CHARACTERIZATION OF LINEN MODIFIED BY LOW TEMPERATURE PLASMA AND ENZYMATIC HYDROLYSIS

A Thesis Presented for the
Degree of Doctor of Philosophy

by
Wong Ka-kee

Institute of Textiles and Clothing
The Hong Kong Polytechnic University
Hong Kong
November 1999

Abstract of thesis entitled:

"CHARACTERIZATION OF LINEN MODIFIED BY LOW TEMPERATURE PLASMA AND ENZYMATIC HYDROLYSIS"

submitted by Wong Ka-kee

for the degree of Doctor of Philosophy

at The Hong Kong Polytechnic University in November 1999

ABSTRACT

This thesis is concerned with a study on the effects of low temperature plasma pretreatment and enzyme treatment as well as their synergy in order to modify the properties of linen. Linen is more expensive due to the difficulties in processing and it faces strong competition with other natural fibers. Fiber modification, preparation and finishing treatments by environmentally friendly processes are essential in order to minimize the chemical waste and associated disposal problem. Characterizations of the modified linen have been carried out and the effects of the treatments have been experimentally determined. Fiber bulk structure and properties have been studied along with the mechanical properties, surface morphology and properties, and dyeing properties of linen. A number of modern characterization techniques have been applied such as the Environmental Scanning Electron Microscopy, Atomic Force Microscopy, X-ray Photoelectron Spectroscopy and a downward wicking measurement.

Low temperature plasma treatments were applied to linen with oxygen and argon gases, various levels of discharge power and exposure time. It was discovered by X-ray Photoelectron Spectroscopy that the surface oxygen content of the low temperature plasma treated linen was increased, along with the formation of voids and cracks on the fiber surface. The fabric weight loss increased with the exposure time. No significant change in x-ray crystallinity and cuprammonium fluidity was found. A slight reduction of the moisture regain was detected. Fabric water uptake and strength first were increased and then decreased with the prolonged exposure

whereas fabric bending rigidity, hysteresis and wrinkle recovery were slightly improved.

Environmental Scanning Electron Microscopy illustrated the time series images of flax surface appearance changed by the low temperature plasma treatment for the first time. With the image processing techniques and Atomic Force Microscopy, a comprehensive understanding of the surface morphology of low temperature plasma treated flax fibers was achieved. The wetting properties of low temperature plasma treated linen were studied by a downward wicking experiment. Wicking properties of linen were greatly improved by the application of low temperature plasma treatment.

Further investigation was conducted in order to study the synergy of low temperature plasma and enzyme treatment. Enzymes have been used extensively in cotton textiles to remove small fiber ends from fabric surface, create a smooth fabric appearance and introduce a degree of softness without using traditional chemical treatments. The low temperature plasma pretreatment enhanced the effectiveness of enzyme treatment. With an oxygen gas for 2.5 minutes exposure time, a faster reaction rate and acceptable strength loss percentage were achieved. The surface roughness created by the low temperature plasma treatment were further deepened and smoothed by the enzyme treatment. Fabric yellowing occurred after plasma exposure and the whiteness was almost recovered after the enzyme treatment. An increase of fabric water uptake was further provided by the enzyme treatment. Fabric bending rigidity, hysteresis and wrinkle recovery were slightly improved by both treatments. Low temperature plasma pretreatment improved dyeing

performance for a direct dye of small molecule size. However, an adverse effect of dyeing performance was obtained after the enzyme treatment.

As a comparison, the study of enzyme treatment on mercerized linen was also carried out. The factors concerned were the mercerization tension, concentration of cellulase, incubation time and mechanical agitation. Experimental results confirmed that the effectiveness of enzyme treatment was strengthened by the mercerization pretreatment. Higher reduction of fabric stiffness, minimization of the loss of tensile strength, shortening of the original treatment time, complete removal of surface fibrils and improvement of dyeing performance for direct dyes were achieved. On the other hand, the effect of mechanical agitation on the efficiency of enzyme treatment has been studied and the results revealed that the reduction of both bending rigidity and hysteresis were achieved by applying a higher mechanical agitation during the enzyme treatment. It was found that low temperature plasma pretreatment was more effective than the mercerization pretreatment in improving the effectiveness of enzyme treatment.

The present thesis illustrates that the application of two environmentally friendly processing technologies can achieve significant improvements of fiber properties in terms of fabric wetting and dyeability, and moderate improvement of fabric strength, wrinkle recovery, bending rigidity and hysteresis.

ACKNOWLEDGEMENTS

The project was completed with the support of many people.

I would like to express my special gratitude to my chief supervisor, Professor X. M. Tao, for providing the opportunity for this project to be undertaken, and for her comprehensive assistance, valuable advice and encouragement. Without her guidance in the course of research, critical discussions and comments, writing up research papers and thesis, I will not be able to complete my Ph.D. study in such a short period of time.

I would like to express my appreciation to my co-supervisors, Dr. C. W. M. Yuen, Assistant Professor and Professor K. W. Yeung, Associate Vice President, Dean of Faculty of Applied Science and Textiles for providing the opportunity and consistent support. Their constructive discussions and comments are important for me to carry out this research.

I would like to express my sincere thanks to the laboratory technical staff in the spinning workshop, finishing laboratory, chemical testing laboratory and physical testing laboratory of the Institute of Textiles and Clothing as well as the technical staff in Materials Research Center, for their kind assistance and valuable advice in the experimental work.

I would like to acknowledge Mr. K. C. Ho, Materials Characterization and Preparation Facility, Hong Kong University of Science and Technology, Mr. W. K. Fok, Department of Earth Sciences, The University of Hong Kong, Dr. J. Cao and Dr. M. G. Huson, CSIRO Wool Technology, Australia, for their kind assistance in the experimental work with helpful suggestions and discussions.

I would like to thank my parents, sisters and brothers for their strong support and encouragement during my study. Special thanks to Mr. W. C. Hui and all of my friends for their support, understanding and patience during my study. Sincere thanks to all my colleagues for their strong support, valuable advice and discussions during my research study.

Finally, I would like to acknowledge with gratitude the Tuition Scholarship for Research Postgraduate Studies, the facilities and financial support of The Hong Kong Polytechnic University which made this Ph.D. research possible.

TITLE: CHARACTERIZATION OF LINEN MODIFIED BY LOW TEMPERATURE PLASMA AND ENZYMATIC HYDROLYSIS

CONTENTS

		Page
CHAPTER 1	**INTRODUCTION**	
1.1	BACKGROUND	1
1.2	OBJECTIVES	3
1.3	METHODOLOGY	4
1.4	SCOPE OF THESIS	5
CHAPTER 2	**LITERATURE REVIEW**	
2.1	INTRODUCTION	8
2.2	FLAX FIBER	9
	2.2.1 Fiber Processing	9
	2.2.2 Fiber Chemical Composition	13
	2.2.3 Fiber Morphological Structure	15
	2.2.4 Fiber Properties	17
2.3	FLAX FIBER MODIFICATION TECHNOLOGY	19
	2.3.1 Low Temperature Plasma Treatment	21
	2.3.1.1 Low temperature plasmas	21
	2.3.1.2 Generation of low temperature plasma	23
	2.3.1.3 Application of low temperature plasma treatment to cellulose materials	27
	2.3.1.4 Advantages and disadvantages of low temperature plasma treatment	30
	2.3.2 Enzyme Treatment	32
	2.3.2.1 Enzymes	32
	2.3.2.2 Enzymatic reaction of cellulase	32
	2.3.2.3 Application of enzyme treatment to cellulose materials	35
	2.3.2.4 Advantages and disadvantages of enzyme treatment	41
2.4	CHARACTERIZATION TECHNIQUES	42
	2.4.1 Changes in Bulk Structure and Properties	43
	2.4.2 Changes in Surface Morphology and Properties	44
	2.4.3 Changes in Other Related Fabric Properties	47
	2.4.4 Changes in Dyeing Properties	47
2.5	CONCLUSION	48

CHAPTER 3	**LOW TEMPERATURE PLASMA TREATMENT OF LINEN**	
3.1	INTRODUCTION	50
3.2	EXPERIMENTAL DETAILS	51
	3.2.1 Sample Preparation	51
	3.2.2 Material Characterization Procedures	54
	3.2.2.1 Bulk structure and properties	54
	3.2.2.2 Surface morphology and properties	55
	3.2.2.3 Other related properties	56
3.3	RESULTS AND DISCUSSIONS	57
	3.3.1Bulk Structure and Properties	57
	3.3.1.1 Fluidity and x-ray crystallinity	57
	3.3.1.2 Moisture regain	58
	3.3.1.3 Fabric weight loss	59
	3.3.1.4 Fabric strength	60
	3.3.2 Surface Morphology and Properties	62
	3.3.2.1 XPS analysis	62
	3.3.2.2 SEM observation	68
	3.3.2.3 Fabric whiteness	71
	3.3.2.4 Fabric water uptake	73
	3.3.3 Other Related Fabric Properties	76
	3.3.3.1 Fabric bending properties	76
	3.3.3.2 Wrinkle recovery	77
3.4	CONCLUSION	78
CHAPTER 4	**SURFACE CHARACTERIZATION OF FLAX FIBER TREATED WITH LOW TEMPERATURE PLASMA**	
4.1	INTRODUCTION	80
	4.1.1 Surface Morphology Study by SEM and ESEM	82
	4.1.1.1 SEM imaging technique	82
	4.1.1.2 ESEM imaging technique	86
	4.1.1.3 Preliminary experiment	88
	4.1.1.3.1 Sample preparation	88
	4.1.1.3.2 Material characterization procedures	89
	4.1.1.3.3 Operation parameters	89
	4.1.1.3.4 Results and summary of the preliminary experiment	92
	4.1.2 Surface Topography Study by AFM	95
	4.1.2.1 Operating principles and main components of AFM	96
	4.1.2.2 AFM imaging modes	100
4.2	EXPERIMENTAL DETAILS	102
	4.2.1 Sample Preparation for ESEM	102

	4.2.1.1 Material characterization procedures and operational parameters of ESEM	103
	4.2.1.2 Application of image processing technique	104
	4.2.1.3 Determination of fiber diameter and fabric weight loss	104
	4.2.2 Sample Preparation for AFM	104
	4.2.2.1 Material characterization procedures and operational parameters of AFM	105
4.3	RESULTS AND DISCUSSIONS	106
	4.3.1 Effect of Plasma Treatment on the Surface Morphology Studied by SEM and ESEM	106
	4.3.1.1 Time-series observation of fiber surface morphology	106
	4.3.1.2 Results from image processing technique	113
	4.3.1.3 Fiber diameter reduction and fabric weight loss	118
	4.3.1.4 Comparison with SEM micrographs	120
	4.3.2 Effect of Plasma Treatment on the Surface Topography Studied by AFM	123
	4.3.2.1 Surface features	123
	4.3.2.2 Surface roughness	127
4.4	CONCLUSION	128
CHAPTER 5	**CRITICAL SURFACE TENSION AND WICKING OF LINEN TREATED WITH LOW TEMPERATURE PLASMA**	
5.1	INTRODUCTION	130
	5.1.1 Measurement of Critical Surface Tension by Contact Angle Method	132
	5.1.2 Measurement of Water Uptake by Downward Wicking Method	136
5.2	EXPERIMENTAL DETAILS	143
	5.2.1 Critical Surface Tension	143
	5.2.1.1 Sample preparation	143
	5.2.1.2 Contact angle measurement	143
	5.2.2 Water Uptake	146
	5.2.2.1 Sample preparation	146
	5.2.2.2 Upward and downward wicking measurements	147
5.3	RESULTS AND DISCUSSIONS	149
	5.3.1 Critical Surface Tension of Plasma Treated Linen	149
	5.3.2 Water Uptake of Plasma Treated Linen	155
	5.3.2.1 Comparison of upward and downward wicking measurements	155
	5.3.2.2 Downward wicking measurement of the	156

plasma treated linen
5.3.3 Effect of Washing 162

5.4 CONCLUSION 163

CHAPTER 6 LINEN TREATED WITH LOW TEMPERATURE PLASMA AND ENZYME

6.1 INTRODUCTION 165

6.2 EXPERIMENTAL DETAILS 166
6.2.1 Sample Preparation 166
6.2.1.1 Plasma pretreatment 166
6.2.1.2 Enzyme treatment 166
6.2.1.3 Dyeing process 167
6.2.2 Material Characterization Procedures 168
6.2.2.1 Bulk properties 168
6.2.2.2 Surface morphology and properties 168
6.2.2.3 Other related properties 168
6.2.2.4 Colorfastness to washing 169

6.3 RESULTS AND DISCUSSIONS 170
6.3.1. Bulk Structure and Properties 170
6.3.1.1 Fluidity and x-ray crystallinity 170
6.3.1.2 Moisture regain 170
6.3.1.3 Fabric weight loss 171
6.3.1.4 Fabric strength 173
6.3.2 Surface Morphology and Properties 177
6.3.2.1 SEM observation 177
6.3.2.2 Fabric whiteness 180
6.3.2.3 Fabric water uptake 182
6.3.3 Other Related Fabric Properties 184
6.3.3.1 Fabric bending properties 184
6.3.3.2 Wrinkle recovery 185
6.3.4 Dyeing Properties 186
6.3.4.1 Effect of plasma treatment 189
6.3.4.2 Effect of enzyme treatment on plasma pretreated linen 191

6.4 CONCLUSION 193

CHAPTER 7 LINEN TREATED WITH MERCERIZATION AND ENZYME

7.1 INTRODUCTION 195

7.2 EXPERIMENTAL DETAILS 195
7.2.1 Sample Preparation 195
7.2.1.1 Mercerization pretreatment 195

	7.2.1.2 Enzyme treatment	196
	7.2.1.3 Dyeing process	197
	7.2.2 Material Characterization Procedures	197
	7.2.2.1 Bulk properties	197
	7.2.2.2 Surface morphology	197
	7.2.2.3 Colorfastness to washing	197
7.3	RESULTS AND DISCUSSIONS	198
	7.3.1 Effect of Mercerization Pretreatment on Enzyme Treatment	198
	7.3.1.1 X-ray crystallinity and moisture regain	198
	7.3.1.2 Fabric weight loss and thickness	199
	7.3.1.3 Fabric strength	202
	7.3.1.4 Fabric bending properties	205
	7.3.1.5 SEM observation	207
	7.3.1.6 Dyeing properties	210
	7.3.2 Effect of Mechanical Agitation on Enzyme Treatment	213
	7.3.2.1 X-ray crystallinity and moisture regain	213
	7.3.2.2 Fabric weight loss and thickness	214
	7.3.2.3 Fabric strength	216
	7.3.2.4 Fabric bending properties	218
	7.3.2.5 SEM observation	220
7.4	CONCLUSION	220
CHAPTER 8	**CONCLUSIONS**	
8.1	SUMMARY	223
	8.1.1 Literature Review	223
	8.1.2 Characterizations of Plasma Treated Linen	224
	8.1.3 Plasma and Mercerization Pretreatments and their Synergy with the Enzymatic Reaction	227
	8.1.3.1 Plasma pretreatments	227
	8.1.3.2 Mercerization pretreatments	229
8.2	CONCLUSIONS	230
8.3	RECOMMENDATION FOR FUTURE WORK	231
REFERENCES		233-253
APPENDIX 4-I		A1-A3

LIST OF TABLES

		Page
Table 2.1:	Chemical composition of flax fibers	14
Table 2.2:	Characterization techniques used to examine the effect of modifications on fiber properties	43
Table 3.1:	Cuprammonium fluidity, x-ray crystallinity and moisture regain of oxygen and argon plasma treated samples	58
Table 3.2:	Relative intensities of chemical composition percentages of surface atoms of linen treated with oxygen and argon plasma	62
Table 3.3:	C_{1s} spectra of linen treated with oxygen and argon plasma	66
Table 3.4:	Water uptake of fabrics treated with oxygen and argon plasma as functions of storage time	76
Table 3.5:	Bending rigidity, bending hysteresis and wrinkle recovery of oxygen and argon plasma treated samples	77
Table 4.1:	Operational parameters of ESEM instrument	103
Table 4.2:	Root Mean Square (RMS) Roughness of untreated, argon and oxygen plasma treated flax fiber surface	128
Table 5.1:	Results of the contact angle measurement of the plasma treated linen	150
Table 6.1:	Cuprammonium fluidity, x-ray crystallinity and moisture regain of plasma and enzyme treated linen	171
Table 6.2:	Bending rigidity, bending hysteresis and wrinkle recovery of samples after plasma and enzyme treatment	185
Table 6.3:	Fabric weight loss percentage, half time of dyeing, final exhaustion and K/S value of plasma pretreated and enzyme treated sample dyeing with CI Direct Red 81 and Green 26	187
Table 6.4:	Colorfastness to washing of plasma pretreated and enzyme treated sample dyeing with CI Direct Red 81 and Green 26	188
Table 7.1:	Fabric specifications	196
Table 7.2:	X-ray crystallinity and moisture regain of untreated and mercerized linen after 4 hours using 2% enzyme	198

Table 7.3:	Fabric weight loss of untreated and mercerized linen after various periods using 1% or 2% enzyme	200
Table 7.4:	Fabric thickness of untreated and mercerized linen after various periods using 1% or 2% enzyme	201
Table 7.5:	Fabric breaking strength of untreated and mercerized linen after various periods using 1% or 2% enzyme	203
Table 7.6:	Fabric bending rigidity of untreated and mercerized linen after various periods using 1% or 2% enzyme	205
Table 7.7:	Fabric bending hysteresis of untreated and mercerized linen after various periods using 1% or 2% enzyme	206
Table 7.8:	Half time of dyeing, final exhaustion and K/S value of untreated, mercerized and enzyme treated sample dyeing with CI Direct Red 81 and Green 26	212
Table 7.9:	Colorfastness to washing of untreated, mercerized and enzyme treated sample dyeing with CI Direct Red 81 and Green 26	213
Table 7.10:	X-ray crystallinity and moisture regain of linen at different levels of mechanical agitation after 4 hours using 2% enzyme	214
Table 7.11:	Fabric weight loss of linen at different levels of mechanical agitation after various periods using 1% or 2% enzyme	214
Table 7.12:	Fabric thickness of linen at different levels of mechanical agitation after various periods using 1% or 2% enzyme	215
Table 7.13:	Fabric breaking strength of linen at different levels of mechanical agitation after various periods using 1% or 2% enzyme	216
Table 7.14:	Fabric bending rigidity of linen at different levels of mechanical agitation after various periods using 1% or 2% enzyme	219
Table 7.15:	Fabric bending hysteresis of linen at different levels of mechanical agitation after various periods using 1% or 2% enzyme	219

LIST OF FIGURES

		Page
Figure 2.1:	Cross-section of the stem of a flax plant shows the bundles of fiber cells lying below the surface layer	16
Figure 2.2:	Cross-sectional and longitudinal view of flax fibers as seen under scanning electron microscope	17
Figure 2.3:	Diagram of a simple plasma reactor	24
Figure 2.4:	Simplified hydrolysis of a cellulose molecule by cellulase	33
Figure 2.5:	Enzymatic degradation of cellulose by cellulase	34
Figure 2.6:	Effect of surface modification of polymer of fiber properties	42
Figure 3.1:	Plasma Polymerization System	52
Figure 3.2:	Fabric surface temperature measured by Thermax irreversible temperature indicator	54
Figure 3.3:	Percentage of fabric weight loss after oxygen and argon plasma treatment	59
Figure 3.4:	Fabric strength of samples after oxygen and argon plasma treatment	60
Figure 3.5:	Fabric strength loss percentage as a function of fabric weight loss percentage	61
Figure 3.6:	Curve fitting of C_{1s} spectra of linen exposed to plasma	64-65
Figure 3.7:	SEM micrographs of oxygen plasma treated linen	69
Figure 3.8:	SEM micrographs of argon plasma treated linen	70
Figure 3.9:	Reduction in whiteness of fabrics treated with oxygen and argon plasma	72
Figure 3.10:	Effect of oxygen and argon plasma on fabric wickability	74
Figure 4.1:	Photon and charged particle emissions from an electron-bombarded surface	83
Figure 4.2:	Interactions of primary electron beam with the emission of secondary electrons and the gas molecules inside the sample chamber of ESEM	87

Figure 4.3:	Observation of flax fiber and oxygen plasma treated flax fiber (200W, 15Pa, 60 minutes) under ESEM	93
Figure 4.4:	ESEM micrographs of wool fibers	94
Figure 4.5:	ESEM micrographs of cotton fibers	94
Figure 4.6:	ESEM micrographs of ramie fibers	95
Figure 4.7:	Force against distance curve observed in AFM experiment	97
Figure 4.8:	Schematic representation of the main components of an AFM and the SEM image of cantilever and tip	99
Figure 4.9a:	ESEM micrographs (x1000) showing the progressive etching by oxygen plasma on flax fiber	107
Figure 4.9b:	ESEM micrographs (x3000) showing the progressive etching by oxygen plasma on flax fiber	108
Figure 4.10a:	ESEM micrographs (x1000) showing the progressive etching by argon plasma on flax fiber	109
Figure 4.10b:	ESEM micrographs (x3000) showing the progressive etching by argon plasma on flax fiber	110
Figure 4.11a:	ESEM micrographs of oxygen plasma treated flax fiber	114
Figure 4.11b:	Surface feature of oxygen treated flax fiber	115
Figure 4.12:	Percentage of weight loss and diameter reduction caused by oxygen and argon plasma at various exposure times (15Pa and 200W)	118
Figure 4.13:	SEM micrographs of flax fiber etched by oxygen and argon plasma (pre-determined etching)	121
Figure 4.14:	SEM micrographs of flax fiber etched by oxygen and argon plasma (accumulative etching)	122
Figure 4.15:	SEM micrographs of flax fiber etched by oxygen and argon plasma after the accumulation of 60 minutes exposure	123
Figure 4.16a:	AFM micrographs of untreated flax fiber	124
Figure 4.16b:	AFM micrographs of argon plasma treated flax fiber (200W, 60 minutes)	125

Figure 4.16c:	AFM micrographs of oxygen plasma treated flax fiber (200W, 60 minutes)	126
Figure 5.1:	Small and large contact angles represent good and poor wetting respectively	133
Figure 5.2:	Schematic diagram of contact angle between a drop of liquid and a solid surface	134
Figure 5.3:	Experimental set-up of contact angle measurement	144
Figure 5.4:	Pictures of contact angle measurement	145
Figure 5.5:	Contact angle determination using Half-Angle measuring method	146
Figure 5.6:	Experimental setting for water uptake measurement	147
Figure 5.7:	Experimental setting for downward wicking measurement	148
Figure 5.8:	Photographs of experimental setting for downward wicking measurement	149
Figure 5.9:	Plots of cos θ of fabric surface contact angle against the surface tension of liquids. The intercept of the line at cos θ = 1 is the critical surface tension γ_c	150-151
Figure 5.10:	Absorption of distilled water on linen fabric under the observation of surface contact angle with a time interval of 1/24 second	152
Figure 5.11:	Absorption of 55% sucrose solution on linen fabric under the observation of surface contact angle with a time interval of 1/24 second	153
Figure 5.12:	Experimental results of comparison between upward and downward wicking	155
Figure 5.13:	Effect of oxygen plasma treatment (100W, various exposure time) on the downward wicking of linen	157
Figure 5.14:	Effect of oxygen plasma treatment (200W, various exposure time) on the downward wicking of linen	157
Figure 5.15:	Effect of argon plasma treatment (100W, various exposure time) on the downward wicking of linen	158
Figure 5.16:	Effect of argon plasma treatment (200W, various exposure time) on the downward wicking of linen	158

Figure 5.17:	Effect of washing on the downward wicking of linen	163
Figure 6.1:	Percentage of fabric weight loss due to plasma treatments and enzyme treatments	172
Figure 6.2:	Fabric strength of plasma treated and enzyme treated samples	174
Figure 6.3:	Fabric strength loss percentage as a function of fabric weight loss percentage	176
Figure 6.4:	SEM micrographs of oxygen plasma treated linen before and after enzyme treatment	178
Figure 6.5:	SEM micrographs of argon plasma treated linen before and after enzyme treatment	179
Figure 6.6:	Reduction in whiteness of fabrics treated with plasma and recovered by washing and enzyme treatment	181
Figure 6.7:	Effect of plasma and enzyme treatments on fabric water uptake	183
Figure 7.1:	Relative breaking loads of untreated and mercerized linen after various periods using 1% enzyme	204
Figure 7.2:	Relative breaking loads of untreated and mercerized linen after various periods using 2% enzyme	204
Figure 7.3:	SEM micrographs of untreated flax fiber and yarn	207
Figure 7.4:	SEM micrograph of linen after 4 hours using 1% enzyme	208
Figure 7.5:	SEM micrograph of linen after 4 hours using 2% enzyme	208
Figure 7.6:	SEM micrograph of slack mercerized linen	208
Figure 7.7:	SEM micrograph of slack mercerized linen after 4 hours using 1% enzyme	208
Figure 7.8:	SEM micrograph of slack mercerized linen after 4 hours using 2% enzyme	208
Figure 7.9:	SEM micrograph of 95% tension mercerized linen	209
Figure 7.10:	SEM micrograph of 95% tension mercerized linen after 4 hours using 1% enzyme	209
Figure 7.11:	SEM micrograph of 95% tension mercerized linen after 4 hours using 2% enzyme	209

Figure 7.12:	SEM micrograph of 100% tension mercerized linen	209
Figure 7.13:	SEM micrograph of 100% tension mercerized linen after 4 hours using 1% enzyme	210
Figure 7.14:	SEM micrograph of 100% tension mercerized linen after 4 hours using 2% enzyme	210
Figure 7.15:	Relative breaking loads of linen at different levels of mechanical agitation after various periods using 1% enzyme	217
Figure 7.16:	Relative breaking loads of linen at different levels of mechanical agitation after various periods using 2% enzyme	218
Figure 7.17:	SEM micrograph of linen after 4 hours using 1% enzyme and 5 stainless steel balls	220
Figure 7.18:	SEM micrograph of linen after 4 hours using 2% enzyme and 5 stainless steel balls	220
Figure 7.19:	SEM micrograph of linen after 4 hours using 1% enzyme and 10 stainless steel balls	220
Figure 7.20:	SEM micrograph of linen after 4 hours using 2% enzyme and 10 stainless steel balls	220

LIST OF PUBLICATIONS

Refereed Journals

1. Wong, K. K., Tao, X. M., Yuen, C. W. M., and Yeung, K. W.,
   Effect of Enzyme Treatment on the Chemically Pre-treated Linen,
   Enzyme Applications in Fiber Processing, ACS Symposium Series 687, 246-261 (1998).

2. Wong, K. K., Tao, X. M., Yuen, C. W. M., and Yeung, K. W.,
   Improvement of Linen Fabric Wickability by Low Temperature Plasma Treatment,
   Journal of China Textile University (English Edition), Vol. 16, No. 2, 1-6 (June 1999).

3. Wong, K. K., Tao, X. M., Yuen, C. W. M., and Yeung, K. W.,
   Low Temperature Plasma Treatment of Linen,
   Textile Research Journal, Vol. 69, No. 11, (November 1999).

4. Wong, K. K., Tao, X. M., Yuen, C. W. M., and Yeung, K. W.,
   Topographical Study of Low Temperature Plasma Treated Flax Fiber,
   Textile Research Journal. (Accepted for publication)

5. Wong, K. K., Tao, X. M., Yuen, C. W. M., and Yeung, K. W.,
   Effect of Plasma Treatment in Further Enzymatic Treatment of Linen Fabrics
   Submitted to Journal of Society of Dyers and Colourists.

6. Wong, K. K., Tao, X. M., Yuen, C. W. M., and Yeung, K. W.,
   Wicking Properties of Linen Treated with Low Temperature Plasma,
   Submitted to Textile Research Journal.

Conference Papers

1. Wong, K. K., Tao, X. M., Yuen, C. W. M., and Yeung, K. W.,
   Effect of Enzyme Treatment on the Chemically Pre-treated Linen,
   American Chemical Society, Abstracts of Papers, 213, Part 1: CELL031, 1 page, April 13-17, 1997. (ACS Conference April 1997. Symposia: "Enzyme Applications in Fibre Processing", Cellulose, Paper & Textile Division & Division of Biochemical Technology.)

2. Wong, K. K., Tao, X. M., Yuen, C. W. M., and Yeung, K. W.,
   Fabric Properties of Linen Treated with Low Temperature Plasma and Enzyme,
   Proceedings of The 5th Asian Textile Conference, Japan, 1241-1243 (October 1999).

3. Wong, K. K., Tao, X. M., Yuen, C. W. M., and Yeung, K. W., Surface Properties of Low Temperature Plasma Treated Linen, Proceedings of The 5th Asian Textile Conference, Japan, 1244-1247 (October 1999).

Non-refereed Journals

1. Wong, K. K., Tao, X. M., Yuen, C. W. M., and Yeung, K. W., Modification of Bast Fibres, (1) Flax and Ramie Structure and Properties, Textile Asia, Vol. XXVIII, No. 2, 46-49 (February 1997).

2. Wong, K. K., Tao, X. M., Yuen, C. W. M., and Yeung, K. W., Modification of Bast Fibres, (2) Chemical Modification Treatments, Textile Asia, Vol. XXVIII, No. 3, 47-52 (March 1997).

CHAPTER 1

INTRODUCTION

1.1 BACKGROUND

Flax is a natural cellulosic fiber belonging to the group of bast fibers. It is derived from the vascular bundles of plant stems which are used for food and water transport in living plants. The fiber consists of long thick-walled cells overlapping and cemented together by non-cellulosic materials to form continuous strands that may run the entire length of the plant stem. Flax is one of the oldest fibers used by man to manufacture textiles. In the modern world, however, the flax fiber faces the challenges of technological developments and ecological concerns at all stages of production, processing and end-uses. Modernization of its processing technology and wide application of the fiber in many fields are important for maintaining and improving its competitiveness.

New methods of fiber modification by means of both physical and chemical techniques have been explored. Concerning the operational safety and environmental protection, two kinds of new technology have been introduced to the textile industry to replace some of the existing chemical treatments. The first kind is the gas phase finishing processes. Among them, low temperature plasma has been used in modifying the fiber surface properties. The second kind is enzymatic treatment. For cellulosic materials, cellulase treatments have been a focus of interest for cotton finishing to improve the fabric softness, as well as to simplify the

manufacturing processes. Both of them have been considered as promising alternatives to replace some of the traditional wet treatments [29, 97, 116, 242].

Processing by plasma assisted techniques is being increasingly used in various areas of production and manufacturing such as the automotive, aerospace, biomedical industries and in the fabrication of microelectronic components. Exposure of materials to suitable low temperature plasma for a short period of time can cause both chemical and physical changes of the surface layers so as to provide a desirable surface without degrading the bulk properties greatly [97]. The accessibility of crystalline regions will be increased by the introduction of cracks on the fiber surface after the low temperature plasma treatment.

On the other hand, enzymes have been used in a variety of applications ranging from production of food and beverages, formulation of detergents, to the processing of pulp, leather and textiles. For instance, enzymes have been applied to processes of desizing and denim washing. The cellulase enzyme treatment can remove fibrils on fabric surface so that a softer handle, smoother, more lustrous and clearer fabric surface appearance can be achieved. Fabrics free from surface hairiness and neps have a lower tendency to pill. Furthermore, fabric wettability may be retained and the colour definition of dyed goods become clearer. Enzymes are completely biodegradable and are always used in low concentrations, thus they pose no disposal problems.

Most of the studies of the low temperature plasma or enzyme treatment have been concentrated on cotton and to a much lesser extent on flax fiber. Flax fiber has a

high crystallinity and unique morphological structure, these features will largely affect the course of modification. There exist many knowledge gaps in our current understanding such as the effect of low temperature plasma treatment on the fiber bulk structure and properties, fabric properties, surface properties, wetting characteristics and fiber surface morphology of flax.

Moreover, previous research showed that the structural features of cellulosic materials influenced the rate and extent of cellulose enzymatic hydrolysis. Two of the most important structural features of fibers are crystallinity and surface area. Structural changes of the cellulose substrate by pretreatments will influence the course of the subsequent process [29]. The progress in the development of effective pretreatment has been very limited, especially the low temperature plasma and mercerization pretreatments on linen have not been explored.

Therefore, the major aims of the investigation are to characterize the variations in the structure and properties of the fibers and fabrics modified by the low temperature plasma and enzyme treatment. A range of advanced analytical instruments and characterization techniques will be employed for the comprehensive and systematic investigation.

1.2 OBJECTIVES

This thesis is concerned with an investigation of the effects of low temperature plasma and enzyme treatments on linen. The principal objectives of the thesis are as follows:

(1) To examine the effects of low temperature plasma treatments on the fiber bulk structure and properties, surface morphology and properties, and mechanical properties of its resultant fabrics. It is aimed to improve the fiber properties in terms of fabric wetting and dyeability, fabric strength, wrinkle recovery, bending rigidity and hysteresis;

(2) To obtain a comprehensive morphological and topographical study of low temperature plasma treated flax fiber by using a range of instrumental techniques;

(3) To develop a downward wicking measuring technique to characterize the wetting properties of low temperature plasma treated linen;

(4) To study the effectiveness of enzyme treatments enhanced by the low temperature plasma and mercerization pretreatments.

1.3 METHODOLOGY

In order to achieve the objectives, the following methodologies will be adopted:

(1) A literature review will be conducted aiming to gain the background knowledge and recent development in the relevant areas.

(2) Low temperature plasma will be applied to linen under different treatment conditions. Preliminary investigations will be conducted to establish suitable working conditions and procedures.

(3) A range of advanced analytical techniques such as XPS, SEM, ESEM, AFM, etc. will be used to obtain a comprehensive evaluation of the surface morphology and chemical composition of the low temperature plasma treated flax fibers as well as other fiber and fabrics properties. Appropriate experimental methods and procedures will be established.

(4) Various testing methods will be used to investigate the wetting characteristic of low temperature plasma treated linen. The changes of wetting properties will be related to the changes in fiber morphology, bulk properties and surface properties.

(5) Linen will be pretreated by low temperature plasma or mercerization prior to enzyme treatments. The effect of the pretreatments will be explored and the effectiveness will be assessed in terms of the changes in fiber bulk structure and properties, mechanical properties, surface morphology and properties, and dyeing properties.

1.4 SCOPE OF THESIS

The thesis comprises eight chapters. Chapter 1 introduces the background information, objectives, methodology and scope of the thesis.

In Chapter 2, results from a literature survey are presented on the processing of techniques of flax fiber, chemical composition, morphological structure, fiber properties and fiber modification technologies as well as the characterization

techniques. The results highlight the needs for further investigation of flax fiber modification through low temperature plasma and enzyme treatment.

Chapter 3 describes an experiment on low temperature plasma treatments of linen with oxygen and argon gases, two levels of discharge powers and various exposure times. A range of analytical methods are used to examine their effects on the properties of linen including fluidity, x-ray crystallinity, moisture regain, fabric weight loss, fabric strength, surface chemistry by XPS analysis, surface morphology by SEM observation, fabric whiteness, fabric water uptake, fabric bending properties and wrinkle recovery.

Chapter 4 presents a study of fiber surface changes brought about by the low temperature plasma treatment using an Environmental Scanning Electron Microscopy (ESEM) and Atomic Force Microscopy (AFM). Suitable operational parameters are selected to examine the fiber surface without being affected by the action of the electron beam degradation. Changes of fiber diameter and fabric weight loss are studied along with the surface morphology characterized by ESEM, SEM and AFM. Moreover, a quantitative description of the surface topography of low temperature plasma treated flax fibers is obtained by the use of image processing techniques.

Chapter 5 investigates the wetting property of low temperature plasma treated linen. First, it describes the measurement of surface contact angles and the determination of critical surface tension by the Zisman's plots. Moreover, the wicking abilities of low temperature plasma treated linen are compared experimentally with a upward water

uptake and a downward water wicking methods. The experimental set-up and testing procedures are developed and the experimental results are discussed in terms of the conditions of low temperature plasma treatments.

In Chapter 6, an experiment is presented on the application of enzyme treatment to low temperature plasma pretreated linen. Oxygen and argon gases are applied for various periods of exposure time. Measurements cover fluidity, x-ray crystallinity, moisture regain, fabric weight loss, fabric strength, XPS analysis, SEM observation, fabric whiteness, fabric water uptake, fabric bending properties, wrinkle recovery and dyeing properties with direct dyes before and after enzyme treatment. The effectiveness of low temperature plasma pretreatment is assessed based on the measured properties before and after the enzyme treatment.

Chapter 7 explores the application of enzyme treatment on mercerized linen. The experimental factors concerned are the mercerization tensions, concentrations of cellulase, incubation times and levels of mechanical agitation. Changes are determined experimentally in x-ray crystallinity, moisture regain, fabric weight loss, fabric thickness, fabric strength, fabric bending properties, SEM observation and dyeing properties with direct dyes. The effectiveness of mercerization pretreatment is assessed.

In Chapter 8, it summaries the major results and findings of the present work, and draws conclusions. The remaining problems are outlined and possible future research work are recommended.

CHAPTER 2

LITERATURE REVIEW

2.1 INTRODUCTION

Flax is a bast fiber used to manufacture linen textiles. At the end of the 1970s, flax was almost forgotten in many western European countries and it was anticipated that the fiber would disappear from the market altogether. However, in the 1990s flax has made a comeback to become one of the biggest fashion stories of the decade. The reasons behind this include the positive physiological properties possessed by the fiber such as good heat conductivity and excellent moisture transport combined with the characteristic rustic structure of linen products which offer comfortable wear properties and fashion prestige. More and more people embrace the 'return to nature' trend and environmental sustainability. Besides the progress of flax fiber technology, the world ecological awareness and the new products developed specifically for flax fiber have also contributed to the comeback of linen [149, 156].

As a fabric, linen is mainly used for furnishing, tableware, handkerchiefs, drying cloths with relatively smaller amounts for apparel, canvas, tenting and industrial fabrics. Recently, there has been a rising demand for linen outer-wear garments. To increase its end uses in certain existing areas and other new areas, research efforts are needed for product development as well as improvement of technical aspects of processing [91-92].

In this chapter, fiber processing, fiber molecular structure, morphological structure, properties of the linen are reviewed. A review of the fiber modification treatments will be presented to explore the possibility of applying new modification techniques to linen. In the later section of this chapter, a range of new analytical equipment will be described for the characterization of fiber structures and properties.

2.2 FLAX FIBER

2.2.1 Fiber Processing

Flax fiber is a natural vegetable fiber based on cellulose and it comes from the stem of an annual flax plant called *Linum usitatissimum* which belongs to the family of *Linaceae*. It grows in many temperature and sub-tropical regions of the world and it is the most important bast fiber having a long tradition of use [51].

Flax fibers lie in bundles within the inner bark of the stem, therefore, they must first be degraded to facilitate the mechanical removal of the woody core so as to allow the fiber bundles to further sub-divide to become sufficiently fine for spinning. In common with other bast fibers, flax is subjected to a biological process known as retting in which fungi and bacteria selectively attack the binding materials by secreting highly specific enzymes in order to achieve the removal of fiber from plant stem [99].

Dew-retting is the most common process employed for the flax fiber. After harvesting, the flax plant is spread on the field for over a period of 3-7 weeks during which the retting organisms grow in the warm, moist conditions of the straw swathe. Since dew-retting is a natural air-drying technique and can be easily mechanized, it

can replace the older water-retting process in which the flax straw is steeped in tanks of water for several days. However, a favorable climate is required for the action of fungi in the case of using dew-retting. Certain disadvantages of using dew-retting include the dependence of geographical regions with appropriate temperatures for retting, coarser and lower quality fibers than with water retting and occupation of agricultural fields for several weeks. Moreover, retting is also carried out by treating the flax straw with chemical solutions such as caustic soda, sodium carbonate, soaps and dilute mineral acids. In general, chemical retting of the straw is a more costly process than biological retting and with poor fiber quality. Because of the disadvantages of the other methods, researchers have expended considerable efforts in the 1980s to develop an enzyme retting system to control the retting process to produce fiber of consistent quality [9-10, 15, 99-100, 115, 220, 222-224, 248].

When the retted straw is dried, the fiber bundles shrink away from the brittle woody core. The fiber will be removed mechanically by the processes of "breaking' and "scutching". The flax straw contains about 25-30% of fiber based on the dry, retted straw weight [15, 100]. Then, the scutched fibers are combed to separate the long fibers from the short fibers by "hackling" processing. The shorter fiber removed is called "tow" which is the raw material for coarser yarns. The long flax is called "line" which is used for the spinning of very fine yarns. The fibers are drawn through a series of pins that separate the fibers and leave them in a parallel arrangement. Fibers are drawn from hackling machines into a sliver for spinning into yarn. This careful and relatively slow processing sequence contributes to the high cost of fine linen [99-100].

There are two methods of spinning flax, i.e., dry spinning and wet spinning. Versatile, high-draft and long-staple spinning frames are used to spin flax to form sliver. Dry spinning, usually from tow, is used for the production of coarser yarns with the limited fineness of around 65 tex or 25 linen "lea". Lea is the traditional linen yarn count and is the number of 300 yards lengths equivalent to one pound weight. Dry-spun yarns are quite soft and open-structured. Wet spinning is used to produce finer yarns either from the high-quality tow or from line. The smooth wiry yarn produced is much stiffer than the dry-spun yarns because the binding materials softened by wetting are still present on the yarn when dry. Most of the coarser dew-retted flax on the rove bobbin before spinning will undergo a chemical treatment, either an alkali boil or a full bleach. The effect of this is to upgrade the fiber quality by assisting fiber subdivision and enabling the fine yarns to be spun from a given raw material. Wet-spun yarns require a costly drying process [99-100].

Flax possesses adhering particles of plant tissue, gums, pectins and coloring matters. Chemical treatment is required to bleach its natural greyish brown colour. A scour in a boiling sodium carbonate solution can remove most of the soluble impurity [99]. The optimum scouring process condition recommended for linen has been worked out using sodium carbonate along with surfactant for 30 minutes near the boil (95°C). This results in saving chemical cost without any adverse effect on quality. On the other hand, discontinuation of the use of caustic soda in an existing mixed alkali scour process has been advised in order to save chemical costs and avoid adverse effect on quality [92, 100].

Linen can be bleached with weak solutions of hypochlorite, peroxide or chlorite

which can oxidize the remaining colored impurities and give fabric the required degree of whiteness [99-100, 141]. Although bleaching of flax-based textiles is more or less equivalent to that of cotton-based textiles, two main factors need to be considered. Firstly, flax contains 15-20% natural impurities in contrast to cotton which acquires only 5%. Secondly, flax is more sensitive to alkali and oxidizing bleaching agents when compared with cotton. This is why bleaching of flax-based textiles is more lengthy and requires more care and precautions than cotton-based textiles [75]. Further modifications in bleaching recipes for achieving similar whiteness like cotton have been attempted, i.e., sodium chlorite-sodium hypochlorite- no rinse-hydrogen peroxide. By using this combination, it has been found to be the best arrangement in terms of cost and quality [91]. Alternatively, a hydrogen peroxide/urea system can also be used for bleaching of linen [75].

Linen can be dyed or printed to high levels of fastness with vat dyes or reactive dyes, and attractive cross-dyed effects can be obtained with blends [99-100]. The strong consumer demand for natural linen fabric without any dyeing involved can further enhance the awareness of environmental safety of linen [138]. To meet the specification and consumer needs, linen may be made crease resistant, flame retardant, stain repellent or water repellent by the application of resin finishes [99]. As an apparel fabric, linen is very comfortable and non-allergenic. The use of knitted fabrics extends its applications beyond warm weather and has the major advantage of not wrinkling unlike linen woven fabric [138].

2.2.2 Fiber Molecular Structure

Bast fibers including flax are natural vegetable fibers based on cellulose. They are derived from the vascular bundles of plant stems which are used for food and water conduction in the living plant. The fibers are constructed of long thick-walled cells overlapping and cementing together by non-cellulosic materials to form continuous strands that may run the entire length of the plant stem. The process of retting or degumming can release the strands of bast fibers from the cellular and woody tissue of plant stem.

The nature and chemical composition of flax fiber are affected by the retting process as shown in Table 2.1. The main factors are generic characteristics of the plant, conditions of growth, type of soil, age, part of the plant from which the sample originates, mode of cultivation, and the atmospheric conditions to which the fibers are directly exposed. To some extent the wide divergence in values may also be due to different methods employed for the determination of a particular component. Heterogeneity in both chemical and structural composition has a direct bearing on the fiber properties and surface morphology of fiber [194]. Plant breeding work has been successful in producing varieties of flax with high fiber content which are resistant to pests and diseases and will stand up well in bad weather. Agricultural research has established the optimum sowing density for flax seed and the correct balance of fertilizers and weed control agents, all of which have further helped to increase fiber yields [99].

The structure of flax is made up of multiple cells meaning that the fiber cells are found in bundles of multiple cells and bound together by natural polymers variously

called resins, gums, cementing materials, encrusting materials and middle lamella [194]. Cellulose is a polysaccharide or polymeric sugar that can be represented by the simple formula $(C_6H_{10}O_5)_n$. When cellulose is completely hydrolyzed in dilute acid solution, it produces the simple sugar glucose which has the molecular formula $C_6H_{12}O_6$. In comparing the two formulae, the repeating unit in cellulose is anhydroglucose.

Table 2.1: Chemical composition of flax fibers [15, 92, 108, 194]

	Unretted flax	Retted flax
Cellulose Content	56.5%	64.1%
Hemicellulose	15.4%	16.7%
Pectin	3.8%	1.8%
Lignin	2.5%	2.0%
Water Soluble Material	10.5%	3.9%
Fat and Wax	1.3%	1.5%
Moisture	10.0%	10.0%

Cellulose is a highly polycrystalline material without forming any discrete crystals like those glucose from which it is derived. Native cellulose fibers consist of crystalline fibrils varying in complexity and length. This fibrillar structure is interspersed with material in which the chain molecules are less well ordered than in a crystal. The same molecule may participate in both crystalline and less crystalline material along different portions of its length. Native cellulose contains very little genuine non-crystalline material. The amorphous region is generally believed to be mainly the accessible surface of some of its crystalline fibrils.

Five allomorphic forms of cellulose have been identified, but only cellulose I and cellulose II are important in textile processing. Cellulose I is the form found in nature and cellulose II is the thermodynamically more stable form produced when cellulose is regenerated from solution or subjected to the process of mercerization.

Crystallite orientation is determined more easily by x-ray diffraction methods. Extensive evidence can be obtained using infrared spectroscopy, deuterium interchange technique and electron diffraction. The dimensions of monoclinic cell are approximately: a = 0.835nm, b = 1.03nm (fiber axis), c = 0.79nm and $\beta = 84°$ in the case of cellulose I. The unit cell of cellulose II is also monoclinic with average dimensions being a = 0.814nm, b = 1.03nm, c = 0.914nm and $\beta = 62°$. The x-ray diagram of purified flax is much more distinct and of better resolution than that of unpurified flax [221].

The outer layer of flax has a Z spiral, followed by an S layer in the thick middle wall, and another Z layer towards the center. The spiral angle has been estimated to be 6.5°. Unlike cotton, there are no reversals in the directions of spirals along the fiber length. On treatment with NaOH solution of mercerization, the cellulose I pattern of purified flax is completely transformed to cellulose II pattern. The degree of crystallinity of flax is estimated to be 70% with the degree of polymerization around 2190-2420 and specific gravity of 1.50-1.55g/cm^3 [15].

2.2.3 Fiber Morphological Structure

The flax fibers lie in bundles within the inner bark of the stem between the woody core and the thin outer skin as shown in Figure 2.1. In a cross-section there are usually about thirty bundles, each containing between 10-40 individual or ultimate flax fibers 2-3cm in length and 15-20μm in diameter. The ultimate flax fibers are bound together within the bundles, and the bundles are also bound to the stem by pectins [100, 194]. The flax plant grows up to a meter tall in temperate climates and has a single slender stem that is devoid of side branches other than those which bear

the flowers [99]. When the plants have flowered and the seeds are beginning to ripen, the crop is pulled up with the roots either by hand or by mechanical pullers. About one-quarter of the stem consists of fiber. Flax fiber strands in the scutched state vary in length from a few centimeters (tow fiber) to as much as one meter (line). By the time the fiber reaches the spinning stages, it will be broken down in length [51].

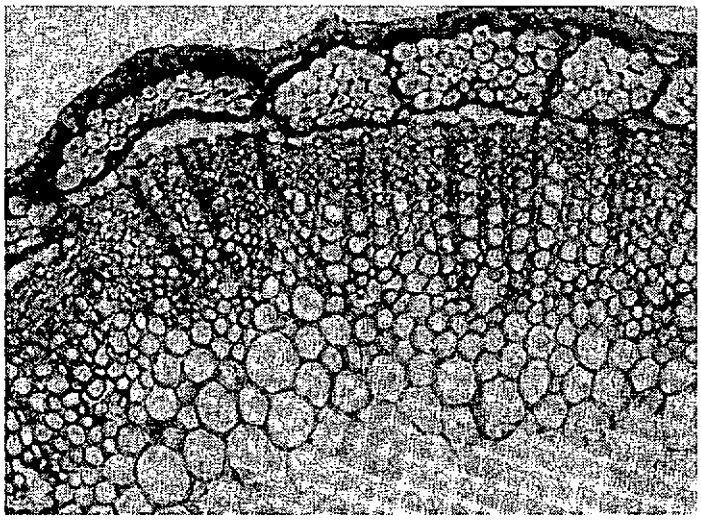

Figure 2.1: Cross-section of the stem of a flax plant shows the bundles of fiber cells lying below the surface layer [100]

Commercial flax is in the form of bundles of individual fiber cells held together by a natural binding material. Scutching and hackling tend to break up the coarse bundles of fibers as they exist in the bast, but do not separate the fiber strands into their individual fiber cells. Flax is usually yellowish-white colour, but the shade of the raw fiber varies considerably depending upon the conditions under which it has been retted, e.g. dew-retted fiber is generally grey.

When the flax fiber is observed under microscope as shown in Figure 2.2, the fiber cells appear as long transparent, cylindrical tubes which may be smooth or striated lengthwise but they do not have the convolutions. The width of the fiber may vary

several times along its length. There are swellings or 'nodes' at many points, and the fibers show characteristic cross-markings. The fiber cell has a lumen or canal running through the center; the lumen is narrow but clearly defined and regular in width. The end of the fiber usually tapers to a point. The cell walls of the flax fiber are thick and polygonal in cross-section. High quality flax has elementary fibers in the shape of polygon with 3-7 sides [206]. Immature and poor flax fibers are more oval in cross-section and the cell walls are thinner. The lumen of the immature fiber is relatively larger than that of the mature fiber [51].

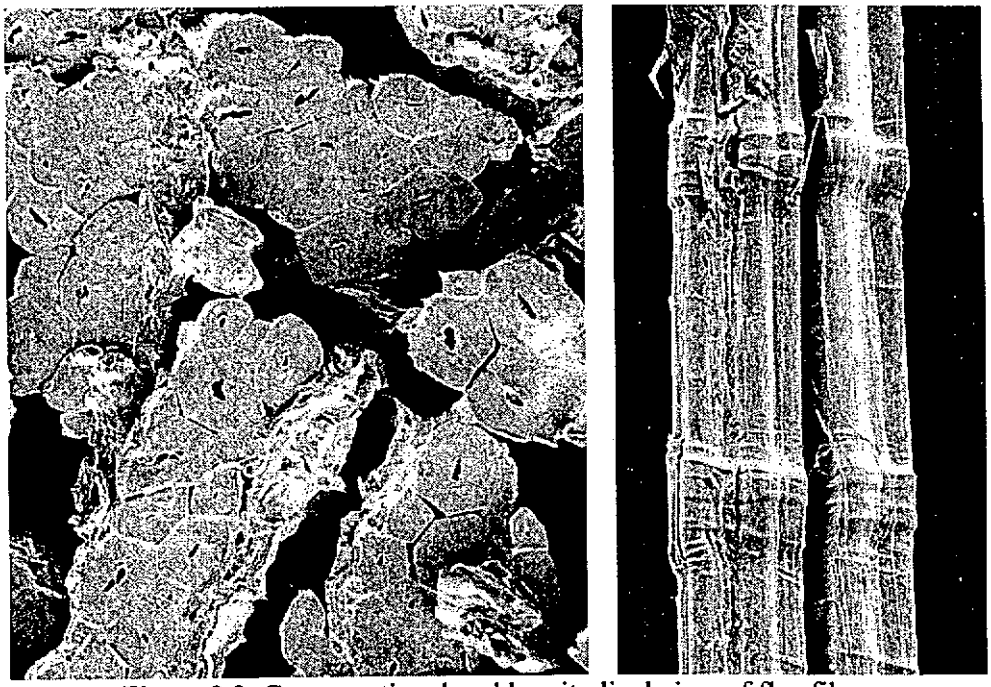

Figure 2.2: Cross-sectional and longitudinal view of flax fibers as seen under scanning electron microscope [218]

2.2.4 Fiber Properties

Flax is usually soft and has a lustrous appearance. The more it is washed, the softer it will be [135]. Luster can be improved as the wax and other surface materials are removed. Flax is a strong and particularly inextensible fiber which can be stretched only slightly as tension increases. Its tenacity ranges between 5.5 and 6.5g/d. The elongation at break is approximately 1.8% in dry and 2.2% in wet condition. Within

its small degree of extensibility, flax is an elastic fiber which will tend to return to its original length when tension is released. It has a high degree of rigidity and can resist bending. Flax is about 20% stronger when wet than dry [51].

The comfort quality of linen involves its cool nature and its ability to absorb perspiration, both of which are related to the structure of the fiber bundle. Little air is trapped between the fibers, and water is retained by capillary action between the fibers [229]. It is a good conductor of heat and so this is the reason why flax sheets feel so cool [51].

Its hygienic, anti-electrostatic and UV preventing properties are needed to prevent the UV radiation or electrostatic fields around human beings (work with computers and electronic devices) [150]. Higher UV-Protection Factors can be provided by the fibers containing natural pigments, lignin and hemicelluloses which act as UV radiation absorbents [185]. Garments made from flax are particularly suitable for hot climates, and also these fibers can be blended with other types of fibers to provide a great variety of fabric properties. Non-static and non-allergic, linen is even claimed to reduce muscle tension [162]. Linen does not have the electrostatic properties like many fibers do, so linen textiles do not have greater affinity for attracting lint, hair and other foreign particles than many textiles do.

The advantages of linen fabrics are seen in its strength, durability, stability, low pilling tendency and low release of individual fiber lint. The moisture regain of flax fiber at standard conditions is 7% [15]. The physiological properties of flax can be characterized as having a pleasant and cooling feel which makes it suitable for

wearing in hot weather [149]. However, the poor dry crease recovery is an inherent property of the pure linen fabric. The reason for this is due to the compact fiber structure and high cellulose crystallinity which make linen particularly susceptible to wrinkling and causes it to react more sensitively to intensive finishing than other cellulose fibers [156]. Fortunately, linen creasing is the natural feature which provoked the designers and wearers to use it, since the decision to buy textiles largely depends on the image and identification [162].

2.3 FLAX FIBER MODIFICATION TECHNOLOGY

Continuous development of fiber processing has been carried out in an attempt to improve the quality of the final products. The flax fiber processing technologies are mainly 'borrowed' from the conventional system used generally for cotton fiber. For example, mercerization is one of the most commonly used preparation steps in the dyeing and finishing of cotton yarns and fabrics [99]. Improved luster, crease resistance and dye uptake can be achieved by mercerization with the caustic soda solution. Alternatively, liquid ammonia treatment can be used for quality improvement. Previous investigations have shown that these two treatments are particularly suitable for linen to improve its quality [43-44, 142, 153].

With the increase in environmental concerns, modification techniques through dry processing or physical means offer more advantages than traditional chemical wet processing. Typical textile fibers have large surface-to-volume ratios, so the surface structure of fibers greatly influences many properties of materials made from them. Additionally, the surface structure of individual fibers often significantly affects their processing behavior during manufacture of other materials. For these reasons,

surface modification techniques which can transform these materials into highly valuable finished products have become an important part of the industries. In recent years, many advances have been made in developing surface treatments to alter the chemical and physical properties of fiber surface without affecting bulk properties. Modern surface modification techniques include treatment by flame, corona, plasmas, photons, electron beams, ion beams, x-rays and ϒ rays.

Surface modification of cotton by low temperature plasma treatment shows promising prospects in improving fiber properties. Exposure of materials to suitable plasma can cause both chemical and physical changes in their surface layers but without interfering with the bulk properties simply because of the very low range of penetration. These changes can produce more reactive surfaces and affect the surface properties of the material while maintaining the desirable properties of the bulk material [97, 188].

On the other hand, fabric conformability and aesthetics are always the ultimate aims pursued by consumers and finishers. A new concept for making cotton fabric softer and smoother is by means of enzyme treatment. It is a kind of treatment using cellulases to decompose the fluff and fibrils on the cotton fabric surface. Through this action to remove the fluff and fibrils, the fabric can be made very soft and its drapeability can also be improved [49].

2.3.1 Low Temperature Plasma Treatment

2.3.1.1 Low temperature plasmas

Plasma is defined as the ionization state of a gas mixture consisting of ions, electrons and electrically neutral particles, in which the number of positive and negative charge carriers is the same. In other words, plasma, on the whole, is electrically neutral [198, 236-238]. The ionized gas system displays significantly different physical and chemical properties compared to its neutral condition. Theoretically, plasma is referred to a 'fourth state of matter' and is characterized in terms of the average electron temperature and the charge density within the system [48, 97, 128, 250].

The plasma can be divided into hot plasma and cold plasma (low temperature plasma). High temperature plasmas are at thermal equilibrium. In low temperature plasma, the fast moving electrons are at extremely high temperature but the other plasma species and substrates to be activated are at ambient temperatures. Although electron temperature rises over several tens thousand K, gas temperature remains at 100K [17, 133, 198, 257, 260-261]. The low temperature plasma is commonly used in material modification. It can be generated by gaseous electric discharge to provide a source of high energy electrons without excessive heating, and is highly reactive chemically [198, 260-261]. The substrates are therefore subjected to bombardment with energetic particles which impart both physical and chemical changes to the treated surfaces. Free electrons which receive increased energy from the imposed electric field generate new chemically-active species of atoms, ions and free radicals through collision with neutral gas molecules. In this way, highly energetic electrons can initiate chemical reactions in the discharge vessel [14, 137].

Gas specific alterations on a surface layer can be achieved by means of surface bombardment with ions, electrons and other high energy particles which knock fragments out of the surface of the polymer material and respectively vaporize it [198].

Depending on the gas pressure, two different forms of discharges are generated which are known as corona and glow discharges. Corona discharge is generated at gas pressures equal to or near to atmospheric pressure with an electromagnetic field at a voltage of higher than 15kV and frequency in the 20-40kHz range for most practical applications today. The glow discharge is generated at the gas pressure in the 0.1-10MPa range with an electromagnetic field at a lower voltage of 0.4-8.0kV and a very broad frequency range of 0-2.45GHz [197-198]. As a result of the possible introduction of different types of gases, specific chemical modifications of the textile surface may be obtained [152]. Corona discharges are suitable for flat products and continuous processing routes, while glow discharges are suitable for all kinds of textile products and their efficiency does not depend on the time elapsed between the treatment and further processing. Strictly speaking, both forms of discharges should be regarded as a source of 'low temperature plasma', but today most papers use the term 'plasma' for its brevity to describe the glow discharge only [151, 197-198]. In the present thesis, low temperature plasma will be referred as 'plasma' unless specified.

In the case of glow discharge, various plasmas with different ionization extents can be produced. The species produced carry high kinetic energy (up to 10eV) [198]. Although the kinetic energy is high, the temperature of the plasma is relatively low.

The activating particles in plasma will lose the energy once they interact with the polymer material. As a result, the penetration of plasma into the polymer material is rather shallow (100Å) and the interior of the material is only slightly affected. Thus plasma species carries high kinetic energy and bombards the polymer causing sputtering or etching effect on the surface. The bombardment alters the surface characteristics of the polymer material. [21, 136, 260-261, 273].

Two principal processes of material ablation that frequently occuring are the physical sputtering and chemical etching. Sputtering of materials by an inert gas such as argon is a typical example of the former case, which is essentially a momentum-exchange process. The energy of the impinging Ar^+ is transferred to the colliding atom and dislodges the atom from the crystalline structure, transferring its energy to a neighboring atom. This energy transfer process continues until one of the atoms is knocked out into the vapor phase. Chemical etching involves the chemical reaction of the impinging species with region of polymer surface which then enable smaller structural units to be dislodged, such as oxidation by oxygen plasma [276].

2.3.1.2 Generation of low temperature plasma

The low temperature plasma is electrically neutral and is generated by electrical discharge, high frequency electromagnetic oscillation or high-energy radiation. Electrical discharge is commonly used in industrial application. The simplest reactors may consist of opposed parallel plate electrodes in a chamber that can be maintained at low pressure, typically ranging from 0.01 to 1 Torr (1.33-133Pa) as shown in Figure 2.3 [80].

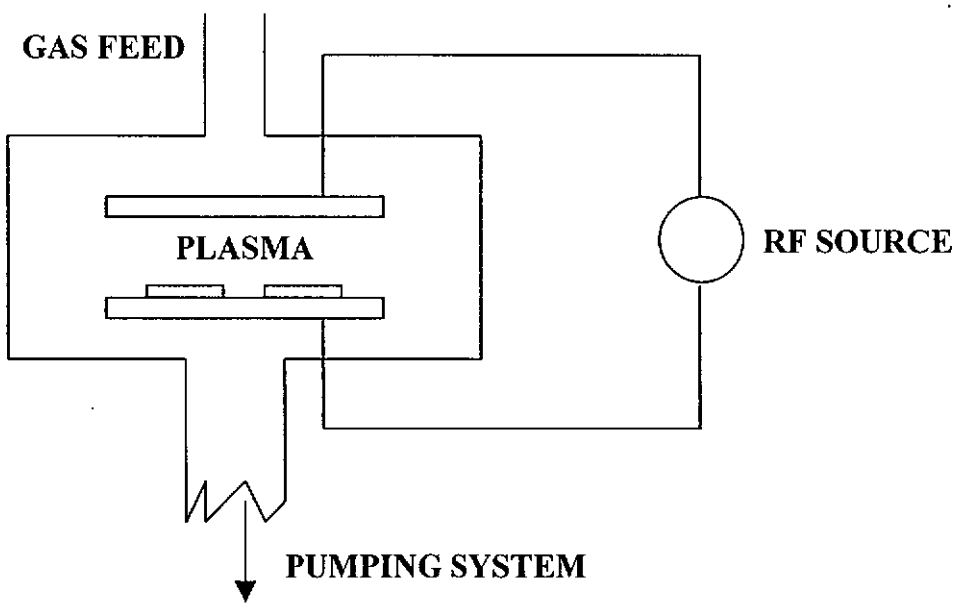

Figure 2.3: Diagram of a simple plasma reactor [80]

The system has the provision for continuously introducing a feed gas and a port for pumping. A source of radio frequency power coupled to the electrodes creates a plasma. Reactive radicals and ions are generated by this electrical discharge. Material on the electrode surface is exposed to reactive, neutral and charged species. Some of these species combine with the substrate to form volatile products that evaporate, thereby etching the substrate [80]. The low temperature plasma is usually excited and sustained electrically by direct current (DC), radio frequency (RF), or microwave (MW) power applied to a gas. The chemistry in a low temperature plasma is controlled mainly by electron temperature and charge density. Therefore, as long as identical conditions can be achieved, the type of discharge used to create plasma is of little importance. The choice of a specific method and equipment to produce discharge is determined by the requirements of flexibility, process uniformity, cost and process rates [97].

The low temperature plasma modifies the physical and chemical nature of fiber surface and surface morphology. Alterations of surface characteristics of material are mainly grouped into three categories namely surface wetting, surface chemical composition and surface morphology [272-273]. Plasma susceptibilities of certain materials have been correlated with their chemical structure, particularly the presence of bonds involving the electro-negative elements such as oxygen. By means of plasma treatment, gas-specific alterations of fiber surface layers can be obtained [55, 198, 277].

Modification of polymer surfaces by plasma treatment has been studied and known for some times. After low temperature plasma treatment, all polymers show a mass loss. The magnitude of loss is dependent on the gas type, gas flow rate, gas pressure, machine power, treatment time, fiber structure and chemical constitution [97, 188, 255, 275, 277]. Three types of plasma treatments may be defined which are governed by the nature of the gas or the vapor used. One is the surface modification under the influence of the glow discharge. It is mostly performed with non-polymerizing gases such as noble gases, nitrogen, oxygen, hydrogen, ammonia or water vapor. Polymer surfaces are modified through the processes such as oxidation, ablation and crosslinking. It should be recognized that the ablation supplies the gas phase with various chemical, some of which may be able to form deposits especially in the mixtures with non-reactive gases such as hydrogen or ammonia. The second is plasma polymerization which is the deposition of a thin and highly crosslinked polymer film on the material surface when subjected to the glow discharge by using organic, organosilicone or organometallic vapors. The deposition of these films is the main factor modifying the polymer surface in these cases. The third is the

plasma grafting after an activation of the surface by means of plasma treatment [188, 251, 277].

The above processes strongly depend on the nature of the gas or the vapor used in the glow discharge. Moreover, the flow rate during low temperature plasma treatment can affect the production of plasma species while the system pressure can affect the energy of the plasma species. If the pressure is high, the probability of collision between plasma species will be increased leading to the loss of energy of the species before interacting with the material. Furthermore, the intensity of plasma is a combined factor of pressure and discharge power. The breakdown energy necessary to produce plasma varies from one gas to another. Therefore, the initiating energy is not a constant and is primarily dependent on the nature of the gas. Normally, the higher the discharge power applied, the more kinetic energy the plasma species will carry, resulting in a strong intensity of plasma action [275].

The duration of treatment plays an important role in plasma treatment. In general, the longer the duration of treatment, the more severe the modification of the material surface, e.g. sputtering or etching. A longer duration will not only affect the material surface but also provide an opportunity for the plasma species to penetrate into the interior regions of the material. This may alter the morphology of polymer material. However, when the treatment duration is too long, this will adversely affect the material and therefore careful control of treatment duration is required [275]. Furthermore, the plasma susceptibility is directly related to the constitution of the corresponding fibers which will have different weight loss under similar plasma exposure [255, 277]. The estimation of the influence of operation parameters by

plasma etching has shown that the discharge power and treatment time are important factor in determining the results of textile modification [207].

2.3.1.3 Application of low temperature plasma treatment to cellulose materials

Low temperature plasma has been shown to be an effective means of modifying the surface properties of textiles such as wool and cotton [17, 21, 32, 96-97, 133, 136-137, 154, 188, 193, 195-198, 208-209, 231, 234, 244, 253, 255, 261, 274-275]. It has also proposed as an alternative scouring process of the cellulosic materials [93, 250].

The glow discharge treatment for fibers was first applied to cotton by Stone *et. al.* in 1962 [231], who found that glow discharge in the presence of air increased the water absorbency and strength of cotton fiber. Analysis showed a slight decrease in the wax content of the irradiated cotton fiber, and also the waxes were degraded by exposure to the plasma. Samples of irradiated cotton fiber felt rough and fibers were difficult to separate from each other.

Byrne *et. al.* in 1972 [32] attempted the glow discharge polymerization of various vinyl monomers including fluoro-compounds onto cotton and other fabrics, and were able to show interesting modifications of fiber properties such as improved water repellency of cotton.

Jung *et. al.* in 1977 [137] investigated the effect of argon cold plasma on water absorption of cotton. The rate of wetting increased until it reached twice that of the untreated cotton. Although the treated cotton was not visibly different from the

untreated cotton, x-ray photoelectron spectroscopy (XPS), infrared absorption spectroscopy (IR) and electron spin resonance (ESR) analyses revealed that its surface was oxidized. The same research group also investigated the effect of plasma treatment on the wicking characteristics and water absorption of cotton and cotton/polyester toweling [136].

In 1981, they investigated the effects of cold plasma of argon, nitrogen, air [17] and ammonia [260-261] in glow and after glow on the surface characteristics of cotton. The cotton treated with argon, nitrogen or air plasma was found to absorb water and oils at faster rates and possess a different feel as compared to the untreated cotton. Analyses by SEM, XPS, IR, chemiluminescense, ESR and other chemical methods indicated that the treatment might have led to the formation of carbonyl groups, α hydroxide groups and free radicals on the surface of cotton. On the other hand, the ammonia plasma treatment resulted in the introduction of nitrogen to the cotton, possibly due to the formation of amide structures. The ammonia-treated fabric exhibited a modest increase in conditioned wrinkle recovery and no changes in wet recovery. The possibility is that, like liquid ammonia treatment, ammonia plasma might cause changes in the crystalline lattice of the cellulose.

Wakida *et. al.* in 1989 [255] found that natural fibers, in particular cellulosic type, showed high levels of free radicals which were induced after plasma treatment with various gases as detected by ESR measurement.

Goto *et. al.* in 1992 [93] looked at the possibility of dewaxing grey cotton fabric by low temperature oxygen plasma treatment instead of the conventional wet scouring

process. They reported that the quality of scoured cotton produced by the glow discharge method was almost the same as those scoured by the conventional method. A practical batch type equipment was proposed with the capacity to process the cotton fabric in 160cm width.

Kubota *et. al.* in 1994 [154] modified the cotton fiber by means of low temperature plasma of air, oxygen and argon leading to decreased flexural rigidity and increased suppleness. Water absorption increased as well as the crease resistance, drying rate and degree of crystallinity. Values for equilibrium moisture regain, dyeability of reactive dye and direct dye decreased. Soil release increased after the air and oxygen plasma treatment. Tear strength retention of the treated cotton fabric was 73.8% in warp and 77% in weft direction.

Vladimirtseva *et. al.* in 1995 [250] proposed the application of low temperature plasma to the preparation processes of linen. The method allows for the preservation of fabric durability, natural coloring of the flax fibers and imparts higher hydrophilicity to the materials. Unbleached fabrics were exposed under the air plasma of glow discharge followed by washing in hot water. This technology is characterized by ecological friendliness, guarantees a high level of linen hydrophilicity and preserves the natural silver-grey colour of flax fabrics and their durability.

Hua *et. al.* in 1997 [126, 281] treated the pure cellulose samples with argon and oxygen RF plasma under various external plasma parameter conditions. It was found that plasma parameters such as power and pressure had a significant influence

on the plasma initiated surface. Argon plasma treatments initiate reactions mainly associated with the cleavage of C1-C2 linkages leading to the formation of C=O and O-CO-O groups, while oxygen plasma treatments are associated with more intense pyranosidic ring C-O-C bonds splitting mechanisms. This opens up practical ways for tailoring the surface characteristics of cellulosic substrates.

2.3.1.4 Advantages and disadvantages of low temperature plasma treatment

Plasma treatments have become important industrial processes in surface modification with the following advantages [39, 74, 151, 251]:

(1) Modification can be confined to the surface layer without modifying the bulk properties of the polymer. Typically, the depth of modification is several hundred angstroms [188, 273, 277].

(2) Excited species in gas plasma can modify the surfaces of all polymers, irrespective of their structure and chemical reactivity.

(3) Modification is fairly uniform over the whole surface.

(4) By selecting the appropriate gas, it is possible to choose the type of chemical modification for the polymer surface.

(5) Using gas plasma can avoid the problems encountered in wet chemical techniques such as residual solvent on the surface and swelling of the substrate.

(6) It may eliminate or reduce the water consumption and related costs such as those associated with water usage for treatments and subsequent washing-rinsing operations, water heating and effluent pollution.

(7) It may reduce the cost of chemicals and auxiliary products used.

(8) Overall preparation time will be reduced and a quick response to the market will be facilitated.

The disadvantages of the plasma processes are as follows [39]:

(1) Most plasma treatments have to be carried out in vacuum except corona discharge. This requirement increases the cost of operation.

(2) The processing parameters are highly system-dependent; the optimal parameters developed for one system usually cannot be adopted for another system.

(3) The scale-up of an experimental set-up to a large production reactor is not a simple process.

(4) The plasma process is extremely complex; it is difficult to achieve a good understanding of the interactions between the plasma and the surface necessary for a good control of the plasma parameters such as RF frequency, power level, gas flow rate, gas consumption, gas pressure, sample temperature and reactor geometry.

In summary, the application of low temperature plasma treatment to the textile industry can improve or replace several pre-treatment processes such as desizing, scouring, bleaching and mercerizing for cotton material. It also can be used to replace some chlorine-based wet treatments and improve dyeing processes of wool. Permanent properties may be added to the textile substrate such as flame-retardant and crease resistance. Improvement of the adhesion power for binding agents used in pigment dyestuffs may be etched as may increases in the adhesion forces for bonding or coating fabric. This include the increase of the binding capacities for non-textile materials with textiles, i.e., twisted tyre cords twists with rubber [120, 133, 151-152].

2.3.2 Enzyme Treatment

2.3.2.1 Enzymes

An enzyme can be defined as a soluble or colloidal organic catalyst produced by an animate object, plant, animal or microbe. Enzymes which are protein in nature are also considered as bio-catalysts [20, 205]. In general, catalysts participate in a chemical or biochemical reaction in such a manner that they remain unchanged at the end of the reaction. Enzyme action is specific and will only participate in very individual reactions of substrate. For example, the enzyme amylase degrades starch only whereas enzyme cellulase cannot degrade any compound other than cellulose. Thousands of enzymes have been isolated, purified and even crystallized, and a large number are being used to benefit human beings. The most common types of enzymes used by the textile industry are amylase, peroxidases, protease, cellulase, pectinases and lipases. All constituents of natural fibers such as cellulose, hemicellulose, pectin and protein are biodegradable with enzymes to a greater or lesser extent. Thus, they can be utilized in the textile world to bring about specific changes and modifications [20].

2.3.2.2 Enzymatic reaction of cellulase

Cellulase is capable of breaking the 1,4 β-glucosidic bonds of cellulose as shown in Figure 2.4 [19, 36, 114, 190, 205, 242]. Natural cellulases are secreted by various fungi and bacteria as complex mixtures of three major kinds namely endoglucanase (EG, EC 3.2.1.4), exocellobiohydrolase (CBH, EC 3.2.1.91) and beta glucosidases (EC 3.2.1.21). These natural mixtures can be described as "total crude" cellulases (TC) [49, 76].

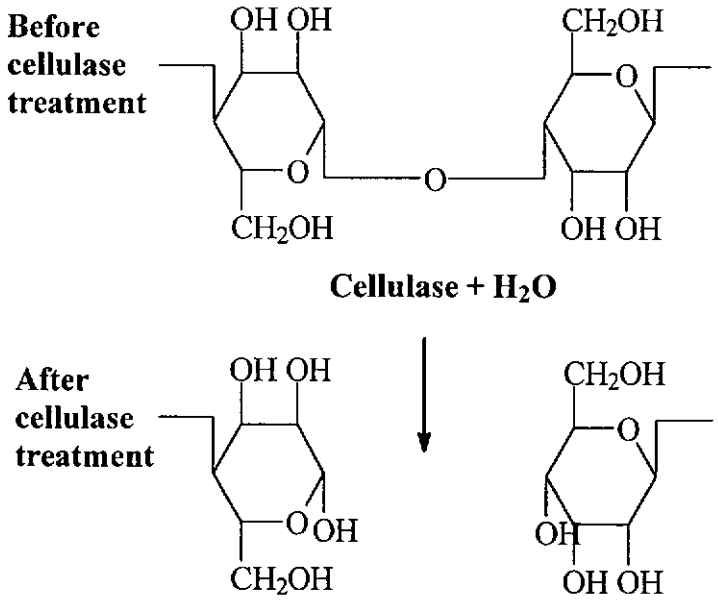

Figure 2.4: Simplified hydrolysis of a cellulose molecule by cellulase [189]

A general model for the action of different components of TCs is shown in Figure 2.5 [49]. First, EGs cause random hydrolytic chain scission at the most accessible points of cellulose chains, producing one new reducing end group and one new non-reducing group at each point of scission (this is often known simply as "endo" activity). Second, CBHs split cellobiose from the non-reducing ends of cellulose chains, leaving a new non-reducing end group that can be further attacked by CBH action; it therefore proceeds in a stepwise manner along cellulose chains (this is also known as exoglucanase activity or simply 'exo' activity). Thirdly, beta glucosidases hydrolyzes cellobiose to form glucose [36, 49, 76, 242].

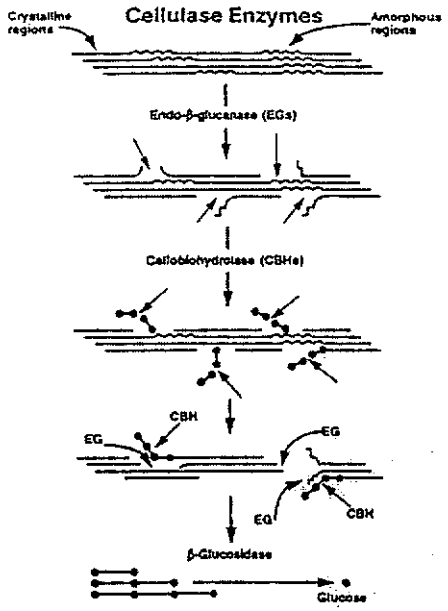

Figure 2.5: Enzymatic degradation of cellulose by cellulase [49]

Since the large molecular enzyme complex is difficult to penetrate into the interior structure of cellulose, therefore the enzymatic action can only take place preferentially on the surface where cleavage of cellulose chains occurs. Micro-fibrils such as the free standing fibers are broken down under the influence of biocatalytic degradation and the additional effects of mechanical agitation. In order to produce such mechanical agitation, it is essential that suitable processing machinery is used, e.g. drum, winch, jet, over-flow machines or similar equipment. Machines without sufficient mechanical washing action such as pad-roll, beam, jigger or open-width washing ranges limit the applicability of the technology [205].

The ability of an enzyme is highly dependent on its environment. For example, cellulases from different organisms and even the same organism may function differently under the same condition. Hence, it is necessary to obtain information about the function and performance of an enzyme under the desired conditions. The

most important factors that affect enzyme are pH, temperature activity, temperature stability, specific activity, substrate binding, product inhibition, substrate specificity and synergy with other components [49]. Like other weight loss treatments, there is an inevitable loss of strength of the fabric. If the process is not precisely controlled, it may induce severe damage to the fabric. Moreover, because the concept is rather new, trials must be made to find out the optimum working conditions.

2.3.2.3 Application of enzyme treatment to cellulose materials

Major applications of biotechnology in the textile industry include [101, 226]:

- improvement of fiber properties and plant varieties used in the production of textile fibers,
- improvement of the properties of animal fibers,
- novel fibers from bio-polymers and genetically modified micro-organisms,
- replacement of harsh and energy-demanding chemical textile processing by enzymes,
- environmentally friendly routes to textile auxiliaries such as dyestuffs,
- novel uses for enzymes in textile finishing,
- development of low energy enzyme based detergents,
- new diagnostic tools for the detection of adulteration and quality control of textiles,
- waste management.

This concept of bio-polishing was first developed in Japan regarding to cellulase treatment of woven fabric [270-271]. The term bio-polishing has been selected by Novo Nordisk to describe a novel finishing treatment for cellulosic fabric [189-190].

It is referred to the finishing of cellulosic materials with the aid of cellulases to achieve the finishing objectives such as elimination of surface hairiness in the pretreatment of fabrics for printing in order to produce sharp outlines; reduction of lint build-up on fabric surfaces thereby lowering the pilling tendency; removal of pills; achievement of a soft handle, luster, smoothness and good quality appearance; and the used-look for the denim fabric [205].

Bio-polishing upgrades the fabric quality so that the fabric continues to look and feel new even after extensive use. This a very important feature of the bio-polishing concept to explain why people throw away their T-shirts with unacceptable surface appearance due to fuzz and pills [19]. Apart from the desirable product characteristics, another main reason for this wide application of enzymes is the steady increase in environmental awareness by the consumers and legislators as the enzymes are environmentally friendly and do not impose environmental threats. Moreover, the substrate-specific reactions of enzymes offer the possibility of controlling the reaction in such a way that no undesirable side reactions take place [205].

Cellulase products are available for textile industry from at least 12 different sources [242]. For the enzyme to be most effective, reaction, pH and temperature must be optimized. In general, there are three major commercial classifications of cellulase enzymes based on optimal pH and temperature ranges. Acid, neutral and alkaline are the categories that are used for textile applications. Acid and neutral enzymes are currently the most popular enzymes used in garment and fabric applications. Alkaline cellulase is being incorporated into some home laundry detergent products

to aid in stain removal and to improve surfaces after multiple laundering [190, 242].

Acid cellulase exhibits the most activity within the pH range of 4.5-5.5 at a temperature of 45°C-55°C while neutral cellulase requires pH of 5.5-8.0 at 50°C-60°C. To obtain the best results, pH adjustments should be made using an appropriate buffering system that will compensate for any fluctuation such as residual alkalinity in the fabric. The hydrolysis of cellulase is not instantaneous. In addition to optimal pH and temperature, an incubation period is required. The length of this period is dependent on the substrate as well as the enzyme dosage. Heavier fabrics and lower enzyme concentrations require longer incubations. The incubation time may be reduced if the dosage is increased [190].

After incubation, the reaction is stopped by deactivating the enzyme. This may be accomplished by adjusting the pH to 10 or increasing the temperature to 75°C for 15 minutes. Either of these actions will distort the physical structure of the enzyme and render it useless for further activity. Cellulase enzymes are biodegradable and usually used at relatively low concentrations, therefore they do not contribute significantly to waste accumulations. These factors make enzymes a favorable alternative to conventional finishing chemical [189-190].

Advances in biotechnology have made a new range of enzymes available for the textile industry. In the last decade, intensive development and research have been carried out on cellulosic fibers such as cotton, linen, ramie and regenerated cellulose [11, 29, 36-38, 45-46, 54, 71, 109, 113, 148, 184, 205, 226, 242, 245]. As a result, many enzyme based processes and products came out to the market such as aged

look denim garments and pills-free cotton fabrics. The cellulase treatment made the 'stonewash' effect on denim fabric a reality, eliminating the use of pumice stones and associated problems such as irregularly lightened areas by excessive mechanical abrasion on the fabric surface [105, 146-147, 182-183, 241-243].

In order to enhance the reactivity of cellulose due to the catalytic reaction, physical and chemical pretreatments were employed [27-28, 43, 52, 82, 144, 172, 179, 186, 258, 279]. One example of chemical pretreatment is mercerization which used for cotton and flax yarn to reduce the fiber crystallinity [27-28, 43, 172, 179, 186] and increases accessibility and yarn strength while tension was applied during the treatment [43]. The relationships between low temperature plasma and enzyme treatment as well as their effect on the mechanical and dyeing properties of wool and cotton fabrics were studied [279]. Besides, the cellulases can be used for the textile recycling to remove the cellulosic fiber constituent from the textile waste [184].

Tyndall *et. al.* in 1990 [241-242] reported a method of improving softness and surface appearance of cotton fabrics and garments by cellulase enzyme treatment. Comparison was made with the use of cellulase alone, cellulase in combination with stones and the regular stone washing.

Buchle-Diller *et. al.* in 1994 [29] investigated the enzymatic hydrolysis of cotton, linen, ramie and viscose rayon fabrics. X-ray crystallinity and moisture sorption of the samples did not change after the treatment, indicating that the mechanism of endwise attack of the cellulase occurred at the accessible cellulose chain on the crystallite surfaces. Pores of the amorphous regions are often too narrow for the

large enzyme molecule to effectively penetrate. As a result, the ratio of crystalline to less ordered regions does not change upon enzymatic degradation. Additionally, mechanical tests demonstrated the increase of stretchability and decrease of stiffness of the fabrics and the mobility of yarns within the samples. Moreover, the effect of enzymatic hydrolysis, acid hydrolysis on the slack and tension mercerized cotton yarn was investigated [28]. It appeared that higher accessibility and decreased crystallinity of the cellulose structure after slack mercerization were the dominating factors for the acceleration of enzymatic hydrolysis.

Koo *et. al.* in 1994 [148, 254] investigated the enzymatic hydrolysis by cellulase enzyme in the presence of dyes on cotton fabrics. The results showed that both direct and reactive dyes on the fabric apparently inhibited the enzyme reaction whereas vat dyes did not. The enzyme was more reactive for the mercerized cotton than for the non-mercerized cotton. The enzyme treatment significantly reduced both tear strength and dye take-up of the fabrics. Moreover, both anionic and cationic surfactants apparently inhibited the cellulase reaction whereas nonionic surfactants did not inhibit the cellulase reaction. These actions have been attributed to the electrostatic interactions between the charged inhibitory compounds and the cellulase enzyme in a treatment solution and on the cotton fabric.

Chikkodi *et. al.* in 1995 [45-46] studied the effects of bio-finishing on cotton/wool blended fabrics by treating it with both cellulase and protease enzymes using two different concentrations. The result showed that the fabric strength, weight and abrasion resistance were reduced whereas the resistance to wrinkling, pilling and shrinkage resistance were increased.

Cavaco-Paulo *et. al.* in 1996 [36] and 1998 [37], implicated that fabric processing history, fabric construction, the level of applied mechanical agitation, the choice of enzyme composition and enzyme concentration were important to determine the consistency and quality of the enzymatic treatment on cotton fabric.

Heikinheimo *et. al.* in 1998 [113] evaluated the effects of the individual cellulase enzyme on the properties of different types of cotton fabrics. The properties of enzyme treated fabrics depended not only on the type and concentration of enzyme used, but also on the structure of fabric being treated.

Hartzell *et. al.* [109-110] and Li *et. al.* [103, 159] in 1998 reported the use of enzymatic scouring to improve cotton fabric wettability. A combination of pectinase and cellulase significantly improved water wetting and retention properties which were similar to those of commercially scoured cotton fabrics. On the other hand, cellulase treatments on the scoured fabrics further enhanced water wettability and whiteness of fabric, however, fabric weight, thickness and strength were significantly reduced.

The effect of cellulase enzymatic pretreatment on the efficient alkaline scouring of cotton fabrics was studied by Csiszar *et. al.* in 1998 [53-54]. The cellulase enzymatic complex made the residual seed-coat fragments more accessible to scouring chemicals. The effect of enzymatic treatment on the removal of seed-coat fragment from desized cotton fabrics was also significant. The tiny fibers that attach the seed-coat fragments to the fabric were hydrolyzed by the enzyme, facilitating the removal of these impurities from the fabric surface. Sawada *et. al.* in 1998 [216-217] also

reported the scouring abilities of a pectinase enzyme system. The quality of scouring by this method was better than that of the conventional alkaline scouring system.

The common cellulosic fibers used in textiles are cotton, flax, ramie and the regenerated fibers derived from pulp such as Tencel and rayon are good candidates for cellulase treatment. The applications of enzyme treatment to bast fibers includes fiber extraction and retting of jute, flax, hemp and mesta fibers, degumming of ramie fiber, fiber pre-treatment in the batching stage in industry, desizing and enzyme bleaching [9-10, 16, 20, 31, 101, 115-116, 222-224, 226-227, 248].

2.3.2.4 Advantages and disadvantages of enzyme treatment

Enzyme treatments have become important industrial processes with the following advantages:

(1) The processing is fairly environmentally friendly with minimal usage of chemicals.

(2) The fabric becomes softer to touch and the improvements are long-lasting.

(3) More uniform stone washing effects are achieved with a shorter treatment time and no addition of pumice stones to the washing machine required.

The disadvantages of the enzyme processes are as follows:

(1) The treatment will reduce the fabric weight and strength.

(2) The processing parameters such as pH and temperature are required to be carefully controlled.

2.4 CHARACTERIZATION TECHNIQUES

It has been shown in Section 2.3 that both low temperature plasma and enzyme treatment cause the modification of fiber properties. Characterization of the modified linen should be carried out to determine the effects of modification. The effects of surface modification on the functional properties of polymeric materials are shown in Figure 2.6.

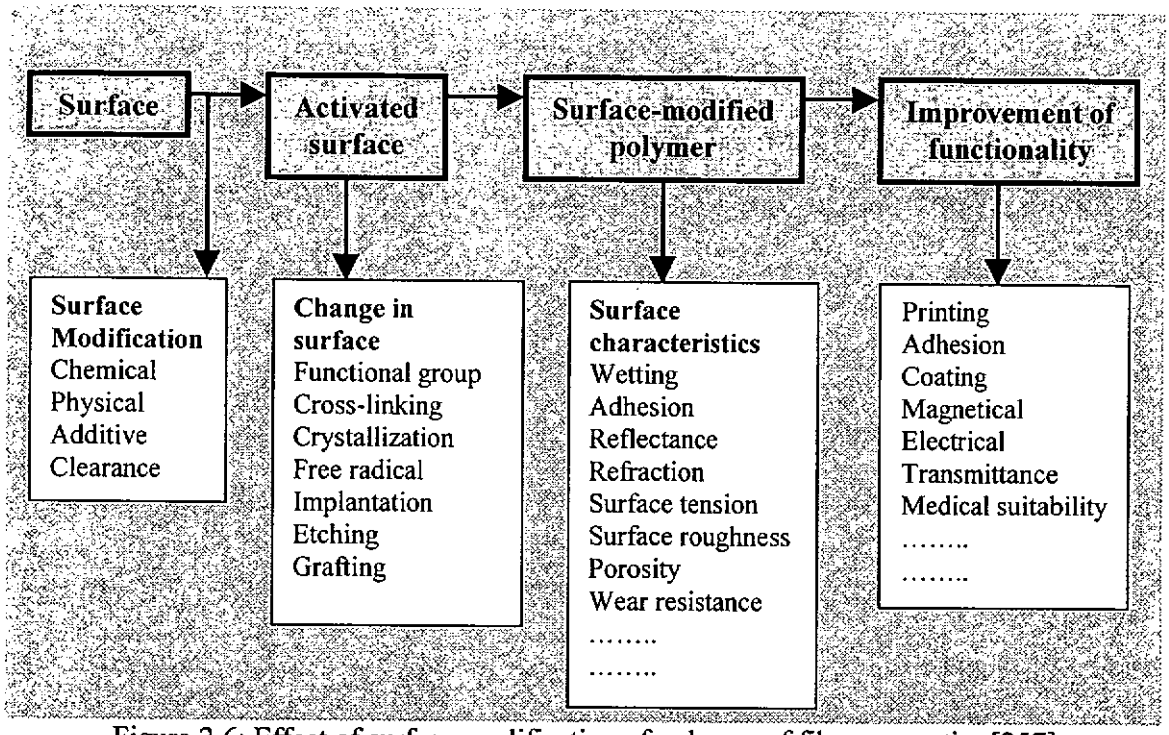

Figure 2.6: Effect of surface modification of polymer of fiber properties [257]

There are many techniques to evaluate the fiber characteristics with regard to fiber modifications. Therefore, it is necessary to select the appropriate techniques complying with the purpose to detect the changes brought about by the modifications. The experimental work may cover different aspects such as bulk structure and properties, surface morphology and properties, related mechanical properties and dyeing properties as shown in Table 2.2.

Table 2.2: Characterization techniques used to examine the effect of modifications on fiber properties

Bulk Structure and Properties	**Surface Morphology and Properties**	**Other Related Fabric and Dyeing Properties**
Cuprammonium fluidity	XPS	Fabric strength
X-ray crystallinity	SEM	Fabric bending properties
Moisture regain	ESEM	Wrinkle recovery
Fabric weight loss	AFM	Dyeing properties
	Fabric whiteness	Color fastness
	Fabric water uptake	

2.4.1 Changes in Bulk Structure and Properties

The flax fiber bulk structure and properties can be examined by the measurements of cuprammonium fluidity, x-ray crystallinity, moisture regain and fabric weight loss. The x-ray crystallinity, calculated based on the ratio of the amorphous and crystalline region of the cellulosic fiber [27, 83, 221], was used to examine the degree of modification on the fiber bulk structure. Meanwhile, the degree of polymerization (DP) can indicate the degree of fiber damage caused by modification treatment as damaged fibers will have a lower DP. The DP is indirectly estimated from the viscosity of a liquid in which a predetermined amount of fibers has been dissolved [247] according to a standardized method [25].

Moisture regain has often been utilized to evaluate the structural change of the fiber [81, 177]. Moisture exists in both amorphous and surface crystalline regions of the fiber. The reduction of fiber accessible or less ordered regions after the modification can be reflected by the value of moisture regain [12]. The fabric weight loss is a key indication of the severity of the applied treatment.

2.4.2 Changes in Surface Morphology and Properties

In general, the structure and morphology of the topmost surface layers (several nanometers thick) are different from those of the bulk polymer. Therefore, comprehensive surface analysis is needed to correlate the surface structures. Advanced analytical techniques can be used to characterize the fiber surface morphology and properties. Changes brought about on the fiber surface can be studied by the X-ray Photoelectron Spectroscopy (XPS) analysis, conventional Scanning Electron Microscopy (SEM), Environmental Scanning Electron Microscopy (ESEM) and Atomic Force Microscopy (AFM). Infrared Spectroscopy (IR), Electron Spin Resonance (ESR) and Chemiluminescence (CL) can also be used to characterize the changes in surface characteristics of fibers [17, 137]. Moreover, measurement of fabric whiteness [1] and fabric water uptake can be used to determine the surface properties of the modified linen.

X-ray photoelectron spectroscopy (XPS) can give information regarding to both the location and oxidation state of atoms [17, 93, 137, 143, 154, 209, 215]. This technique yields qualitatively information concerning the chemical composition (elemental analysis), chemical state (bonding and oxidation) and location of atom types within the sample. The technique involves measuring the kinetic energy E_k of the emitted photoelectron and from this calculating the electron binding energy E_B. The value of the electron binding energy enables the emitting atoms and oxidation states to be identified and ascertained.

Scanning electron microscopy (SEM) is a powerful tool to observe the fiber surface morphology. The SEM micrographs are produced by collecting the secondary

electrons emitted by the sample due to the bombardment of the electron beam. The collected secondary electrons yield the production of the micrograph that provides surface information. Particularly for polymers with low atomic numbers, metallic coatings are normally applied to eliminate charging effects of the sample [160].

Environmental Scanning Electron Microscope (ESEM) was developed to overcome some of the disadvantages of the regular SEM instrument [232]. The development of ESEM has satisfied the long-time desire of researchers to view specimens and processes in their natural state. Samples in ESEM no longer have to be observed at ultra-high vacuum. ESEM permits a higher resolution of sample image at relatively high pressures than the conventional SEM. This relatively new modification of SEM allows materials to be examined in the presence of gases or liquids, and whose specimens do not require conductive coatings [33, 50, 232]. The development of the machine itself has been published in a series of papers [56-58, 61-63, 65-66].

Apart from textiles, research by ESEM has been made on other areas including the study of fresh and living plant materials, wetting and drying of papers, microstructure in ceramics and composites, and the corrosion studies of stainless steel piping [24, 67, 82, 225]. In textile research, many of the initial developments of ESEM have been carried out mainly on wool [57, 59-60]. Besides, it has been used for studying the time series images of textile absorption and structure change under wetting and heating condition [232]. Methods have also been developed for observing the transverse swelling of cellulosic fibers [134].

The in-situ examination of material surfaces is not possible when using the conventional SEM since the conductive coating and high vacuum environment are essential. Moreover, ESEM is a powerful tool for observing the structural change in textile materials under various treatment conditions such that 'on-going' examination (time series images) of treatment effect is possible to carry out.

A new microscopic method, Atomic Force Microscopy (AFM) has been used to study the surfaces of different carbon fibers and compared the results with those from SEM [161, 228]. Imaging surface features ranging from macroscopic scale (hundred of microns scale) down to angstroms by these techniques look very attractive. It has been shown that AFM gives a more direct approach to microtopography.

AFM is based on the principle that intermolecular repulsive force or attractive force between the scanning tips and the fiber surface gives a more direct surface visualization. Better resolution of surface features by AFM is undoubted [161]. It has been used for imaging the surface of wool scales to give a complementary views of surface features [192]. At present, AFM has been widely used to study ceramic and metal surfaces, little attention has been given to textile fibers, especially for quantifying the micropores created by the low temperature plasma etching.

Modification of fabric wetting properties is expected as a result of the alteration of fiber surface and changes in surface chemical groups brought about by the surface modifications [17, 54, 93, 109, 136-137, 154, 159, 216, 231, 250]. Vertical wicking methods have been used extensively for determination of water uptake of textile

materials [18, 69, 73, 86, 104, 130, 145, 203]. During vertical wicking, there are several factors which affect liquid flow. Wicking in a vertical capillary will reach to a ceiling due to gravity. To minimize the gravity effect on the vertical wicking measurement, Miller *et. al.* [165] has developed and proposed a set-up where the liquid path is downward. It is also useful to determine the effect of surface modification treatments on fabric water uptake properties generally.

2.4.3 Changes in Other Related Fabric Properties

The surface and bulk properties of fiber play an important role on the fabric mechanical properties. The tensile strength, bending properties and wrinkle recovery are often measured by conventional test methods [3, 13] as an indication of the changes occurring [29].

2.4.4 Changes in Dyeing Properties

Since most of the textile goods are dyed, it is important to study their interaction with dyes especially after treatments. In a previous study, two direct dyes with different molecular size and shape were used to illustrate the changes in dyeing properties of treated materials [44, 155]. CI Direct Red 81 is a dye of a low molecular weight with a faster rate of diffusion while the other is CI Direct Green 26 with a non-linear shape and slower rate of diffusion. Using projections from molecular models, it was assumed that the area occupied by a molecule of CI Direct Red 81 was $30nm^2$ while the CI Direct Green 26 was $67.5nm^2$ [155]. Dyeing behavior of the linen includes the exhaustion curve, dyeing rate (half time of dyeing) and final exhaustion at the equilibrium of dyeing [1], along with the colorfastness to washing of dyed linen can be evaluated [2, 5-6, 249].

All the above measurements were carried out under the standard condition (65% RH and 21°C). All the samples included both untreated and treated were conditioned for 24 hours before characterization. The paired comparison *t*-test was used to determine whether any statistical significant difference occurred with a confidence limit of 95%.

2.5 CONCLUSION

Flax fibers have unique molecular and morphological structures. Although all cellulosic fibers are of identical chemical composition, there are some major differences in the fine structure and morphology of these fibers which will largely determine the course of modification. A flax fiber has higher crystallinity and the pitch of the spiral structure is less than cotton. Furthermore, spiral reversal and convolutions only occur in cotton. Significant differences in their pore structures and crystallite sizes have also been found. In contrast to cotton which consists only of a single cell, linen is made up of a multiple cellular system. Multi-cellular fiber contains natural gums and resins that keep the entire cells together.

Attempts have been tried at modify the properties of linen which aim to simplify the preparation and finishing processes. In order to minimize the chemical waste and associated disposal problem, modification of fibers through dry or environmentally friendly processing is essential if we are replace the harsh and energy-demanding chemical processes. Previous studies have been concentrated on cotton. From the review of flax fiber processing and the modification treatment, only a few attempts have been reported on the use of low temperature plasma and enzymatic treatment.

The major drawbacks of the commercialization of enzymatic hydrolysis by cellulase are the relatively low reaction rates and the high cost of the enzyme [258]. Low temperature plasma treated fabric appears to cause alteration of surface morphology, chemical composition and surface wetting properties while the mercerized fabric appears to have the higher accessibility and decreased crystallinity of the cellulose structure, which are the dominating factors for the acceleration of enzymatic hydrolysis [46]. Hence, these two processes may be promising candidates for the pretreatment of enzymatic reaction.

The recent developments in the advanced characterization techniques have provided many powerful tools such as XPS, ESEM and AFM. However, it was also found that main applications to date have been limited to wool owing to its popularity and special surface features. There has been a gap in research where such applications of these advanced techniques may help to determine effectively the effects of fiber modification on the surface properties of flax fiber.

Therefore, the major objectives of the present thesis are to study the effects of low temperature plasma and enzyme treatment, as well as their possible synergy, in order to modify the structure and properties of linen. With the recent development of analytical instruments and the above mentioned characterization techniques, the effects brought about by the applied treatments will be investigated systematically.

CHAPTER 3

LOW TEMPERATURE PLASMA TREATMENT OF LINEN

3.1 INTRODUCTION

Low temperature plasma treatment has been used as an effective means of modifying the surface properties of natural textile fibers such as wool and cotton [17, 32, 96-97, 136-137, 154, 188, 198, 209, 231, 255, 260-261]. It was also proposed for the scouring process of cellulosic materials [93, 250]. Exposure to a suitable plasma can produce a more reactive surface and thus affect the surface properties of the material while maintaining the desirable properties of the bulk material [97, 188]. Two principal processes of material ablation frequently occur during the plasma surface modification are physical sputtering and chemical etching. Sputtering of materials by an inert gas, e.g. argon, is a typical example of the former case, while the latter involves the chemical reaction of the impinging species with the dislodging elements such as oxidation by oxygen [276].

By means of plasma treatment, gas-specific alterations of fiber surface layer can be obtained [198, 277]. Plasma susceptibilities of certain materials have been correlated with their chemical structure, particularly the presence of bonds with electro-negative elements such as oxygen. The effect is dependent on the machine power, gas type, gas pressure, treatment time and fiber structure. Alterations of surface characteristics of material by low temperature plasma are mainly due to the prominent surface property discrimination caused by ion bombardment. The evidence of the alterations

has been grouped into three categories namely surface wetting, surface chemical composition and surface morphology [272]. These changes may lead to desirable enhancement in dyeability, color shade, handle and water take up.

Among the cellulosic fibers, flax does not have the versatility of cotton. Flax has a compact structure and a high cellulose crystallinity. It is more expensive partly due to the difficulties of textile processing. Linen fabric made from flax tends to have harsh handle. Numerous attempts have been tried to improve fiber properties, processing performances and final product. The current practices of wet spinning and finishing have disadvantages such as high energy cost, requirement of special spinning machine, waste water disposal and environmental pollution. It is highly desirable to modify the fibers through the dry processing such as low temperature plasma treatment. In the past, little information has been reported in the literature on such modification although the plasma treatment has already been applied to the natural fibers such as cotton and wool. This chapter reports the results of the recent investigation on low temperature plasma treatment of linen fabrics.

3.2 EXPERIMENTAL DETAILS

3.2.1 Sample Preparation

Scoured and semi-bleached linen woven fabric used in this experiment was supplied by a fabric manufacturer in China. Fabric weight was 154g/m^2 with a sett 21/20 per cm (54/50 per inch) and yarn count 118tex/118tex (14lea/14lea).

A plasma Polymerization System SPP-001 (Showa Co. Ltd., Japan) with a radio frequency of 13.56Mhz was used for this study. The fabric samples (20cm x 20cm)

were placed between the pair of water-cooled electrodes and exposed to oxygen or argon plasma at a pressure of 15Pa for various exposure times of 2.5, 5, 10, 20, 40 and 60 minutes respectively. The treated fabric sample was removed from the chamber and then conditioned under the standard condition (65% RH and 21°C) for 24 hours before characterization. The sample used for x-ray photoelectron spectroscopy (XPS) analysis was stored in a sealed storage bag and then tested within 4 hours after the plasma treatment.

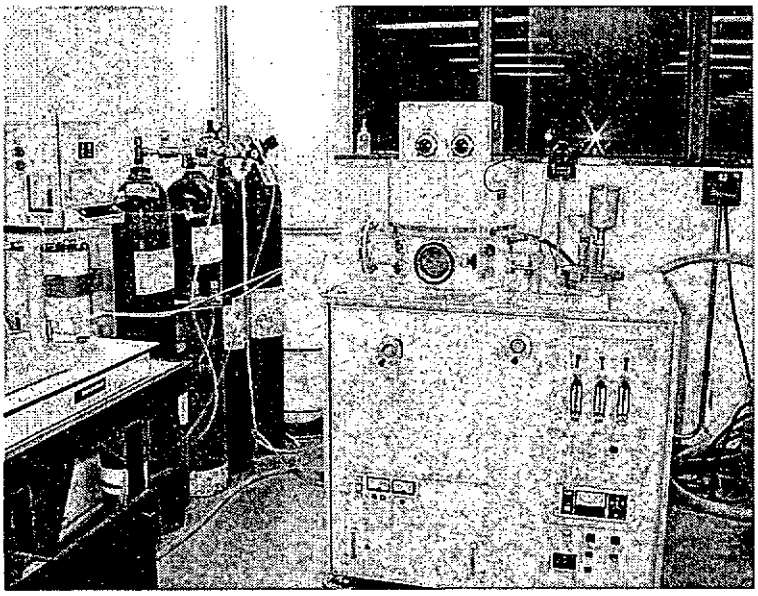

Figure 3.1: Plasma Polymerization System

Theoretically, plasma is characterized in terms of the average electron temperature and the charge density within the system [48, 97, 128]. Plasma diagnostic often used to obtain the information about the state of the plasma by means of experimental examination of the physical processes occurring in it. Appropriate and reliable diagnostic tools are therefore necessary to provide an understanding of the plasmas and the actual phenomena taking place, which in turn will enable the control of the process. The diagnostic techniques can be classified into ex-situ and in-situ techniques. The most used techniques for plasma diagnostic are mass spectrometry,

electric probes and optical methods [80, 97]. Due to the unavailability of the measuring equipment and the limitation of the reaction chamber as well as the time constraint, the measurement of the plasma density and electron temperature is not possible in the present thesis. However, fabric surface temperature under plasma treatment has been measured and will be discussed.

Oxidation is known to cause evolution of heat during the plasma treatment and lead to thermal degradation [277]. Therefore, a preliminary study was carried out to determine the appropriate level of power and exposure time in order to avoid excessive heating of fibers. Thermax irreversible temperature indicators were attached to the fabric samples prior to the plasma treatment. During the treatment, when the fabric surface temperature was above the indicating point, the indicator became darker. Triplicate readings were obtained for each condition and the mean values were recorded.

Figure 3.2 shows the temperature change of the fabric surface during the plasma treatment with three levels of power and two gases. For both gases, oxygen and argon, higher temperatures were recorded when using higher levels of discharge power. The fabric surface temperature increased with time until reaching a stable level and remained almost constant afterwards. In addition, the oxygen plasma was associated with a slightly higher temperature than the argon plasma. Intensive heating of the material took place when using 300W discharge power for both types of gas, and the temperature was quite close to the onset of thermal degradation temperature of cellulose materials [111]. In order to minimize the effect of over-

heating, the discharge powers of 100W and 200W were selected for the rest of the experiments.

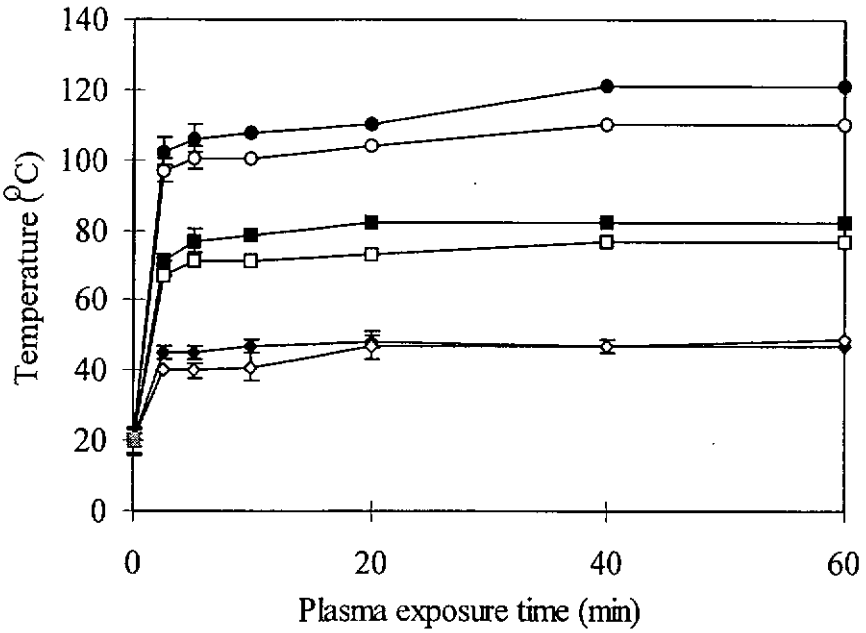

Figure 3.2: Fabric surface temperature measured by Thermax irreversible temperature indicator (▣) Untreated sample, (♦) Oxygen plasma 100W, (◊) Argon plasma 100W, (■) Oxygen plasma 200W, (□) Argon plasma 200W, (●) Oxygen plasma 300W, (○) Argon plasma 300W.

3.2.2 Material Characterization Procedures

3.2.2.1 Bulk structure and properties

The determination of cuprammonium fluidity of linen was carried out according to BS3090 [25] and the average of three measurements was reported for each sample. X-ray crystallinity was measured by the Philips PW3710 diffractometer using CuK_α radiation at an operating voltage of 40kV and current of 35mA from angles 5° to 30°. Pellets were prepared from 0.25g ground fibers [27] and the crystallinity ratio was calculated [221] according to the equation:

$$Cr.R. = 1 - I_1/I_2,$$

where I_1 is the minimum intensity of 2θ between 18° and 19°,

I_2 is the maximum intensity of crystalline peak at 2θ between 22° and 23°.

Moisture regain of the fabric sample was determined according to ASTM D2654-89a [12] and twelve specimens were measured for each type of sample. The fabric weight loss was determined based on the conditioned weight at 65% RH and 21°C before and after the plasma treatment, and the average of twelve readings was taken. Fabric strength was measured by an Instron tensile tester model 4466 according to ASTM D5035-95 [13] under the standard testing atmospheric condition with the cross-head speed of 304mm/minute. The width of sample was 5.08cm (2 inch) and the gauge length was 7.62cm (3 inch), and the results obtained were the average values of ten specimen readings.

3.2.2.2 Surface morphology and properties

Surface chemical composition analysis was conducted by the PHI 5600 XPS System (Perkin-Elmer) with an AlKα source at 14kV and 25mA. The residual pressure in the chamber was approximately 3 x 10^{-8}Pa. The kinetic energy E_k of the emitted photoelectron was measured and the electron binding energy E_B was calculated using the following relationship:

$$E_B = h_v - E_k$$

where h_v is the photon energy.

The derived value of the electron binding energy enables the emitting atoms to be identified so that the oxidation state can be ascertained. In addition, the spectral line intensities allow the relative abundance of species on the surface to be determined [143]. Surface charge build-up was corrected by considering the C_{1s} peak at 285eV. The relative peak areas of the C_{1s} spectra were determined by the wave form separation.

Scanning electron microscopy (SEM) examination was carried out on the spots of gold coated fabric surfaces randomly selected from different areas of the untreated and treated fabrics using the Lecia Cambridge Stereoscan 440 at 10kV. Change of fabric whiteness after the plasma treatment was quantified by CIE Whiteness index. Measurement of fabric whiteness using an Elrepho 2000 reflectance spectrophotometer (DataColor International) according to AATCC Test Method 153-1985 [1]. The results reported were the average values of three readings.

Fabric water uptake, the ability of a fabric to absorb water through a wicking or capillary action, was measured according to DIN 53924 [73] with a specimen size of 200mm x 25mm. Depth of fabric immersion in the reservoir was 20mm and the test duration was 5 minutes. The results obtained were the average of ten readings. Fabric water uptake was calculated by the following equation:

$$W = M \times H / 100$$

where H is the height (mm) of distilled water wicked above the reservoir level,

M is the weight of distilled water wicked above the reservoir level relative to the conditioned weight of H length of the fabric strip.

3.2.2.3 Other related properties

Fabric bending properties were measured by a KES-FB2 instrument from Kato Tech. Co. Ltd. The sensitivity was selected at 5x1 to provide the full-scale reading of 50gfcm. Twelve samples were measured and the sample width was 10cm. The bending rigidity was calculated from the slope between the curvature K = $0.5cm^{-1}$ and $1.5cm^{-1}$, and the bending hysteresis was calculated at the curvature K = $0.5cm^{-1}$.

Wrinkle recovery was measured according to AATCC66 (under 500g for 5 minutes) with a specimen size of 1.5cm x 4cm [3]. The values reported were the average results in the warp and weft directions. Results were expressed as the average wrinkle recovery percentage of twelve samples.

All the above measurements were carried out under standard conditions. The paired comparison *t*-test was used to determine whether any statistical significant difference occurred with a confidence limit of 95%.

3.3 RESULTS AND DISCUSSIONS

3.3.1 Bulk Structure and Properties

3.3.1.1 Fluidity and x-ray crystallinity

The experimental results of the cuprammonium fluidity test are shown in Table 3.1 and suggest a slight reduction of the degree of polymerization of the cellulose chain with prolonged exposure of plasma as reflected by higher fluidity values. However, based on the paired comparison *t*-test of the untreated sample, these differences are not significant statistically. When comparing the control with all the plasma treated sample, no significant change in crystallinity ratio can be found from all the cases under investigation. This indicates that the plasma ablation may attack only the ends of accessible chains on the crystallite surface and amorphous regions, and does not cause any significant change in the fiber bulk crystallinity.

Table 3.1: Cuprammonium fluidity, x-ray crystallinity and moisture regain of oxygen and argon plasma treated samples

		Plasma exposure time, min.					
	Untreated	2.5	5	10	20	40	60
Oxygen Plasma, 100W.							
Cuprammonium fluidity	17.7	18.6	-	-	-	-	18.4
CV%	2.7	0.6					0.5
X-ray crystallinity	0.81	0.82	-	-	-	-	0.81
CV%	0.9	1.1					0.3
Moisture regain, %.	7.7	7.4	7.5	7.4	7.5	7.4	7.3
CV%	3.3	4.0	2.5	2.2	2.6	2.6	4.4
Oxygen Plasma, 200W.							
Cuprammonium fluidity		16.7	-	-	-	-	17.9
CV%		1.6					0.8
X-ray crystallinity		0.80	-	-	-	-	0.81
CV%		1.3					0.7
Moisture regain, %.		7.4	7.4	7.4	7.4	7.3	7.4
CV%		4.5	2.3	3.5	2.8	3.8	2.1
Argon Plasma, 100W.							
Cuprammonium fluidity		16.9	-	-	-	-	17.8
CV%		1.1					1.2
X-ray crystallinity		0.81	-	-	-	-	0.81
CV%		1.5					1.2
Moisture regain, %.		7.3	7.5	7.4	7.3	7.5	7.4
CV%		2.4	1.6	2.5	2.6	2.6	2.5
Argon Plasma, 200W.							
Cuprammonium fluidity		18.1	-	-	-	-	19.3
CV%		0.6					0.5
X-ray crystallinity		0.80	-	-	-	-	0.82
CV%		1.4					0.1
Moisture regain, %.		7.5	7.5	7.4	7.3	7.5	7.4
CV%		2.8	3.8	3.0	3.7	2.6	3.3

3.3.1.2 Moisture regain

Table 3.1 shows the moisture regain of fabric samples measured before and after the plasma treatment. Only a slight reduction is found after 2.5 minutes of plasma exposure for all cases and no further reduction can be observed even when the exposure time is prolonged to 60 minutes. All the treated samples exhibit a similar reduction of moisture regain when subjected to different types of gas with various powers and exposure times. Owing to the very little changes occurring in x-ray crystallinity and degree of polymerization, a small decrease in moisture regain may

reflect a reduction in the accessible or the less ordered regions of the fiber. This may be due to the removal of amorphous regions on the fiber surface caused by the plasma etching within the limited depth of penetration.

3.3.1.3 Fabric weight loss

Figure 3.3 shows the plot of fabric weight loss against exposure time at two levels of discharge power. In the case of oxygen plasma, the weight loss increases with both the discharge power and treatment time. When doubling the power from 100W to 200W, nearly twice the weight loss is obtained which is also linearly correlated with the exposure time. The highest weight loss occurs with 200W oxygen plasma followed by the 100W oxygen plasma, and the 200W and 100W argon plasma samples for 60 minutes of exposure. In the case of argon plasma, it seems that there is no significant difference between the weight loss rates at 100W and 200W. The oxygen plasma treatment brings about a much higher loss (10.3%) than the argon plasma (1.7%) under the same conditions (200W, 60 minutes).

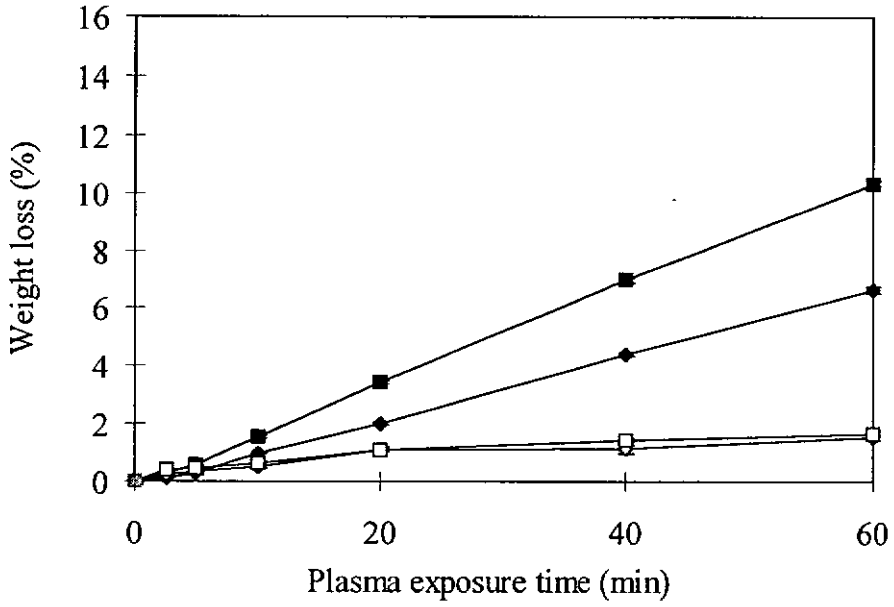

Figure 3.3: Percentage of fabric weight loss after oxygen and argon plasma treatment (▩) Untreated sample, (♦) Oxygen plasma 100W, (◊) Argon plasma 100W, (■) Oxygen plasma 200W, (□) Argon plasma 200W.

3.3.1.4 Fabric strength

Figure 3.4 shows the plot of fabric strength against exposure time. In the first 10 minutes, the fabric strength increases slightly and then decreases with the exposure time. This initial increase of strength may be due to the effects caused by the plasma etching on the fiber surface such as roughening of fiber, thereby increasing the inter-fiber friction. For the oxygen plasma, a significant reduction is found after 20 minutes of exposure and the reduction is more severe at 200W discharge power. Fabric strength of the argon plasma treated samples change only slightly even after a prolonged exposure for 60 minutes.

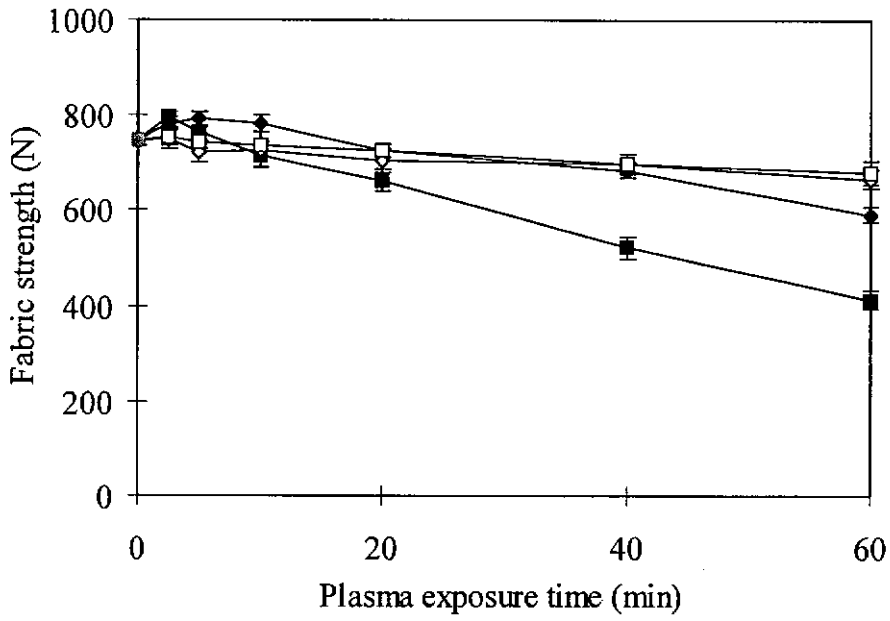

Figure 3.4: Fabric strength of samples after oxygen and argon plasma treatment (▩) Untreated sample, (♦) Oxygen plasma 100W, (◊) Argon plasma 100W, (■) Oxygen plasma 200W, (□) Argon plasma 200W.

The results of x-ray crystallinity, cuprammonium fluidity and moisture regain indicated that the treatments employed for this study did not alter the bulk structure of the flax fiber. However, the surface bombardment by electrons, ions and excited atoms can cause the breakage of polymer bonds making the resulting polymer fragments more easily crosslink with each other. This crosslinking may lead to the

formation of a brittle polymer layer which can act as a crack initiator [97]. Besides, ultraviolet light can cause oxidation reaction which may severely damage the fiber. The level of degradation is reflected by the measured values of fabric strength.

The relationship between the percentage of strength loss and weight loss is shown in Figure 3.5. Apart from the initial increase in fabric strength after a short period of exposure time, fabric weight loss is linearly correlated with the strength loss. A similar phenomenon was observed when ramie was exposed to air plasma [277]. Excessive strength loss occurs when the exposure time to a oxygen plasma is beyond 20 minutes at 200W discharge power. Under this condition, tendering (with possible formation of oxycellulose) may occur to the prolonged plasma treated cellulose at elevated temperature.

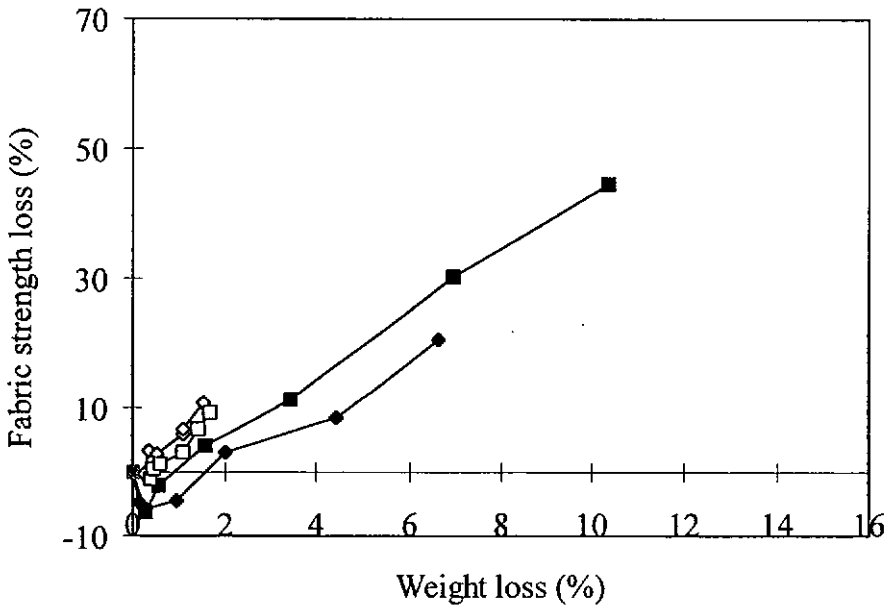

Figure 3.5: Fabric strength loss percentage as a function of fabric weight loss percentage (▣) Untreated sample, (♦) Oxygen plasma 100W, (◊) Argon plasma 100W, (■) Oxygen plasma 200W, (□) Argon plasma 200W.

3.3.2 Surface Morphology and Properties

3.3.2.1 XPS analysis

The oxygen and argon plasmas are known to be effective in modifying fiber surfaces and improving the hydrophilic properties by inducing polar functional groups such as -CO-, -C=O and -COOH [93, 154]. Thus the x-ray photoelectron spectroscopy (XPS) analysis was applied to provide more information concerning the changes in chemical composition (via elemental analysis) and the chemical state (via bonding and oxidation) of atom types on the fabric surface (a typical penetration depth of sampling is 3-5nm) qualitatively and quantitatively.

Table 3.2 shows the relative intensities of C_{1s} and O_{1s} representing the chemical composition percentages on the fiber surface. It is found that all the plasma treatments can lead to lower C_{1s} and higher O_{1s} intensities except argon plasma at 200W for 2.5 minutes. As a result, the O_{1s}/C_{1s} ratio (oxygen to carbon ratio) increases considerably for most of the cases. For the samples treated with a shorter exposure time (2.5 minutes), the change in chemical composition is not very significant with respect to all gases and discharge power levels.

Table 3.2: Relative intensities of chemical composition percentages of surface atoms of linen treated with oxygen and argon plasma

Relative intensities of chemical composition, %.	C_{1s}	O_{1s}	O_{1s}/C_{1s}
Untreated Linen	67.65	32.35	0.48
Oxygen Plasma			
100W, 2.5min.	62.50	37.50	0.60
100W, 60min.	52.12	47.88	0.92
200W, 2.5min.	67.32	32.68	0.49
200W, 60min.	47.38	52.62	1.11
Argon Plasma			
100W, 2.5min.	67.58	32.42	0.48
100W, 60min.	61.02	38.98	0.64
200W, 2.5min.	68.85	31.15	0.45
200W, 60min.	44.03	55.97	1.27

After a prolonged exposure for 60 minutes, the O_{1s}/C_{1s} ratio increases significantly in the ascending order of 100W argon plasma < 100W oxygen plasma < 200W oxygen plasma < 200W argon plasma. From this result, it can discriminate the effect into two different aspects according to the discharge power used. After 60 minutes of exposure at a lower discharge power (100W), the oxygen plasma is more effective than the argon plasma in terms of increasing the O_{1s}/C_{1s} ratio. The higher incorporation of oxygen components into the fiber structure under the oxygen plasma is achieved. It is initially assumed that the oxygen plasma at a higher discharge power will further lead to stronger incorporation of oxygen atoms on the fiber surface. However, the results showed that the argon plasma was more effective than the oxygen plasma (200W, 60 minutes) at the higher discharge power. This phenomenon might be related to the slow ablation rate of the physical sputtering caused by the argon plasma. Under the same condition of 200W discharge power for 60 minutes, the weight loss for the oxygen plasma treated sample is 10.3% while the weight loss for the argon plasma is only 1.7%. As a result, the oxidized components that could not be removed effectively by the argon plasma etching would accumulate on the fiber surface. This will be further examined in Section 3.3.2.3 concerning fabric yellowing.

Chemical states of atoms represented by the relative peak area can be obtained by the wave separation of C_{1s} spectrum. The carbon component was further divided into four sub-components assuming that peak 1 at 285eV corresponding to -CH, peak 2 at 286.5eV to -CO-, peak 3 at 287.9eV to -C=O and peak 4 at 289.1eV to -COOH [209, 215]. Figure 3.6 illustrates the wave separation of C_{1s} and the relative peak areas of chemical component percentages are shown in Table 3.3.

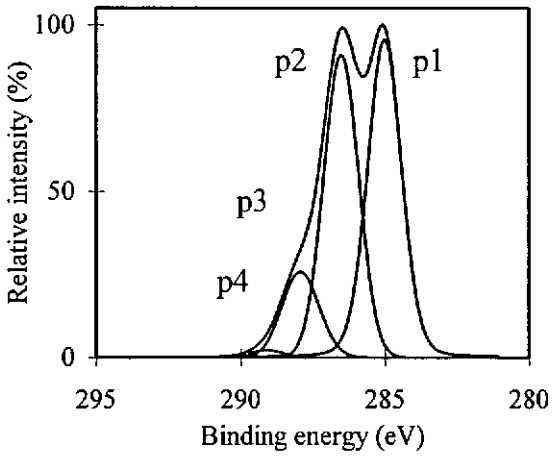
100
50
0
Relative intensity (%)
p1
p2
p3
p4
295
290
285
280
Binding energy (eV)

(1)

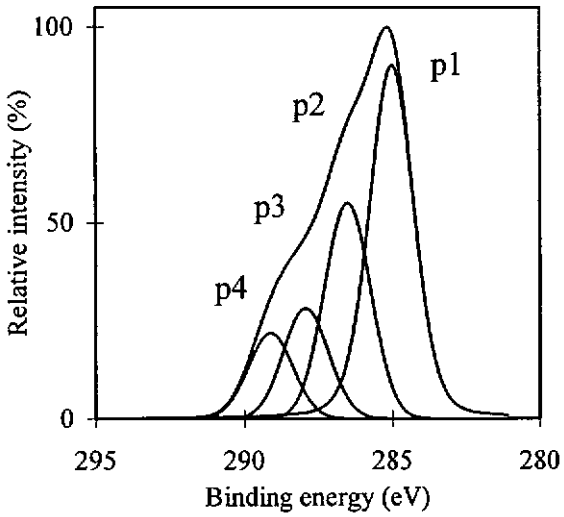
100
50
0
Relative intensity (%)
p1
p2
p3
p4
295
290
285
280
Binding energy (eV)

(2)

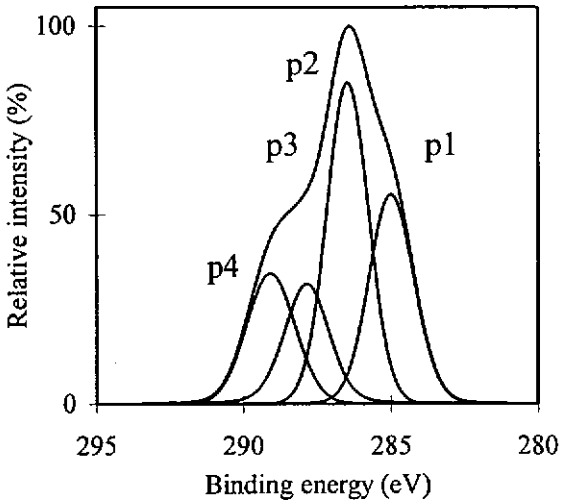
100
50
0
Relative intensity (%)
p1
p2
p3
p4
295
290
285
280
Binding energy (eV)

(3)

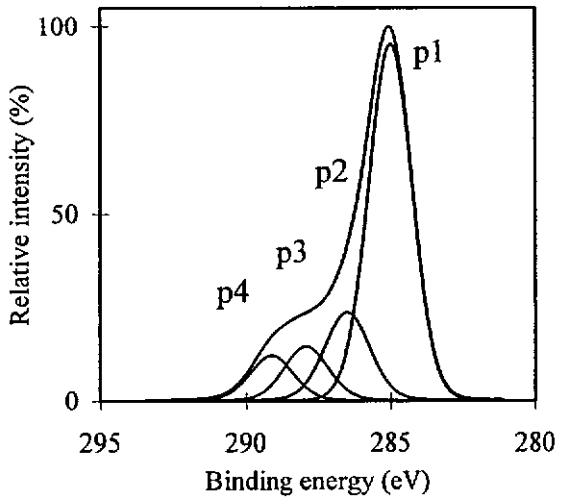
100
50
0
Relative intensity (%)
p1
p2
p3
p4
295
290
285
280
Binding energy (eV)

(4)

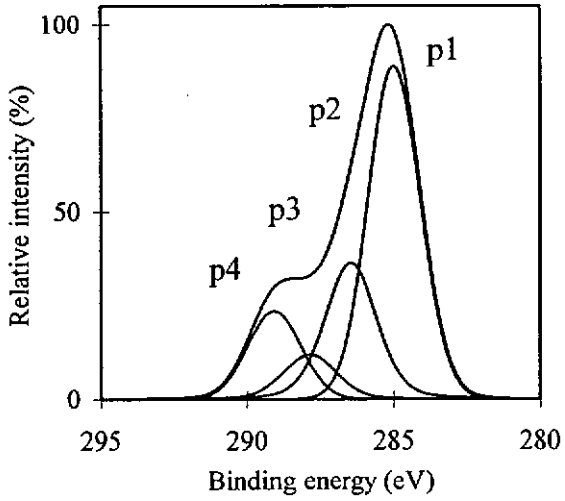
100
50
0
Relative intensity (%)
p1
p2
p3
p4
295
290
285
280
Binding energy (eV)

(5)

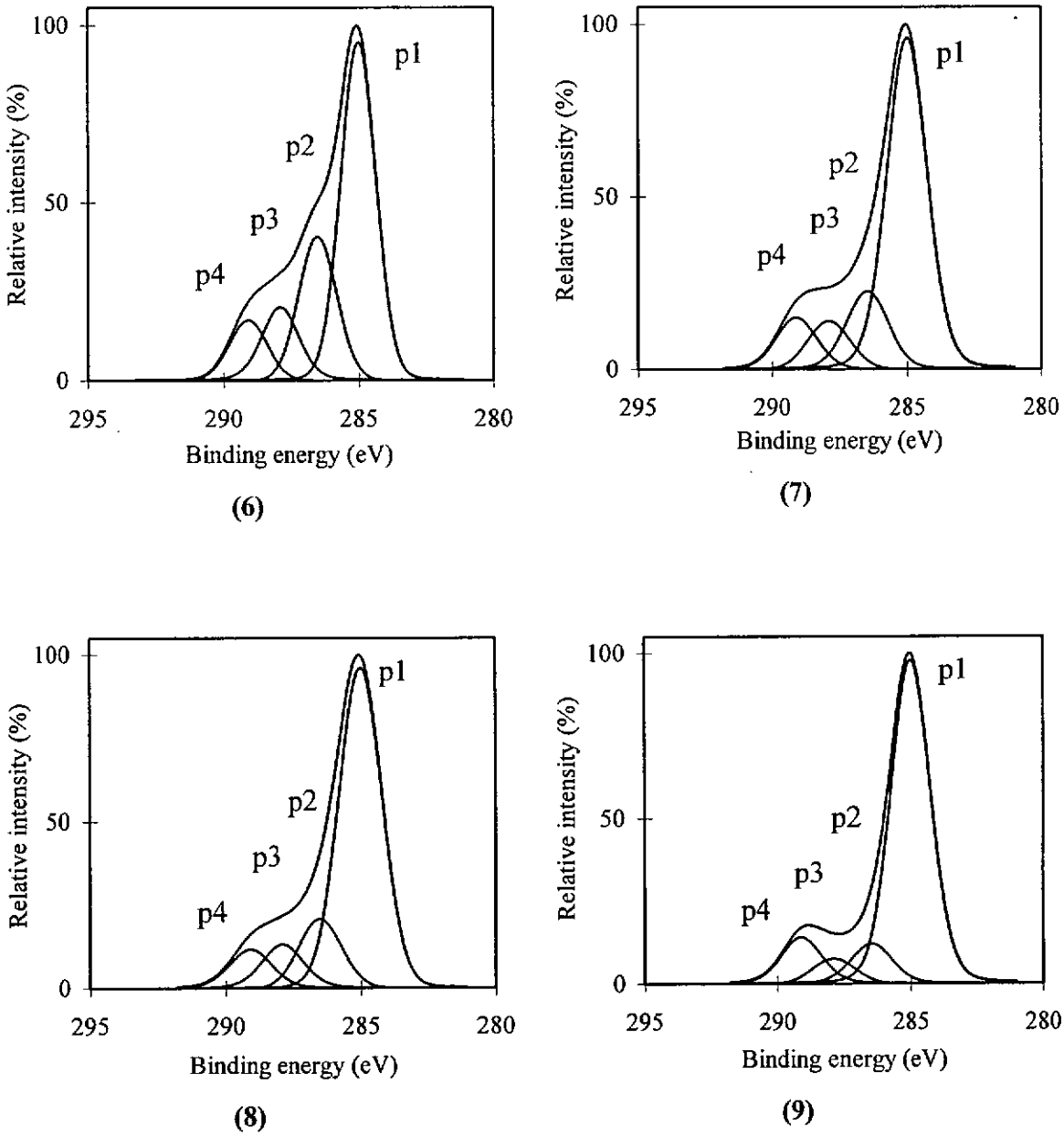

Figure 3.6: Curve fitting of C_{1s} spectra of linen exposed to plasma (peak 1, peak 2, peak 3 and peak 4 correspond to -CH, -CO-, -C=O and -COOH respectively)
(1) Untreated, (2) Oxygen plasma 100W, 2.5min, (3) Oxygen plasma 100W, 60min,
(4) Oxygen plasma 200W, 2.5min, (5) Oxygen plasma 200W, 60min,
(6) Argon plasma 100W, 2.5min, (7) Argon plasma 100W, 60min,
(8) Argon plasma 200W, 2.5min, (9) Argon plasma 200W, 60min.

Table 3.3: C_{1s} spectra of linen treated with oxygen and argon plasma

Relative peak area of chemical component, %	-CH	-CO-	-C=O	-COOH
Untreated Linen	45.6	40.9	12.4	1.1
Oxygen Plasma				
100W, 2.5min.	48.4	26.9	13.9	10.8
100W, 60min.	27.2	38.6	16.3	17.9
200W, 2.5min.	63.4	17.2	10.6	8.8
200W, 60min.	53.6	24.1	7.9	14.4
Argon Plasma				
100W, 2.5min.	52.7	23.9	13.4	10.0
100W, 60min.	65.3	15.6	9.0	10.1
200W, 2.5min.	67.1	14.2	9.9	8.8
200W, 60min.	73.8	9.6	5.5	11.1

The -COOH component is increased dramatically on the fiber surface after being treated with either the oxygen or argon plasma. The -CH component is also increased after being exposed to the argon plasma under all the conditions and to the oxygen plasma under most of the conditions, except for the oxygen plasma at 100W for 60 minutes. The results agree with the previous findings on low temperature plasma treatment of cotton fiber [154]. The increment of oxidized and -CH components was attributed by the increase of free radical intensity and the breakage of glucoside bonds to form the activated carbonyls on the fiber surface respectively [154, 276].

Different discharge power levels and gases seem to provide various degrees of polar group incorporation. Higher percentages of -C=O and -COOH incorporation were found for the oxygen plasma than the argon plasma when using lower discharge power for both 2.5 minutes and 60 minutes exposure. These results are in agreement with the previous results where at low discharge power, the oxygen plasma is more effective than the argon plasma in terms of increasing the O_{1s}/C_{1s} ratio.

When using higher discharge power (200W) with shorter exposure time as shown in Table 3.2, the increment of oxidized component is smaller than that with the lower discharge power (100W). The amount of increment for oxygen plasma is higher than those of the argon plasma at the same power and time. The reverse is observed when the exposure time reaches 60 minutes in the case of -COOH. In the case of argon plasma, the component of -CH is significantly increased (refer to Table 3.3) especially when a higher discharge power is used. This may be explained by the accumulation of -CH due to the slower ablation rate and lower weight loss value. Perhaps, it may be assumed that the argon plasma mainly provides physical sputtering while the oxygen plasma provides chemical etching. This explanation is consistent with the previously observed phenomenon that the -CH component increases sharply after argon plasma exposure and the oxidized component increases tremendously with the oxygen plasma treatment [154, 276].

In the case of using higher discharge power (200W), the oxygen plasma induces 10.3% weight loss with a O_{1s}/C_{1s} ratio of 1.11 and 53.6% of -CH component, while the argon plasma induces only 1.7% weight loss with the O_{1s}/C_{1s} ratio of 1.27 and 73.8% of -CH component. It demonstrates that the strong incorporation of oxygen component by the oxygen plasma under this condition is offset by the high weight loss. Thus the hypothesis of oxidized (yellowed) component accumulation can be adopted. The higher value of -CH for the argon treated sample implies that physical sputtering is the main effect provided by the argon plasma.

In the case of using the lower discharge power (100W), the oxygen plasma induces 6.7% weight loss with an O_{1s}/C_{1s} ratio of 0.92 and 27.2% of -CH component, while

the argon plasma induces 1.5% weight loss with an O_{1s}/C_{1s} ratio of 0.64 and 65.3% of -CH component. It indicates that a strong incorporation of oxygen component by the oxygen plasma under this condition can be retained since the weight loss is not severe. The principal effect of the argon plasma is the breakage of cellulose bonding with less oxidizing effect when lower discharge power is used. Therefore, the hypothesis of oxidized component accumulation cannot be applied when lower discharge power (100W) is used.

3.3.2.2 SEM observation

Figure 3.7 shows the SEM micrographs of samples treated with oxygen plasma illustrating a progressive change in the fiber surface morphology with the treatment time. It reveals the formation of voids and cracks on the fiber surface caused by the plasma ablation. Progressive pitting and surface damage appear on the fiber surface and the surface area is significantly increased when using a higher discharge power (200W). It seems that certain spots on the fiber surface are more susceptible to etching resulting in the formation of cracks with a pronounced empty corncob structure. The typical dimension of the surface structure is in the micrometer range. The effect becomes more significant when the sample is treated at the discharge power of 200W rather than 100W. Cracks and micro-pores start to appear on the surface of the sample which has 1.6% weight loss at 200W and 10 minutes of exposure. The voids and cracks become more pronounced as the exposure time is increased. The enlarged cracks at 200W, 40 minutes and 60 minutes (corresponding to 7.0% and 10.3% weight loss respectively) are perpendicular to the fiber axis and similar to an empty corncob.

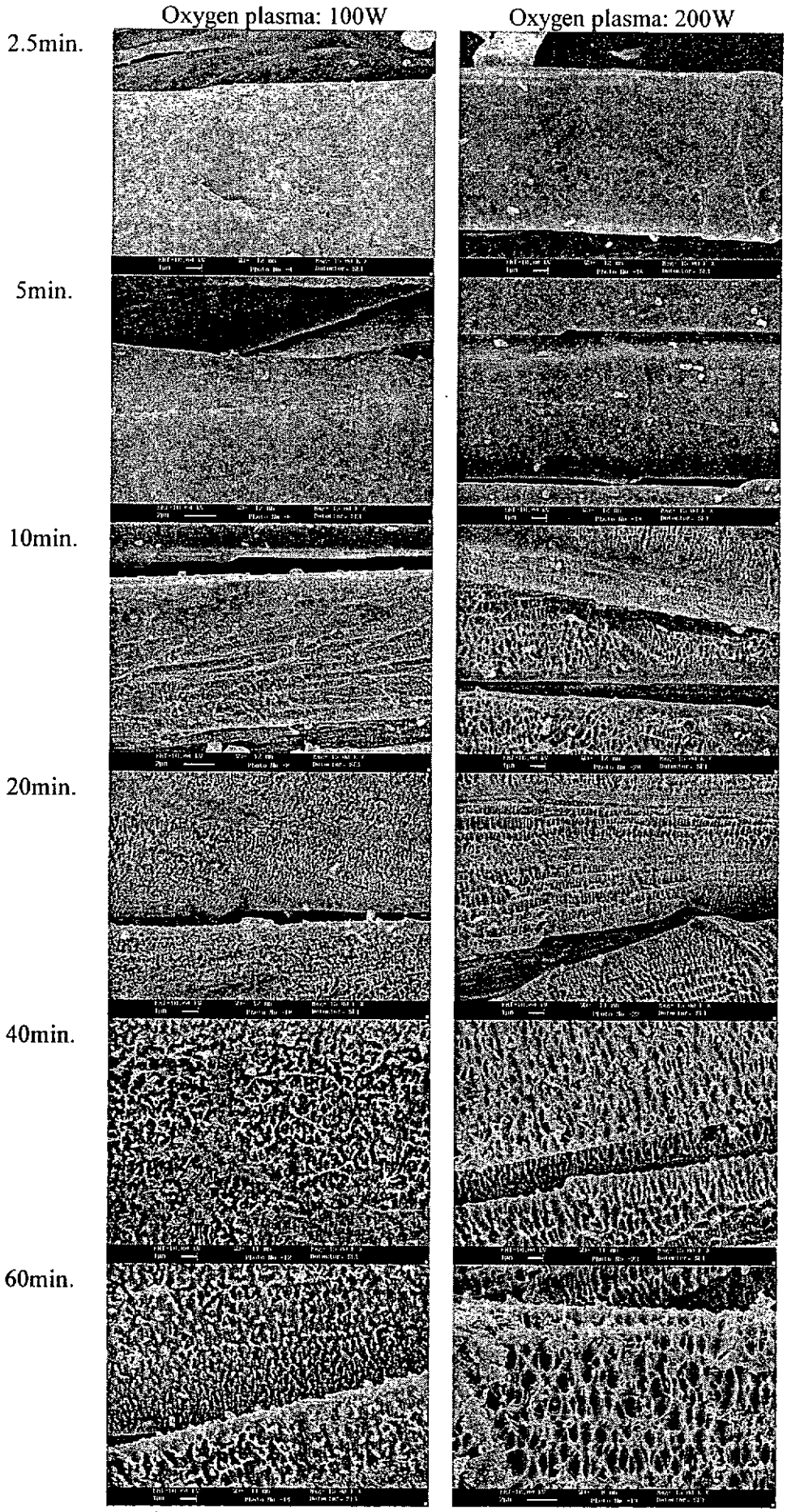

Figure 3.7: SEM micrographs of oxygen plasma treated linen

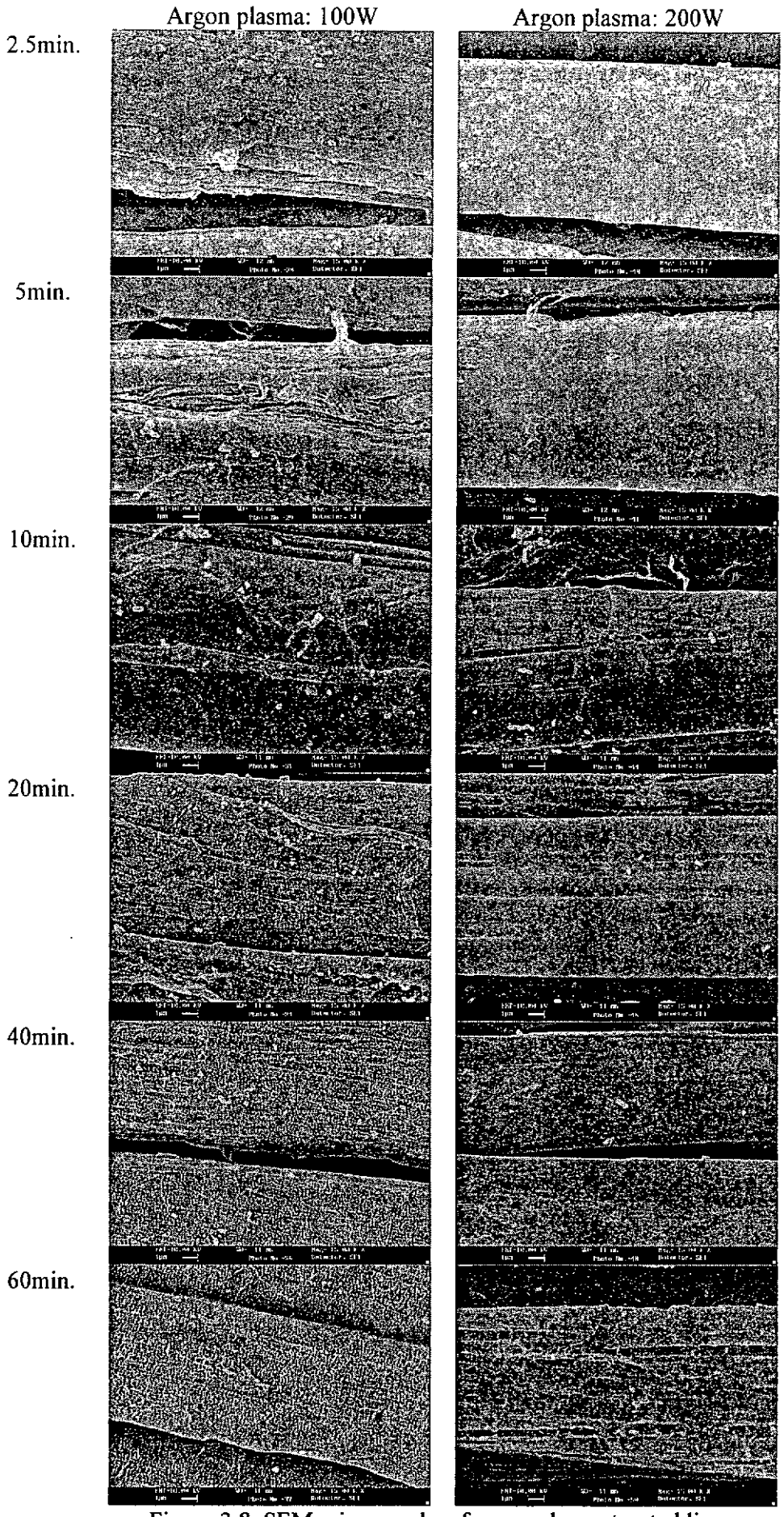

Figure 3.8: SEM micrographs of argon plasma treated linen

When comparing to the oxygen plasma, the argon plasma is not so effective in changing the surface morphology as shown in Figure 3.8. This might be due to the relatively slow rate of physical etching introduced by the argon plasma samples as reflected by the lower weight loss values, i.e., ranging from 0.2% to 1.7%.

The changes in fiber surface morphology observed after the plasma treatment could be explained by the localized ablation of the surface layer. The presence of micro-pores indicates the predominant effect of the oxygen plasma (chemical etching) on the fiber surface. Differential etching of crystalline and amorphous regions might be the origin of the roughness. This process leads to an almost complete breakdown of relatively small numbers of molecules on the surface into very low molecular components which eventually vaporize in the low pressure system when the exposure time is prolonged. As a result, the development of cracks and voids perpendicular to the fiber axis is similar to the case of air plasma treated synthetic fibers [277].

3.3.2.3 Fabric whiteness

Figure 3.9 shows the reduction of fabric whiteness against the plasma exposure time. The yellowness increases with higher discharge power and longer exposure time. This increase of yellowness is less severe with the oxygen plasma at 100W even when the exposure time is prolonged to 60 minutes, but severe yellowing takes place when using 200W discharge power. The argon plasma makes the fabric yellower than the oxygen plasma for all cases under investigation.

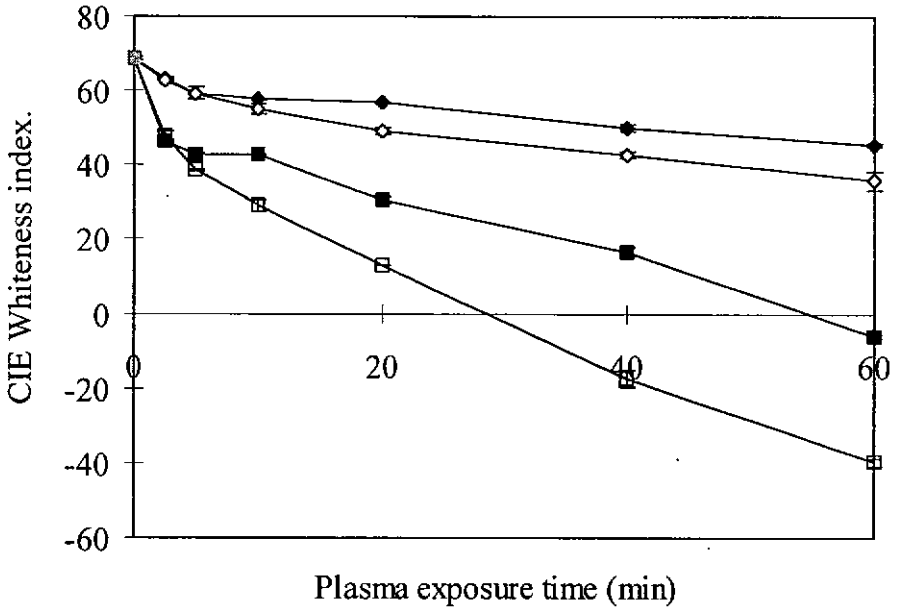

Figure 3.9: Reduction in whiteness of fabrics treated with oxygen and argon plasma (▩) Untreated sample, (♦) Oxygen plasma 100W, (◊) Argon plasma 100W, (■) Oxygen plasma 200W, (□) Argon plasma 200W.

On one hand, it is expected that the oxidative effect brought about by the oxygen plasma should be more prominent than that by the argon plasma in terms of fabric yellowing. On the other hand, a higher ablation rate caused by the oxygen plasma may lead to the subsequent and fast removal of the yellow component. The differences in yellowness brought about by the oxygen and argon plasma might be due to the slower ablation rate of the inert gas (argon gas) resulting in the accumulation of more yellow oxidized component on the fiber surface. This explanation is supported by the higher weight loss value of the oxygen plasma treated sample as discussed in Section 3.3.1.3.

However, this observation seems to be partially related to the O_{1s}/C_{1s} ratio measured by XPS. The explanation that the accumulation of oxidized components occur under higher discharge power and it is not occur under lower discharge power as the descending sequence of the O_{1s}/C_{1s} ratio is 200W argon plasma, 200W oxygen

plasma, 100W oxygen plasma and 100W argon, at 60 minutes of exposure support the whiteness results. Thus comparing the results obtained, it is shown that the first two cases using higher discharge power were matched but not for the latter two samples using lower discharge power. Apart from the O_{1s}/C_{1s} ratio, the percentage of -CH component seems to match the sequence of fabric yellowness. The result shows that the sample treated with 100W argon plasma is yellower than that with 100W oxygen plasma after 60 minutes of exposure even though the latter one has a higher O_{1s}/C_{1s} ratio. Moreover, the -CH percentage of the sample treated with 100W argon plasma is much higher than that with 100W oxygen plasma [154]. Therefore, in addition to the lower weight loss (slow ablation), the 100W argon plasma could make a fabric yellower than the 100W oxygen plasma.

3.3.2.4 Fabric water uptake

Irradiation of fiber in the plasma may cause the introduction of polar groups onto the fiber surfaces, thereby increasing the rate of water uptake and making it more water absorbent. The effect of oxygen and argon plasma on linen fabric water uptake is shown in Figure 3.10. Similar to cotton [136], a significant improvement of fabric water uptake is found after being exposed to both types of gas for all cases.

The highest rate of increment of fabric water uptake can be achieved and the fabric water uptake value is nearly double when using 100W discharge power at 5 minutes of argon plasma or 100W discharge power at 10 minutes of oxygen plasma. The fabric water uptake then declines from the peak but it is still higher than that of the untreated sample. There is no significant difference between sample exposed to two

types of gas in most of the cases when using the same discharge power level. Higher fabric water uptake appears to occur when the discharge power is lower (100W).

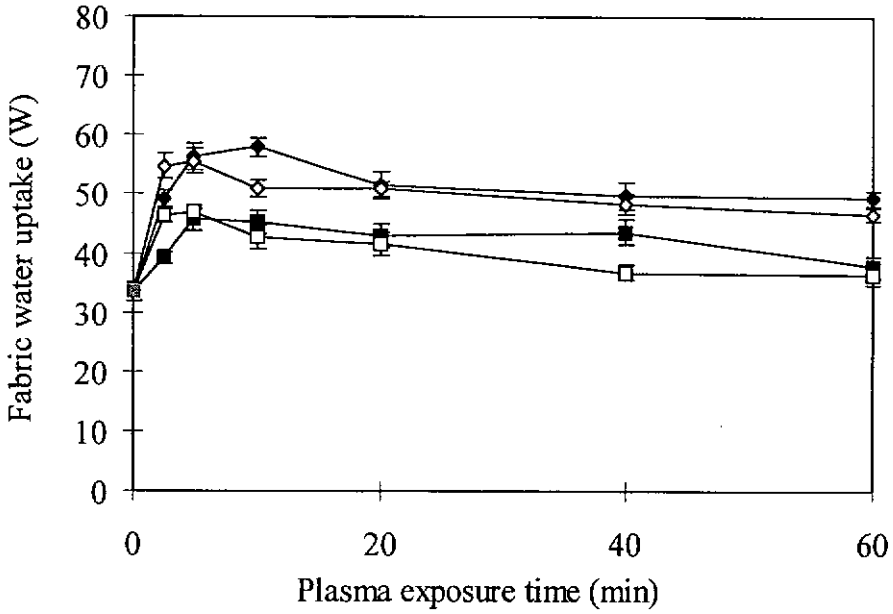

Figure 3.10: Effect of oxygen and argon plasma on fabric wickability
(▨) Untreated sample, (♦) Oxygen plasma 100W, (◊) Argon plasma 100W,
(■) Oxygen plasma 200W, (□) Argon plasma 200W.

The wettability of the material depends on the surface morphology (roughness and dimension) and its polarity. The plasma modification of the fiber surfaces causes an increase in surface area and a reduction of fiber fineness leading to an increase in capillary effects. Both the SEM observations and weight loss measurements showed that the changes were progressive with time. Apart from the capillary effect, increased hydrophilic characteristics with the incorporation of polar groups, as reflected by XPS results, can explain the changes of fabric water uptake.

Fabric water uptake increases in all cases after a short exposure time. As the weight loss percentage and the changes in fiber surface appearance are not significant, thus the causes of these increases should only be attributed to the change in surface hydrophilic properties. This increases occurred when the oxidized components and

especially -COOH, increased significantly after a short exposure time of 2.5 minutes in all cases. This agrees with the previous study [209] that these groups play an important role in increasing the hydrophilic properties of the fibers.

However, after a prolonged exposure, the initial increase of fabric water uptake was reversed in all cases. The results appear to be contradictory to the findings obtained from SEM, weight loss and XPS measurements. They show that the prolonged exposure can lead to surface pitting and reduction of fiber fineness as reflected by the higher weight loss percentage especially in the case of oxygen plasma as well as higher O_{1s}/C_{1s} ratio. The adverse degradation effect of prolonged exposure on the fabric strength caused by the oxygen plasma treatment is attributed to the tendering as shown in Figure 3.4. This may have a relation to the reduction of fabric water uptake increment that also occurs after 10 minutes of exposure.

In order to study the effect of storage time (under standard conditions) the after the plasma treatment, a further study was carried out by using two fabric samples treated by the oxygen and argon plasmas respectively at 100W for 5 minutes. The results shown in Table 3.4 indicate that the effect of storage time on the fabric water uptake is small within the range from 0 to 1000 hours. The highest fabric water uptake of the sample is found at zero storage time which can probably be explained by the drying effect of the treatment. The fabric was dry initially when removing it from the plasma chamber because the moisture content of the fiber was removed during the vacuum process of plasma treatment. Thus a maximum fabric water uptake is expected from the immediate measurement. As the moisture content of the sample reaches its equilibrium, the stable fabric water uptake values can be obtained.

Table 3.4: Water uptake of fabrics treated with oxygen and argon plasma as functions of storage time

Storage time after plasma exposure, h.	Oxygen Plasma: 100W, 5min. (CV%)	Argon Plasma: 100W, 5min. (CV%)
0	70.2 (6.6)	66.1 (5.8)
1	61.1 (4.1)	62.8 (4.8)
10	61.7 (5.8)	63.5 (4.9)
24	56.3 (6.5)	55.6 (6.4)
100	58.7 (5.3)	60.2 (5.9)
1000	60.7 (7.0)	57.1 (6.2)

3.3.3 Other Related Fabric Properties

3.3.3.1 Fabric bending properties

The bending rigidity and hysteresis of the fabric against exposure time are shown in Table 3.5. The reduction of fabric bending rigidity and hysteresis caused by the oxygen plasma is not significant at 100W discharge power, but the effect becomes more noticeable at 200W discharge power especially at 2.5 minutes of exposure time. Afterwards, the two bending properties are slightly increased. Similar profiles are also found when using the argon plasma but the time employed for the lowest bending rigidity and hysteresis to appear is 10 minutes of exposure time at 200W discharge power.

When plasma etches the fiber surface, the breakage of polymer molecules will occur, thus making the fiber more soft and flexible for bending. Higher discharge power (200W) is more effective in the breakage of polymer molecule for both gases. However, the sample subjected to the prolonged exposure under the plasma condition would lead to over drying and hardening, as well as cross-linking which in

turn affected the reduction of bending rigidity adversely. This phenomenon was also reflected by the reduction of fabric strength and water uptake.

Table 3.5: Bending rigidity, bending hysteresis and wrinkle recovery of oxygen and argon plasma treated samples

		Plasma exposure time, min.					
	Untreated	2.5	5	10	20	40	60
Oxygen Plasma, 100W.							
Bending rigidity, $gfcm^2/cm$.	0.68	0.64	0.66	0.68	0.67	0.71	0.69
CV%	8.4	5.9	8.3	8.5	10.7	7.3	8.9
Bending hysteresis, gfcm/cm.	0.54	0.51	0.53	0.55	0.56	0.56	0.57
CV%	9.1	11.5	8.8	8.7	10.5	8.4	8.1
Wrinkle recovery, %.	25.1	27.2	26.2	26.5	26.3	27.0	26.8
CV%	7.1	6.8	5.9	5.7	5.0	4.9	6.2
Oxygen Plasma, 200W.							
Bending rigidity, $gfcm^2/cm$.		0.51	0.56	0.60	0.58	0.51	0.50
CV%		6.5	5.0	5.7	8.2	8.5	10.9
Bending hysteresis, gfcm/cm.		0.41	0.45	0.51	0.47	0.40	0.37
CV%		11.7	6.4	5.9	9.8	7.2	16.9
Wrinkle recovery, %.		27.1	26.9	27.4	27.6	28.0	28.5
CV%		5.4	5.6	3.4	4.8	3.2	5.4
Argon Plasma, 100W.							
Bending rigidity, $gfcm^2/cm$.		0.71	0.71	0.56	0.75	0.74	0.80
CV%		6.6	9.0	9.0	3.1	4.3	5.8
Bending hysteresis, gfcm/cm.		0.60	0.60	0.48	0.72	0.69	0.75
CV%		6.8	7.0	10.6	6.2	5.5	3.9
Wrinkle recovery, %.		28.6	27.9	28.0	27.4	26.9	25.8
CV%		5.6	5.6	7.6	5.8	7.7	6.1
Argon Plasma, 200W.							
Bending rigidity, $gfcm^2/cm$.		0.69	0.69	0.54	0.76	0.74	0.73
CV%		6.4	5.1	4.7	3.4	6.3	7.1
Bending hysteresis, gfcm/cm.		0.58	0.58	0.45	0.67	0.67	0.64
CV%		5.7	7.4	6.6	6.4	5.0	6.0
Wrinkle recovery, %.		26.2	28.0	27.3	26.4	26.4	25.0
CV%		6.4	5.0	6.1	5.0	5.0	3.7

3.3.3.2 Wrinkle recovery

Table 3.5 shows the fabric wrinkle recovery percentage as a function of plasma exposure time. A slight improvement is found after 2.5 minutes of plasma exposure for all cases but no significant change can be observed after the exposure time of 60 minutes. The plasma treatments do not change the wrinkle recovery of the linen significantly.

3.4 CONCLUSION

It has been shown that the exposure of linen to the oxygen or argon low temperature plasma will result in the change of the surface morphology and chemical property. By employing XPS to quantify the change in both chemical composition and chemical state, it was found that the oxygen content (O_{1s}/C_{1s} ratio) of the plasma treated samples was dramatically increased particularly at higher discharge power (200W) for both gases at 60 minutes of exposure. SEM investigation revealed that the cracks and voids appeared on the fiber surface after being exposed to the oxygen plasma at 200W discharge power and to a less extent at 100W. However, the appearance of cracks and voids was less noticeable when using the argon plasma. Fabric whiteness was reduced after being exposed to the argon plasma at the higher discharge power. No significant change in degree of polymerization and crystallinity occurred to the samples as shown by the x-ray crystallinity and fluidity tests. A slight reduction of the moisture regain was detected in all the treated samples after 2.5 minutes of treatment. The loss of fabric weight and strength increased with the exposure time for both levels of power, and the effects were more severe when using the oxygen plasma. A significant reduction of fabric bending rigidity and hysteresis was achieved after 2.5 minutes of oxygen plasma or 10 minutes of argon plasma exposure. With regard to the type of gases used, the fabric treated with the oxygen plasma generated higher heat level and also suffered higher weight loss and strength losses when compared with the argon plasma treated sample, although a higher level of yellowing was found in the argon plasma treated sample. More severe effects were obtained by using 200W discharge power except the case of fabric water uptake.

Considerable initial improvement of water fabric water uptake was achieved during treatment and the effect remained almost constant with the storage time up to 1000 hours. Maximum improvement of fabric water uptake was achieved by exposing the fabric sample to the oxygen plasma for 10 minutes or to the argon plasma for 5 minutes at a discharge power of 100W. It was observed that the prolonged exposure time, irrespective of the type of gas and power, did not give better fabric water uptakes and might even cause adverse effects on the fabric such as excessive reduction of fabric strength, increased bending stiffness and reduction in fabric water uptake. In conclusion, low temperature plasma with short treatment times on linen was very effective for surface modification as shown by substantial increases of polar group contribution and water uptake. Furthermore, a slight improvement of fabric strength, bending rigidity, hysteresis and wrinkle recovery could be achieved, without interfering the bulk fiber structure and with minimal loss of fabric weight and whiteness.

CHAPTER 4

SURFACE CHARACTERIZATION OF FLAX FIBER TREATED WITH LOW TEMPERATURE PLASMA

4.1 INTRODUCTION

The surface properties of materials are often the important determinants of their usefulness, and many of the chemical treatments now in use are aimed at modifying these properties [94, 161]. The important properties of polymer materials such as adhesion, friction, wetting, swelling, penetrability and biological compatibility are strongly influenced by their surface characteristics. In general, the structure and morphology of the topmost surface layers (several nanometers thick) differ from those of the bulk polymer. Therefore, a comprehensive surface analysis is needed to correlate the surface structures with the physical or chemical property [7, 158, 160, 219].

The microscope has played an important part in formulating structural concepts in polymeric materials. Scanning Electron Microscopy (SEM) is traditionally used for this purpose [94, 161, 228]. It is an important instrument for the observation, analysis and examination of phenomena occurring at the micrometer and sub-micrometer scales. Since textile fibers have diameters within this range, thus SEM is a powerful tool for examining the structural features of fibers. It produces a high resolution and depth of field images of the sample surface [232]. While SEM has been firmly established as a standard analytical tool, however, there have been some limitations on its application [33]. The in-situ examination of material surfaces under ambient condition is not possible using the conventional SEM since a

conductive coating and high vacuum environment are employed. Environmental Scanning Electron Microscopy (ESEM) is a relatively new instrument and there is very little published information on textile application. As the conductive coating of the sample under a high vacuum evacuation is not necessary with the ESEM, it allows viewing of textile materials without any extensive sample preparation and possible change of structural details. ESEM can be employed to observe the structural change in textile materials under various treatment conditions so that the 'on-going' examination (time-series images) of treatment effects can be studied.

The invention of the Scanning Probe Microscopy (SPM) created a new research tool to study the material surface down to the atomic scale. Scanning Tunnelling Microscopy (STM) and Atomic Force Microscopy (AFM) are the most advanced scanning probe methods to provide atomic-resolution images. At present, STM has been used for analyzing metallic and semi-conducting surfaces. The most important feature of STM is the real space visualization of the surfaces or the atomic scale. The image is converted to either the spatial variation of the tunnelling current or the spatial variation of the tip height. The tunnelling current decreases exponentially with increasing distance between the tip and sample. However, the STM application is mostly limited to metals and semi-conductors since tunnelling currents are employed [160-161].

To enable the characterization of insulating surfaces, AFM was invented. By using this technique, an image presents a three-dimensional profile of inter-atomic force between a sharp probe and surface atoms. It gives a more direct approach to the microtopography of the fiber surface [160-161]. It has been found to have much

broader application than STM and is currently the dominant scanning probe technique.

For textile materials, it is important to understand their appearance in the natural state since it can be easily changed under the ultra-high vacuum condition experienced under SEM. Therefore, the potential application of using ESEM and AFM should be explored for the examination of processing effects on textiles. In this chapter, the surface morphology and topography of flax fibers treated by plasma treatment will be studied by using ESEM, SEM and AFM techniques.

4.1.1 Surface Morphology Study by SEM and ESEM

4.1.1.1 SEM imaging technique

In SEM, a very fine probe of electrons with energies up to 30-40 kV is focused at and scanned over the surface of the specimen as a raster or parallel line. When the primary electron beam strikes the specimen, a number of different emissions and absorption processes occur. The emission of low energy secondary electrons from the uppermost layers of the specimen is important for signal induction.

The secondary electrons are collected, processed and translated continuously on a cathode ray tube or monitor. For each point where the electron beam strikes the specimen and generates secondary electrons, a corresponding intensity is displayed on the viewing monitor. The brightness of the point is directly proportional to the number of secondary electrons generated from the specimen surface. The electron beam is scanned rapidly over the specimen, the numerous minute points appear to blend into a continuous-tone image composed of many density levels or shades of

gray where light and dark areas give the impression of depth. The magnification produced by the SEM is the ratio between the dimensions of the final image displayed and the field scanned on the specimen [22, 262].

In addition to the production of secondary and back scattered electrons, the interaction of the specimen with the beam generates Auger electrons and x-rays. These emissions, a characteristic of particular atoms, can be used to identify surface elements of the specimen. The various products of the interaction are shown schematically in Figure 4.1. These are (1) Secondary electrons, (2) Reflected or Backscattered electrons, (3) Transmitted electrons, (4) X-radiation, (5) Auger electrons, (6) Cathodoluminescence radiations, (7) Absorbed (specimen) current. Of these, (3) are used for imaging in transmission electron microscopy, (1) and (2) in scanning electron microscopy, whilst (4)-(7) can provide additional analytical information about the specimen in other type of microscope [262].

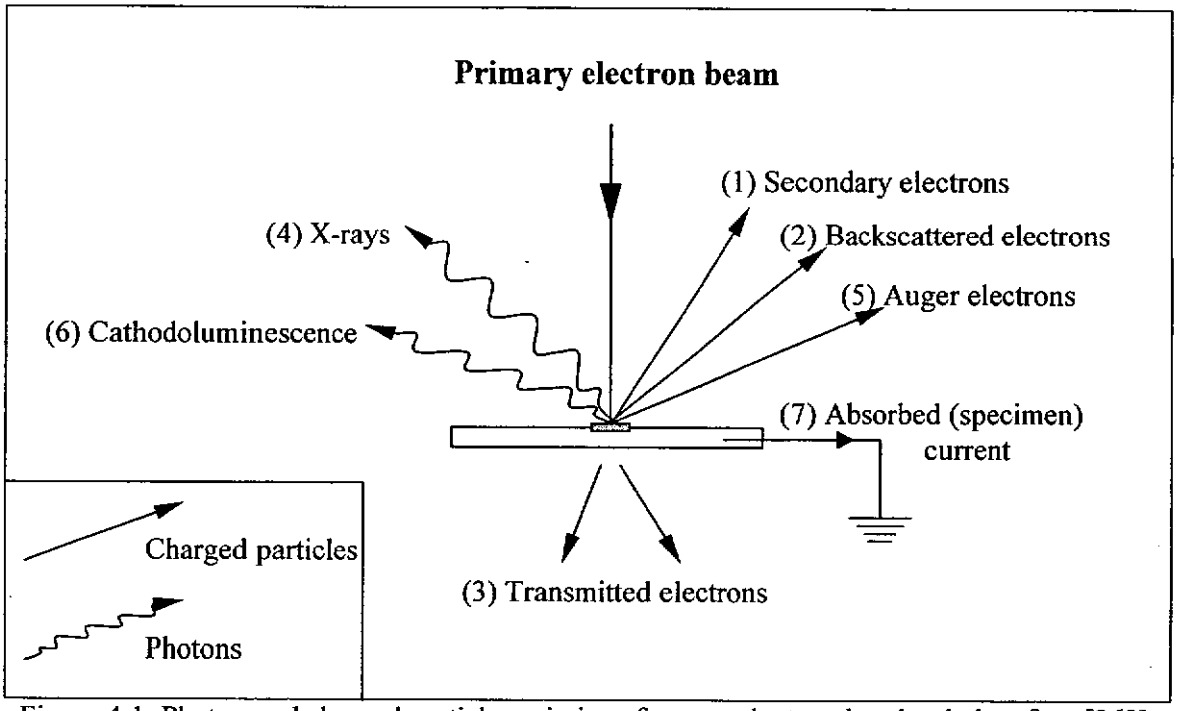

Figure 4.1: Photon and charged particle emissions from an electron-bombarded surface [262]

It has been shown that a moving electron can be regarded as a moving charged particle or as a radiation with associated wavelength. The wavelength of the radiation varies inversely with the square root of the accelerating voltage, therefore the electron wavelength is in fact many orders of magnitude shorter than that of light. Thus, a 100kV electron has a wavelength of 0.0037nm. The significance of the electron wavelength in the resolving power relationship is shown as follows:

$$d_o = 0.6\lambda / n\sin\alpha$$

where d_o = minimum resolvable separation in the object,

λ = wavelength of the illuminant,

α = half-angle subtended by the objective at the object,

n = refractive index in the space between object and objective lens.

This relationship can be used to work out the theoretical limit of resolution of any microscope system. The product $n\sin\alpha$ is called the numerical aperture (NA) of the objective lens, and is usually engraved by the manufacturer in the lens mount. It is obvious if an electron objective lens of NA1.4 was available, then a 100kV electron microscope would be capable of resolving detail as fine as 0.016nm or about a hundredth of the size of an atom [262].

In the SEM, the object detail is sampled point by point continuously and the resolving power of the instrument is directly determined by the smallest area where it can sample, i.e., by the diameter of the electron probe. Minimizing the probe diameter requires a system of lenses with small aberrations and high electrical stability. In practice, the smallest probe which can formed with enough electrons in it to be useful depends on the focal length or working distance of the final probe-

forming lens, the electron gun and the operating voltage. For a conventional tungsten-filament gun with a working distance of about 10mm and the smallest usable probe size of about 3-4nm, the secondary electron resolving power is between 3.5nm and 7nm. Better resolving power is only obtainable by working with a stronger lens or brighter electron source [33, 262].

The entire column of SEM is normally under a high vacuum environment for the passage of the high energy primary electrons down to the column as well as to permit the low energy secondary electrons to travel to the detector with the minimal beam-scattering effects [22, 232, 262]. Electron microscopy has a high resolution but requires special sample preparation, and the electron beam may damage polymer samples [95, 160, 232]. Therefore, it is necessary to coat non-conducting specimens with a thin layer of gold, carbon or other conductor so as to provide a path to earth for the negative charge imparted by the electron beam. This is to overcome 'charging effects' (the sporadic discharge and deflection of the electron beam caused by the accumulated negative charge in the specimen) and to prevent thermal and/or electrical breakdown of the specimen. However, the conductive coating prevent the possibility of subsequent treatment of the specimen and subsequent re-examination of the same area of the specimens is not possible.

The other limitation of the conventional SEM used for hydrophilic materials is that it is necessary to operate the microscope under a high vacuum in order to obtain an image. Any specimen containing moisture or volatile substances will therefore be desiccated before being studied and the image obtained may not represent the true natural state of the material [95].

4.1.1.2 ESEM imaging technique

ESEM is a modification of SEM which allows materials to be examined in the presence of gases or liquids, and whose specimens do not require conductive coatings [33, 50, 232]. ESEM permits a higher resolution of sample image at relatively high pressure than a conventional SEM. The development of the machine itself has been described in a series of papers [56, 58, 61-63, 65-66].

Essentially, ESEM operates by having a differential-pumped specimen chamber placed very close to a pressure-limiting aperture at the bottom of main electron optical column. The main electron optical column operates under a standard vacuum condition such that when the electron probe passes through the aperture, it is scattered by the gas molecules present in the short space between the aperture and the specimen [64, 95]. The primary electron beam hits the specimen causing the emission of secondary electrons which are scattered to the positively charged detector electrode. As they travel through the gaseous environment, collisions occur between an electron and a gas particle which will result in emission of more electrons and ionization of the gas molecules as shown in Figure 4.2 [33, 233].

The environmental secondary electron detector is mounted around the final pressure-limiting aperture. A voltage is applied between the sample and the detector which accelerates secondary electrons towards the detector. The increased number of the electrons will effectively amplify the original secondary electron signal. The detection process uses gas molecule and electron interaction for signal amplification in imaging. The positively charged gas ions are attracted to the negatively based

specimen and the excessive electron charge on the specimen surface, allowing the non-conducting materials to be examined without any surface coating [33, 232].

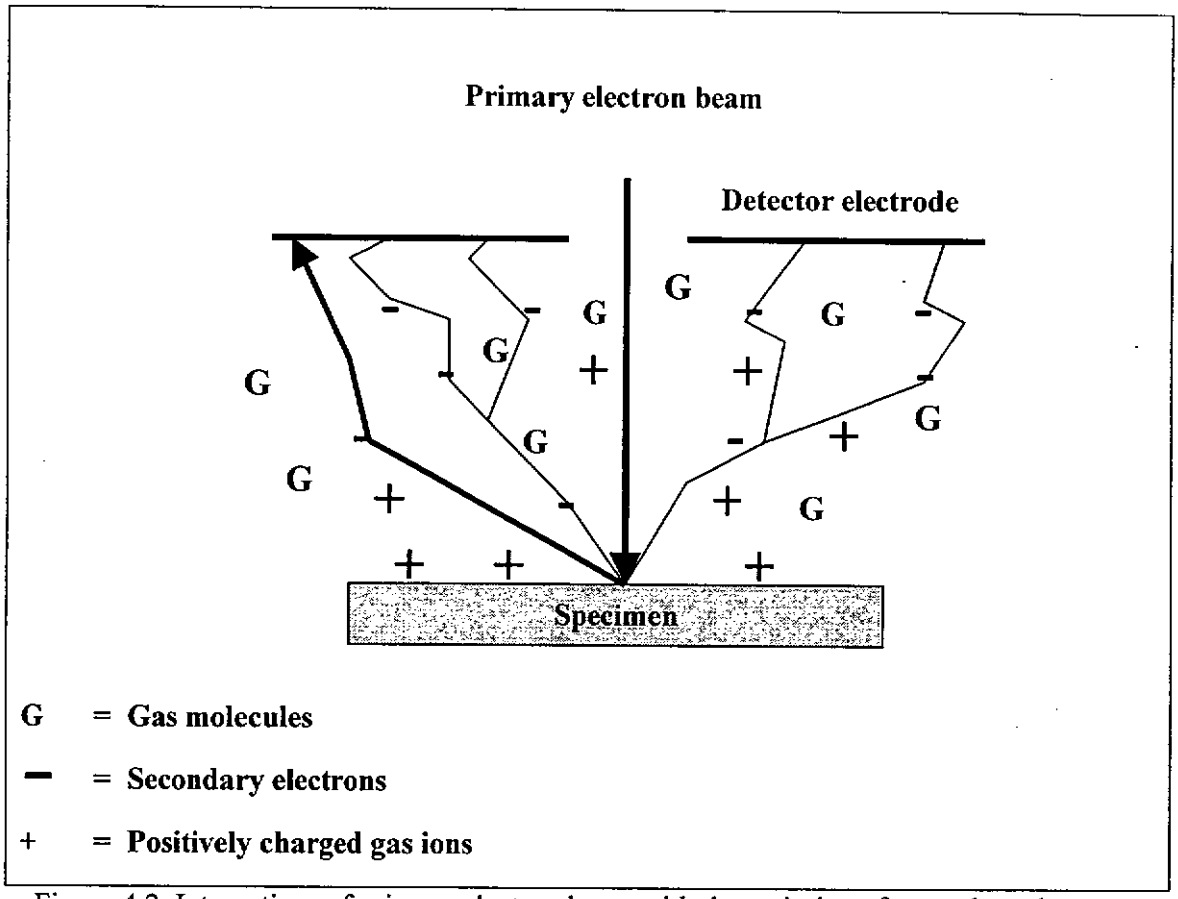

Figure 4.2: Interactions of primary electron beam with the emission of secondary electrons and the gas molecules inside the sample chamber of ESEM [64]

The most common imaging gas used in the sample chamber is water vapor, it enables viewing of non-coated hydrated samples. Reactive or other gases such as oxygen, carbon dioxide, ethylene, hydrogen, propylene, styrene, acetone, toluene and alcohol may be introduced in small quantities by injecting them directly over the sample using the micro-injector. Alternatively, if they are stable to an applied voltage, they may by used as the only gas in the sample chamber instead of the usual water vapor [50, 64].

In textile research, the initial developments of ESEM have been carried out mainly on wool research [57, 59-60]. In additional, it has been used for studying the time

series images of textile absorption and structure change under wetting and heating condition [232]. Methods have also been developed for observing the transverse swelling of cellulosic fibers [134]. Apart from textiles, research has been made on some other areas like the study of fresh and living plant materials, wetting and drying of papers, microstructure in ceramics and composites, and the corrosion studies of stainless steel piping [24, 33, 67, 85, 193, 225].

4.1.1.3 Preliminary experiment

A preliminary experiment was carried out with the objective of studying the fiber surface morphology under a low vacuum condition without gold coating. The time-series experiment was conducted to investigate the changes of fiber surface morphology between successive plasma exposures. Hence, suitable operational parameters had to be chosen in order to retain the natural fiber properties and surface morphology with a minimum of post irradiation.

4.1.1.3.1 Sample preparation

Various textile fibers such as wool, cotton, ramie, flax and plasma treated flax were observed. Plasma treatment of flax fiber was conducted with a procedure specified in Section 3.2.1. Fiber samples were fixed on a carbon-based, electrically-conductive, double-sided adhesive tape and exposed to the oxygen plasma at a pressure of 15Pa and 200W discharge power for 60 minutes. The sample was removed from the chamber and then transferred to the ESEM chamber for morphological characterization.

4.1.1.3.2 Material characterization procedures

The instrument used was a Hitachi S-2380N Scanning Electron Microscope. Samples were mounted on a stub with the carbon-based, electrically-conductive, double-sided adhesive discs. The samples were viewed without drying and coating. The specimen chamber pressure was 1Pa.

4.1.1.3.3 Operational parameters

Although the principle of ESEM is promising, it does not provide optimal operating conditions for textiles in actual practice. The operational parameters, including the accelerating voltage, working distance, chamber pressure, beam current, scanning rate and magnification, are important to regulate properly in order to optimize the resolution of the micrographs. ESEM fiber images often have bright edges with poor contrast, and do not relate well to the images obtained from SEM. The sides of the fibers appear brighter than the top because the low take-off-angle of the back-scattered electrons travels at a longer distance than the high take-off-angle ones, a fact which allows more ionizing collisions of the former than the latter [63]. Care also has to be taken to ensure that the surfaces do not have water condensed on them otherwise details of the fiber surface can be obscured [94].

Poor sample conductivity will cause the build up of surface electrons, producing variations of surface potential or charging. Charging up of electrons on sample surface will lead to various image distortions and excessively bright 'over glow' which prevents true image production. Poor conductivity also reduces thermal dissipation which may lead to local sample movement or even heat damage [60, 94, 262]. In addition, low atomic density polymeric materials are readily penetrated by a

high voltage electron beam causing a great loss of surface detail. Coating with a thin layer of metal is the most widely used method to suppress charging and decrease beam penetration in the conventional SEM [94]. As non-coated materials are studied by ESEM, the question arises as to what degree the examined surface remains unaffected by the action of electron beam.

Firstly, the effects brought about by various types and intensities of beam depend on several aspects such as the accelerating voltage, current intensity, scanning rate and scanning mode (raster or other linen density, magnification). Secondly, the nature of the sample chamber environment such as the pressure and temperature of the gas need to be considered during examination. Thirdly, the specimen composition, structure, texture and orientation also affect the level of beam irradiation [22, 60, 64, 84, 132].

Since the sample being investigated is a non-conducting material and no metal coating has been applied to the sample, it would become charged by the primary electron beam during scanning. When using a high gun voltage, the energy given by the charged electrons will be in the form of heat and the heating effect is frequently sufficient to cause a permanent damage to the specimen [262]. Low density polymer generally allows greater penetration of the electron beam than a sample of higher atomic number and density. If a high energy electron beam is used, the penetration will produce signal from the areas of specimen below the surface resulting in the formation of images of lower contrast with a loss of detail.

Therefore, when examining organic and polymeric materials, it is necessary to restrict the electron beam voltage to 10kV and refrain from prolonged examinations at high magnifications so as to avoid producing localized thermal stresses in the specimen caused by the electron beam. The use of lower voltages is especially important when very thin specimens such as fibrillated or sectioned fibers are studied. Even with coated specimens, low voltages are recommended to be an additional means of reducing charging in fibers. However, the resolution of micrographs will be decreased with the reduction of operation voltage [94, 225, 262]. Further reduction of the beam voltage to 5kV gives a detailed image but reduces the resolving capability [94, 230]. Since resolution is lost by the use of low voltage, care must be taken to set other parameters so as to give the greatest possible resolution.

The use of a shorter working distance is another means of increasing resolution [22, 59, 62]. The working distance from the bottom of the objective lens to the specimen surface is around 5-35mm in both SEM and ESEM [204]. Since beam scattering will occur in the sample chamber of ESEM due to the presence of gas, therefore, the electron beam should travel a minimum distance in the high pressure environment in order to avoid the excessive beam scattering of the gas molecules. Pictures with clearer quality can be observed at a high magnification with the usage of a suitable beam voltage. With careful operation, acceptable resolutions can be obtained even at very low voltages [94], thus the best compromise between the resolution of the detail of interest and the minimization of onset of beam damage on the specimen under different working conditions can be achieved. Under this condition, any minute charging-up effect will be minimized.

4.1.1.3.4 Results and summary of preliminary experiment

The first aim of the preliminary experiment was to undertake repeat observing of both the untreated and treated fiber in order to minimize any damage caused by the electron beam between each observation. The second aim was to establish the optimum working conditions under which the post irradiation is minimal.

A secondary electron detector was employed by which the electrons emanated from the upper 25 angstroms of the specimen surface and the related topographical information could be received [50, 225]. The pressure of the sample chamber was 1Pa. After a number of trials, acceptable quality of micrographs was obtained using a working distance of 8mm [94, 230], operating voltage of 8kV with the emission current of 30μA and the magnification could be up to x3000.

By repeating the observation of an untreated fiber over the same field of view at various time intervals as shown in Figure 4.3, it was evident that the fiber damage caused by the electron beam was not significant. The charging effect was not serious and could be de-charged inside the chamber within a short period of time without any observable damage. The surface appearance of the plasma treated fiber also remained unchanged after the observation. When comparing the plasma treated sample with the initial observation under ESEM in Figure 4.3 with the SEM micrographs in Section 3.3.2.2, both exhibited a similar surface appearance after ESEM exposure. Therefore, it is reasonable to assume that the initial exposure of flax fiber under ESEM did not affect the features introduced by plasma treatment.

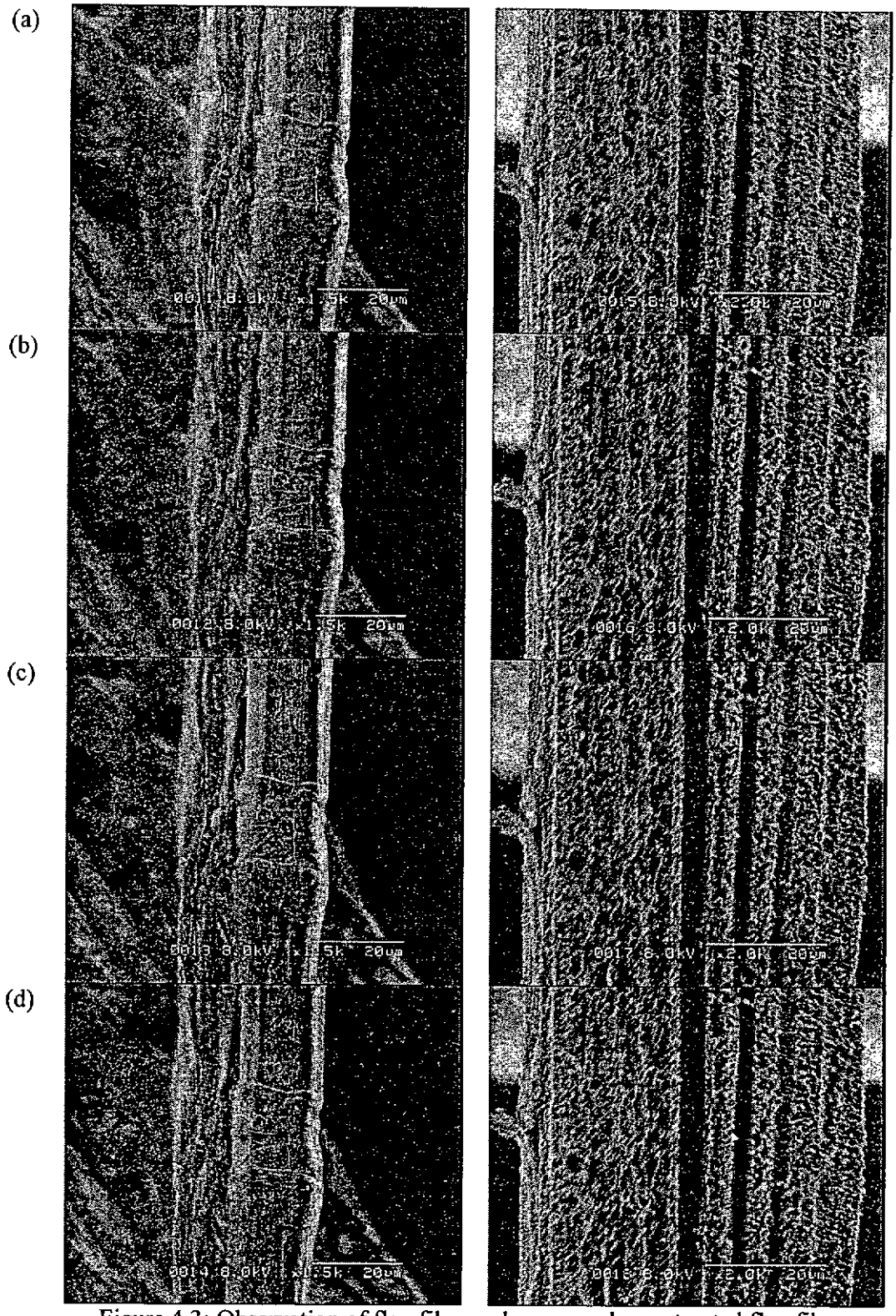

Figure 4.3: Observation of flax fiber and oxygen plasma treated flax fiber (15Pa, 200W, 60 minutes) under ESEM
(a) first observation, (b) second observation, repeated immediately,
(b) third observation, repeated after 10 minutes, and
(d) fourth observation, repeated after 30 minutes.

However, some damage appeared on the wool, cotton and ramie fibers. From the micrographs, the image quality was not very clear with the appearance of overly bright area as shown in Figures 4.4, 4.5 and 4.6. The extent of damage depended on the accelerating voltage, current intensity, scanning rate, magnification and the nature of the specimen. The micrographs were obtained at a lower accelerating voltage of 5kV in order to reduce charging and damage to the fibres. The magnification produced by a scanning electron microscope is actually the ratio between the dimensions of the final image display and the field scanned on the specimen. Since a smaller area would be scanned when a higher magnification was used, thus the primary electron beam was brought to rest within the sample during scanning. As a result, the localized thermal stress on the fiber would be increased resulting in fiber damage. With the heat sensitive and low conductivity materials being examined by ESEM without coating, the acceptable image could therefore only be produced with a limited magnification.

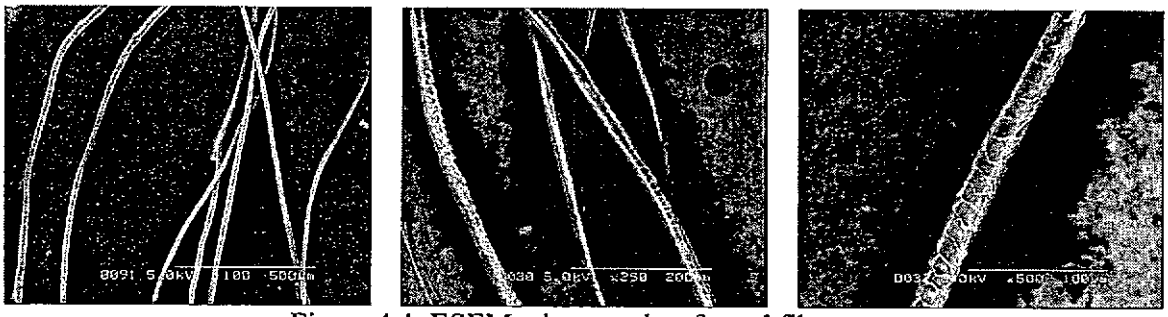

Figure 4.4: ESEM micrographs of wool fibers

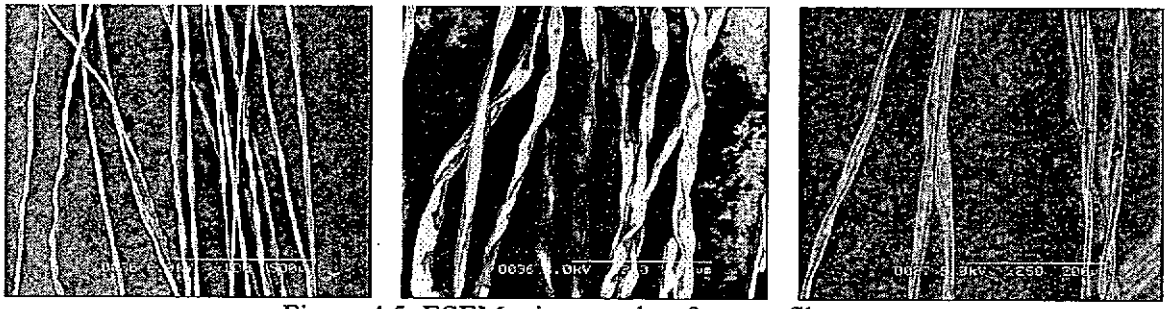

Figure 4.5: ESEM micrographs of cotton fibers

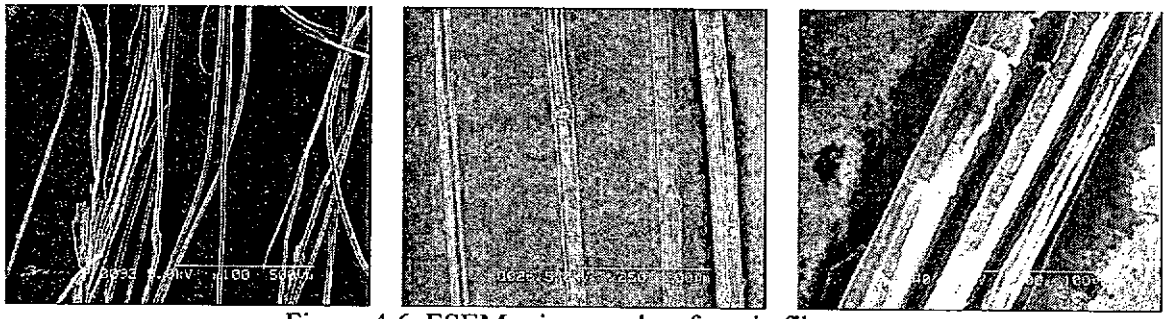

Figure 4.6: ESEM micrographs of ramie fibers

With the primary electron beam scanning the surface of the non-coated fiber, permanent damage to the fiber due to the thermal degradation would occur [262]. The effect of fiber charging and thermal degradation acting upon the fiber depends on the electrical conductivity and the thermal resistance of the fiber. When compared to the cellulose materials, the conductivity of wool fiber is lower [111, 118, 178] and this might be the reason why the severe charging effect appeared. Apart from the conductivity, the presence of lignin in the flax fiber also provides a protection against the damage induced by the electron beam [84]. Moreover, flax fiber also has a higher thermal resistance temperatures than wool, cotton and ramie [111], therefore, flax fiber is a good candidate for the morphological study under ESEM [84].

4.1.2 Surface Topography Study by AFM

It is known that poor vertical sensitivity of SEM is related to the fact that only a large intensity variation (in flux of secondary electrons) of over 5% can show differences in contrast. Thus the image resolution detail is limited. For the Scanning Probe Microscopy (SPM) like Atomic Force Microscopy (AFM) or Scanning Tunneling Microscopy (STM), it is strongly dependent on surface probe interaction between the tip and surface, hence the vertical resolution is higher. More direct surface visualization of fiber surface based on the registration of the intermolecular

repulsive force can be achieved [161]. Moreover, the fibers cannot be modified or treated for further studies after SEM imaging as they have a coating on them [192].

AFM studies of carbon fibres have been compared with those from SEM and show that the conductivity of carbon fibres permits direct visualization by SEM without metallic coating. AFM enables more resolved three-dimensional surface profile to be achieved [161, 228]. A complementary study of the surface features such as the scale height of wool fibers was reported by using AFM [192]. For composites, wher surface features of the reinforcing fibers are important in determine their interface with the matrix, AFM and SEM have been used to obtain a better understanding of surface topography of three different kinds of glass fibers [7]. The nano-scale morphology, friction, adhesion and elastic modulus of a spin finish layer on a polypropylene fiber surface has also been studied by AFM [158].

4.1.2.1 Operating principles and main components of AFM

AFM can be used for non-coated or wet samples or even samples in solution. AFM measures the repulsive or attractive force between a tip located at the end of a cantilever and the sample on the basis of a cantilever deflection. Figure 4.7 shows the forces between the probe and sample when the probe approaches to the sample surface. The spatial variation of the tip-sample repulsive force or that of the tip height is converted into an image. Because the repulsive or attractive force is universal, AFM is applicable to conducting as well as insulating materials. In general, AFM enables one to detect surface morphology, nano-scale structures, and molecular- and atomic scale lattices [77, 102, 160, 164].

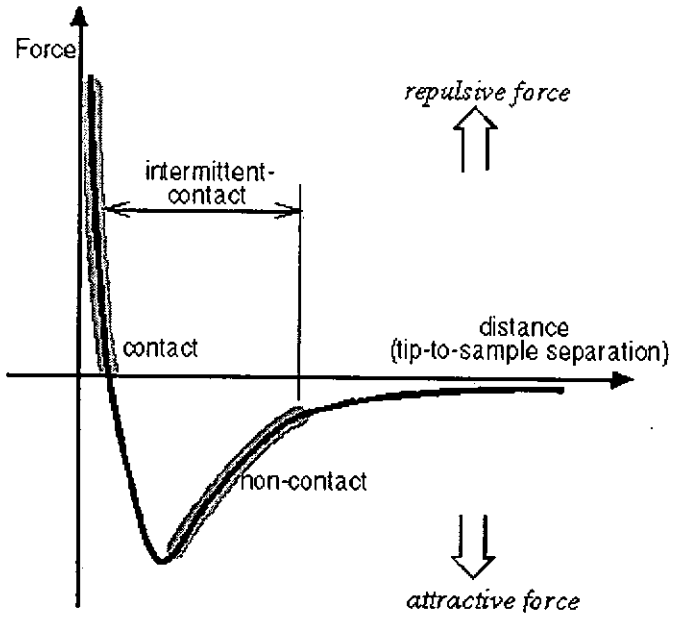

Figure 4.7 Force against distance curve observed in AFM experiment [72]

The AFM probes the surface of a sample with a sharp tip, a couple of microns long and often less than 100Å in diameter. The tip is located at the free end of a cantilever that is 100 to 200μm long. Forces between the tip and the sample surface cause the cantilever to bend or deflect. A detector measures the cantilever deflection as the tip is scanned over the sample, or the sample is scanned under the tip. The measured cantilever deflections allow a computer to generate a map of surface topography.

The probe operating in AFM may be explained by considering the curve in Figure 4.7, where the force between two atoms as a function of separation are considered. As the atoms are gradually brought together, they first weakly attract each other. This attraction increases until the atoms are so close together that their electron clouds begin to repel each other electrostatically. This electrostatic repulsion progressively weakens the attractive force as the inter-atomic separation continues to decrease. The force goes to zero when the distance between the atoms reaches a

couple of angstroms, about the length of a chemical bond. When the total van der Waals force becomes positive (repulsive), the atoms are in contact.

The slope of the van der Waals curve is very steep in the repulsive or contact regime. As a result, the repulsive van der Waals force balances almost any force that attempts to push the atoms closer together. In AFM, this means that when the cantilever pushes the tip against the sample, the cantilever bends rather than forcing the tip atoms closer to the sample atoms. In addition to the repulsive van de Waals force, two other forces are generally present during contact AFM operation namely the capillary force exerted by the thin water layer often present in an ambient conditioned ample and the force exerted by the cantilever itself. The capillary force arises when water wicks its way around the tip, applying a strong attractive force that holds the tip in contact with the surface. The force exerted by the cantilever is similar to the force of a compressed spring. The magnitude of the capillary force depends upon the tip-to-sample separation, the deflection of the cantilever and its spring constant.

In a scanning probe microscope, the sample surface is scanned with the sharp probe at a distance of less than a few nanometers or in mechanical contact. For scanning, either the tip moves against the fixed sample or the sample moves against the fixed tip. Since the nature of the probing interactions is different in STM and AFM, they have different probes and detecting mechanisms. The common parts of a scanning probe microscope are a piezo-electrical scanner on which the moving element is mounted, and a coarse mechanism by which the tip and sample are brought close together so that the probing interactions can be measured with an appropriate

detector. The detected signal is used for feedback control to adjust the tip-sample distance during scanning.

The schematic diagrams of the main components of AFM are shown in Figure 4.8. The microscope head contains the scanner, coarse mechanism, probing tip and detector. Instrument operations are performed through the electronic unit controlled by the computer station. The software allows monitoring of the tip-sample approach, and records the strength of the probing interaction as a function of the tip position, before it converts the collected information into the image on the screen and stores the data in the computer. Contemporary scanning probe microscopes are designed to perform both STM and AFM measurements by simply switching the heads [160].

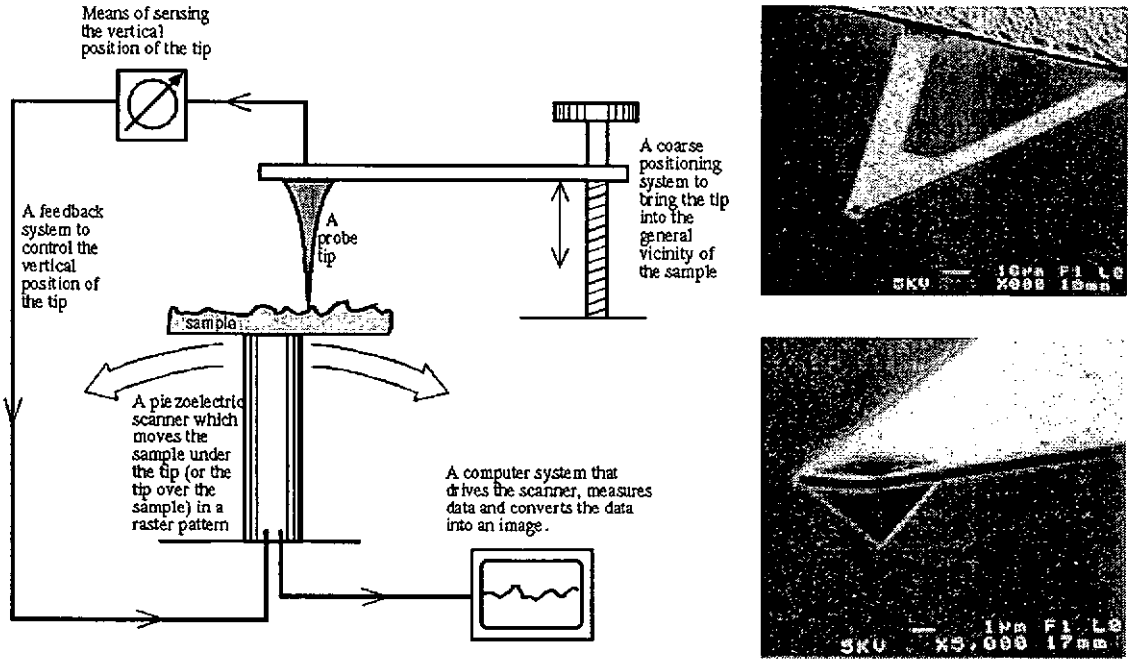

Figure 4.8: Schematic representation of the main components of an AFM and the SEM image of cantilever and tip [72]

The driving motion in scanning probe instruments is normally performed by a piezo-electrical scanner which changes its dimension under an applied voltage. The

strength of the local probing interactions between the tip and the sample becomes measurable only when the tip is positioned close enough to the sample surface. To prevent any possible damage of the sample by a tip-sample contact, the approach of the tip to the sample should be delicate.

Initially, the tip and sample are put close to each other by manually rotating the high precision mechanical screws which are incorporated into the microscope stage. This procedure is facilitated by an optical control when a scanning probe microscope is combined with an optical microscope or optical camera system. Closer approach is performed by the stepper motor which brings the tip to the sample at the separations that can be controlled by the scanner. The final adjustment of the tip and sample separation to the value at which the probing interaction reaches the 'set-point' level determined by the user is performed by the scanner. During scanning, the vertical movement of the tip is adjusted according to the chosen feedback gain, while the lateral motion proceeds independently. Conventionally, the fast and slow scanning directions are taken to be the x- and y- direction respectively [160].

4.1.2.2 AFM imaging modes

The AFM imaging can be done in the contact (repulsive) mode, the non-contact (attractive) mode or the tapping (intermittent) mode as shown in Figure 4.7. In contact image (repulsive mode), the AFM tip is pressed against the surface, causing the cantilever to deflect away from the sample. Thus the AFM tip makes soft physical contact with the sample. The sample surface is tracked by the tip using a feedback system that maintains a constant preset force on the cantilever by controlling the sample height (z-coordinate) as the sample is rastered under the tip

(x- and y- coordinates). The deflection of the cantilever is usually monitored through the displacement of a laser beam reflected off the cantilever onto a segmented detector. Imaging in the contact mode has been used to investigate wool, glass and polypropylene fibers [7, 158, 192].

Non-contact (attractive mode) imaging maintains the AFM tip several nanometers above the sample surface and detects the weak attractive forces that are present in this region. An AC voltage is applied to the cantilever, causing it to oscillate. Variation of the cantilever resonance will occur if the attractive force as well as the distance between the tip and sample (z-coordinate) are changed. Images of wool fibres are not taken in the attractive mode because these small forces cannot easily be detected in liquid [192]. There is also a decrease in resolution from the repulsive to the attractive mode because of the greater distance between the tip and the surface.

For soft materials, the application of the smallest force in the contact mode might still damage the weak surface structures. One of the factors causing this problem is the lateral force that the tip applies to the sample surface. To avoid this lateral force, the tapping mode can be employed. In the tapping mode, the energy delivered to the sample from the vibrating tip is determined by the amplitude of the free vibration and the 'set-point' drop in the amplitude. When the sample approaches the vibrating tip, they come into intermittent contact (tapping), thereby lowering the vibration amplitude. The amplitude drop is used for the feedback. In this mode, the tip-sample lateral force is greatly reduced and the short tip-sample contact time prevents inelastic surface change [160].

Imaging in the contact mode is heavily influenced by frictional and adhesive forces which can damage the sample and distort the image data. The non-contact mode generally provides a lower resolution and can also be hampered by the contaminant layer which can interfere with oscillation. The tapping mode reduces the lateral forces by intermittently contacting the surface and oscillating with sufficient amplitude to prevent the tip from being trapped by adhesive meniscus forces from the contaminant layer [72, 187, 239]. Tapping mode AFM has become an important technique since it overcomes the limitations of both contact and non-contact AFM methods.

4.2 EXPERIMENTAL DETAILS

4.2.1 Sample Preparation for ESEM

The material used was the scoured and bleached flax fibers. The time-series examination was illustrated by applying plasma treatment on a flax fiber with various accumulated exposure times. Plasma treatment was conducted using the same conditions as specified in Section 3.2.1. In each plasma treatment, fiber samples were fixed on the carbon-based, electrically-conductive, double-sided adhesive discs and exposed to oxygen or argon plasma at a pressure of 15Pa and 200W discharge power. After being treated for the pre-determined exposure time, the sample was removed from the chamber and then transferred to the ESEM chamber for morphological characterization. By repeating the plasma treatment, the time-series examination of the surface with the accumulated exposure time varying from 0min, 2.5min, 5min, 10min, 20min, 40min and 60min were carried out.

For re-locating the fiber section in the time-series experiment, carbon adhesive tapes perpendicular to the fiber axis was used with crossing-marks for reference. A covering adhesive tape was put on the top of the fiber.

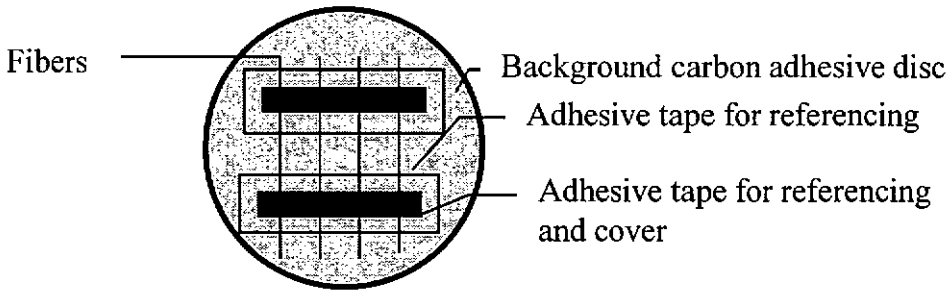

4.2.1.1 Material characterization procedures and operational parameters of ESEM

A Hitachi S-2380N Scanning Electron Microscope was used. Samples were mounted on a stub covered with the carbon-based, electrically-conductive, double-sided adhesive discs. The samples were viewed by using ESEM without drying and coating. The operational parameters of ESEM instrument are specified in Table 4.1

Table 4.1: Operational parameters of ESEM instrument

	Operation Parameters
Working distance (mm)	8mm
Accelerating voltage (kV)	8kV
Emission current (μA)	30μA
Beam scan time (s)	0.5s
Acquiring time (s)	80s
Chamber pressure (Pa)	1Pa
Magnification	up to x3000

Comparison of the structural identification and image quality was done by re-examining the same sample using the conventional SEM. After the ESEM examination, the 60 minutes treated samples were gold coated and viewed under

Lecia Cambridge Stereoscan 440 SEM at 10kV which was operated at a pressure of 10^{-6}Torr.

4.2.1.2 Application of image processing technique

Imaging processing techniques were used to quantify the surface features of the plasma treated fiber at different stages of treatment based on the ESEM micrographs. MATLAB Imaging Processing software was used for quantitative analysis.

4.2.1.3 Determination of fiber diameter and fabric weight loss

Changes of fiber diameter with plasma exposure time were measured based on the ESEM micrographs. The fiber diameter was determined before and after plasma treatment. The difference in observed fiber diameter was used to calculate the fiber diameter reduction percentage and the average of fifteen readings was taken. Fabric samples subjected to the plasma treatment with the corresponding exposure time and other conditions as specified in Section 3.2.2.1 and discussed in Section 3.3.1.3 will be used to compare with the reduction in fiber diameter. The paired comparison *t*-test was used to determine whether any statistical significant difference occurred with a confidence limit of 95%.

4.2.2 Sample Preparation for AFM

Untreated, argon and oxygen plasma treated flax fiber samples were imaged by AFM to determine the nature of the surface features as well as the lateral and vertical dimensions of the surface pits resulting from the plasma treatments. The fibers were exposed to the oxygen or argon plasma at a pressure of 15Pa and 200W discharge power for 60 minutes as described in Section 3.2.1. Afterwards, the sample was

removed from the chamber and stored in a sealed nitrogen gas environmental before characterization.

4.2.2.1 Material characterization procedures and operational parameters of AFM

Individual flax fibers were mounted onto double-sided tape with the plasma treated sides facing upwards and it would be imaged within 24 hours of being exposed to air. The AFM imaging was preformed at CSIRO, Division of Wool Technology, Australia, with a Digital Dimension^{TM} 3000 Scanning Probe Microscope. Measurements were conducted under room conditions.

The imaging was done with the fast scanning direction parallel to the fiber axis using a Digital Instruments Etched silicon tip (TESP). The tip radius is 5-10nm while the tip height is 10-15μm. Tip half cone angle is 18° front, 25° back and 10° side. A single beam cantilever was used with the corresponding length of 125μm, 30μm-40μm width and 2.5μm-5μm thick.

The reported scan area was 7.5μm x 7.5μm. AFM images were collected at 1Hz with 512x512 pixels. Phase images were acquired at the same time as the height image. Images were flattened (3rd order polynomial) to remove fiber curvature in the slow scanning direction before the image analysis was taken. The 'flatten' command removes the Z offset between scan lines and the tilt in each scan line by calculating a third order least-squares fit for the selected segment and subtracting it from the scan line. Bowing effects along the Y-axis are also removed. All images presented are the original pictures without any filtering or contrast enhancement.

4.3 RESULTS AND DISCUSSIONS

4.3.1 Effect of Plasma Treatment on the Surface Morphology Studied by SEM and ESEM

4.3.1.1 Time-series observation of fiber surface morphology

ESEM was used to observe the time-series fiber surface appearance treated by plasma for various accumulated exposure times. The micrographs in Figure 4.9 and Figure 4.10 show the longitudinal views of flax fibers including nodes which are the dislocations of the fibrils. The variation in fiber diameter depends on how many fibrils are present in the fiber. The untreated fiber shows a slightly charging effect. After plasma exposure over 5 minutes, the charging effect during ESEM observation disappears. After an initial exposure to either argon or oxygen plasma, the change in fiber appearance is not distinguishable. As the exposure time is prolonged, the change of fiber surface appearance becomes more obvious.

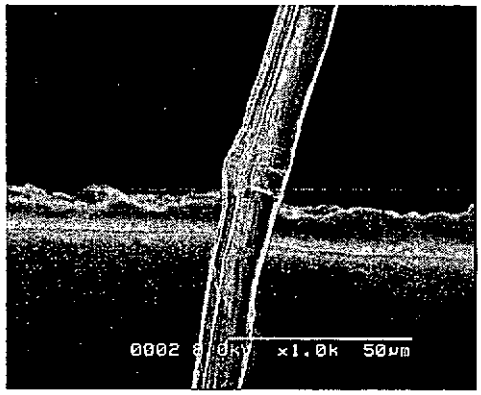

Untreated

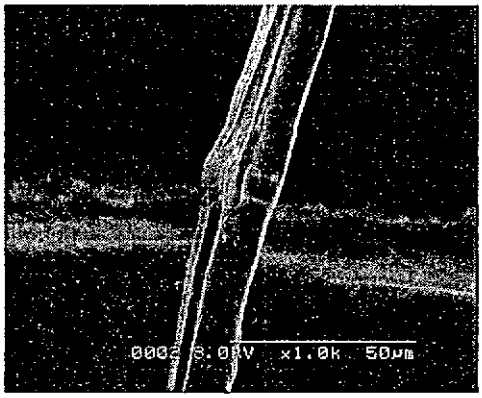

2.5 min.

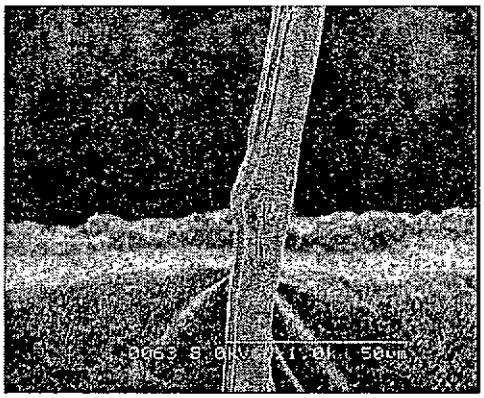

20min.

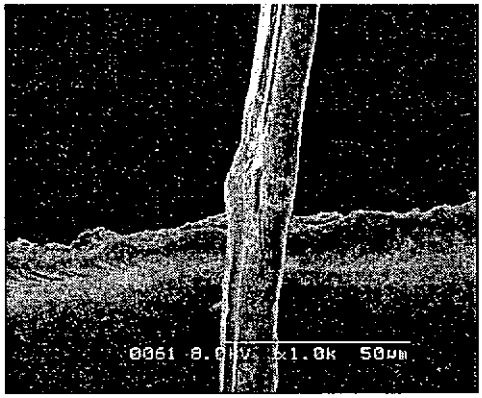

5min.

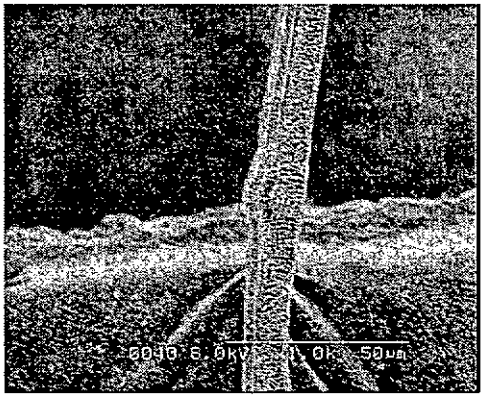

40min.

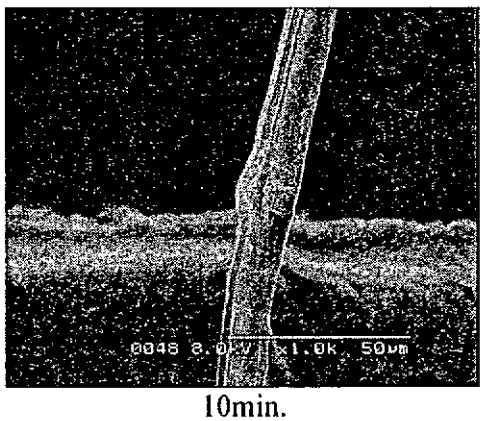

10min.

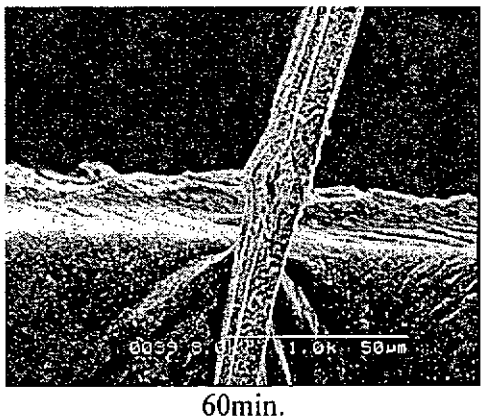

60min.

Figure 4.9a: ESEM micrographs (x1000) showing the progressive etching by oxygen plasma on flax fiber

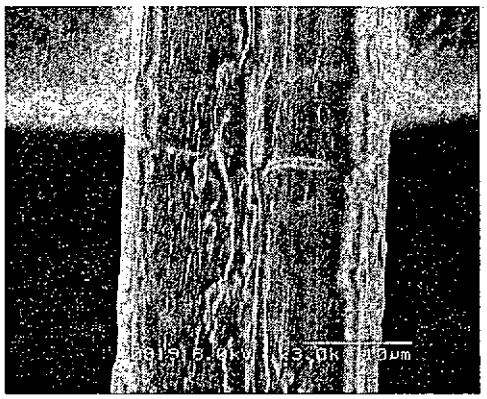

Untreated

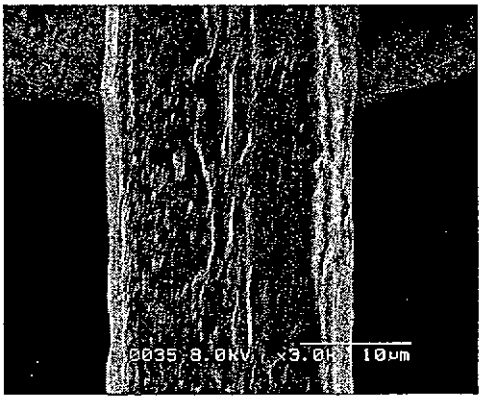

2.5min.

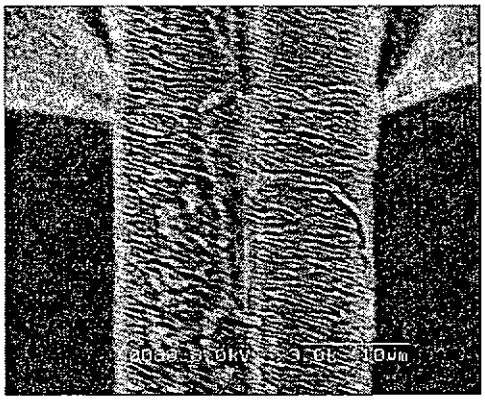

20min.

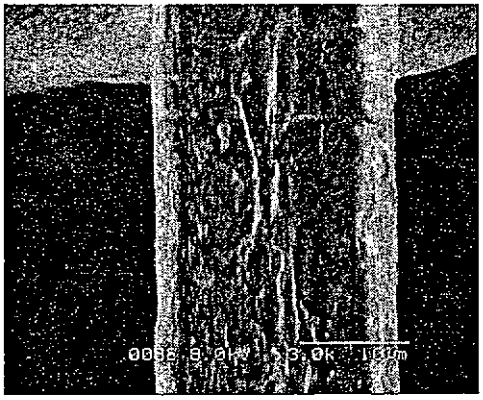

5min.

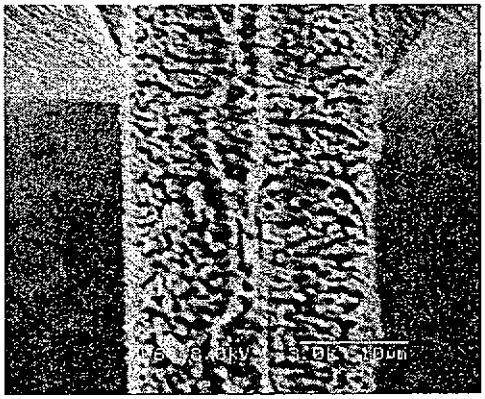

40min.

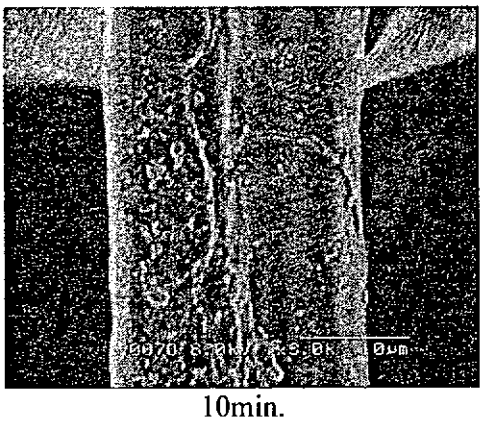

10min.

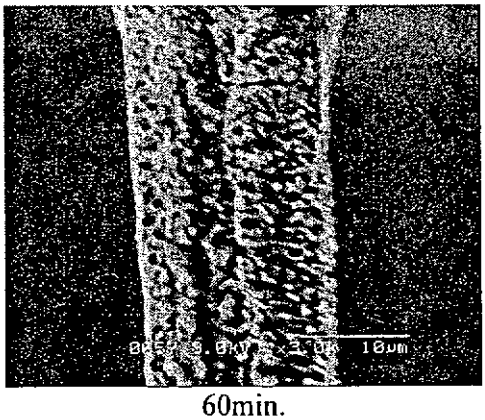

60min.

Figure 4.9b: ESEM micrographs (x3000) showing the progressive etching by oxygen plasma on flax fiber

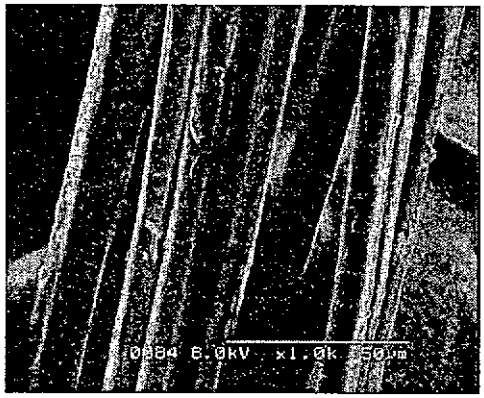

Untreated

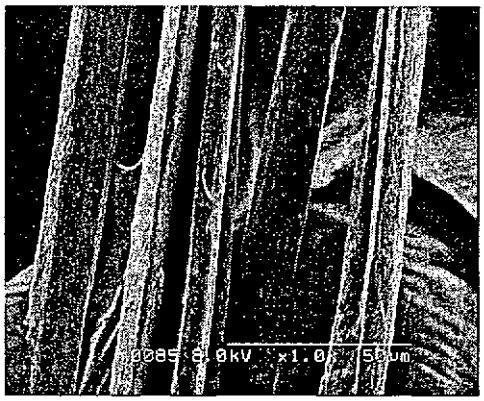

2.5min.

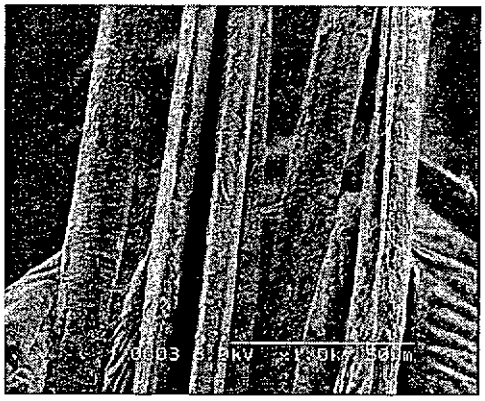

20min.

5min.

40min.

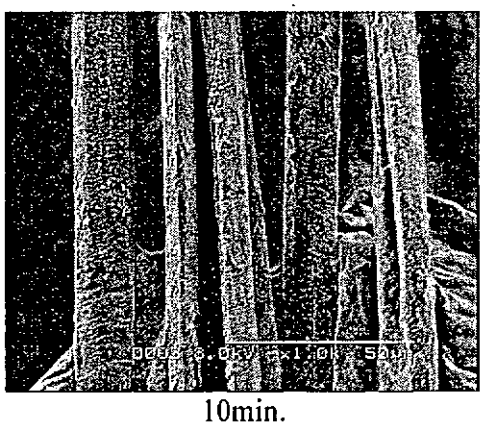

10min.

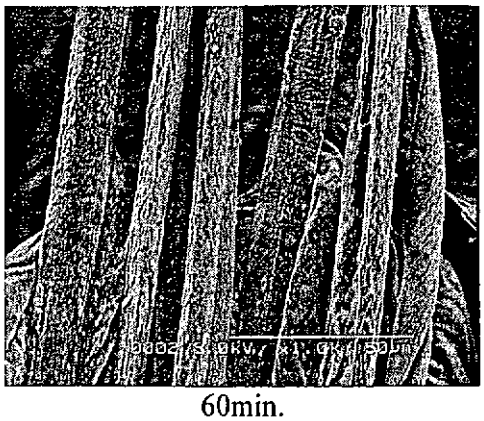

60min.

Figure 4.10a: ESEM micrographs (x1000) showing the progressive etching by argon plasma on flax fiber

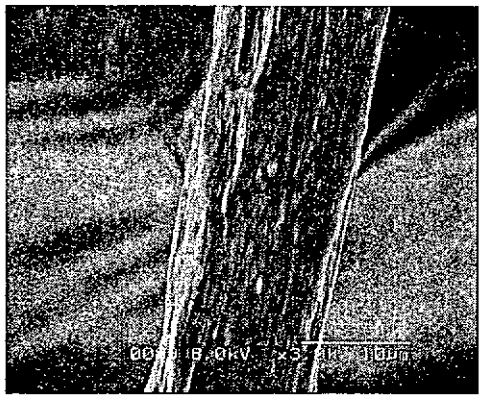

Untreated

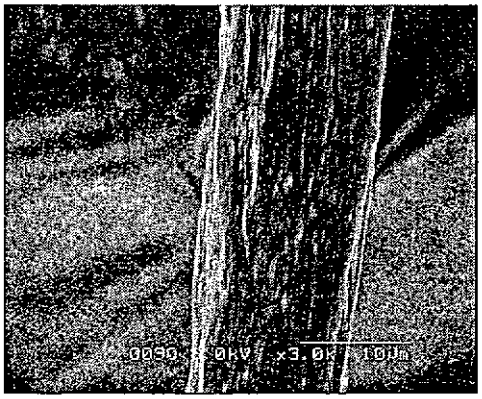

2.5min.

20min.

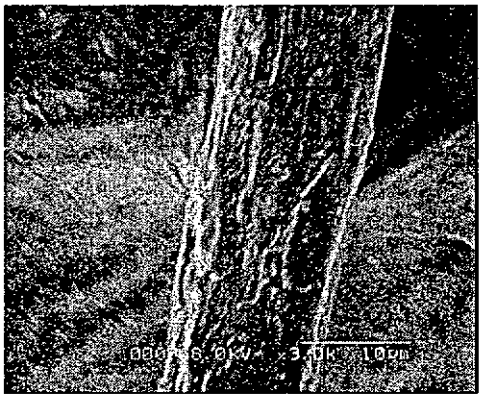

5min.

40min.

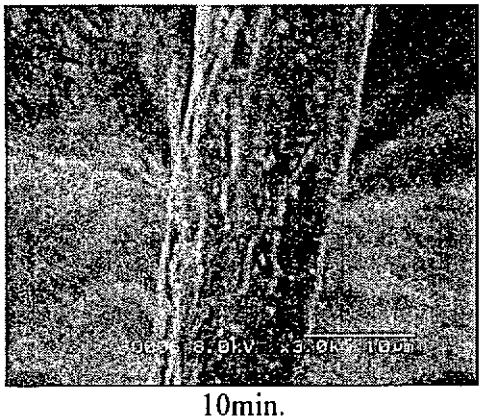

10min.

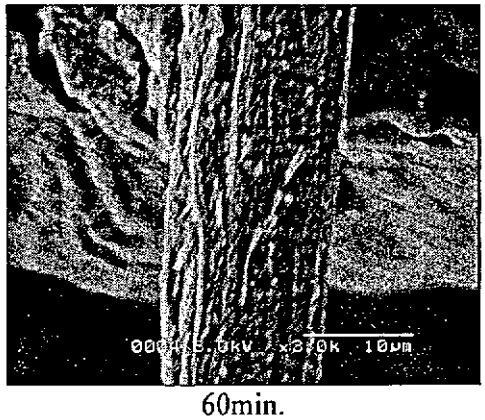

60min.

Figure 4.10b: ESEM micrographs (x3000) showing the progressive etching by argon plasma on flax fiber

The micrographs of the fibers treated with the oxygen plasma illustrate a progressive change of the fiber surface morphology with the treatment time as shown in Figures 4.9a and 4.9b. They reveal the formation of voids and cracks on the fiber surface due to the plasma ablation. Progressive pitting and surface damage on the fiber surface implies that the surface area is significantly increased. It seems that certain spots on the fiber surface are more susceptible to plasma etching to form cracks with a pronounced empty corncob structure. The typical dimension of the surface structure is within the micrometer range after a prolonged exposure. In some cases, the occurrence of fiber etching starts from the nodes along the fiber.

The oxygen plasma shows a faster etching rate by exhibiting a progressively spitted and etched pattern after only 10 minutes of accumulated exposure. On the other hand, argon plasma treatment shows a relatively slower etching rate and the etched pattern appears significantly after 40 minutes of accumulated exposure as shown in Figures 4.10a and 4.10b. When comparing to the oxygen, the argon plasma was not as effective in changing the surface morphology.

The changes in the fiber surface morphology can be explained by the localized ablation of the surface layer. The presence of micro-pores indicates this predominant effect of the interaction of oxygen plasma (chemical etching) with the fiber surface. Differential etching of crystalline and amorphous regions might be the origin of the roughness. This process leads to almost a complete breakdown of molecules on the surface into very low molecular components which eventually vaporize in the low pressure system when the exposure time is prolonged [277].

As seen from the oxygen plasma treated sample, the depth of etching increases progressively with increasing exposure time. It also shows that the etched micro-pores are deepened after prolonged exposure. With increased exposure time, continual pore enlargement occur indicating that the plasma etching action is a continuous process. As pore deepens, so, fiber bulk damages will occur especially when the oxygen plasma is used. The adhering material on the fiber surface may remain on the fiber surface even after 60 minutes of argon plasma exposure. When the oxygen plasma is used, the adhering material is completely removed after 40 minutes of exposure. This implies that the weight loss is due to the breakdown of small molecules on the fiber surface which eventually vaporize inside the exposure chamber. This is mainly attributed to the creation of micro pores resulting in the reduction of fiber diameter [277].

Apart from the fiber pitting and etching, with reference to the bottom carbon adhesive tape, fiber contraction also occurs during the plasma treatment as the exposure time is increased. The cross-marking between the fiber and carbon adhesive tape is changed with the exposure time. When compared to the micrographs of 60 minutes plasma treated fibers (Figure 4.9a), the creasing mark under the fibers becomes more obvious. However, this occurs only to the portion under the fiber while the rest of the carbon tape remains in a straight condition. This suggests that changes of crease marks originate from fiber contraction during the treatment. If fiber contraction occurs during the plasma treatment, it will counter balance the reduction of fiber fineness to a certain extent.

4.3.1.2 Results from image processing technique

The ESEM micrographs of the same portion of the fiber surface were analyzed further by the use of MATLAB Image Processing software. The samples selected for this study included the untreated flax fiber, and the 200W oxygen plasma treated fiber with exposure time of 10 minutes, 20 minutes and 40 minutes.

A monochrome picture is made up of numerous areas that differ in brightness. In sampling a picture to produce a digital image, discrete brightness values are assigned to each picture element or 'pixel'. In MATLAB, the image is stored as a single matrix. Normally, the intensity matrix contains double-precision values ranging from 0.0 to 1.0, with each element of the matrix corresponding to an image pixel. The elements in the intensity matrix represent various intensities or grey levels, where the intensity 0.0 represents black and the intensity 1.0 represents full intensity, or white [233, 264]. In this study, the intensity images are named as indexed images with an implied gray scale colormap having a length of 256. Similarly, the intensity 0 represents black and the intensity 256 represents full intensity or white.

In Figure 4.11a, the images in the left column are the original ESEM images obtained while those in the second column are the images selected from the original image for image processing. The latter cut images each consists of 512 x 512pixels. The 512 x 512 pixels image was used as an input file and the data points were selected in alternative rows and columns in order to produce an 256 x 256 pixels indexed matrix. The choice of these sizes was determined mainly by the computation time, and it seemed to be quite suitable for this analysis [265].

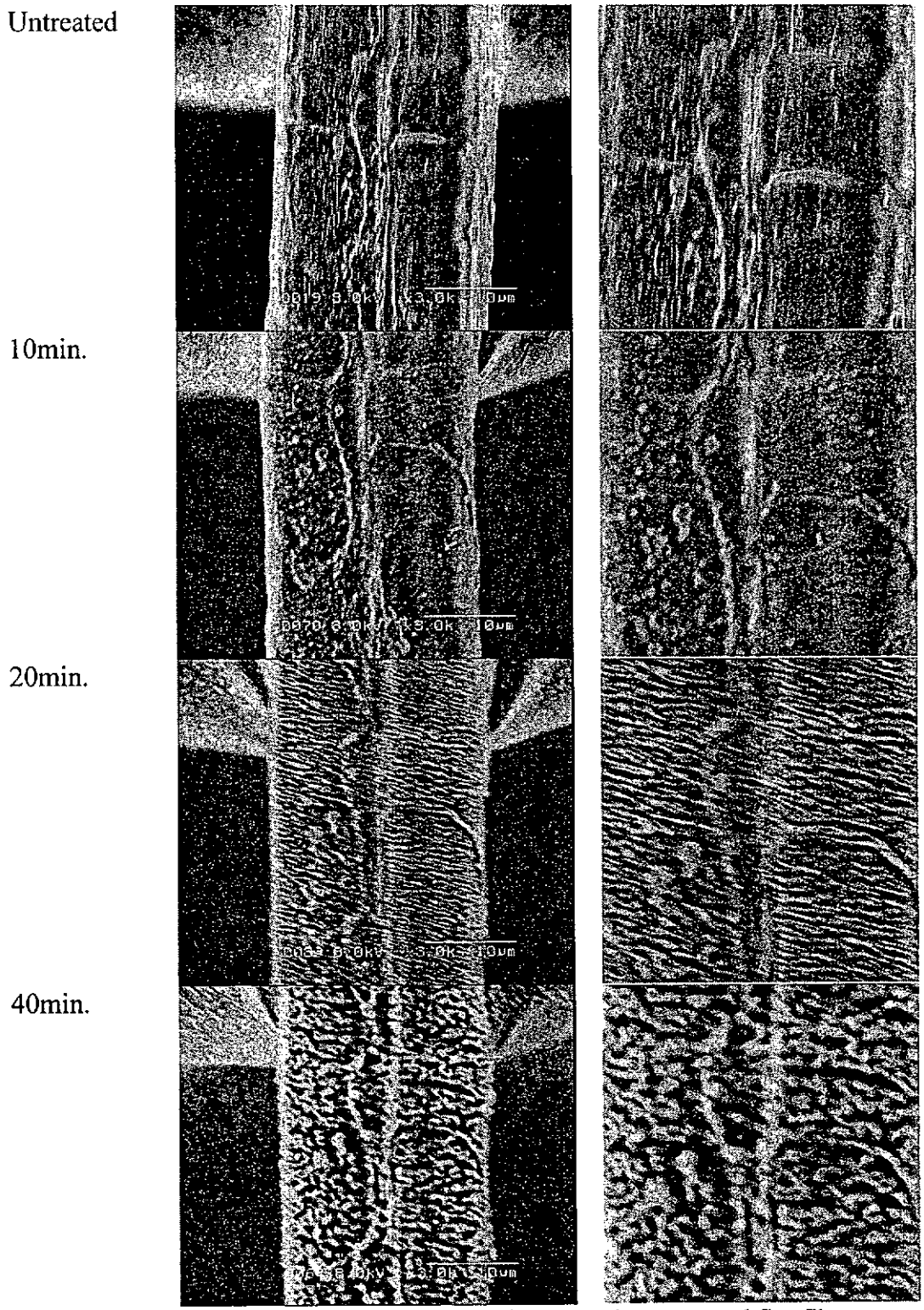

Figure 4.11a: ESEM micrographs of oxygen plasma treated flax fiber

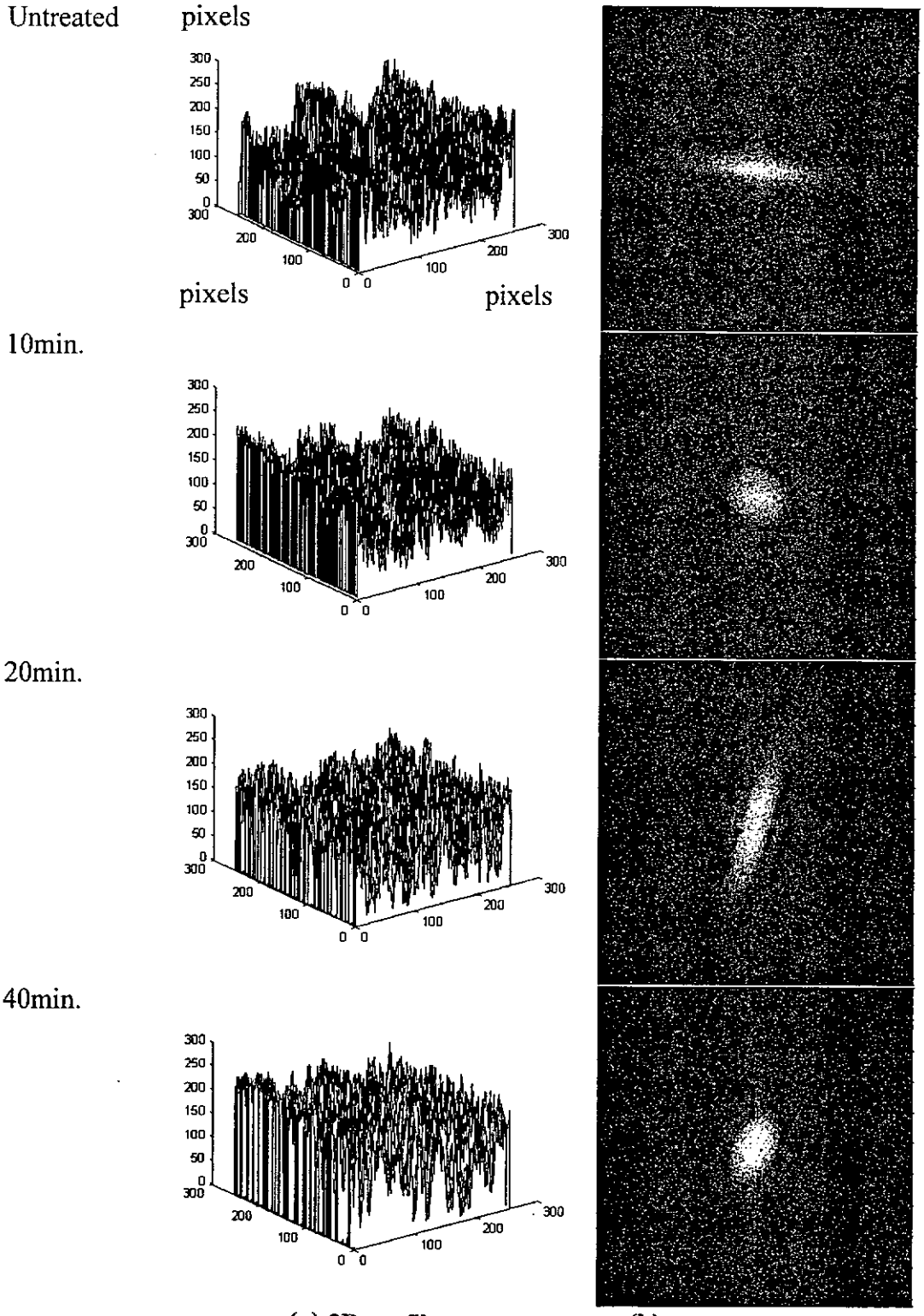

Figure 4.11b: Surface feature of oxygen treated flax fiber

In Figure 4.11b, the first column shows the intensity plots of data points of the indexed matrix. The x-axis of the plot of the indexed matrix represents the data point along the width of the fiber while the y-axis of the plot represents the length of the fiber along the fiber axis. The size of this cut part is around 20μm x 20μm. The z-axis represents the intensity range of the fiber surface which reflects the surface roughness or the surface profile of the fiber. From the plots, it can be found that the surface profile of the flax fiber has changed with the increase of the treatment time. The plane of x = 0 or y = 0 shows the respective 2-dimensional profiles of the surface pitted pattern.

The ESEM micrographs illustrate the changes from relatively flat to a rougher surface as the plasma exposure time is increased. The depth and width of the pits seem to increase with the exposure time from sub-micrometer to micrometer in size. With the consideration of the vertical sensitivity of electron microscopy (only over 5% of variation in flux of secondary electron can show the difference in contrast) [192], it is still reasonable to represent the fiber surface profile by using a range of data points with different levels of intensity in each micrograph. Therefore, the data are further analyzed by using the Fast Fourier Transform (FFT) technique.

The FFT has been used as an efficient computational tool in a wide range of applications. FFT converts the image into a two-dimensional complex function (magnitude and phase) in a frequency domain. A power spectrum image can be derived from the FFT function, in which different components will inevitably be separated by their spatial frequencies. A periodic structure in the image will result in a peak (a high magnitude area) in the power spectrum, whose value and location

reveal the periodicity and directionality of the periodic structure. The Fourier transform provides the link between a waveform in the time (or spatial) domain and its spectrum in the frequency domain. Since locating peaks in the power spectrum is relatively easy, thus the power spectrum is a very useful resource for identifying the periodic structure of an image [265, 269].

The centered power spectra of the images are shown in the right column of the Figure 4.11b. The power at the origin indicates the so-called direct component (DC) reflecting the average brightness of the original image and the power values at other locations show frequency terms. Points on the same radius from the origin represent the same frequency term spreading in different directions. Points at a region near the origin represent low-frequency terms that provide the overall structure of the image, while points at a region far from the origin represent high-frequency terms. Since frequency terms can be readily isolated in a power spectrum, the spectrum is particularly useful for identifying periodic structure [269]. If the periodic structure has a dominant orientation angle, the power spectrum will exhibit a line distribution which is perpendicular to the orientation line of the structure [23].

The power spectrum shows that the surface of the untreated flax fiber with a dominant surface feature has an orientation angle of 5° or so. For the flax fiber treated for 10 minutes, its surface features are relatively random as shown by the FFT diagram. The FFT diagram shows that most of the intensities are concentrated near the origin, which represent low-frequency terms by providing the overall structure of the image.

For the 20 minutes treatment, the fiber surface has a dominant effect with an obvious pattern line can be found. This indicates that a relatively high frequency of surface pattern appears on the fiber surface with an orientation angle of approximately 75-80°. For 40 minutes, the surface features are changed into a more random pattern and lose the high frequency terms. By means of the FFT technique, the surface features of the plasma treated fiber can be described.

4.3.1.3 Fiber diameter reduction and fabric weight loss

The diameter of the fiber is also reduced after the plasma treatment. Figure 4.12 plots both the fabric weight loss and fiber diameter reduction against the plasma exposure time.

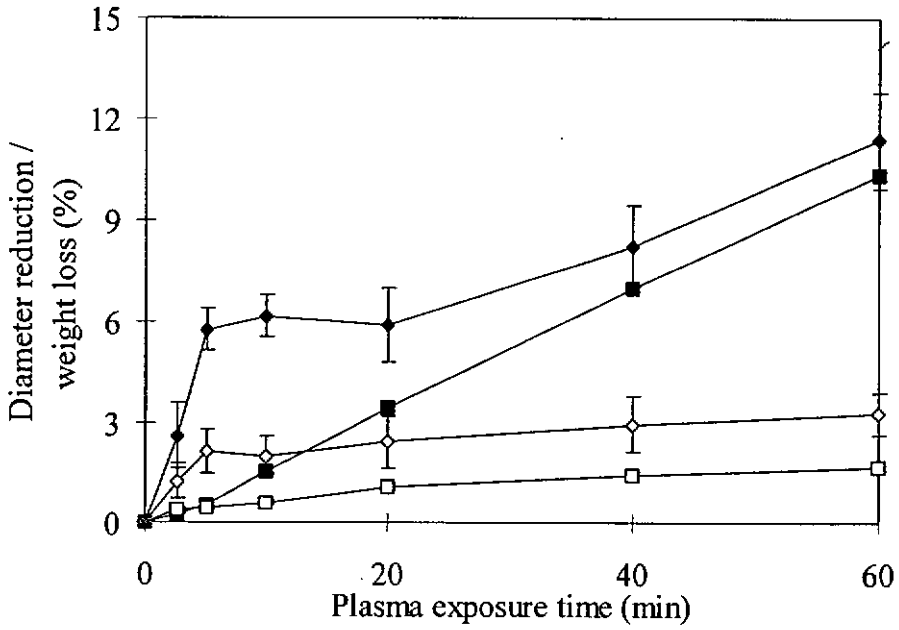

Figure 4.12: Percentage of weight loss and diameter reduction caused by oxygen and argon plasma at various exposure times (15Pa and 200W) (■) Untreated sample, (♦) fiber diameter reduction caused by oxygen plasma, (◊) fiber diameter reduction caused by argon plasma, (■) fabric weight loss caused by oxygen plasma, (□) fabric weight loss caused by argon plasma.

In the case of oxygen plasma, the weight loss increases with the treatment time linearly. The oxygen plasma brought about a much higher weight loss (10.3%) than

the argon plasma (1.7%) under the same conditions (60 minutes). The measured results obtained from 15 different fibers show that the reduction in fiber diameter ranges from 2.6% to 11.4% for the oxygen plasma treated sample and 1.3% to 3.3% for the argon plasma treated sample with the accumulated exposure time ranging from 2.5 minutes up to 60 minutes.

Cracks and micro-pores start to appear on the surface of the sample which has 6.2% reduction in diameter after 10 minutes of exposure of oxygen plasma. The voids and cracks become more pronounced as the exposure time is increased. The enlarged cracks at 40 and 60 minutes (corresponding to 8.3% and 11.4% reduction in diameter respectively) are similar to an empty corncob and perpendicular to the fiber axis (Figure 4.11a). Owing to the relatively slow rate of physical etching introduced by the argon plasma samples, the lower reduction levels of diameter (ranging from 1.3% to 3.3%) are obtained.

From the results obtained, the percentages of fabric weight loss are always lower than the fiber diameter reduction. However, the weight of the fiber should be proportional to the square of the fiber diameter, so that the fabric weight loss should be much higher than the fiber diameter reduction. When referring to the measurement methods, the value of fabric weight loss was obtained from comparing the fabric weight before and after the plasma treatment while the fiber diameter was obtained from the direct measurement of fiber diameter on the ESEM micrograph. As plasma treatment is mainly acting on the fabric surface, therefore, the reduction of fiber diameter may not take place on every fiber of the fabric. Hence, this is the

on possible reason why the fabric weight loss values are always lower than the fiber diameter reduction under the same exposure conditions.

4.3.1.4 Comparison with SEM micrographs

Figures 4.13 and 4.14 show the SEM micrographs of the plasma treated linen obtained under pre-determined and accumulated exposure. In Figure 4.13, the samples were treated under oxygen or argon plasma at various pre-determined exposure times, i.e., 2.5, 5, 10, 20, 40, 60 minutes as described in Section 3.3.2.2. In Figure 4.14, the samples were treated by accumulating oxygen or argon plasma exposure as described in Section 4.2.1. The objective of this surface morphological comparison is to determine the effect of plasma treatment under predetermined exposure and accumulated exposure.

When comparing the surface morphology obtained by the pre-determined and accumulated exposure under oxygen plasma, the micrographs obtained show similar surface features. However, the surface appearance of the argon plasma treated sample exhibits different extents of etching between two types of exposure conditions. Since the etching effect for the accumulated exposed sample shows a deeper etching than the pre-determined exposed sample, thus this implies that the effectiveness of argon physical etching can be enhanced by intermediate exposure.

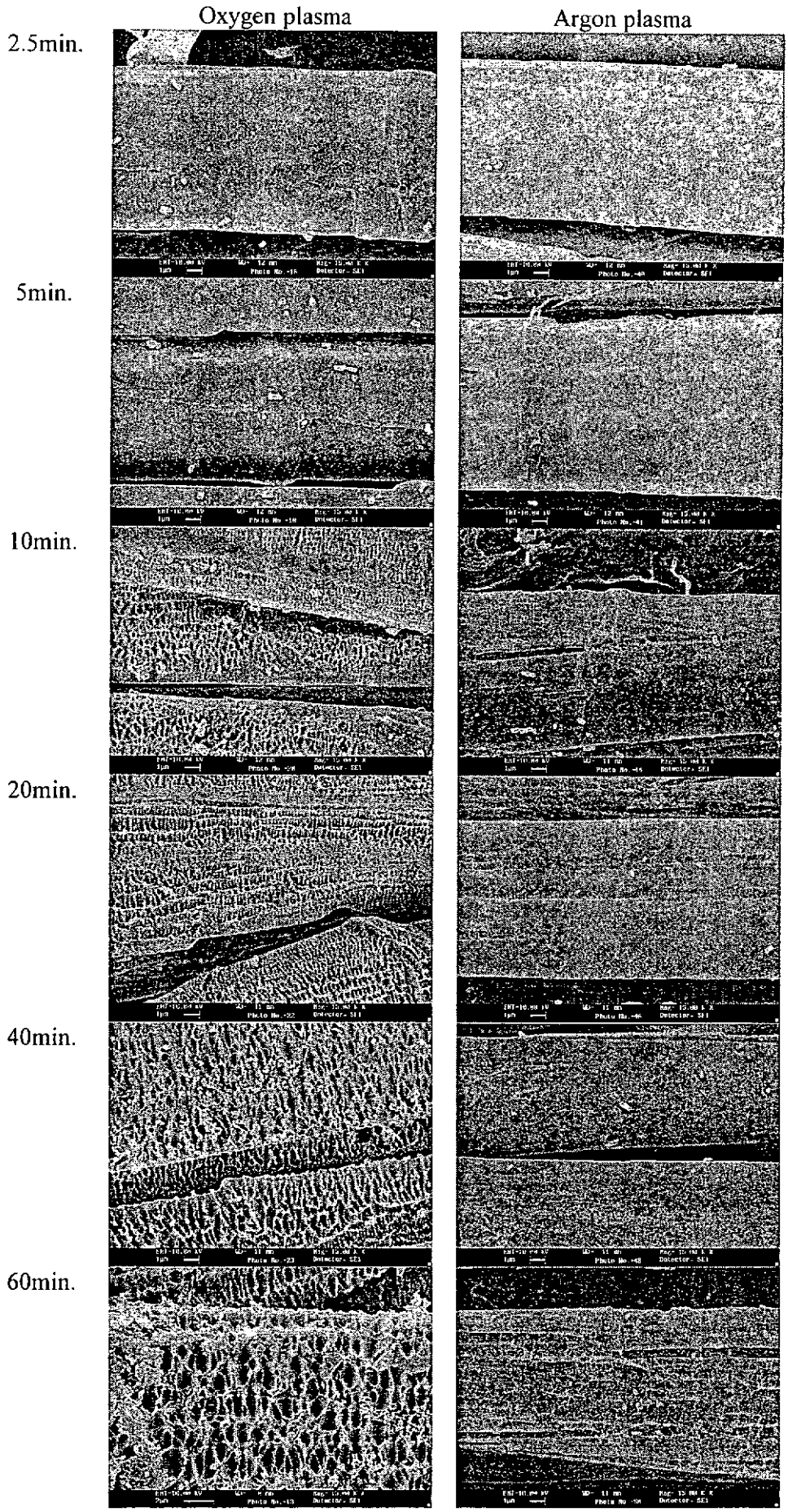

Figure 4.13: SEM micrographs of flax fiber etched by oxygen and argon plasma (pre-determined etching)

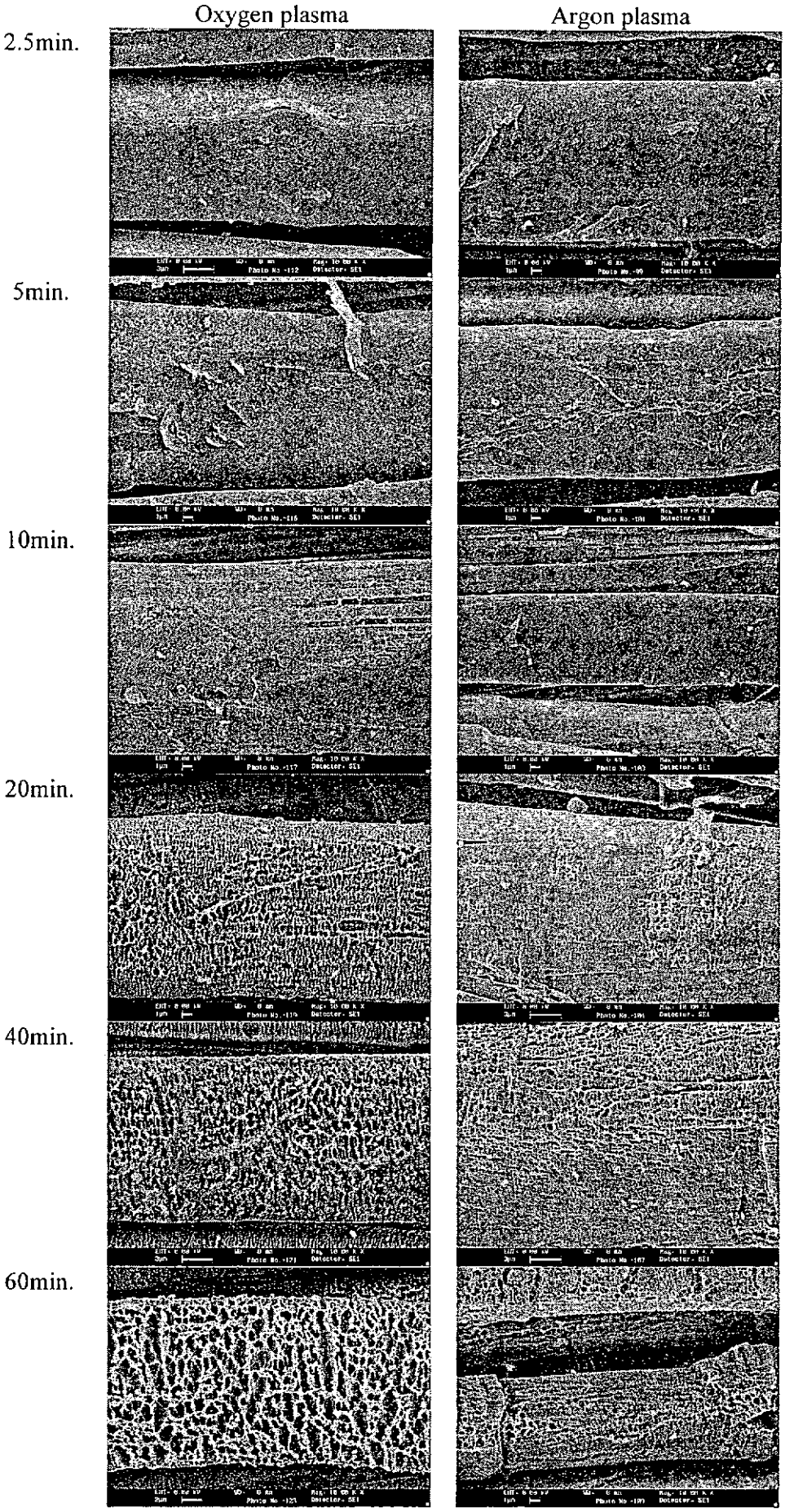

Figure 4.14: SEM micrographs of flax fiber etched by oxygen and argon plasma (accumulative etching)

In order to confirm the observation by ESEM was real and reproducible, the 60 minutes (accumulated) treated samples were further studied by SEM. The micro-pores in Figure 4.15 are much clearer than those obtained from ESEM in Figures 4.9 and 4.10. However, ESEM provides sufficient details on the surface features of the plasma treated samples.

Oxygen plasma treated fiber

Argon plasma treated fiber

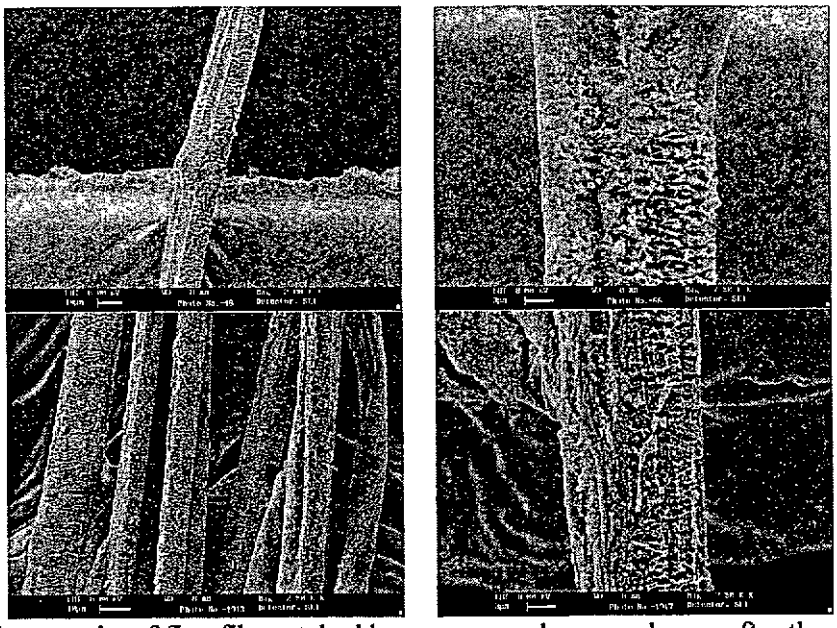

Figure 4.15: SEM micrographs of flax fiber etched by oxygen and argon plasma after the accumulation of 60 minutes exposure

4.3.2 Effect of Plasma Treatment on the Surface Topography of Flax Fibers Studied by AFM

4.3.2.1 Surface features

AFM images of the untreated, argon and oxygen plasma treated (both under the exposure conditions of 15Pa, 200W for 60 minutes) flax fiber are shown in Figure 4.16. As previously discussed in Section 3.3.2.2 and Section 4.3.1.1, the surface of the untreated flax fiber always consists of residual material. When comparing to the plasma treated flax fiber, the surface of the untreated fibers is relatively flatter and associated with distinguishable residual materials. The results obtained are consistent with the FeSEM images in Appendix 4-I.

Untreated flax fiber

Raw image

Flattened image

3-D image

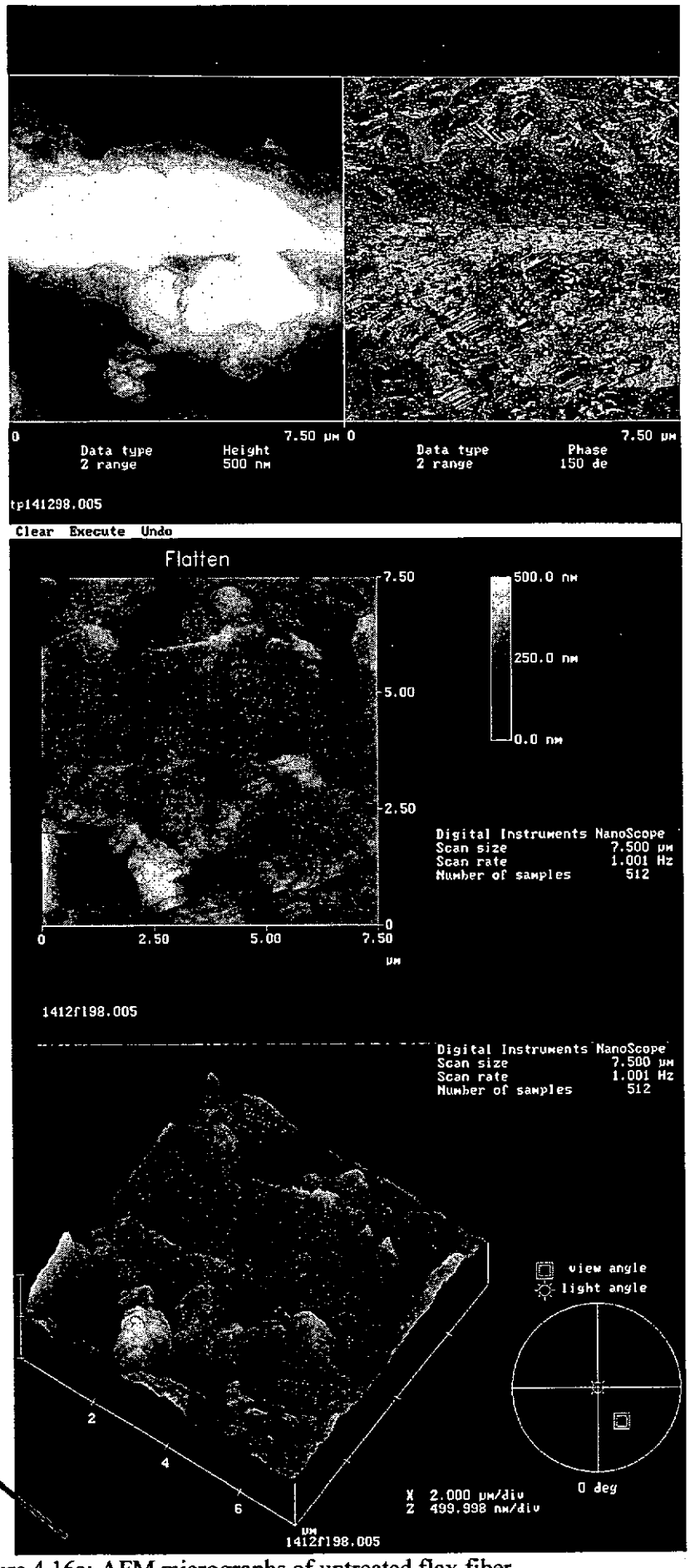

Fiber axis

Figure 4.16a: AFM micrographs of untreated flax fiber

Argon plasma treated flax fiber

Raw image

Flattened image

3-D image

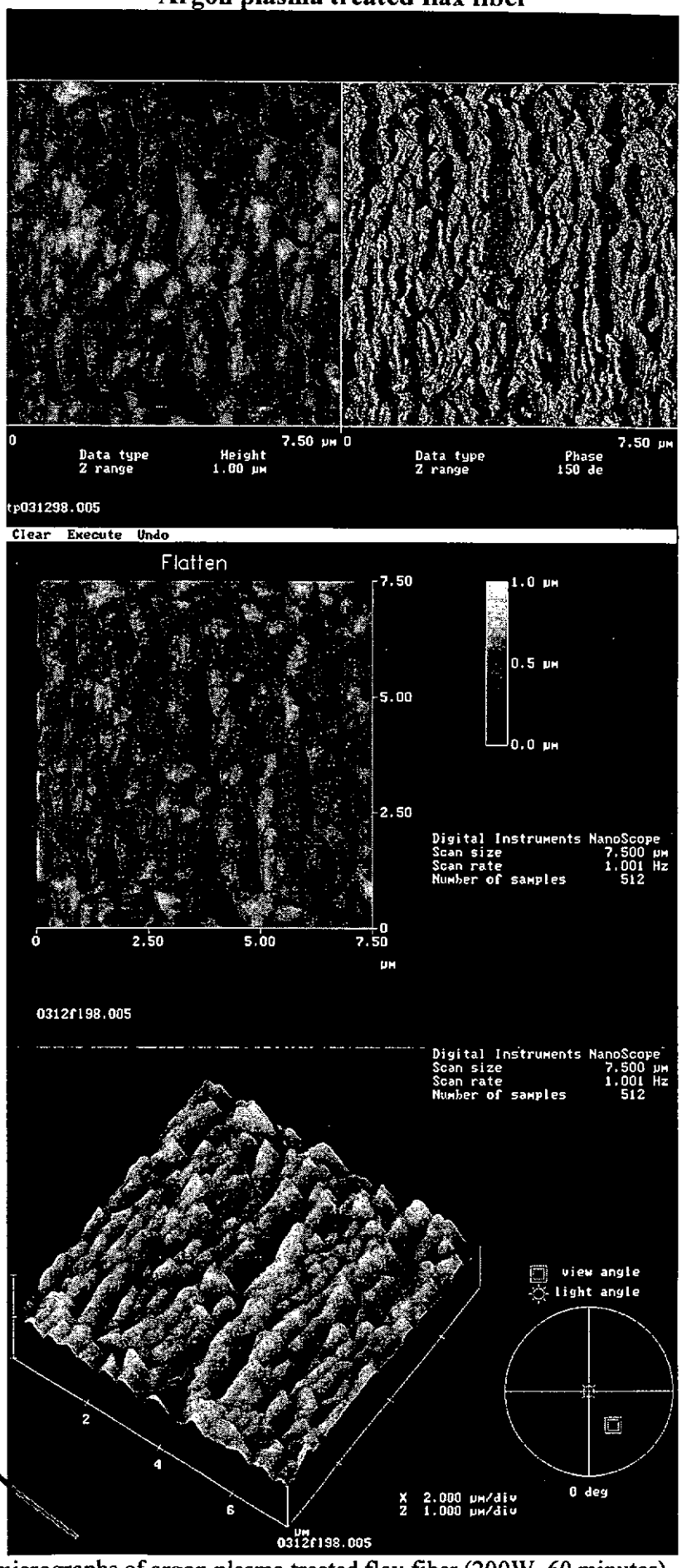

Fiber axis

Figure 4.16b: AFM micrographs of argon plasma treated flax fiber (200W, 60 minutes)

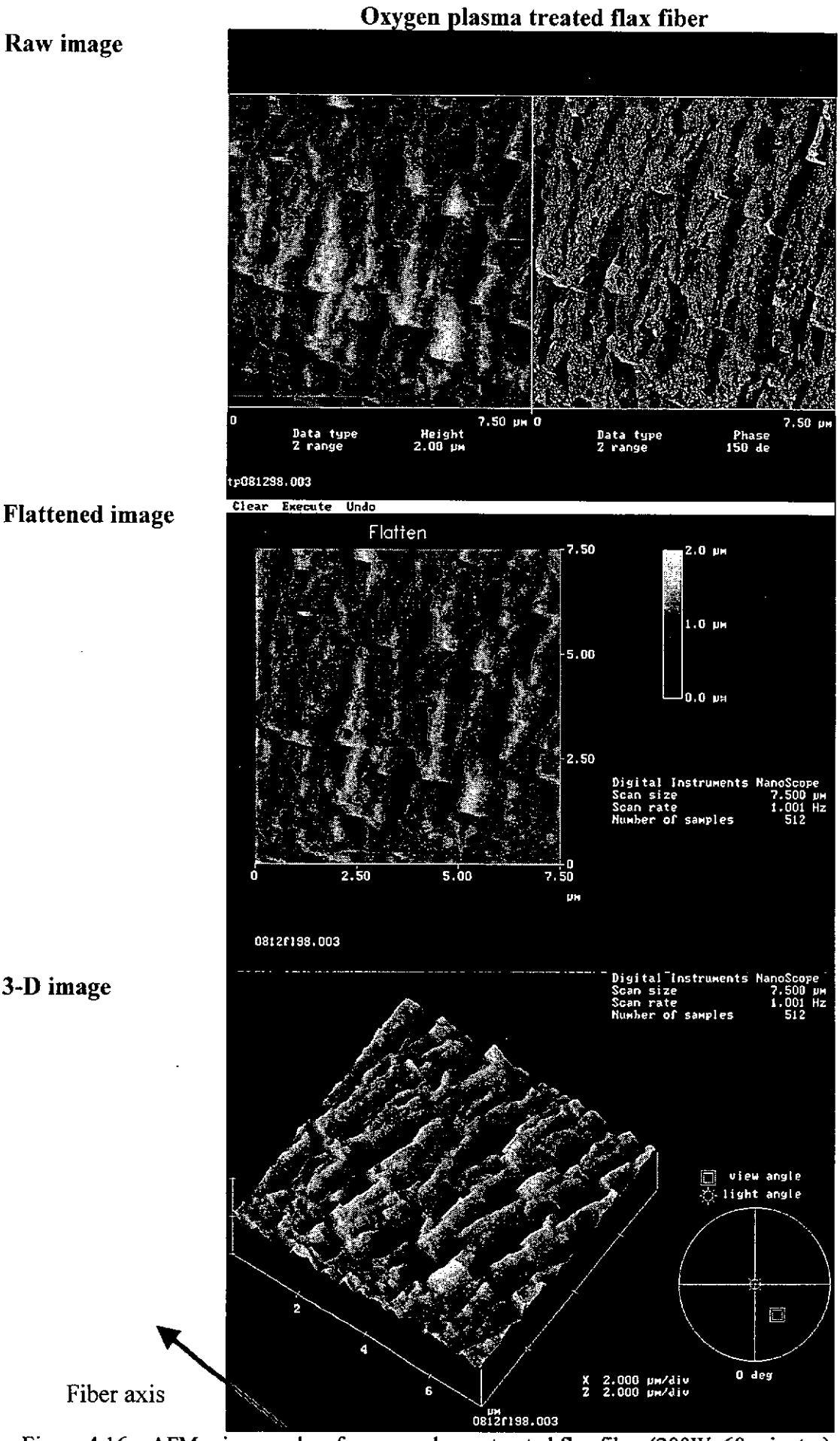

Figure 4.16c: AFM micrographs of oxygen plasma treated flax fiber (200W, 60 minutes)

The argon plasma has selectively attacked less resistant areas on the fiber surface, leaving a network of pitted areas of around micrometers in diameter. They appear to have elongated shape. Large pits appear to have depths of 200nm-400nm with the diameter ranging from 500nm-2000nm. The smaller features can be seen superimposed on these larger features. They are typically 50nm-150nm in depth and generally less than 100nm in diameter.

The surface of the oxygen plasma treated flax fiber is very rough. The random images show more variability and a high level of surface degradation in surface structures. The features between the pits appear to be broader and the details that can be seen here are not visible in the argon treated plasma flax fiber. Larger pits appear to have the depths of 1000nm-2000nm with the diameter ranging from 1500nm-2500nm. Smaller features are seen less frequently than for the argon treated flax fiber and are typically 200nm-500nm in depth and generally 250nm-500nm in diameter.

4.3.2.2 Surface roughness

Fiber surface roughness can be determined by the measurement of the pit sizes. Root Mean Square (RMS) roughness was calculated to highlight the change in the surface due to treatments. Table 4.2 shows the results from ten flattened images. Surface roughness measurements indicate an increasing level of damage from the control to the argon plasma treated flax fiber to the oxygen plasma treated flax fiber. The RMS value was increased from 40.9 of untreated sample to 98.0 of argon and 308.4 of oxygen plasma treated fiber.

Table 4.2: Root Mean Square (RMS) Roughness of untreated, argon and oxygen plasma treated flax fiber surface

	Untreated flax fiber	Argon plasma treated flax fiber	Oxygen plasma treated flax fiber
	47.2	79.1	412.4
	20.4	135.4	392.6
	44.3	84.8	177.6
	51.1	90.4	207.0
	81.2	90.7	303.3
	36.1	85.4	345.8
	19.0	101.8	260.5
	44.9	105.5	267.8
	35.3	81.4	391.8
	29.4	125.2	325.3
Average (nm)	**40.9**	**98.0**	**308.4**
S. D. (nm)	17.9	19.1	80.2
C. V (%)	43.8	19.5	26.0

4.4 CONCLUSION

ESEM has been used to study the time-series fiber surface appearance under plasma exposure. As the exposure time is increased, the depths as well as the size of the micro-pores etched by the plasma are increased. FFT has been used to quantify the periodic surface features of plasma treated fibers. The reduction in fiber diameter has been measured from the ESEM micrographs of the accumulated treated fiber. The results show that the oxygen plasma possesses more severe effects. Fiber contraction has been observed during the plasma treatment. The dominant weight loss during plasma treatment was mainly attributed to the surface etching of the fibers on the fabric surface. When comparing with the SEM micrographs, the ESEM micrographs show a good correlation without obscuring the surface details of the fibers.

AFM measures the depth of etching pits induced by the argon and oxygen plasma. For a relatively smoother surface of an untreated flax fiber, the argon plasma creates

pits with the sizes (both depth and diameter) mainly in the sub-micrometer range while the oxygen plasma creates pits with the sizes of the order of a few micrometers on the flax fiber surface. Moreover, the changes in surface roughness of the plasma etched samples have been quantified by the RMS values.

CHAPTER 5

CRITICAL SURFACE TENSION AND WICKING OF LINEN TREATED WITH LOW TEMPERATURE PLASMA

5.1 INTRODUCTION

Wetting is important for processing and performance of textiles. The comfort of clothing made from the cellulosic fiber is closely associated with moisture absorbency. The hydrophilic properties of cellulosic fibers also have great industrial importance for many processes, e.g., scouring, dyeing and finishing. In addition, the fiber mechanical properties vary with the moisture content. Wettability can be valuable for characterization of fiber surfaces, transportation of liquid, interaction of fibers with liquids and surfactants as well as adhesion with polymers. Various wetting tests have been devised to obtain information on wettability, absorbency, repellency, resistance and moisture transport [106, 163, 170].

Wetting is a dynamic process, it is the displacement of a solid-air (vapor) interface with a solid-liquid interface. To move in a fibrous medium, a liquid must wet the fiber surfaces before being transported through the inter-fiber pores by means of the capillary action. The fiber-liquid surface attraction force which causes the liquid to wet the fibers is determined by fiber surface properties and liquid properties. The manner in which the liquid is transported through the pores depends on the capillary forces present in the pore structures of the medium. Capillary action is governed by the properties of liquid, fiber surface wetting characteristics and geometric configurations of the porous medium [123].

Wetting and wicking are two related processes. A liquid that does not wet fibers cannot wick into a fabric. Wicking can only occur when fibers assembled with capillary spaces between them are wetted by a liquid. The resultant capillary forces drive the liquid into the capillary spaces. Fiber wettability is therefore a prerequisite for the occurrence of wicking [145]. Wetting of a fibrous assembly, e.g., a fabric, is a complex process. Various wetting mechanisms such as spreading, immersion, adhesion, and capillary penetration may operate simultaneously. Wickability describes the ability to sustain capillary flow whereas wettability describes the initial behavior of a fabric, yarn or fiber in contact with liquid [86-87, 104, 145].

The wetting and wicking behavior of fabrics reflect the absorption of sweat from individual droplets on the skin surface or from localized regions of high sweat gland population density or restricted evaporation, e.g., underarms region. It is an important aspect to clothing comfort. If the perspiration can spread and distribute over a large surface area quickly, the evaporative moisture loss will be increased thus helping to keep the skin dry and comfortable [104].

The interactions between fiber assemblies (yarns or fabrics) and liquids depend on the chemical nature of the fiber surface, the geometry of fiber assemblies including the pore size distributions, fiber diameter and surface roughness, and the liquid properties such as surface tension, viscosity and density [40-41, 123-124, 145, 163, 240]. In the case of a fibrous material such as woven or non-woven structure, the fiber surface properties and pore structure of the material are the main determinants of its liquid wetting and wicking properties [166-167, 174, 199, 201]. Changing

fiber chemical compositions in a fibrous material can alter its overall surface wetting behavior [124].

Plasma treatment is one of the methods available to improve the wettability of surfaces by the introduction of polar groups onto the fiber surfaces, thereby increasing the rate of water uptake and making it more water absorbent [17, 70, 93, 136-137, 154, 231, 244, 250]. Besides, fiber surfaces are etched away with the corresponding changes in fiber diameter and surface roughness, thus alteration of fabric pore structure is expected especially with increased severity of plasma exposure. In this manner, modification of fabric wetting and wicking properties will be expected. In this chapter, further work on the wetting and wicking properties of the plasma treated linen will be reported.

5.1.1 Measurement of Critical Surface Tension by Contact Angle Method

Atoms and molecules located on or at a surface experience a different environment when compared with those in the bulk of the structure. In the bulk, a molecule is attracted equally in all directions by its neighboring molecules. The surface molecules, which are subjected to intermolecular attraction from one side only, tend to leave the surface region and return to the bulk until a pressure gradient caused by the concentration gradient is set up to stop further migration of the surface molecules. At the equilibrium state, the lower density in the surface layer increases the intermolecular distance, putting it in a state of tension. Thus surface tension is a direct measurement of intermolecular forces at the surface [40].

When a drop of liquid is placed on a solid surface, the surface tension of the liquid is larger than the surface tension of the solid, thus making a definite angle of contact between the liquid and the solid phases. When the same liquid is placed on the surfaces of increasing surface tension, the contact angle is decreased correspondingly as shown in Figure 5.1. Finally, total wetting ($\theta = 0°$) occurs if the surface tension of the liquid is equal to or smaller than the surface tension of the solid [40].

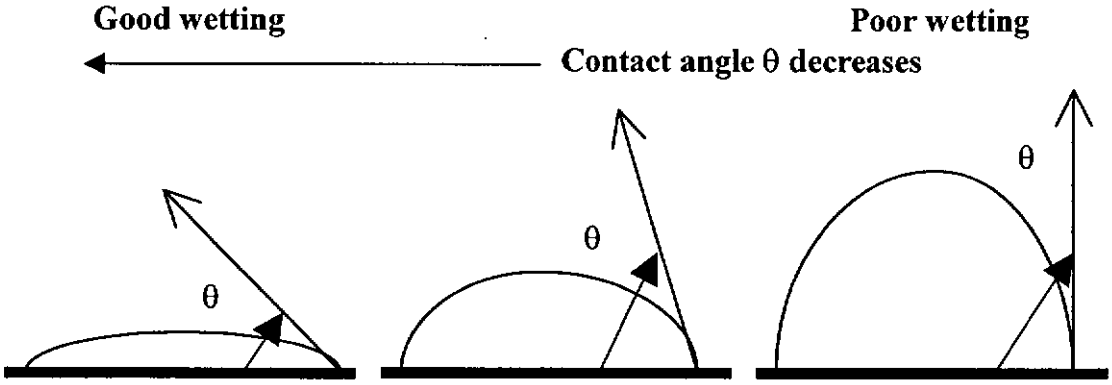

Figure 5.1: Small and large contact angles represent good and poor wetting respectively [40]

The contact angle shown in Figure 5.2 is governed by the force balance at the three-phase boundary and is defined by Young's equation:

$$\gamma_{lv} \cos\theta = \gamma_{sv} - \gamma_{sl}$$

where γ_{lv} is the surface tension of the liquid in equilibrium with its saturated vapor, γ_{sv} is the surface tension of the solid in equilibrium with the saturated vapor of the liquid, γ_{sl} is the interfacial tension between the solid and the liquid. θ is the equilibrium contact angle. The term $\gamma_{lv} \cos\theta$ has been called ' adhesion tension' or 'specific wettability' [40, 145].

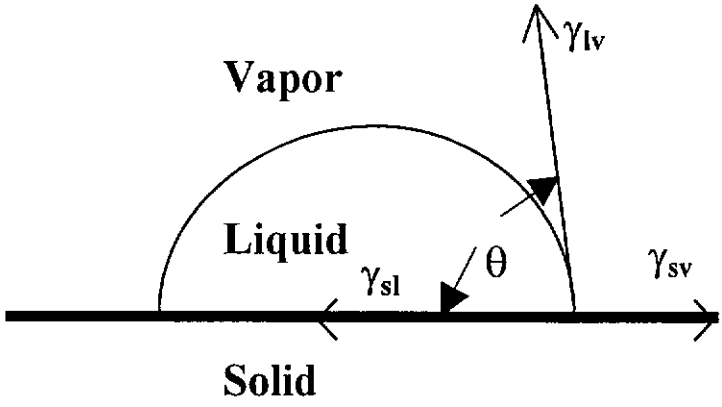

Figure 5.2: Schematic diagram of contact angle between a drop of liquid and a solid surface [40]

Although the equation is valid only for a droplet resting at equilibrium on a smooth, homogeneous, impermeable and non-deformable surface, the equation has been widely used to explain wetting and wicking phenomena [40]. For a system satisfying all these conditions, there is one equilibrium contact angle. However, these conditions are seldom completely met for practical systems.

Contact angle has been used to study the wetting and wicking processes. Although the contact angle is a very useful tool for surface characterization, however, it is not the main cause of wetting but a consequence of it. The contact angle depends on three interfacial tensions γ_{lv}, γ_{sv} and γ_{sl}. If γ_{sv} is larger than γ_{sl}, cos θ and is positive and the contact angle must be between 0° to 90°. If γ_{sv} is smaller than γ_{sl}, the contact angle must be between 90° to 180°. The contact angle will decrease whereas cos θ will increase with increasing wettability. Complete wetting implies a zero contact angle, but equating θ = 0° may lead to and incorrect conclusion. It is better to visualize that when the contact angle approaches zero, wettability has its maximum limit [145, 171].

Contact angle measurements have been used extensively for studying changes in polymer surface composition caused by various surface treatments. In many studies concerning the surface modification of polymers, water and solvents are used as the testing liquid. The changes in the chemical composition of polymer surfaces can be quantified in terms of water / solvent droplet penetration time (wetting time) [4, 26, 117, 127, 173, 209, 211-212 240, 252, 256, 268] or the contact angle [34-35, 78, 88, 98, 117, 127, 129, 139-140, 157, 173, 191, 210-212, 213-214, 235, 240, 246, 252, 254, 256, 259, 278, 280, 282].

Currently, there are no direct, reliable methods for determining surface tension or surface energy of solids. However, a number of indirect methods have been developed based on contact angle measurement [40-41, 89-90, 107, 145, 163, 171, 181, 246]. Contact angle and absorption by imaging the drops of liquid on the surface as a function of time, and monitoring the change in shape of the drop profile can be used to quantify the wettability of a material. Various approaches and applications developed include the determination of the critical surface tension γ_c by means of Zisman's plot [210, 252, 254, 256, 282], Wu's equation [210, 214], Fowkes's theory and the extended Fowkes equation [211, 252, 254], Kaelble's methods [127, 129] and Wilhelmy techniques [117, 121-125, 169, 202-203, 278].

Zisman and co-workers measured the advancing contact angles of a homologous series of liquids on a solid and plotted cos θ values against the surface tension of the liquids. The lines extrapolated approximately to the same γ_{lv} value at cos θ =1. Zisman named this γ_{lv} value the critical surface tension of the solid and proposed that

only those liquids having surface tensions below this value could spread on the solid [282]. Although the critical surface tension is an empirical concept with several deficiencies and limitations, its data are very useful for evaluating the wettability of fibers and developing products such as water- and oil-repellent finishes for textiles and paper [124, 145, 169, 171, 259].

5.1.2 Measurement of Water Uptake by Downward Wicking Method

The interaction of liquids with textiles may involve several physical phenomena, i.e., wetting of a fiber surface, transport of liquid into an assembly of fibers, adsorption on the fiber surface and diffusion of liquid into the interior of fibers [145]. Liquid that penetrates into a fabric can be taken up into two sites. The first site is the capillary space between the fibers while the second site is inside the fiber where the absorption will take place [69]. Liquid retention is governed by the pore structures as well as the wetting properties of substrate [121].

For a theoretical treatment of capillary flow, the fibrous assemblies are usually regarded as consisting of a number of parallel capillaries. The advancement of a liquid front in a capillary can be visualized as occurring in small jumps. The advancing wetting line in a single capillary stretches the meniscus of liquid until the extensibility of meniscus and the inertia of flow are exceeded. The meniscus contracts, pulling more liquid into the capillary to restore the equilibrium state of meniscus [145].

The magnitude of the capillary pressure P_c is described by the Laplace equation as applied in idealized capillary tube as follows [8, 41-42]:

$$Pc = \frac{2\gamma \cos\theta}{r}$$

where γ is the surface tension of the liquid,

$\cos\theta$ is the contact angle at the liquid / solid / air interface,

r is the capillary radius.

From the equation, the capillary pressure is inversely related to the capillary radius. Since the capillary spaces in a fabric are not uniform, the effective capillary radius is used instead of the radius r. Moreover, the fibers with a small contact angle will have a large capillary pressure to drive liquid movement [86, 107, 145].

In any fibrous structure of woven, non-woven or knitted fabrics, a distribution of pore sizes along any planar direction is expected. Wicking rate and liquid transported in a fabric depend on its pore sizes and pore size distribution. The capillary principle dictates that smaller pores are filled first and responsible for liquid front movement. As the smaller pores are completely filled, the liquid then moves to the larger pores [125]. The sizes and shapes of fibers as well as their alignment will influence the geometric configurations and topology of the interfiber spaces or pores, which are the channels that have wide shape and size distributions and may or may not be interconnected [121, 123-124]. The shape of fibers in an assembly affects the size and geometry of the capillary spaces between fibers and consequently the rate of wicking. The flow in a capillary may stop when geometric irregularities allow the meniscus to reach an edge and flatten [145].

Optimal absorbent performance, whether measured by the travel distance of liquid spreading or total liquid retention, can be achieved by controlling the pore sizes and their distribution. The distance of liquid advancement is greater in a smaller pore because of the higher capillary pressure but the mass of liquid retained in this pore is also small. Larger liquid mass can be retained in larger pores but the distance of liquid advancement is limited. Therefore, fast liquid spreading in fibrous materials is facilitated with small, uniformly distributed and interconnected pores, whereas high liquid retention can be achieved by having a large number of large pores or a high total pore volume [123].

Changing fiber chemical compositions in a fibrous material can alter its overall surface wetting behavior because each fiber type has distinct wetting and surface properties [121, 124]. Wetting can be enhanced by increasing the surface polar groups after the plasma treatment. The increased surface tension is apparently due to oxygen incorporation [256]. Introduction of oxygen elements to fiber surface in the form of –OH, C=O and –COOH can increase the hydrophilicity [214]. Hydrophilic properties of the surface during fabric printing, for example, are related not only to the wetting of colour paste on the fiber surface but also to its penetration into the fiber assembly in the padding process.

On the basis of the relative amount of liquid involved and the mode of liquid-fabric contact, the wicking processes can be divided into two groups namely wicking from an infinite liquid reservoir (immersion, transplanar wicking and longitudinal wicking), and wicking from a finite (limited) liquid reservoir (a single drop wicking into a fabric) [104, 145]. It is a common practice to use in-plane wicking

measurements to evaluate the absorbing power or liquid transport capabilities of fibrous sheet materials [18, 69, 73, 86-87, 104, 130, 145, 203]. Most versions of the test methods used for this purpose start out by dipping one end of a sheet into liquid and monitoring the subsequent upward movement into the sheet, either by following the position of the liquid front or by gravimetric or volumetric changes. If the upward distance traveled by the liquid becomes long enough, there will be a noticeable effect of gravity on the flow rate. The equilibrium will happen when the capillary action is balanced by gravity, that is, by the weight of raised liquid [41, 145, 163, 165]. Moreover, water uptake in a vertically hung cotton fabric shows a gradient distribution pattern with a saturated zone near the water-fabric interface followed by diffused and steadily distributed zones [121].

During the vertical upward wicking, gravity affects the unsteady-state flow of liquid. At the onset of absorption in a vertical capillary system, the absorbed liquid is relatively close to the liquid source, the effect of gravity can be neglected at this situation. However, after a longer period of time (or upward wicking distance), gravity plays an increasingly important role [41]. In 1996, Miller *et. al.* [165] theoretically considered the case where the liquid path was downward. Downward wicking differs from its upward counterpart in several significant ways. The equations describing these two processes have somewhat different forms, and both theory and experiment indicate that downward wicking can produce an essentially constant feed rate over a very long time period or length of travel. In contrast, water uptake rates decrease continuously with time or length. Downward wicking rates become more constant than upward rates as the process continues.

For upward direction [165]:

$$Lc \ln\left[\frac{1}{1-\frac{L}{Lc}}\right] - L = \frac{\rho g K}{\eta} t$$

where L is the height of rise at any time,

Lc is the height of the liquid column that would produce the equivalence of the capillary pressure,

ρ is the liquid density,

g is the gravitational constant,

K is the effective mean cross sectional area (i.e., permeability),

η is the liquid viscosity,

t is the wicking time.

For downward direction [165]:

$$L + (Lo - C) \ln\left[\frac{C + L}{Lo + L}\right] = \frac{\rho g K}{\eta} t$$

where Lo is the initial upward wicking length before downward wicking,

L is the downward wicking length,

C is a constant (equal to $Lc - Lo \cos\beta$).

It has been shown that the capillary pressure and the permeability of the fabric are important in determining the liquid movement inside the fabric structure [165]. The fabric water uptake is governed by the interfacial tension and wettability of the fibers, fabric properties, the effective pore size and capillary dimensions (i.e., permeability and effective mean cross sectional area), and liquid properties (i.e., the

surface tension and viscosity [121, 145, 168]. The variations of fabric wicking properties brought about by plasma treatment can be interpreted as the results of the changes in the fiber surface chemical composition (surface tension and water contact angle), fiber surface geometry (roughness and dimension) and capillary geometry (dimension) of the fibrous assembly.

Surface chemical composition greatly affects the interaction of liquids and textiles as stated above. Hydrophilization with the incorporation of polar groups on the fiber surface could improve the fiber wettability. XPS analysis showed that the oxygen content was increased dramatically after plasma treatment as discussed in Section 3.3.2.1. The permeability of fabric structure is related by the structural and geometrical factors such as the capillary geometry of the fibrous assembly, porosity, fiber shape, fiber surface roughness and dimensions. The plasma modification of fiber surface causes the progressively increased reduction in fabric weight (Section 3.3.1.3) and fiber diameter with the treatment time (Section 4.3.1.3). Moreover, the increment of surface area and roughness were shown by the SEM, ESEM and AFM observation in Chapter 3 and Chapter 4. Under such modification, the changes of capillary pressure would be expected. The effect of liquid properties will not be considered in this study because only distilled water was used for all the experiments related to wicking.

Fiber swelling due to the sorption of liquid may reduce the capillary spaces between fibers [145]. As wicking proceeds in a fibrous structure, water continuously diffuses into fibers resulting in a continuous change of the dimensions of wet capillaries. The structure as a whole may expand or collapse resulting in changes in the capillary

radius of the system. To various extents, all natural fibers swell in water and the swelling is always as a function of time. Therefore, the average radius of the capillaries present in the system is never a constant factor [41, 200]. It has been shown previously that flax fiber does not increase in size or shape as a result of mercerization treatment [43-44]. In this study, it is assumed that both untreated and plasma treated fibers will behave similarly and have much lower swelling tendency (no increase in size or shape as a result of mercerization treatment), therefore, the effect brought about by the plasma treatment will not be considered for discussion.

Irregular shapes and sizes of fibers can contribute to the variations in single fiber wetting. Wetting properties can be obtained more conveniently with simpler and easier handling from fabrics than from single fiber measurement. It has been demonstrated that the surface wetting characteristic of any fabric containing a single fiber type is the same as that of its constituent single fibers. Wetting characteristics are not affected by fabric factors such as length, fabric-water interface depth and direction. The variation of fiber dimensions will affect the determination of changes in fabric wetting properties following plasma by the following plasma treatment. Since fabric measurements represent the collective effects of all fibers, then they encompasse all fiber variations. In addition, measurement in fabric form offers the advantage of simultaneous detection of dynamic liquid transport and retention information [122-123, 125].

Hence, the objectives of the present chapter are to illustrate the wetting and wicking properties of linen fabrics treated under different plasma conditions. The contact angles of various solutions on the fabric surface will be measured for the

determination of critical surface tension by means of Zisman's plot. Afterwards, an experimental set-up and testing procedures will be developed for studying the fabric downward wicking. The abilities of water upward and a downward wicking of plasma treated linen will be compared experimentally.

5.2 EXPERIMENTAL DETAILS

5.2.1 Critical Surface Tension

5.2.1.1 Sample preparation

Scoured and semi-bleached linen fabrics used in this experiment were obtained from the same batch as specified in Section 3.2.1. Plasma treatments were conducted under the conditions as described in Section 3.2.1. Linen materials were exposed to oxygen or argon plasma at a pressure of 15Pa, discharge powers of 100W and 200W for the exposure time of 5 minutes. The treated fabric sample was removed from the chamber and then conditioned under the standard condition (65% RH and 21°C) for 24 hours before characterization.

5.2.1.2 Contact angle measurement

The equipment used was the Contact Angle Micrometer (Tantec Inc.) which was connected to an Electro-microscope (U-TEXT UT-901) and a VHS Video Cassette Recorder (JVC HR-J747MS). The purpose of the experimental set-up was to capture, magnify and record the image, and then view it through a TV and a computer monitor. The image capturing was obtained by a capture board and the Leica EWS 2100 software. The experimental set-up is shown in Figure 5.3.

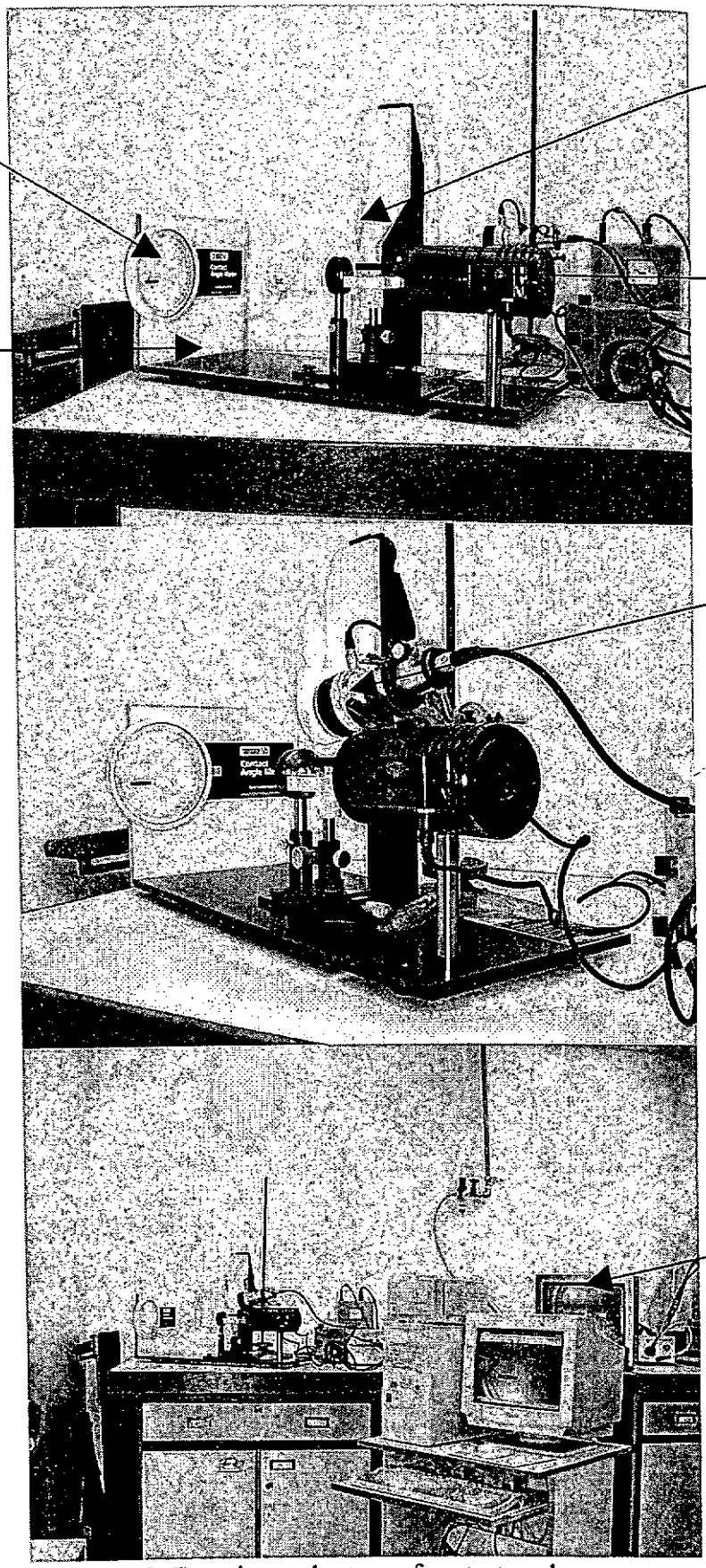

Figure 5.3: Experimental set-up of contact angle measurement

After a liquid drop is placed on the fabric surface, the timing of the experimental measurement is important. The contact angle was measured from the images at 0.125s (3 x 1/24s) after the drop was placed on the surface [117, 119] as shown in Figure 5.4. The value reported was the average of 20 drops of each solution. The droplet size was 1μl and the distance between the syringe and sample was 0.5cm. Six types of solution were used including distilled water (71.99mN/m), sucrose solutions of 10% (72.50mN/m), 20% (73.00mN/m), 30% (73.40mN/m), 40% (74.10mN/m) and 55% (75.70mN/m) concentration [26, 68].

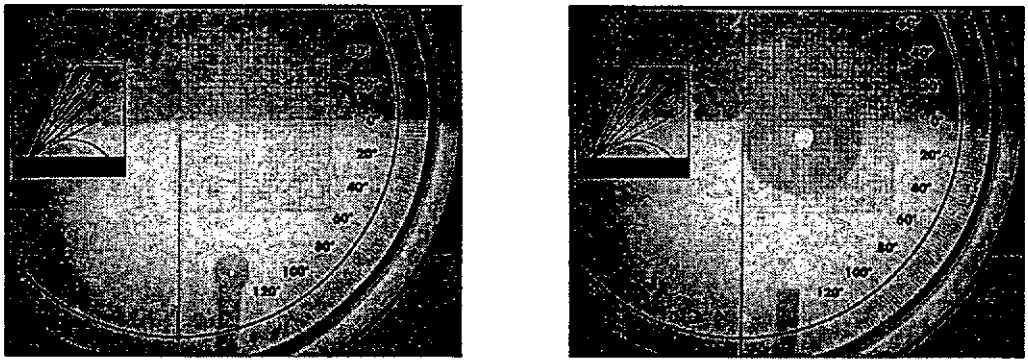

Figure 5.4: Pictures of contact angle measurement

Tantec's Half-Angle method was used for determining contact angles measured from the droplet dimensions and based on the formula [131]:

$$\theta = 2 \text{ x arc tan } (H/R)$$

where θ is the contact angle,

H is the height of a droplet, and

R is the radius of droplet's base as shown in Figure 5.5.

It becomes apparent from this formula that the angle between a line connecting the contact point C with the apex A of the droplet and the base line CO itself actually is a

half of the contact angle. This Half-Angle, θ/2, can be easily determined and used for further calculation.

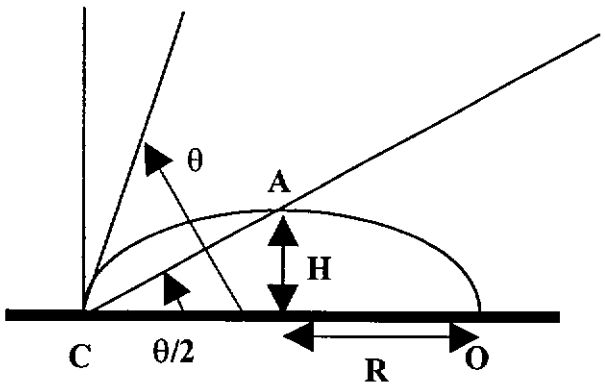

Figure 5.5: Contact angle determination using Half-Angle measuring method

5.2.2 Water Uptake

5.2.2.1 Sample preparation

Scoured and semi-bleached linen fabrics used in this experiment were the same batch as specified in Section 3.2.1. Plasma treatments were conducted under the conditions as described in Section 3.2.1. Linen materials were exposed to oxygen or argon plasma at a pressure of 15 Pa, discharge powers of 100W and 200W for the exposure time of 2.5, 5, 10, 20, 40 and 60 minutes respectively. The treated fabric sample was removed from the chamber and then conditioned under the standard condition (65% RH and 21°C) for 24 hours before characterization.

Effect of washing on the plasma treated linen was also studied. The fabric sample was washed according to AATCC Test Method 61-1994 Colorfastness to Laundering, Home and Commercial: Accelerated [2]. Sample was washed based on the Test Method 61-IA with 0.5% of non-ionic detergent and 10 stainless steel balls at 40°C for 45 minutes in a Launder-Ometer. The washed sample was rinsed with distilled water for 5 minutes and then spin dried for 5 minutes to remove excessive

water. A warm iron was applied to remove the wrinkles and then the sample was air dried under the standard conditions for 24 hours before characterization.

5.2.2.2 Upward and downward wicking measurements

For the upward experiment, a strip of fabric sample with the width of 2.5cm and 15cm long, a graduated scale with 1cm markings by a water-soluble pen was lowered into the distilled water as shown in Figure 5.6. Depth of fabric immersion in the reservoir was 20mm. The time required for the water to rise along each mark was recorded. The experiment would be terminated when the distance of water traveled arrived 12cm or the measuring time exceeded 2 hours. The distance of water traveled along the fabric as a function of time was determined.

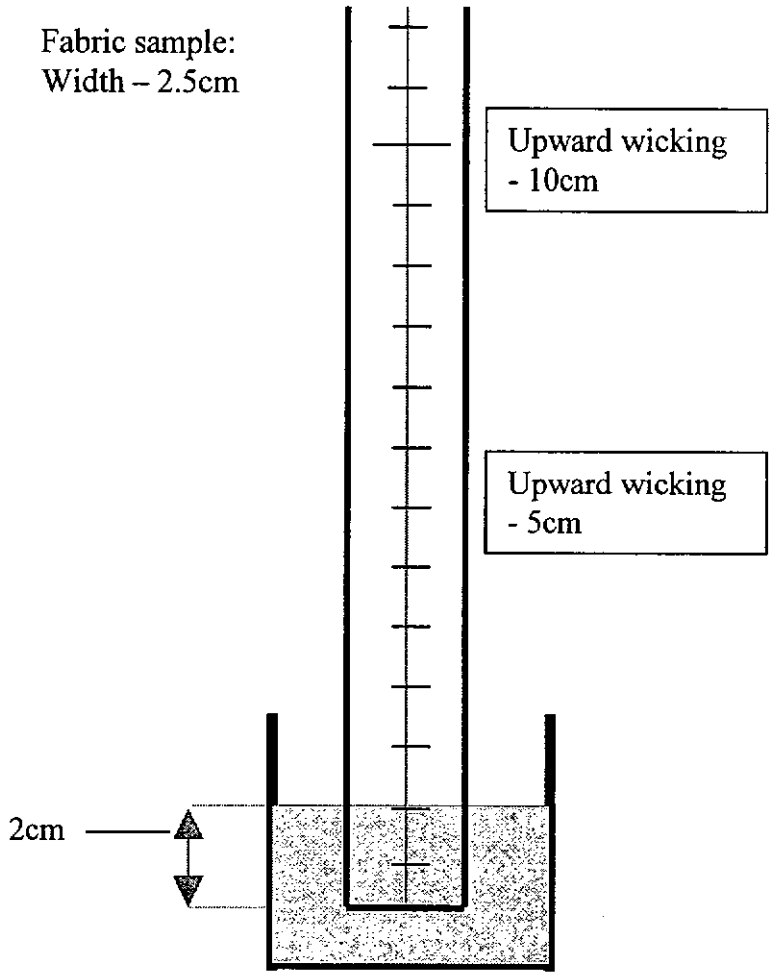

Figure 5.6: Experimental setting for water uptake measurement

For the downward wicking experiment, a strip of fabric sample with the width of 2.5cm and 20cm long, a graduated scale with 1cm markings by a water-soluble pen was passed over a glass rod in order to turn the direction as shown in Figure 5.7. Afterwards, the distilled water was added to the tank and the wicking time was commenced. The time required for the water to drop along each mark from the top of the glass rod was recorded. The experiment would be terminated when the distance of water traveled 12cm or the measuring time exceeded 2 hours. This experiment set-up can therefore be used to determine the distance of water traveled along the fabric as a function of time. The photographs of the experimental set-up are shown in Figure 5.8.

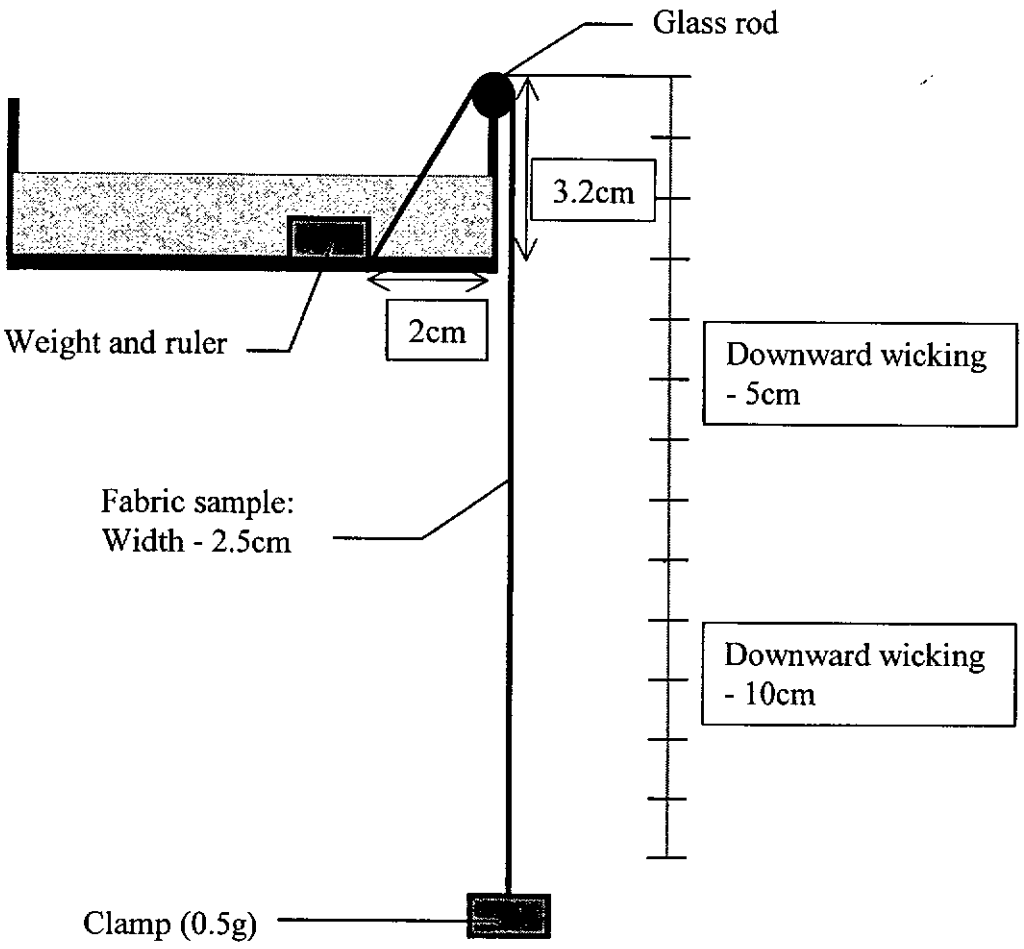

Figure 5.7: Experimental setting for downward wicking measurement

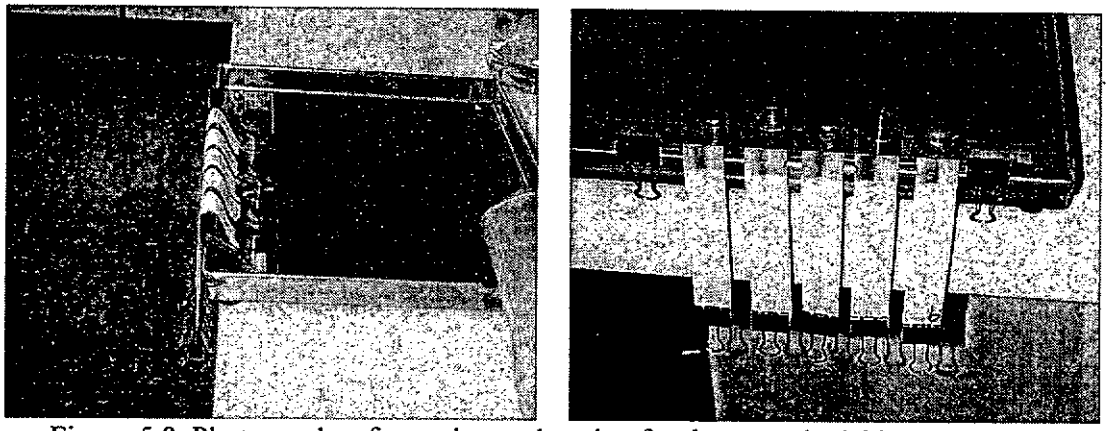

Figure 5.8: Photographs of experimental setting for downward wicking measurement

All the above measurements were carried out under the standard condition. The paired comparison *t*-test was used to determine whether any statistical significant difference occurred with a confidence limit of 95%.

For both upward and downward wicking measurements, the following assumptions and limitations are considered. First of all, the water-soluble pen was used for marking the graduated scale on the fabric surface, therefore, it was assumed that the water front travelling on the fabric surface was consistent with the interior as well as the back of the fabric. Second, since the capillary spaces in a fabric are not uniform, the liquid may not spread as a continuous front and also it may penetrate into some capillaries before others. Therefore, the wicking distance was determined when the marked graduate scale (middle of the fabric strip) started to burr. The mass of water absorbed during the wicking process was not measured.

5.3 RESULTS AND DISCUSSIONS

5.3.1 Critical Surface Tension of Plasma Treated Linen

The critical surface tension was determined by plotting the cosine contact angles against the surface tension of the liquids with known surface tension. By using the

linear regression method, the intercept of the line at cos θ = 1 is derived as the critical surface tension γ_c. The plot of cos θ versus γ_{lv} is known as the Zisman's plot. The experiment results are shown in Table 5.1 and Figures 5.9 - 5.11 respectively.

Table 5.1: Results of the contact angle measurement of the plasma treated linen

	Surface tension of the solution (mN/m)						
	Distilled water	10% sucrose solution	20% sucrose solution	30% sucrose solution	40% sucrose solution	55% sucrose solution	Critical surface tension
Contact angle, °.	71.99	72.50	73.00	73.40	74.10	75.70	(mN/m)
Untreated Linen	40.4	52.0	59.4	63.1	61.3	68.3	68.3
CV%	8.6	7.3	7.6	6.0	8.9	6.0	
Oxygen plasma 100W, 5min.	*	*	*	*	*	30.2	72.8
CV%						15.9	
Oxygen plasma 200W, 5min.	*	*	*	*	32.9	36.4	72.5
CV%					10.0	13.2	
Argon plasma 100W, 5min.	31.7	39.5	48.1	45.7	44.7	46.0	65.0
CV%	15.2	14.0	9.7	12.1	10.3	9.8	
Argon plasma 200W, 5min.	46.0	51.4	56.7	51.2	61.3	71.8	68.9
CV%	12.3	10.0	9.7	8.4	9.4	7.3	

Note: * refers to the case where θ = 0

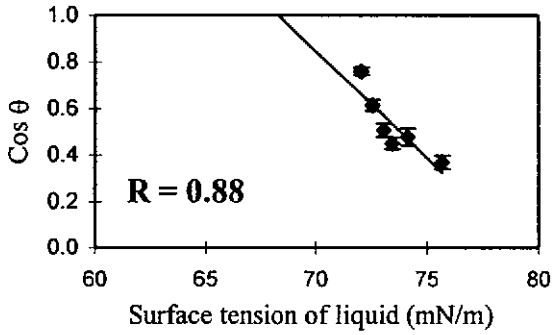

Untreated linen

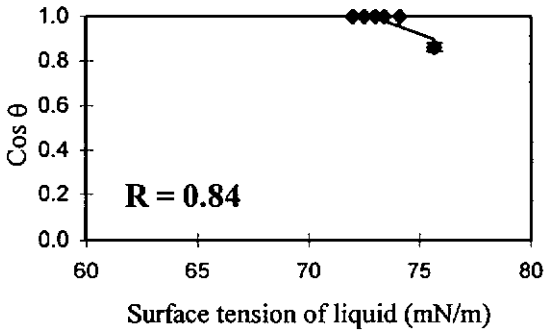

Oxygen plasma (100W, 5min.)

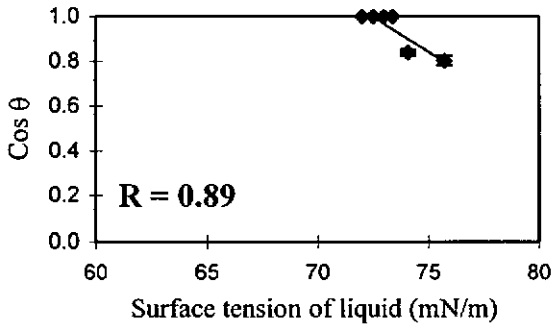

Oxygen plasma (200W, 5min.)

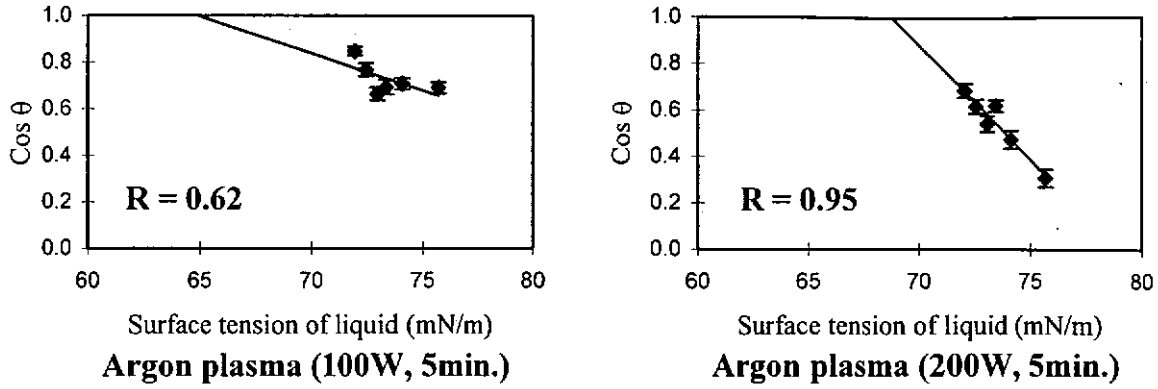

Figure 5.9: Plots of cos θ of fabric surface contact angle against the surface tension of liquids. The intercept of the line at cos θ = 1 is the critical surface tension γ_c

Since the surface oxygen content was increased after the plasma treatment as discussed in Section 3.3.2.1, the increased wettability was expected [214, 252, 254, 256]. Cellulose material has a large number of OH groups on the surface leading to a higher surface tension and wettability [107, 200]. Surface chemical composition is the most important factor affecting the fiber surface wettability because it determines the surface bonding forces with liquid, i.e., dispersion forces, polar forces and H-bonding [240]. It has been shown in Table 3.3 that both oxygen and argon plasma treatment will introduce oxygen elements on the material fiber surfaces in the form of –OH, C=O and –COOH, thereby increasing the hydrophilicity [70, 124, 126, 140, 214, 256, 281].

From the results obtained, the contact angles of most plasma treated samples were reduced as compared to the untreated sample. In particular, the oxygen plasma treated sample exhibited zero contact angles when using the solutions of lower surface tension. As a result, the critical surface tension was increased accordingly. As refer to the definition of critical surface tension, it stated that only those liquids having the surface tension below this value could spread on the solid surface. In the

case of the sample treated by oxygen plasma at 100W for 5 minutes, the critical surface tension value obtained is 72.8mN/m, however, the 40% and lower concentration sucrose solutions with the surface tension of 74.1mN/m and below could spread on the fabric surface as shown in Table 5.1. Similar wetting phenomena occurred when 200W discharge power was used and this illustrated the error of this method and its lack of ability to quantify the surface wetting properties. In the case of the argon plasma treated sample having the lower discharge power of 100W, the results showed that lower contact angle with respect to untreated linen was obtained with a lower critical surface tension in contrary to expectation. The data is scattered around the regression lines with the poor correlation of 0.62 as shown in Figure 5.9. Again, a contradictory result was also obtained from the 200W argon plasma treated sample in which some higher contact angles were measured with a higher critical surface tension.

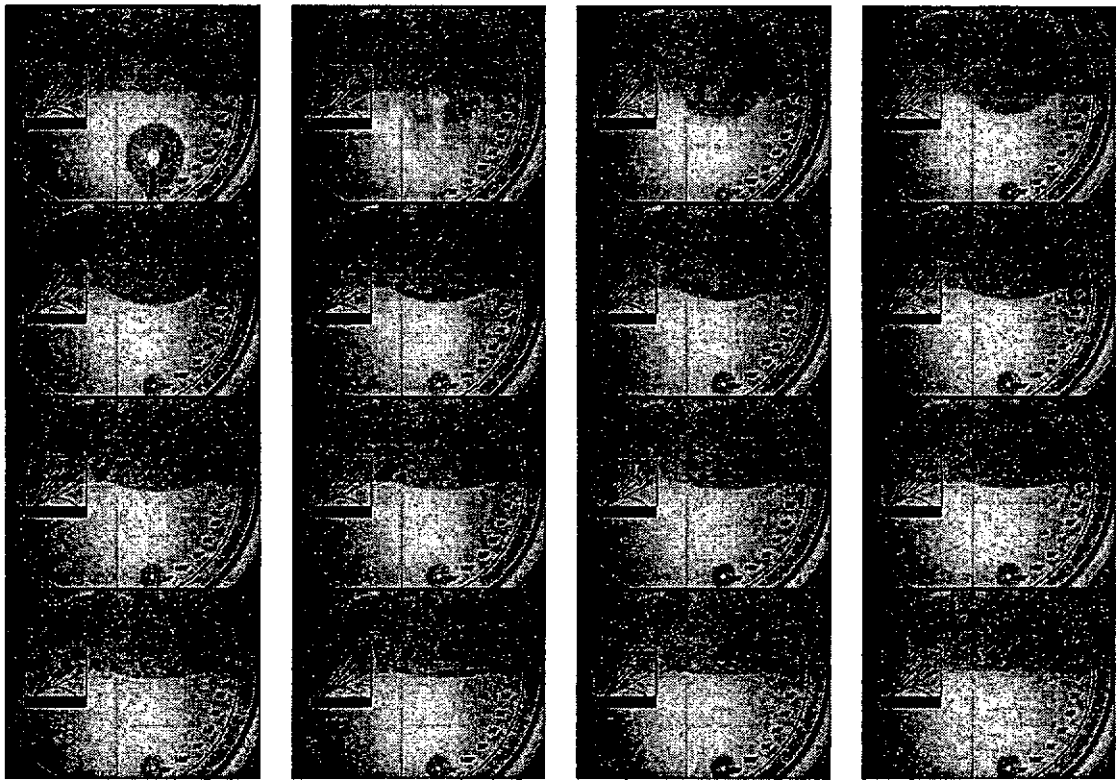

Figure 5.10: Absorption of distilled water on linen fabric under the observation of surface contact angle with a time interval of 1/24 second

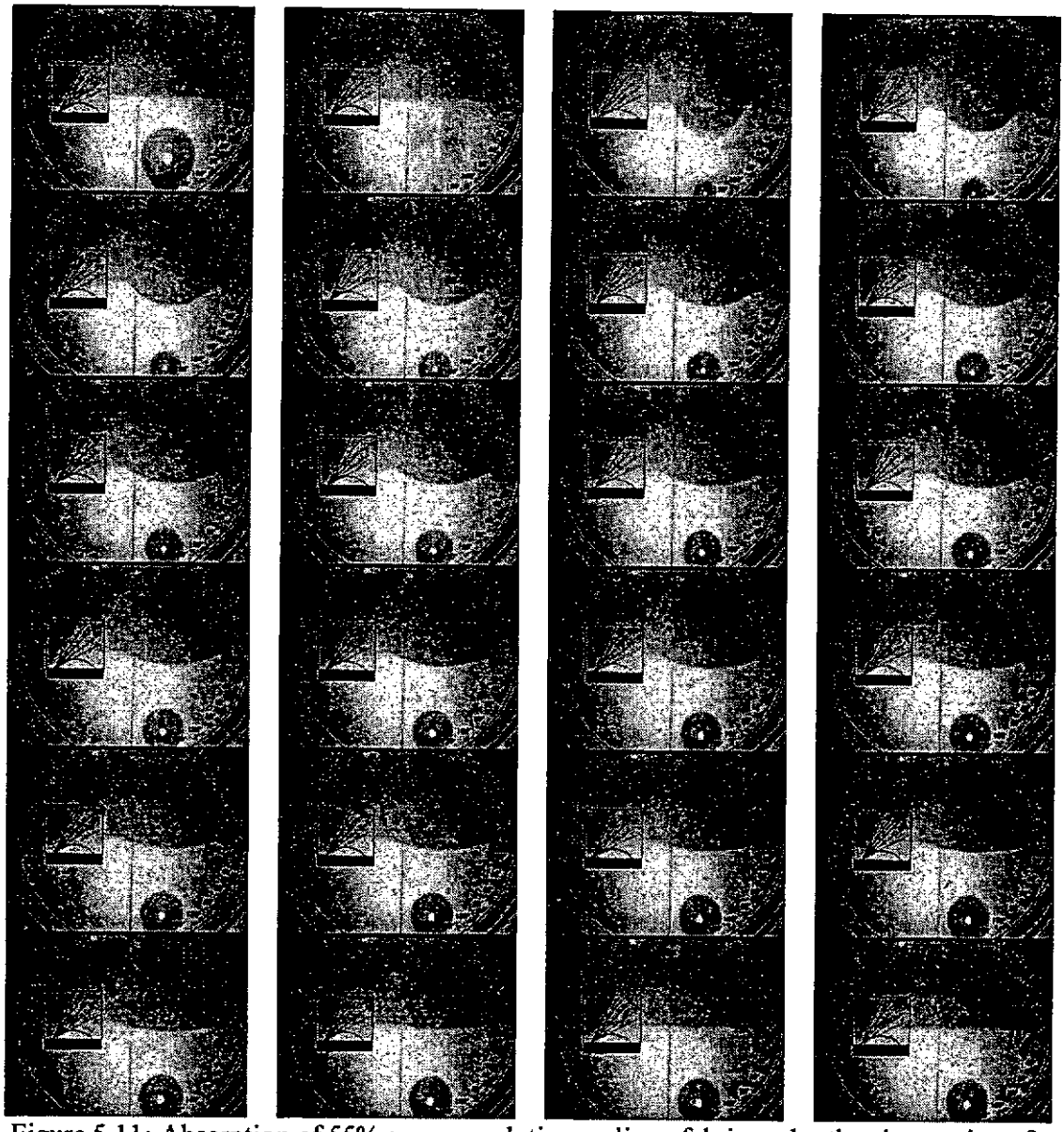

Figure 5.11: Absorption of 55% sucrose solution on linen fabric under the observation of surface contact angle with a time interval of 1/24 second

The determination of critical surface tension by means of the Zisman's plot has a few problems. First, the relationship between cos θ and γ_{lv} becomes extremely curvilinear as θ approached to zero [169, 171]. Second, the established experimental technique is used for evaluating flat and isotropic surfaces. Stable equilibrium can be obtained only when the surface is rigid, immobile, smooth, compositionally homogenous, and there are no interactions between the liquid and solid surface [40]. Hence, the fabric surface wettability measured by such an approach can be erroneous because of the inherent complexity and roughness of the surface.

Increasing the roughness of fabric surfaces can promote wetting by decreasing the apparent contact angle even when the intrinsic wettability of the fiber remains the same. Under such conditions, the observation and measurement of contact angle, when a droplet of liquid is placed on a horizontal textile fabric are difficult to accomplish [122, 124, 145, 169, 171, 199, 259]. Moreover, the differences in fiber diameter, stiffness and coefficient of friction inside the woven structure will lead to appreciable differences in structure and pore size distribution [181]. Furthermore, textile fabrics do not have ideal surface, thus the wetting phenomena will be complicated by the surface roughness, heterogeneity and absorption of liquids [145].

However, the contact angle is sensitive to the chemical composition of the fiber surface molecular layers and is a relatively simple and inexpensive technique for characterizing polymer surfaces. If two materials are compared using the same wetting liquid, a difference in the contact angle will indicate which solid has a greater attraction for the liquid. Therefore, changes in cosine θ can only indicate the relative difference [171]. In the case of comparisons between systems especially when different liquids are involved, this can be extremely misleading.

The measurement results show that the critical surface tension may be not very appropriate to quantify the surface wetting properties of the plasma treated linen. However, the measured results show that the contact angle between the liquid and fabric surface is reduced after the treatment. As a lower contact angle implies a better wettability, it is necessary to use another approach to quantify the effect of plasma treatment. Previous experiments in Section 3.3.2.4 confirmed that the fabric

water uptake was significantly increased after the plasma treatment. Therefore, further study of the wicking measurement [165] was conducted.

5.3.2 Water Uptake of Plasma Treated Linen

5.3.2.1 Comparison of upward and downward wicking measurements

The effects of oxygen and argon plasma on the water uptake of linen fabric have been shown in Section 3.3.2.4. The water uptake of fabric was measured according to the standard testing method and the results were calculated based on the height and weight of distilled water wicked above the reservoir within 5 minutes of measurement time. The highest increment of water uptake was achieved using the oxygen plasma at 100W for 10 minutes and the argon plasma at 100W for 5 minutes. However, the effect of gravity might affect the measurement of water uptake [165]. For this reason, a downward wicking experiment as described in Section 5.2.2.2. has been set-up and the results are shown in Figure 5.12.

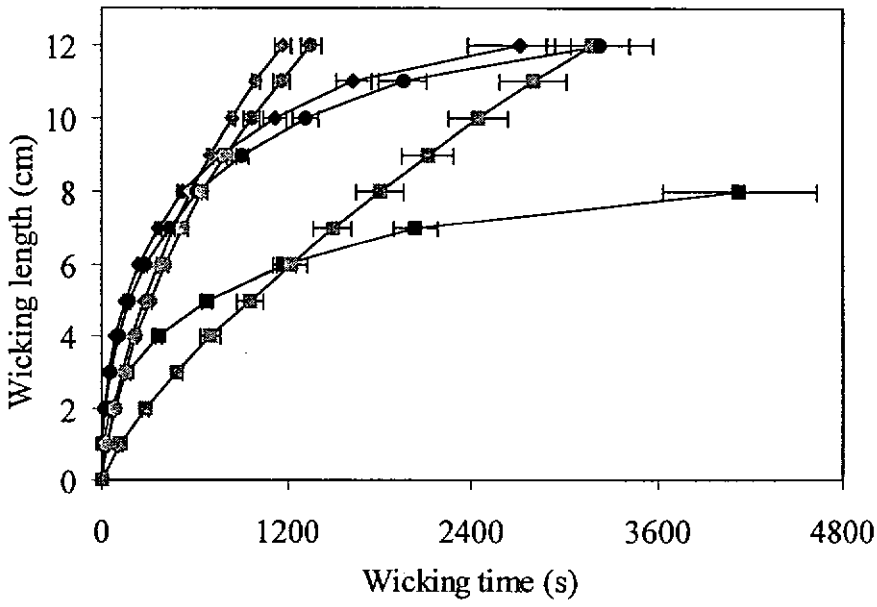

Figure 5.12: Experimental results of comparison between upward and downward wicking (■) Untreated sample, upward, (■) Untreated sample, downward, (♦) Oxygen plasma 100W, upward, (♦) Oxygen plasma 100W, downward, (●) Argon plasma 100W, upward, (●) Argon plasma 100W, downward.

Three samples have been used to compare the effects of upward and downward wicking, namely untreated linen, oxygen plasma treated linen (100W, 5 minutes) and argon plasma treated linen (100W, 5 minutes). For upward wicking, it is obvious that if the distance traveled by the liquid becomes long enough, there will be a noticeable effect of gravity on the flow rate leading to the reduction of uptake length. For the downward wicking, it agrees well with the prediction by Miller *et. al.* that after an initial deceleration, the rate of downward wicking should become essentially constant. The wicking length becomes longer as the wicking time is increased. It has been explained that the inhibiting effect of gravity is not acting to affect the filling of different pores dimension, therefore, downward wicking can produce essentially constant front movement rate over a long period of time or length of travel [165].

Apart from the reduction of uptake rate, Figure 5.12 also shows the limitation of upward measurement. In the previous experiment (Section 3.3.2.4), the length of water travel within 5 minutes (300s) was measured where different fabrics would appear to have the similar water uptakes. When observing a short travel distance or wicking time, the upward measurement is unable to distinguish the water uptake of different fabrics as they might exhibit similar wicking rates at the early stage. Therefore, it is concluded that more accurate representation of fabric wicking properties can be obtained by the downward water wicking measurement.

5.3.2.2 Downward wicking measurement of the plasma treated linen

The effects of plasma treatment on the downward wicking properties of linen fabric are demonstrated in Figures 5.13 - 5.16.

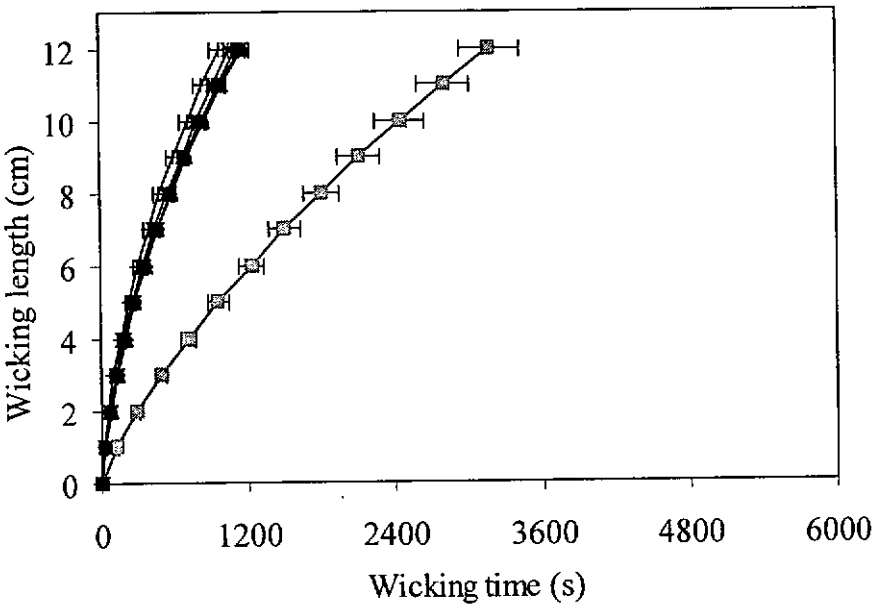

Figure 5.13: Effect of oxygen plasma treatment (100W, various exposure time) on the downward wicking of linen
(▣) Untreated sample, (◆) 2.5 minutes, (▲) 5 minutes, (×) 10 minutes, (✳) 20 minutes, (●) 40 minutes, (|) 60 minutes.

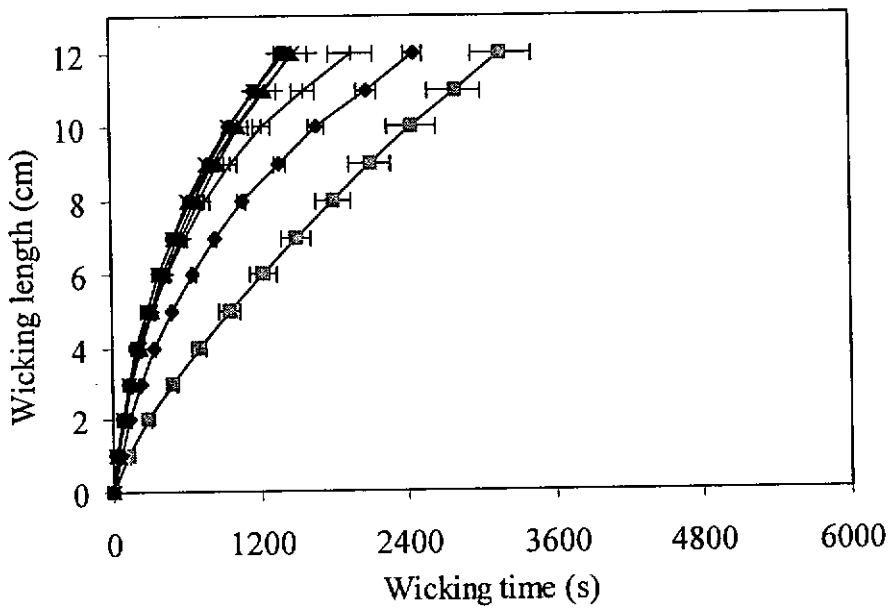

Figure 5.14: Effect of oxygen plasma treatment (200W, various exposure time) on the downward wicking of linen
(▣) Untreated sample, (◆) 2.5 minutes, (▲) 5 minutes, (×) 10 minutes, (✳) 20 minutes, (●) 40 minutes, (|) 60 minutes.

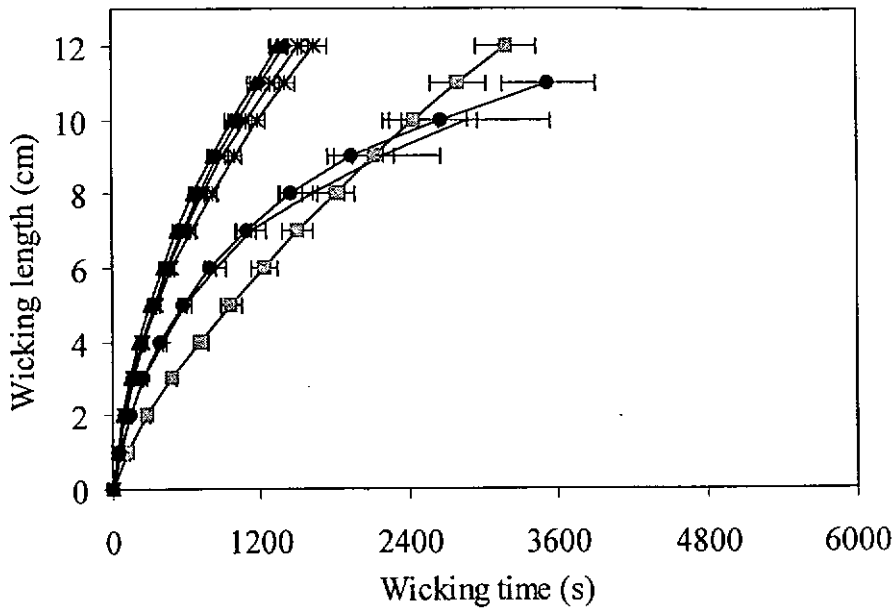

Figure 5.15: Effect of argon plasma treatment (100W, various exposure time) on the downward wicking of linen
(▣) Untreated sample, (◆) 2.5 minutes, (▲) 5 minutes, (×) 10 minutes, (✳) 20 minutes, (●) 40 minutes, (|) 60 minutes.

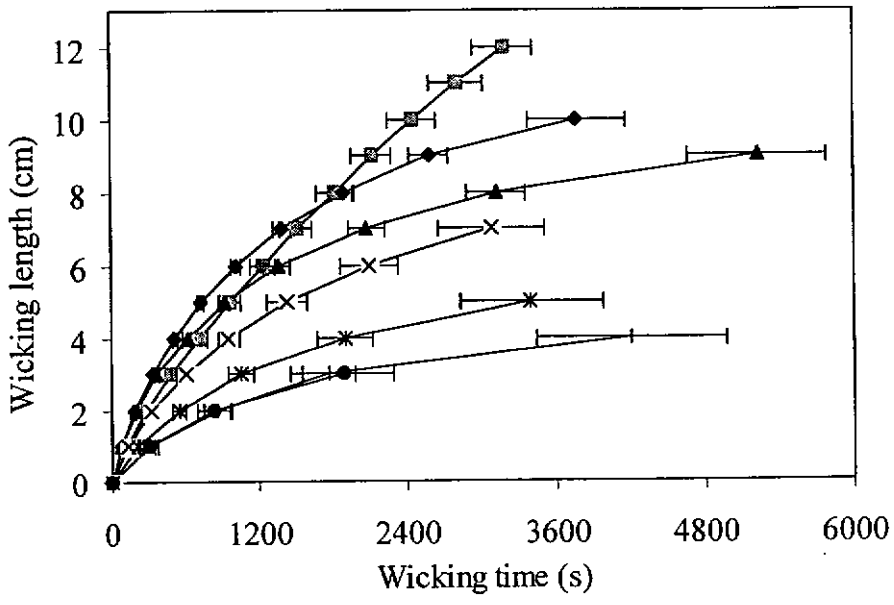

Figure 5.16: Effect of argon plasma treatment (200W, various exposure time) on the downward wicking of linen
(▣) Untreated sample, (◆) 2.5 minutes, (▲) 5 minutes, (×) 10 minutes, (✳) 20 minutes, (●) 40 minutes, (|) 60 minutes.

There is a significant difference between the effect of these two types of gas in most of the cases. Oxygen plasma treatment at 100W leads to a higher increment of fabric downward wicking. At 200W, it produces immediately an increment until 40 minutes of exposure, then the wicking length reduces. In the case of argon plasma, a similar trend occurs when using 100W discharge power, the transit time for the reversing trend being reduced to 20 minutes. The phenomenon of reduction becomes much obvious when 200W is used, and the reversing point starts at 2.5 minutes.

Oxygen plasma with 100W discharge power shows the fastest downward wicking rate among all the treated samples. There are no significant differences between the samples with the exposure time ranging from 2.5 minutes to 60 minutes. Under these treatment conditions, the result obtained is consistent with the increased surface oxygen content, slight reduction of fiber diameter, creation of small pores and great reduction of water contact angle as shown in Table 5.1.

Figure 5.14 shows the plot of wicking length against wicking time of oxygen plasma treated samples using 200W discharge power. The wicking rates of all plasma treated samples are faster than the untreated sample but lower than the sample treated at 100W. The samples with 2.5 minutes and 60 minutes of exposure time show slightly lower wicking rates than the other treated samples.

Under the oxygen plasma exposure with a stronger discharge power (200W), the fabric weight loss is much higher than the sample using lower discharge power (100W). This implies that reduction of fiber diameter will be higher. Excessive separation of fiber may occur when over 10% weight loss is achieved. As a result,

the effective pore size present in the fabric structure may increase and adversely reduce the capillary pressure. Moreover, the surface roughness induced by the higher discharge power is more severe. From the AFM experiments described in Chapter 4, the oxygen plasma treated sample (200W, 60 minutes) has a high surface roughness as reflected by the RMS values. As the textile fabric is composed of rough and irregular modified fibers, it will be more difficult to wet completely than those composed of smooth fibers [180], thus the wicking length is reduced. For the 2.5 minutes treated sample, the reason for a lower wicking rate may be due to the lower level of polar groups on the fiber surface as shown in Tables 3.2 and 3.3.

Figure 5.15 plots the wicking length against wicking time of argon plasma treated samples using 100W discharge power. For a shorter exposure time ranging from 2.5 minutes to 20 minutes, the downward wicking rates are improved. However, a prolonged exposure of 40 minutes or greater leads to the reduction of downward wicking length. A similar phenomenon is also found when using 200W discharge power. These findings agree with the higher water contact angle value as shown in Table 5.1.

The surface chemical composition (related to the contact angle) and fiber surface morphological and fabric geometrical configuration (related to the permeability and effective capillary radius) play a major role when considering the effects brought about by the plasma treatment on the fabric wickability. For the argon plasma treated sample, XPS results show that the oxygen content always increases with the exposure time and discharge power. However, both the weight loss value and the SEM micrographs confirm that the fabric density together with the fiber surface

morphology do not change much with a short exposure time. Under such conditions, the initial increase of surface oxygen may cause the increase in wicking length (100W, 2.5 minutes to 40 minutes in Figure 5.15). On the contrary, a larger increment of surface oxygen content without the modification of pore structure may lead to the retention of water instead of transporting it through the porous structure, thus the wicking length is reduced (100W, 40-60 minutes in Figure 5.15 and 200W, 5-60 minutes in Figure 5.16). In this situation, it may indicate that the water retention ability can be improved by the argon plasma with a longer exposure time or stronger discharge power.

Previous results in Chapter 3 showed that the fabric water uptake (upward wicking length after 5 minutes and with the consideration of mass of water absorbed) was nearly double after the plasma treatment. There was no significant difference between oxygen plasma and argon plasma in most of the cases when using the same discharge power level. However, higher fabric water uptake appeared to occur when the discharge power was lower (100W). As the exposure time is increased, the fabric water uptake decrease.

By comparison, the results obtained from the downward wicking measurement are different from fabric upward wicking in two aspects. First of all, the oxygen plasma treated samples behave differently in the downward wicking when compared with argon plasma treated samples. Since the water uptake value is the product of the height and weight of water wicked above reservoir, therefore, a fabric with a higher water retention capability and a shorter wicking length may have a water uptake value similar to that of a fabric with a longer wicking length and a lower water

retention capability. This suggests that the water uptake measurement is unable to distinguish different plasma treated fabrics as described above.

Second, the fabric downward wicking length for the 100W oxygen plasma treated samples does not decline as the exposure time is increased except a slight decline occurred when the 200W discharge power was used. However, the argon plasma treated samples show significant decrease in wicking length as the exposure time is increased especially when 200W discharge power is used. This finding suggests that the downward wicking measurement is more useful in quantifying the difference in the wicking properties of different treated samples.

5.3.3 Effect of Washing

As the washing process might alter the surface properties and internal structure of both untreated and plasma treated linen, so the effect of washing on the water downward wickability was also studied. The samples investigated are the untreated, oxygen plasma (100W, 5min) and argon plasma (100W, 5 minutes) treated samples, and their results are shown in Figure 5.17. As expected, the removal of oxidized components on the plasma treated samples causes the reduction of downward wicking length after washing. However, the values are still higher than the untreated sample. On the other hand, the removal of non-cellulosic material on the fabric surface and perhaps the changes of fabric structure during the washing lead to the improvement of downward wicking.

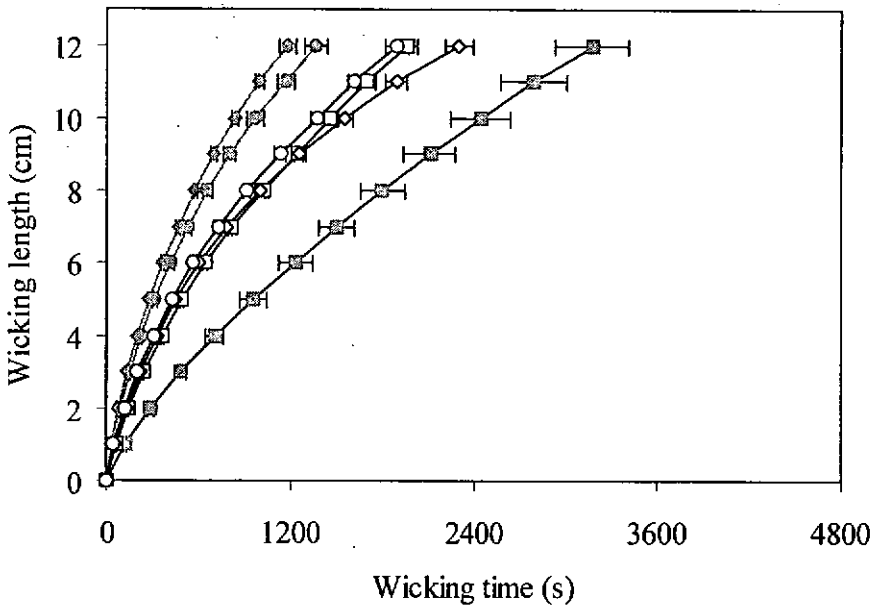

Figure 5.17: Effect of washing on the downward wicking of linen
(■) Untreated sample, (□) Untreated sample after washing,
(♦) Oxygen plasma 100W, (◊) Oxygen plasma after washing,
(●) Argon plasma 200W, (O) Argon plasma after washing.

5.4 CONCLUSION

Two characterization techniques were used to determine the effect of plasma treatment on the wetting and wicking properties of linen. The measurement of contact angles was conducted and the critical surface tension was determined by using the Zisman's plots. The measured results showed that the contact angle between the liquid and the plasma treated fabric surface was reduced.

A downward wicking measurement was proposed to study the wicking properties of plasma treated linen. The experimental set-up and testing procedures were developed. The phenomena of both upward and downward water wicking were compared experimentally. It was found that the downward wicking measurement provided a relatively constant wicking rate. The oxygen plasma treatment could increase the downward wicking rate under all the treatment conditions. However,

prolonged exposure of linen under 100W argon plasma and 200W discharge power would lead to a significant reduction of downward wicking rate. The results were discussed in terms of the changes in surface chemistry, fiber dimension and morphology as well as fabric structure (permeability).

CHAPTER 6

LINEN TREATED WITH LOW TEMPERATURE PLASMA AND ENZYME

6.1 INTRODUCTION

Linen is more expensive due to the difficulties in processing and it faces strong competition with other natural fibers. Fiber modifications by environmentally friendly processing are essential in order to simplify the preparation and finishing processes, in addition to minimize the chemical waste and associated disposal problem. In this regard, enzymes have been used extensively in yarn, fabric and garment treatments. The cellulase enzyme treatment can remove the small fiber ends from the yarn surface to create a smooth fabric appearance and introduce a degree of softness without using traditional chemical treatment. However, a significant strength reduction and slow reaction rate of the enzymatic reaction limit its industrial application.

Studies of the other cellulosic fibers such as linen, ramie and regenerated cellulose have been carried out [29, 46]. In the course of enzymatic hydrolysis of cellulosic materials, fiber structural features were found to be the most important factor which governed the yield and rate of reaction [82]. Key structural features such as crystallinity and accessible surface area determine the susceptibility of cellulosic materials to enzymatic degradation. In order to enhance the reactivity of cellulose to the catalytic reaction, physical pretreatments by plasma etching could alter the fiber surface wetting, chemical composition and surface morphology. The accessibility of crystalline region would be increased by the introduction of cracks and voids on the

fiber surface after the plasma treatment. Besides, the large molecular size of enzyme could not penetrate the fiber structure but only attacked the ends of accessible chain present on the crystalline surface. The application of plasma as a pretreatment may increase the efficiency of enzyme treatment and further modify fiber properties. Thus the objective of this chapter is to investigate the effect of plasma pretreatment on enzymatic hydrolysis of linen material with the mercerization as a comparison.

6.2 EXPERIMENTAL DETAILS

6.2.1 Sample Preparation

Scoured and semi-bleached linen fabrics used in this experiment were obtained from the same batch as specified in Section 3.2.1.

6.2.1.1 Plasma pretreatment

Plasma treatments were conducted as described in Section 3.2.1. Linen fabrics were exposed to oxygen or argon plasma at a pressure of 15Pa and discharge power of 200W for various exposure times of 2.5, 5, 10, 20, 40 and 60 minutes. An additional set of sample using 100W was produced for studying the effect of discharge power on the dyeing performance. The treated fabric sample was removed from the chamber and then conditioned under the standard condition (65% RH and 21°C) for 24 hours before characterization.

6.2.1.2 Enzyme treatment

A commercial cellulase, Cellulsoft L from Novo Nordisk was used, with its specified activity being 1500NCU/g. All the other chemicals used were of reagent grade. Enzyme treatments were carried out at 2% concentration based on the weight of

fabric sample after the plasma treatment. The treatment time was 1 hour at a temperature of 50°C with the liquor-to-goods ratio of 30:1 in a Launder-Ometer using a 1 liter pot. The machines ran at 42 rpm to provide mechanical agitation during the enzyme treatment.

For the enzymatic hydrolysis, 1g of cellulase was dissolved at room temperature in 500ml of sodium acetate buffer at pH4.5 to prepare 0.2% cellulase stock solution. For each gram of conditioned fabric, 10ml of cellulase stock solution was added. Fabric samples were immersed in the buffer solution and the temperature was raised to 50°C within 10 minutes. After the fabric samples were treated for 1 hour, the cellulase was deactivated by washing thoroughly in hot water at 70°C for 10 minutes. Finally, the samples were spin dried for 5 minutes to remove excessive water and then dried in air under standard conditions.

6.2.1.3 Dyeing process

In this study, the linen was treated by the plasma or enzyme or their combination. Since most textile goods will be subjected to dyeing subsequently, it is important to study their interaction with dyes. Moreover, the mercerization prior to the enzyme treatment was also investigated to compare with the plasma pretreatment. Dyeing behavior of the fabric sample was studied including the exhaustion curve, dyeing rate (half time of dyeing) and final exhaustion at the equilibrium of dyeing. Two direct dyes were selected with different in molecular size and shape. CI Direct Red 81 is a dye of low molecular weight with a faster rate of diffusion while the other is CI Direct Green 26 with a non-linear shape and slower rate of diffusion [44, 155].

Fabric samples were dyed with 0.5% dye and 20g/l sodium chloride at liquor-to-goods ratio of 100:1 for one hour at the boil. It had previously been established that an equilibrium could be attained within that period of time [155]. The quantity of dye taken up by the fabric sample to exhaustion, $\%E$, was determined from the difference in light absorbency of the original and exhausted dyebath solution at different times of dyeing. The light absorbancy was measured at the wavelength of maximum absorption of each dye using a Philips PU 8620 UV/VIS/IR spectrophotometer. Half time of dyeing, $t_{1/2}$, calculated from the exhaustion curves was the time taken for the material to absorb 50% of the dye at equilibrium. K/S value was calculated by the equation:

$$K/S = (1-R)^2/2R$$

where R is the measured reflectance from the dyed fabric sample.

6.2.2 Material Characterization Procedures

6.2.2.1 Bulk structure and properties

Determination of the cuprammonium fluidity, x-ray crystallinity, moisture regain, fabric weight loss and fabric strength were conducted as described in Section 3.2.2.1.

6.2.2.2 Surface morphology and properties

Scanning electron microscopic (SEM) examination, change of fabric whiteness and fabric water uptake were determined as described in Section 3.2.2.2.

6.2.2.3 Other related properties

Fabric bending properties and wrinkle recovery were measured as described in Section 3.2.2.3.

6.2.2.4 Colorfastness to washing

Colorfastness to washing of dyed linen was evaluated according to the AATCC Test Method 61-1994, Colorfastness to Laundering, Home and Commercial: Accelerated [2, 249]. AATCC Standard Reference Detergent WOB and Multifiber Test Fabric No. 10 (composed of six components including acetate, cotton, nylon, polyester, acrylic and wool) were used to assess the color change and color staining of the dyed fabric sample. However, staining to other fibers such as acetate, nylon, polyester, acrylic and wool were not distinguishable. Therefore, grading of color staining to cotton fabric was reported. The samples were prepared in accordance with the procedures stated in AATCC Test Method 61-IA. After colorfastness washing test, the samples were dried and conditioned under the standard condition.

The color change of the samples was evaluated using Grey Scales for Color Change (AATCC evaluation procedure 1) [5] and the assessment of staining on the multifiber fabrics was evaluated using the Grey Scales for Staining (AATCC evaluation procedure 2) [6]. Both evaluations were conducted under the illumination of D_{65}. The average grade number of each specimen rated by three raters was reported.

All the above measurements were carried out under standard conditions. The paired comparison *t*-test was used to determine whether any statistical significant difference occurred with a confidence limit of 95%.

6.3 RESULTS AND DISCUSSIONS

6.3.1 Bulk Structure and Properties

6.3.1.1 Fluidity and x-ray crystallinity

The experimental results of cuprammonium fluidity shown in Table 6.1 seem to show a slight reduction of the degree of polymerization of the cellulose chain after a prolonged exposure of argon plasma as higher fluidity values were observed. Besides, the fluidity value of the samples exposed to 60 minutes plasma after the enzyme treatment was slightly increased. However, based on the *t*-paired tests, no statistically significant difference could be found between the treated and control samples for all cases. Similarly, no significant change in crystallinity ratio could be found from all cases. This indicates that the plasma ablation as well as the combination with enzyme treatment attack only the ends of accessible chains on both the crystallite surface and surface amorphous region causing no significant change in the fiber bulk crystallinity.

6.3.1.2 Moisture regain

Table 6.1 shows the moisture regain of the fabric sample measured before and after the plasma treatment. A slight reduction was found after 2.5 minutes of the plasma exposure for all cases but there was no further reduction even when the exposure time was prolonged to 60 minutes. All the treated samples showed a similar reduction of moisture regain when subjected to both oxygen and argon gases at various exposure times. In the case of enzyme treatment, the sample without pretreatment showed a slight reduction of moisture regain. For the plasma pretreated samples, further reduction did occur but no significant difference could be found among all the samples pretreated at different exposure times for both gases.

As very little change occurred in the x-ray crystallinity of fibers, the reduction in moisture regain might reflect the reduction in the accessible or less ordered regions of the fiber. It might be due to the removal of amorphous region on the fiber surface caused by the limited depth of plasma penetration and so the large enzyme molecule could not penetrate the inner fiber structure.

Table 6.1: Cuprammonium fluidity, x-ray crystallinity and moisture regain of plasma and enzyme treated linen

	Plasma exposure time, min.						
	0	2.5	5	10	20	40	60
Oxygen Plasma							
Cuprammonium fluidity	17.7	16.7	-	-	-	-	17.9
CV%	2.7	1.6					0.8
X-ray crystallinity	0.81	0.80	-	-	-	-	0.81
CV%	0.9	1.3					0.7
Moisture regain, %.	7.7	7.4	7.3	7.3	7.3	7.3	7.3
CV%	2.5	3.3	2.0	2.3	3.2	4.1	2.2
Oxygen Plasma and Enzyme							
Cuprammonium fluidity	18.2	16.9	-	-	-	-	19.8
CV%	1.4	0.8					1.4
X-ray crystallinity	0.82	0.81	-	-	-	-	0.81
CV%	0.4	0.3					0.2
Moisture regain, %.	7.5	7.3	7.2	7.3	7.2	7.2	7.0
CV%	6.2	3.2	3.4	5.1	2.8	2.2	2.7
Argon Plasma							
Cuprammonium fluidity	17.7	18.1	-	-	-	-	19.3
CV%	2.7	0.6					0.5
X-ray crystallinity	0.81	0.80	-	-	-	-	0.82
CV%	0.9	1.4					0.1
Moisture regain, %.	7.7	7.3	7.3	7.3	7.3	7.3	7.4
CV%	2.5	3.2	3.4	5.1	2.8	2.2	2.7
Argon Plasma and Enzyme							
Cuprammonium fluidity	18.2	16.7	-	-	-	-	19.7
CV%	1.4	1.3					1.4
X-ray crystallinity	0.82	0.80	-	-	-	-	0.79
CV%	0.4	0.2					0.9
Moisture regain, %.	7.5	7.0	7.1	7.1	7.1	7.2	7.2
CV%	6.2	2.6	3.1	4.9	3.4	2.5	3.4

6.3.1.3 Fabric weight loss

Figure 6.1 plots the weight loss percentage against the plasma exposure time. It includes the fabric weight loss percentage of the samples after the plasma treatment,

after the enzyme treatment and the total weight loss for both types of gases. The fabric weight loss of the oxygen plasma treated samples increased with the exposure time while the time effect of the argon plasma was less significant. The oxygen plasma treatment brought about a much higher weight loss (from 0.4% to 9.5%) than the argon plasma (from 0.6% to 1.9%) under the same conditions (from 2.5 minutes to 60 minutes).

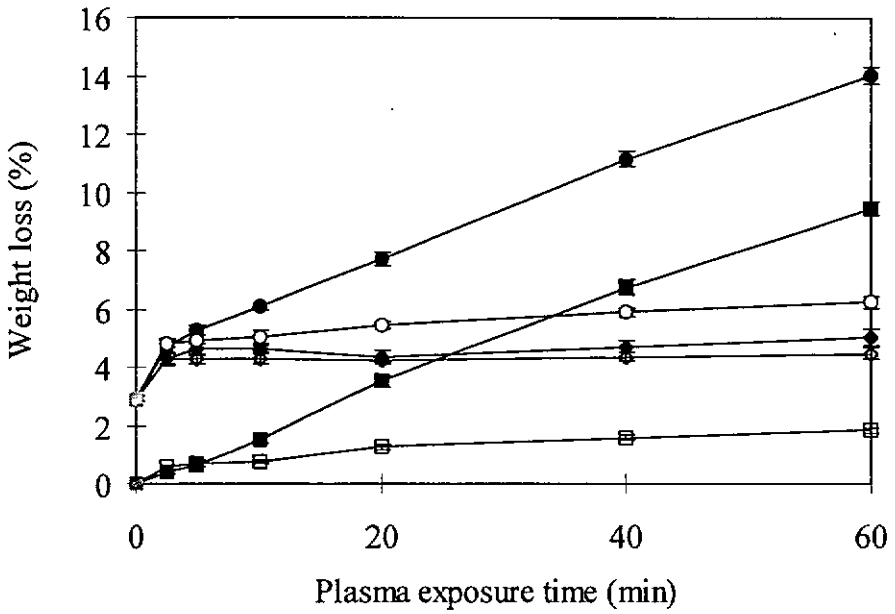

Figure 6.1: Percentage of fabric weight loss due to plasma treatments and enzyme treatments (▣) Untreated sample, (□) Un-pretreated sample after enzyme treatment, (■) After oxygen plasma treatment (200W), (♦) Weight loss % of oxygen plasma treated sample caused by enzyme treatment, (•) Total weight loss after oxygen plasma and enzyme treatment, (□) After argon plasma treatment (200W), (◊) Weight loss % of argon plasma treated sample caused by enzyme treatment, (o) Total weight loss after argon plasma and enzyme treatment.

During the enzyme treatment, the weight loss of the sample without pretreatment was 2.9%. When the enzyme treatment was applied to the plasma pretreated samples, its weight loss was higher than the sample without pretreatment, i.e., ranging from 4.3% to 5.1%. The enzyme treatment becomes more effective when the plasma pretreatment is employed. The weight loss caused by enzyme treatment of the oxygen plasma pretreated samples is slightly higher than the argon plasma pretreated samples but the difference is not significant. On one hand, the oxygen

plasma pretreated samples exhibit a higher weight loss which is dominated by the enzyme treatment for a shorter exposure time (less than 10 minute), and then by the oxygen plasma treatment after a prolonged exposure. On the other hand, the fabric weight loss of the argon plasma pretreated samples is dominated by the enzyme treatment.

After the plasma treatment, the fiber accessibility is increased due to the introduction of cracks and voids on the fiber surface as shown by the SEM micrographs in Section 6.3.2.1. Under this condition, it was assumed that the fiber structure would make the enzyme easier to penetrate. Thus the weight loss caused by the enzymatic hydrolysis was increased. Since the initial weight loss was increased by the prolonged plasma exposure (using oxygen gas with exposure time longer than 20 minutes), it is believed that a certain amount of surface polymeric material is removed resulting in a limit to the availability of accessible region to enzyme. However, the percentage of fabric weight loss was similar to those samples that had shown lower initial weight losses. Therefore, it is confirmed that the reactivity of flax fiber towards enzyme treatment is enhanced by the plasma pretreatment (by both gases and various exposure times) as reflected by a higher weight loss.

6.3.1.4 Fabric strength

Figure 6.2 shows the plot of fabric strength against the plasma exposure time. For the first 10 minutes, the fabric strength increased slightly and then decreased with the exposure time for both gases. This initial increase of strength might be due to the effects caused by the plasma etching of fiber surface such as roughening of fiber, thereby increasing the inter-fiber friction. For the oxygen plasma, a significant

reduction was found after 20 minutes of exposure. After 60 minutes of exposure to the oxygen plasma, its strength loss percentage was 44.7%. Fabric strength of the argon plasma treated sample changed slightly even after 60 minutes of exposure (9.1%).

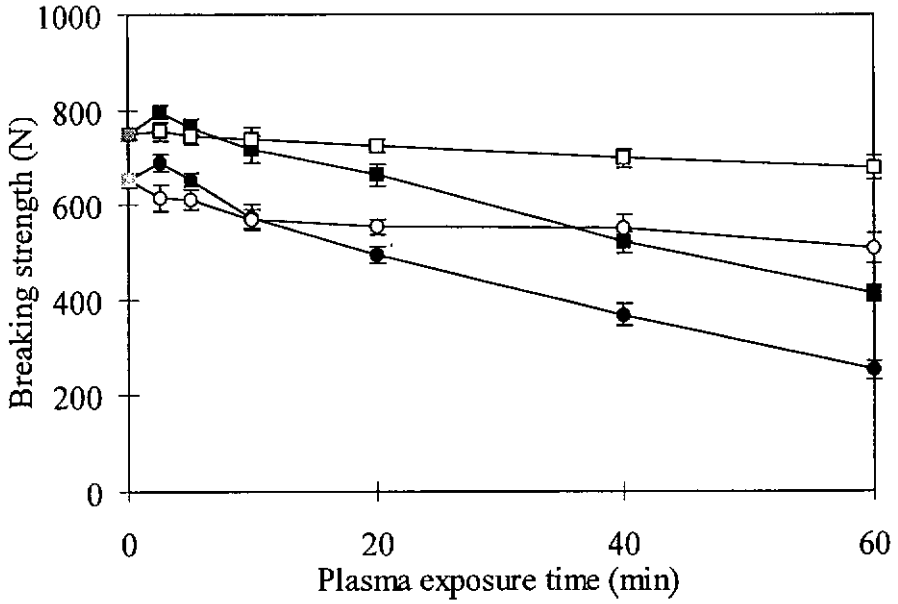

Figure 6.2: Fabric strength of plasma treated and enzyme treated samples
(▣) Untreated sample, (⊡) Un-pretreated sample after enzyme treatment,
(■) After oxygen plasma treatment (200W), (•) After oxygen plasma and enzyme treatment,
(□) After argon plasma treatment (200W), (o) After argon plasma and enzyme treatment.

When the enzyme treatment was applied to the linen without pretreatment, the fabric strength loss percentage was 12.7%. On the other hand, when the enzyme treatment was applied to the oxygen plasma pretreated samples, the fabric strength was further reduced. The accumulated strength losses ranged from 8.0% to 66.0%. In addition, the strength reduction of the argon plasma pretreated sample was increased from 17.8% to 31.9%. As the plasma exposure time was increased, the strength loss caused by the enzyme was also intensified. When the plasma pretreatment was employed prior to the enzyme treatment, the accessibility of crystalline region would be increased owing to the introduction of cracks and voids on the fiber surface.

Thus, the penetration of enzyme molecule to the fiber was increased as reflected by the higher weight loss percentage.

The results of x-ray crystallinity, cuprammonium fluidity and moisture regain have indicated that the treatments employed for this study did not alter significantly the bulk structure of flax fiber. However, the surface bombardment caused by electrons, ions and excited atoms may induce the breakage of polymer bonds creating polymer fragments with free radicals that easily crosslink with each other. This crosslinking may lead to the formation of a brittle polymer layer which in turn can act as a crack initiator [97]. In addition, the ultraviolet light generated during the plasma treatment may also cause oxidative reaction which may severely damage the fiber. The level of degradation caused by the plasma and enzyme treatment is reflected by the measured values of fabric strength.

The relationship between the percentage of strength loss and weight loss is shown in Figure 6.3. Apart from the initial increment of fabric strength after a short period of exposure time, the fabric weight loss is linearly correlated with the strength loss. A similar phenomenon was observed when ramie was exposed to an air plasma [277]. Excessive strength loss occurred when the exposure time was beyond 20 minutes using the oxygen plasma. Under this condition, tendering due to the formation of oxycellulose would occur with a prolonged exposure of cellulose in an environment above its heat resistance temperature and containing oxygen.

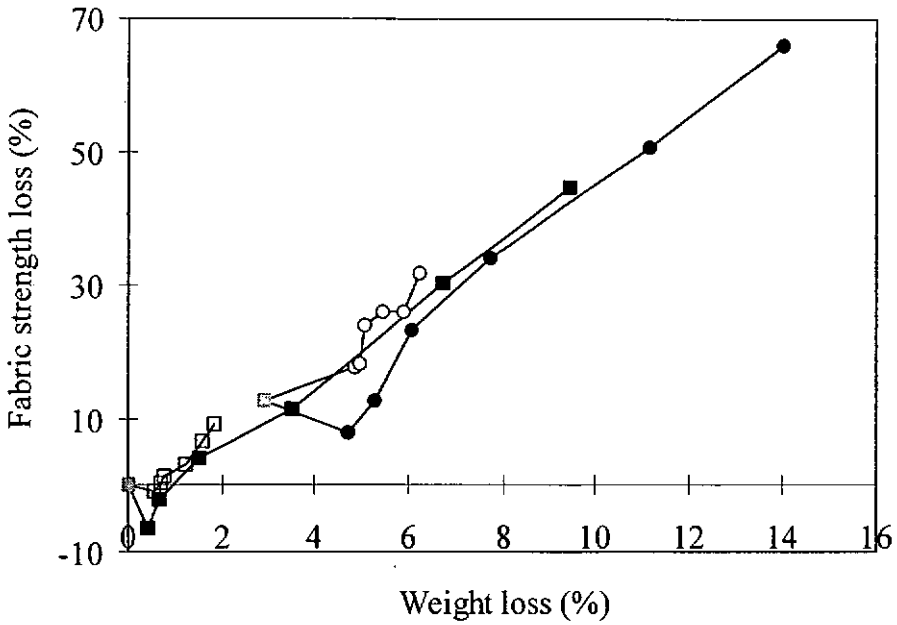

Figure 6.3: Fabric strength loss percentage as a function of fabric weight loss percentage (▨) Untreated sample, (▫) Un-pretreated sample after enzyme treatment, (■) After oxygen plasma treatment (200W), (•) After oxygen plasma and enzyme treatment, (□) After argon plasma treatment (200W), (o) After argon plasma and enzyme treatment.

The enzyme treatment leads to a more severe reduction of weight loss which again shows a linear relationship with the reduction in strength. When the accumulated weight loss reached 14.0% (60 minutes oxygen plasma and enzyme treated), the severe reduction of fabric strength is realized is obtained to be 66.0%. The accumulated weight loss of the 60 minutes argon plasma pretreated sample was found to be 6.3% after the enzyme treatment, and the strength loss was 31.9%. This phenomenon shows that the higher initial weight loss caused by the pretreatment for both gases will result in a severe strength loss. This again implies that after such pretreatment, the accessibility to the enzyme treatment is greatly increased.

However, if the oxygen plasma treatment with a shorter exposure time is followed by the enzyme treatment, a higher weight loss value will be obtained together with a small amount of fabric strength loss. This is illustrated by a sample treated for 2.5 minutes oxygen plasma and enzyme with the corresponding total weight loss of

4.7% and a total strength loss of 8.0%. It implies that an appropriate short exposure of sample to the plasma can effectively achieve a faster reaction rate and with an acceptable resultant strength loss.

6.3.2 Surface Morphology and Properties

6.3.2.1 SEM observation

Figure 6.4 shows the SEM micrographs of flax fibers treated with the oxygen plasma, illustrating a progressive change of fiber surface morphology with the treatment time and revealing the formation of voids and cracks on the fiber surface by the plasma ablation. A significant increase in progressive pitting and surface damage is observed on the fiber surface. It seems that certain spots on the fiber surface are more susceptible to etching to form cracks with the empty corncob structure being the most pronounced. Differential etching of the crystalline and amorphous regions might be the origin of roughness. The typical dimension of surface structure is in the micrometer range.

Cracks and micro-pores start at 10 minutes of exposure to appear on the surface of sample with a weight loss of 1.5%. The voids and cracks become more pronounced as the exposure time is increased. The enlarged cracks after 40-60 minutes, corresponding to 6.8% and 9.5% weight loss respectively, are perpendicular to the fiber axis and are similar to an empty corncob. When compared to the oxygen plasma, the argon plasma is not so effective in changing the surface morphology as shown in Figure 6.5. This is supported by the relatively slow rate of physical etching introduced by the argon plasma samples as reflected by the lower weight loss values, i.e., ranging from 0.6% to 1.9%.

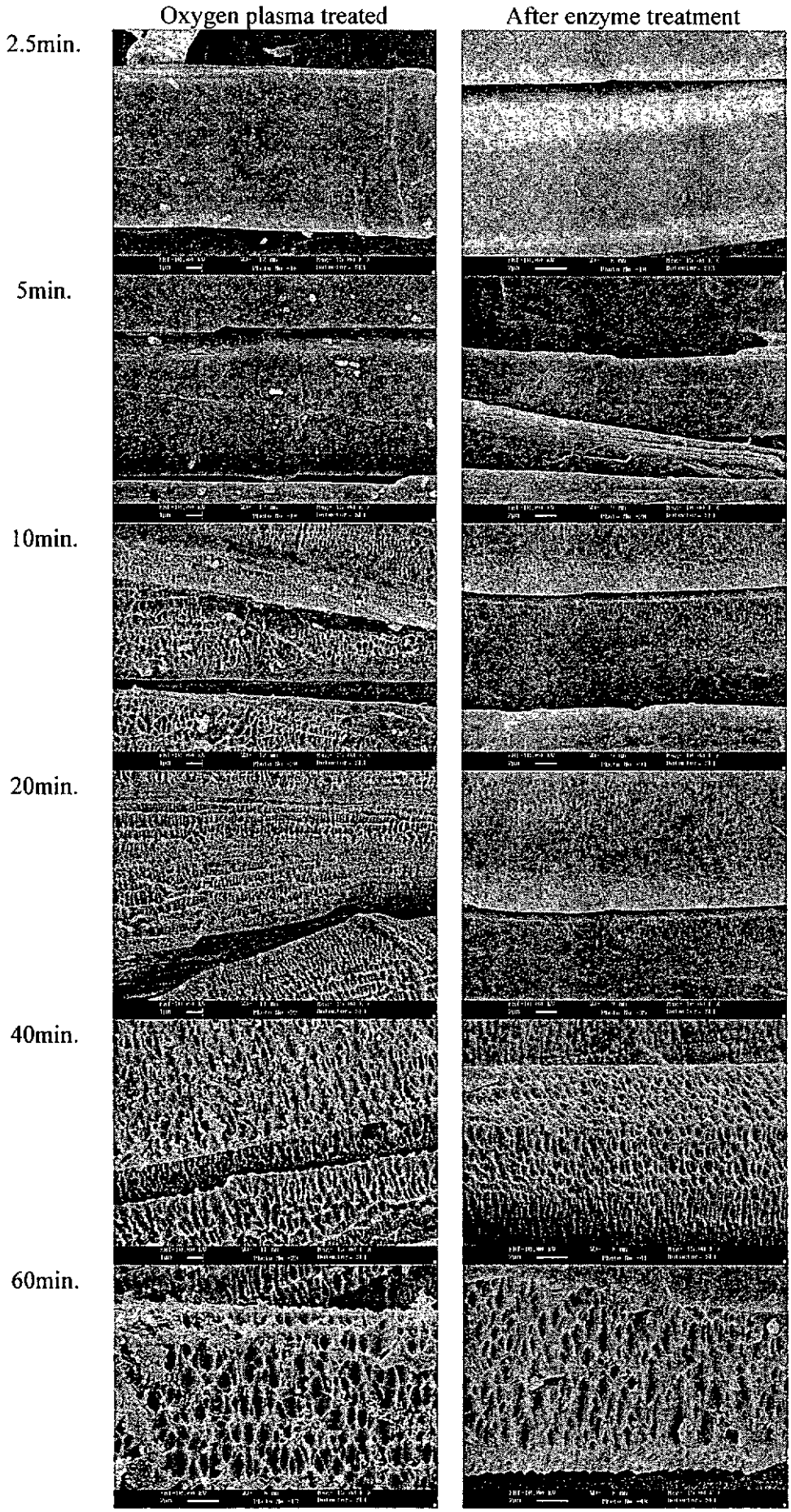

Figure 6.4: SEM micrographs of oxygen plasma treated linen before and after enzyme treatment

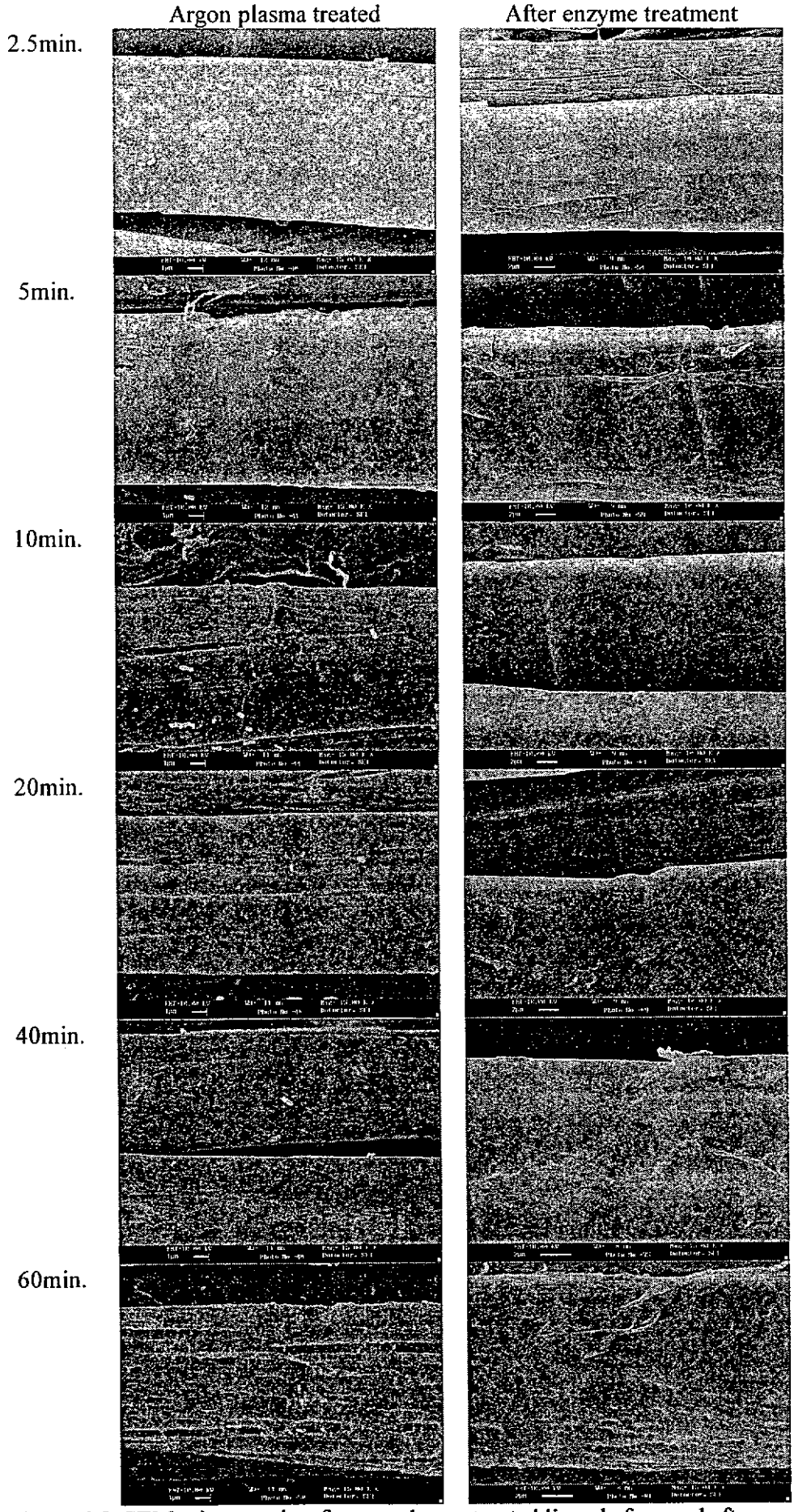

Figure 6.5: SEM micrographs of argon plasma treated linen before and after enzyme treatment

The changes in fiber surface morphology observed after the plasma treatment can be explained by the localized ablation of surface layers. The presence of micro-pores indicates the predominant effect of the interaction of the oxygen plasma (chemical etching) on the fiber surface. This process leads to an almost complete breakdown of relatively small numbers of molecule on the surface molecular chain into very low molecular components which are eventually vaporized in the low pressure system when the exposure time is prolonged. The development of cracks and voids perpendicular to the fiber axis is similar to the air plasma treated synthetic fiber studied elsewhere [277].

Largest voids and cracks in micrometer scales appear on the sample treated by oxygen plasma for 60 minutes (Figure 6.4). There is a quite large amount of starting residues left on the top of those cracks. The voids are enlarged, deepened and smoothed by the enzyme treatment. In addition to the deepening of the cracks and fissures of the rough surface created by the plasma pretreatment, most of the residual materials are also removed after the enzyme treatment. As a result, the enzyme treatment further enlarges the original surface features created by the plasma treatment.

6.3.2.2 Fabric whiteness

Figure 6.6 shows the reduction of fabric whiteness with increased plasma exposure time including the pretreated sample after the washing and enzyme treatment. The condition of washing was similar to the enzyme treatment except that the distilled water alone was used to replace the enzyme solution. It was used as a control to compare the effect of whiteness recovery after the enzyme treatment.

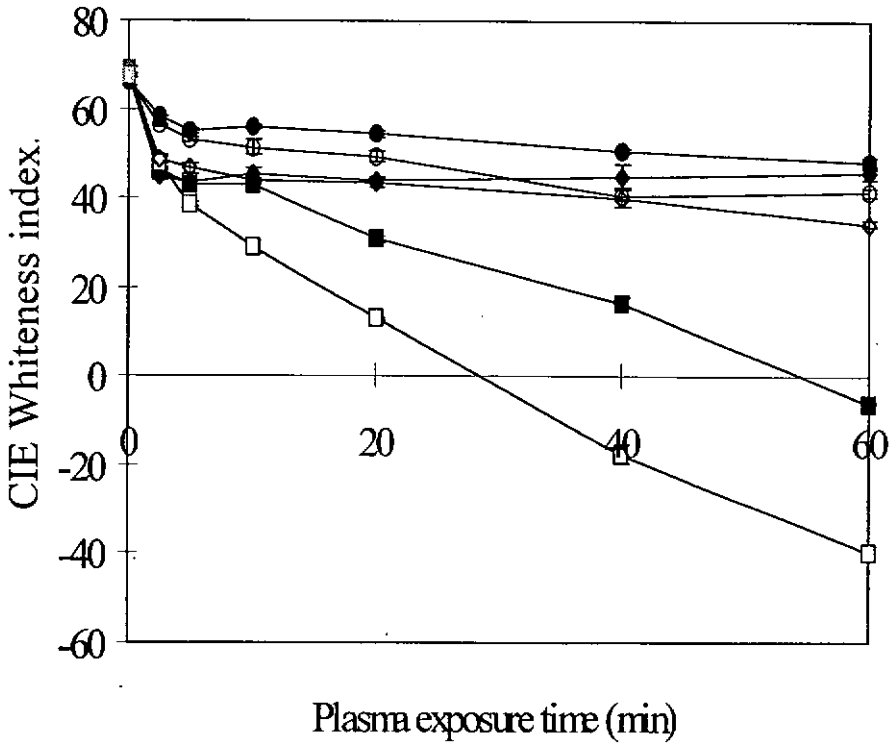

Figure 6.6: Reduction in whiteness of fabrics treated with plasma and recovered by washing and enzyme treatment (▣) Untreated sample, (□) Un-pretreated sample after enzyme treatment, (□) Un-pretreated sample after washing,
(■) After oxygen plasma treatment (200W), (♦) Oxygen plasma treated sample after washing,
(•) Oxygen plasma treated sample after enzyme treatment,
(□) After argon plasma treatment (200W), (◊) Argon plasma treated sample after washing,
(o) Argon plasma treated sample after enzyme treatment.

The experimental results show that the fabric yellowness increases with the plasma exposure time. While the yellowness due to the oxygen plasma treatment is severe and the argon plasma makes the fabric even yellower in all cases. On one hand, it is expected that the oxidative effect brought about by the oxygen plasma should be more prominent than the argon plasma in terms of fabric yellowing. On the other hand, a higher ablation rate caused by the oxygen plasma might lead to the fast removal of yellow component subsequently. The differences in yellowness brought about by the oxygen and argon plasma might be due to the slower ablation rate of the inert gas (argon gas) resulting in the accumulation of more yellow oxidized component on the fiber surface. This explanation is supported by the higher weight loss value of the oxygen plasma treated sample as discussed in Section 6.3.1.3. The yellowness should be reduced to a certain level after the enzyme treatment. The

results show that the yellowness caused by the plasma treatment is almost totally removed after the enzyme treatment. When considering the effect of washing on the plasma pretreated sample, the enzyme treatment is more effective in recovering the fabric whiteness especially for the argon plasma treated samples.

6.3.2.3 Fabric water uptake

Irradiation of cotton fiber in the plasma was found to cause the introduction of polar groups onto the fiber surfaces, thereby increasing the rate of fabric water uptake and making it more water absorbent [231]. The effect of oxygen and argon plasma on the fabric water uptake is shown in Figure 6.7. A significant improvement of fabric water uptake is found after exposure to both types of gas for all cases. The highest rate of increment of fabric water uptake is obtained initially and the value is nearly double after 5 minutes of exposure. Subsequently, the rate of fabric water uptake increment declines as the exposure time is increased. There is no significant difference between these two types of gas for most of the cases.

It is known that the fabric water uptake of the material depends on the surface morphology and its polarity. It is expected that the physical modification of fiber surfaces might be one of the main factors influencing its fabric water uptake as reflected by the increment of surface area and reduction of fiber fineness leading to the increase of capillary effect. These effects are supported by SEM observation and the weight loss measurement. Apart from the capillary effect, increased hydrophilicity together with the incorporation of polar groups, as reflected by the results of XPS analysis in Section 3.3.2.1, can be used to describe the changes of fabric water uptake.

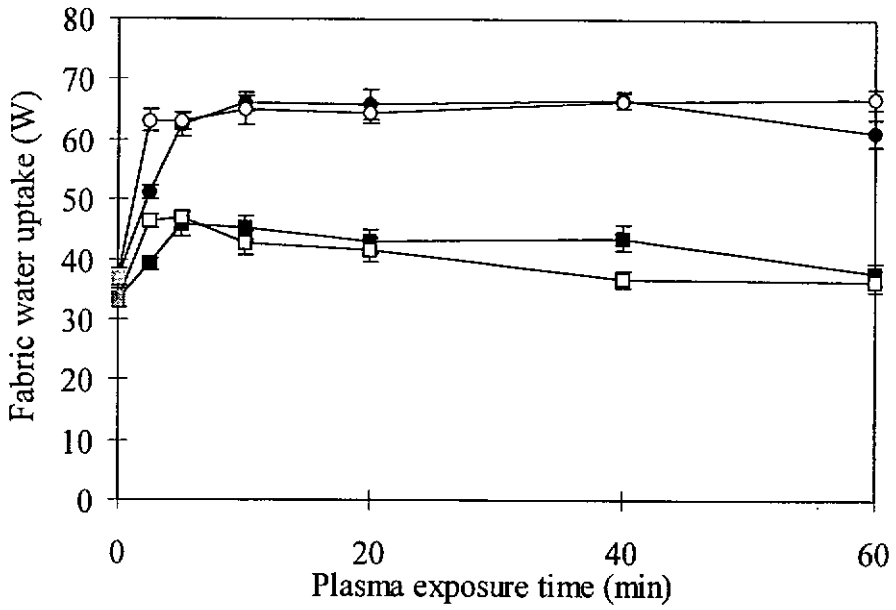

Figure 6.7: Effect of plasma and enzyme treatments on fabric water uptake
(▩) Untreated sample, (▨) Un-pretreated sample after enzyme treatment,
(■) After oxygen plasma treatment (200W), (•) After oxygen plasma and enzyme treatment,
(□) After argon plasma treatment (200W), (o) After argon plasma and enzyme treatment.

Fabric water uptake is increased for all cases after a short exposure time. As the weight loss percentage and the changes of fiber surface appearance are not so significant at such short times, the modification should only be attributed to the change of surface hydrophilic property. XPS results indicated that the oxidized components especially the -COOH group increased significantly after a short exposure time of 2.5 minutes for all cases, which was in agreement with previous findings mentioned in the literature [209]. However, after a prolonged exposure, the fabric water uptake is reduced for both gases. The results are contradictory to the findings that a higher reduction of fiber fineness (higher weight loss), a significant increase of fiber surface area (SEM micrographs) and improved hydrophilicity of fiber surface (XPS analysis) occur at prolonged exposure.

After the enzyme treatment, a further considerable increase of fabric water uptake was found. This may be attributed to the higher reduction of fiber fineness caused

by the enzyme treatment resulting in about 5% of additional weight loss. In addition, a further improvement of fabric water uptake may also be attributed to the removal of hydrophobic non-cellulosic component from the fabric surface by the enzymatic treatment of cellulose [109].

6.3.3 Other Related Fabric Properties

6.3.3.1 Fabric bending properties

The measured values of bending rigidity and hysteresis are shown in Table 6.2. The reduction in fabric bending rigidity and hysteresis caused by the oxygen plasma is more noticeable especially at 2.5 minutes exposure time. Afterwards, they slightly increase. Similar profiles are also found with the argon plasma but the exposure time required to achieve the lowest bending rigidity and hysteresis is 10 minutes. During the plasma treatment, the breakage of polymer molecules may occur and the fiber becomes finer, thus making the fiber softer and flexible for bending. However, a prolonged exposure of sample under the plasma condition would lead to over drying and hardening, cross-linking, as well as the increased fiber surface roughness (SEM micrographs as shown in Figure 6.5) would affect the reduction of bending rigidity adversely. This phenomenon was also reflected by the reduction of fabric strength and water uptake.

A reduction of bending rigidity occurred among all the enzyme treated samples. By the 'bio-polishing' effect provided by the enzyme treatment, the fiber surface roughness is reduced. Therefore, the inter-fiber friction would reduce as reflected by the measured values of bending rigidity and hysteresis. The effect of the oxygen plasma pretreatment on the reduction of bending rigidity after the enzyme treatment

is less apparent. However, a significant reduction of bending rigidity occurs to the argon plasma pretreated sample after the enzyme treatment. Similar results were also obtained from the value of measured bending hysteresis. In conclusion, enzyme treatment is more effective in reducing both bending rigidity and hysteresis of the argon plasma pretreated sample than the oxygen plasma pretreated sample.

Table 6.2: Bending rigidity, bending hysteresis and wrinkle recovery of samples after plasma and enzyme treatment

	Plasma exposure time, min.						
	0	2.5	5	10	20	40	60
Oxygen Plasma							
Bending rigidity, gfcm^2/cm.	0.68	0.51	0.56	0.60	0.58	0.51	0.50
CV%	8.4	6.5	5.0	5.7	8.2	8.5	10.8
Bending hysteresis, gfcm/cm.	0.54	0.41	0.45	0.51	0.47	0.40	0.37
CV%	9.1	11.7	6.4	5.9	9.8	7.2	16.9
Wrinkle recovery, %.	25.1	27.1	26.9	27.4	27.6	28.0	28.5
CV%	7.1	5.4	5.6	3.4	4.8	3.2	5.4
Oxygen Plasma and Enzyme							
Bending rigidity, gfcm^2/cm.	0.57	0.49	0.54	0.55	0.54	0.51	0.49
CV%	7.5	5.2	5.0	7.5	9.9	6.9	6.7
Bending hysteresis, gfcm/cm.	0.55	0.42	0.43	0.44	0.43	0.37	0.37
CV%	5.5	9.1	9.7	6.9	7.2	7.7	8.1
Wrinkle recovery, %.	30.1	30.2	30.1	31.4	30.2	30.9	31.5
CV%	6.7	5.8	5.0	6.7	5.7	3.5	4.1
Argon Plasma							
Bending rigidity, gfcm^2/cm.	0.68	0.69	0.69	0.54	0.76	0.74	0.73
CV%	8.4	6.4	5.1	4.7	3.4	6.3	7.1
Bending hysteresis, gfcm/cm.	0.54	0.58	0.58	0.45	0.67	0.67	0.64
CV%	9.1	5.8	7.4	6.6	6.4	5.0	6.0
Wrinkle recovery, %.	25.1	26.2	28.0	27.3	26.4	26.4	25.0
CV%	7.1	6.4	5.0	6.1	5.0	5.0	3.7
Argon Plasma and Enzyme							
Bending rigidity, gfcm^2/cm.	0.57	0.58	0.59	0.57	0.57	0.57	0.58
CV%	7.5	5.9	6.7	6.0	8.6	7.0	4.5
Bending hysteresis, gfcm/cm.	0.55	0.55	0.54	0.46	0.52	0.50	0.52
CV%	5.5	9.5	8.2	6.1	4.9	7.1	6.1
Wrinkle recovery, %.	30.1	30.8	30.8	31.4	31.3	32.6	32.5
CV%	6.7	4.4	3.1	5.7	6.6	4.2	4.5

6.3.3.2 Wrinkle recovery

Table 6.2 also shows the measured fabric wrinkle recovery percentage as a function of plasma exposure time before and after the enzyme treatment. A slight

improvement is found after 2.5 minutes of plasma exposure for all cases but there is no further change up to the exposure time of 60 minutes. The plasma treatment alone does not change the wrinkle recovery of the linen significantly. Similarly, a slight improvement of wrinkle recovery is found after the enzyme treatment and the degree of improvement is approximately the same for all the samples including the control. This indicates that the plasma pretreatment does not enhance the improvement of wrinkle recovery percentage if followed by enzyme treatment.

6.3.4 Dyeing Properties

Dyeing performance of the fabric sample after the treatments was evaluated by the half time of dyeing, final exhaustion percentage and K/S values with the results being shown in Table 6.3. Colorfastness values to washing of the dyed sample are shown in Table 6.4. Direct dye usually enters the less ordered areas of the cellulosic fiber through water-filled pores. They attach themselves through weak interactions and additional physical entrapment by means of dye association in these areas and on the fiber surface. It is believed that a direct dye is capable of forming stronger interactions with cellulose chains simply because of its large size [30]. The final depth of shade achieved by a dyed sample is affected by the actual dye content, modification of internal scattering and the changes of fiber size or shape after the treatment [44]. When dyeing the plasma or enzyme treated samples, it was assumed that two kinds of region could be accessible to dye. The first region is amorphous initially and should be readily etched or digested by the plasma or enzyme while the second region is the amorphous region newly developed or revealed by the plasma and enzyme treatments.

Table 6.3: Fabric weight loss percentage, half time of dyeing, final exhaustion and K/S value of plasma pretreated and enzyme treated sample dyeing with CI Direct Red 81 and Green 26

			CI Direct Red 81							CI Direct Green 26						
			Plasma exposure time, min.							Plasma exposure time, min.						
			0	2.5	5	10	20	40	60	0	2.5	5	10	20	40	60
Case 1	100W Oxygen	Wt loss, %.	-	0.1	0.3	1.0	2.0	4.4	6.7	-	0.1	0.3	1.0	2.0	4.4	6.7
	plasma treated	½ time of dyeing, min.	3.0	2.9	2.9	2.8	3.0	2.9	3.1	4.2	4.5	4.4	4.4	4.6	4.5	4.4
		Final exhaustion, %.	54.4	54.4	54.3	54.9	56.6	56.2	57.9	63.6	64.5	64.0	63.8	65.7	63.6	65.5
		K/S value	3.4	3.5	3.5	3.6	3.6	3.5	3.6	5.1	5.0	4.9	4.8	4.6	4.4	4.6
Case 2	200W Oxygen	Wt loss, %.	-	0.3	0.6	1.6	3.4	7.0	10.3	-	0.3	0.6	1.6	3.4	7.0	10.3
	plasma treated	½ time of dyeing, min.	3.0	2.9	2.8	2.9	3.2	3.1	2.9	4.2	4.3	4.4	4.3	4.3	4.3	4.2
		Final exhaustion, %.	54.4	54.9	55.5	57.6	61.0	59.3	59.1	63.6	66.6	66.5	66.3	67.4	66.4	69.8
		K/S value	3.4	3.4	3.5	3.4	3.6	3.5	3.5	5.1	4.9	4.9	4.5	4.7	4.4	4.6
Case 3	200W Oxygen	Wt loss, %.	2.9	4.7	5.3	6.1	7.7	11.2	14.0	2:9	4.7	5.3	6.1	7.7	11.2	14.0
	plasma and	½ time of dyeing, min.	2.9	3.0	3.2	3.0	3.3	3.0	3.0	5.7	8.9	8.6	8.8	8.3	8.7	9.5
	enzyme treated	Final exhaustion, %.	53.9	53.7	55.9	56.5	58.0	58.1	58.8	62.7	63.0	64.0	64.6	64.9	67.7	68.6
		K/S value	3.5	3.6	3.5	3.6	3.6	3.6	3.6	5.0	4.6	4.7	4.5	4.4	4.4	4.6
Case 4	100W Argon	Wt loss, %.	-	0.2	0.4	0.5	1.1	1.1	1.5	-	0.2	0.4	0.5	1.1	1.1	1.5
	plasma treated	½ time of dyeing, min.	3.0	3.0	2.9	2.8	3.0	3.1	3.1	4.2	4.4	4.4	4.3	4.3	4.4	4.3
		Final exhaustion, %.	54.4	54.4	53.7	53.7	53.4	53.9	53.3	63.6	67.2	66.9	66.2	67.5	66.3	66.4
		K/S value	3.4	3.6	3.6	3.6	3.7	3.6	3.5	5.1	5.0	4.7	4.8	4.8	4.4	4.3
Case 5	200W Argon	Wt loss, %.	-	0.4	0.5	0.6	1.1	1.4	1.7	-	0.4	0.5	0.6	1.1	1.4	1.7
	plasma treated	½ time of dyeing, min.	3.0	2.9	2.8	2.8	3.0	2.9	3.0	4.2	4.7	4.8	4.8	4.8	4.9	4.9
		Final exhaustion, %.	54.4	57.5	57.3	56.9	58.0	57.9	57.4	63.6	66.5	67.5	67.4	68.2	67.7	68.2
		K/S value	3.4	3.6	3.6	3.6	3.5	3.4	3.4	5.1	4.8	4.7	4.5	4.4	4.2	4.1
Case 6	200W Argon	Wt loss, %.	2.9	4.8	4.9	5.0	5.4	5.9	6.3	2.9	4.8	4.9	5.0	5.4	5.9	6.3
	plasma and	½ time of dyeing, min.	2.9	3.0	3.1	3.0	2.9	3.2	3.1	5.7	7.3	7.3	7.3	7.2	7.5	7.1
	enzyme treated	Final exhaustion, %.	53.9	54.2	55.7	56.6	57.2	57.9	57.5	62.7	62.7	67.5	67.2	68.0	67.5	67.0
		K/S value	3.5	3.6	3.7	3.7	3.7	3.7	3.5	5.0	4.7	4.5	4.4	4.3	4.3	4.2

Table 6.4: Colorfastness to washing of plasma pretreated and enzyme treated sample dyeing with CI Direct Red 81 and Green 26

	CI Direct Red 81							CI Direct Green 26						
	Plasma exposure time, min.							Plasma exposure time, min.						
	0	2.5	5	10	20	40	60	0	2.5	5	10	20	40	60
Colour Change														
100W Oxygen plasma treated	3.7	4.3	4.3	4.0	4.2	4.2	4.0	4.5	4.7	4.5	4.5	4.5	4.3	4.7
200W Oxygen plasma treated	3.7	4.3	4.2	4.2	4.3	4.2	4.2	4.5	4.7	4.8	4.5	4.8	4.3	4.8
200W Oxygen plasma and enzyme treated	3.5	3.8	4.3	4.3	4.0	4.0	3.8	4.7	4.7	4.8	4.5	4.5	4.8	4.7
100W Argon plasma treated	3.7	4.2	4.5	4.2	4.3	4.3	4.2	4.5	4.7	4.7	4.5	4.7	4.2	4.7
200W Argon plasma treated	3.7	4.3	4.2	4.3	4.2	4.5	4.3	4.5	4.8	4.7	4.8	4.8	4.7	4.5
200W Argon plasma and enzyme treated	3.5	4.2	4.5	4.3	4.2	4.2	4.3	4.7	4.8	4.7	4.7	4.8	4.7	4.5
Colour Staining on Cotton														
100W Oxygen plasma treated	2.2	2.2	2.7	2.5	2.5	2.5	2.5	4.5	4.7	4.7	4.8	4.5	4.8	4.8
200W Oxygen plasma treated	2.2	2.3	2.3	2.5	2.3	3.0	2.8	4.5	4.7	4.7	4.7	4.8	4.7	4.8
200W Oxygen plasma and enzyme treated	2.0	2.7	2.5	2.5	2.5	3.0	2.5	4.8	5.0	4.8	5.0	4.7	4.8	4.8
100W Argon plasma treated	2.2	2.5	2.7	2.7	2.8	2.7	2.7	4.5	4.8	4.7	4.5	4.7	4.7	4.8
200W Argon plasma treated	2.2	2.5	2.7	2.2	2.0	2.2	2.2	4.5	4.8	5.0	4.8	5.0	4.8	4.7
200W Argon plasma and enzyme treated	2.0	2.5	2.3	2.5	2.3	2.2	2.5	4.8	4.7	5.0	5.0	5.0	4.8	4.8

6.3.4.1 Effect of plasma treatment

When the oxygen plasma treated samples were dyed with the direct dye of a smaller molecular size (red dye), the dyeing rate was first increased and then returned back to the initial level as shown in Cases 1 and 2 in Table 6.3. At the initial stage of plasma treatment, a new surface was created together with a considerable increment of absorption as reflected by the measurement of fabric water uptake. However, as the exposure was prolonged, the removal of the surface amorphous region would cause eventually the reduction of dyeing rate. On the other hand, improvement of final exhaustion percentage was achieved by using 200W discharge power. In addition, the K/S value increases slightly. This increment may be basically due to the porous surface structure created by the plasma etching and the increased dye adsorption.

With the direct dye of a larger molecular size (green dye), the dyeing rate is slightly reduced. However, the final exhaustion percentage is increased in contrast to the reduced K/S value. This may be explained by the fact that the changes of fiber size and shape after the plasma treatment greatly affect the color reflection of the material dyed with a larger dye molecule. As the plasma etching on linen creates numerous surface features, thus the reflection of color is reduced.

A similar dyeing behavior of the argon plasma treated samples is found. As shown by Cases 4 and 5 in Table 6.3, the change of dyeing rate profile for smaller dye molecule is similar to that of the oxygen plasma treated sample. The dyeing rate is first increased and then returned back to the initial level. The final exhaustion is increased for the 200W argon plasma treated sample but only slightly changed in the

case of 100W discharge power. Furthermore, the depth of shade reflected by the K/S value has increased slightly. When dyeing with a larger dye molecule, samples treated by the argon plasma using 200W discharge power show the slowest dyeing rate. The final exhaustion percentage is increased while the K/S value is reduced which is again similar to the oxygen plasma treated sample.

Cases 1 and 2 in Table 6.3 show that the dyeing rate of smaller dye molecule is slightly increased with the short exposed time but the dyeing rate of larger dye molecule is reduced. The final exhaustion is increased for both types of dyes. The use of 200W discharge power shows a greater increase of dyeing performance in terms of the final exhaustion percentage for most of the cases. Higher exhaustion percentages are achieved by both the oxygen plasma treated sample dyed with a smaller dye molecule and the argon plasma treated samples dyed with a larger dye molecule in most of the cases.

Because the plasma etches the fiber surface and creates new surface structures with a larger area and after a prolonged exposure, the removal of surface amorphous region plus the etching of the surface crystalline region results, the surface changes on surface chemical composition or water uptake is increased as demonstrated by the XPS analysis and water uptake test respectively. Therefore, the dyeing performance of the plasma treated sample would be expected to improve. Table 6.4 confirms that the color change of the sample and color staining on cotton fabric of the plasma treated linen have been improved in most of the cases. This implies that the plasma treatments can enhance the interaction of dye molecules with the fiber surface as reflected by the higher final exhaustion percentage and improved color fastness.

6.3.4.2 Effect of enzyme treatment on the plasma pretreated linen

The enzymatic treatment of cellulosic textile materials is a non-toxic 'bio-finishing' process which has gained an increasing practical importance for various kinds of textile goods to enhance softness and surface appearance, and reduce pilling propensity [190, 242]. It is particularly important to investigate the effect of enzymatic hydrolysis on the dyeability of the treated fibers.

As shown in Table 6.3, the change of dyeing performance due to the enzyme treatment is not very significant for most of the cases. In the case where the oxygen plasma treated samples dyed with the direct dye of smaller molecular size (red dye), the dyeing rate first increases and then returns back to the initial level. The dyeing rate does not have any significant change after the subsequent enzyme treatment as shown in Case 3. The final exhaustion of the oxygen plasma treated sample increases but the extent of increase is reduced after the enzyme treatment. Similarly with repect to the dyeing rate, no significant change can be found in the K/S value.

An exception can be observed for the direct dye of larger molecular size (green dye) with the dyeing rate (half-time) being greatly reduced. In addition, the final exhaustion of the oxygen plasma pretreated samples is reduced by the enzyme treatment which is similar to the result of dyeing using the smaller dye molecule. No significant change can be found in the K/S values brought about by the enzyme treatment. The susceptibility of the oxygen plasma pretreated linen towards the larger dye molecule is reduced.

The results of Case 6 in Table 6.3 show that similar changes occur with the argon plasma pretreated samples after the enzyme treatment to those with the oxygen plasma pretreated samples when dyeing with smaller dye molecule. The dyeing rate is also reduced but the magnitude is less than the oxygen plasma pretreated sample when dyeing with larger dye molecule. The final exhaustion is not affected by the enzyme treatment and also no significant change can be found in the K/S value. The effect of changing the dyeing performance by the enzyme treatment is greater for the oxygen plasma pretreated sample than the argon plasma pretreated sample.

Enzymatic hydrolysis is primarily a surface reaction consisting of complex steps. Cellulases are large-sized protein, most of them are unable to access the crystalline area of the substrate due to the geometric constraints [29-30]. Thus the enzymatic action is to weaken the fiber surface fibrils and amorphous regions, and remove them through the mechanical action applied during the treatment. As the enzyme may remove the surface amorphous region of the fiber, the dyeability of the enzyme treated sample is expected to reduce [47, 175-176, 148], which is confirmed by the results of plasma treated samples in Case 3 and Case 6 as shown in Table 6.3.

Plasma alone apparently slightly increases the dyeing rate with a short exposure but reduces it with a prolonged exposure. The cellulase treatments further reduce the dyeing rate especially when dyeing with the larger dye molecule. This suggests that the cellulase can digest the amorphous regions and reduce the accessibility of the larger dye molecule to the fiber resulting in the reduction of final exhaustion percentage and shade depth. The effect is more prominent for the oxygen plasma pretreated sample.

The experimental results in Table 6.4 show that the effect of enzyme treatment on the colorfastness properties of both the untreated and plasma pretreated linen is not very significant. This implies that enzyme treatment only affects the dyeing rate of the sample but not the interaction and adhesion between the fiber and dye.

6.4 CONCLUSION

The potential of using the oxygen or argon plasma as the pretreatment prior to the enzyme treatment on linen has been studied. The pretreatment changes the surface morphology and chemical property as reflected by the appearance of small voids and increase in oxygen content. No detectable fiber damage was observed after the plasma and enzyme treatment as evidenced by the x-ray crystallinity and fluidity measurement. A slight reduction in moisture regain was detected for all the plasma pretreated samples after 2.5 minutes treatment, and further reductions of similar amount could be seen when further subjected to the enzyme treatment. The losses of both fabric weight and strength increased with exposure time. The results confirmed that the plasma pretreatment did enhance the effectiveness of enzymatic hydrolysis. The cracks of the rough surface created by the plasma pretreatment were removed, and the depth and width of the pore were further deepened, smoothed and enlarged by the enzyme treatment. Fabric whiteness was reduced after the exposure to the plasma pretreatment and could be effectively recovered by the enzyme treatment. A significant improvement of fabric water uptake was found after the sample was exposed to the plasma pretreatment and it was further improved greatly for all cases after the enzyme treatment. A slight improvement of fabric bending rigidity, hysteresis and wrinkle recovery could be achieved by both treatments. By means of the plasma pretreatment with a shorter exposure time, i.e., 2.5 minutes of oxygen

plasma treatment, the effectiveness of enzyme treatment could be enhanced as a faster reaction rate and acceptable resultant strength loss could be achieved.

With the aid of plasma pretreatment, the dyeing rate of the smaller dye molecule (red dye) was slightly increased with a shorter exposure time for all cases, but the dyeing rate of the larger dye molecule (green dye) was reduced. With regard to final exhaustion, it was increased for both types of dyes. The K/S value of the sample dyed with smaller dye molecule was slightly improved, but slightly reduced while dyeing with larger dye molecule. Prolonged plasma exposure alone apparently would reduce the dyeing rate slightly, while the cellulase treatment further reduced the dyeing performance especially with the direct dye of larger molecular size. When considering the washing fastness properties, improvement could be achieved by the plasma pretreatment, whereas enzyme treatment did not affect the fastness property apparently.

CHAPTER 7

LINEN TREATED WITH MERCERIZATION AND ENZYME

7.1 INTRODUCTION

Structural features such as crystallinity can determine the susceptibility of cellulosic materials towards enzymatic hydrolysis. In order to enhance the reactivity of cellulose in the catalytic reaction, mercerization is often used for cotton yarn to reduce the fiber crystallinity [28, 172]. The application of sodium hydroxide (mercerization) to flax yarns have been shown to increase their accessibility and yarn strength while the tension was applied during the treatment [43]. Besides, previous literature have reported that a certain level of mechanical agitation during the enzyme treatment can affect the resultant enzymatic hydrolysis [36-37]. Thus the objective of this chapter is to investigate the effect of both mercerization pretreatment and mechanical agitation on the enzyme treatment of linen.

7.2 EXPERIMENTAL DETAILS

7.2.1 Sample Preparation

Scoured and semi-bleached linen woven fabrics used in this experiment were obtained from the same batch as specified in Section 3.2.1.

7.2.1.1 Mercerization pretreatment

Three levels of mercerization tension were applied to the linen material, i.e., slack, 95% tension (with 5% shrinkage during mercerization) and 100% tension

mercerization (restricted to the original length during mercerization). For slack mercerization, the fabric samples were immersed in 20% sodium hydroxide solution for 10 minutes at 20°C. Neutralization was carried out by rinsing the mercerized samples in distilled water for 10 minutes followed by the addition of 1% acetic acid and then rinsed again until the rinse water was neutral. A stainless steel needle frame was used for controlling the fabric tension. The tension mercerized fabric sample was removed from the frame after final rinsing and then allowed to dry in air without restraint. The samples were spin dried for 5 minutes to remove excessive water and then air dried under the standard condition (65% RH and 21°C). Table 7.1 lists the fabric specifications.

Table 7.1: Fabric specifications

Fabric type	Fabric count[a], warp/weft	Weight/area, g/m^2
Linen	21/20	154
100% Tension mercerized	22/20	164
95% Tension mercerized	24/21	180
Slack mercerized	25/24	226

[a] Number of yarns per cm.

7.2.1.2 Enzyme treatment

Enzyme treatments were conducted as described in Section 6.2.1.2. Enzyme treatments were carried out separately at 1% and 2% concentrations based on the weight of fabric sample with the treatment time ranging from one to four hours. The effect of mechanical agitation on the enzyme treatment was studied at two levels. Five or ten stainless steel balls were added to each washing pot to attain a medium and high agitation respectively for the enzyme treatment. The stainless steel balls were used to provide an increased level of mechanical agitation in various standard fastness test methods.

7.2.1.3 Dyeing process

Dyeing process was conducted as described in Section 6.2.1.3

7.2.2 Material Characterization Procedures

7.2.2.1 Bulk properties

X-ray crystallinity, moisture regain, fabric weight loss and fabric strength were measured as described in Section 3.2.2.1. Fabric thickness was measured by the FAST-1 (Compression Meter of FAST system) and fifteen samples were used. The untreated control samples were washed in distilled water and air dried before measurement. Fabric thickness was measured at $2gf/cm^2$ and $100gf/cm^2$, and the surface thickness was calculated from the thickness difference between $2gf/cm^2$ and $100gf/cm^2$. Fabric bending properties were measured as described in Section 3.2.2.3.

7.2.2.2 Surface morphology

Scanning electron microscopy (SEM) examination was carried as described in Section 3.2.2.2.

7.2.2.3 Colorfastness to washing

Colorfastness to washing of dyed linen was evaluated as described in Section 6.2.2.4.

All the above measurements were carried out under the standard condition. The paired comparison *t*-test was used to determine whether any statistical significant difference occurred with a confidence limit of 95%.

7.3 RESULTS AND DISCUSSIONS

7.3.1 Effect of Mercerization Pretreatment on Enzyme Treatment

7.3.1.1 X-ray crystallinity and moisture regain

The x-ray crystallinity ratio of the cellulosic material was used to determine the degree of modification of the fiber accessibility. The crystallinity was calculated based on the ratio with respect to the sum of the amorphous and crystalline region of the cellulosic material. The experimental results are shown in Table 7.2.

Table 7.2: X-ray crystallinity and moisture regain of untreated and mercerized linen after 4 hours using 2% enzyme

	X-ray crystallinity		Moisture regain, %	
Fabric type	Before enzyme treatment	After enzyme treatment	Before enzyme treatment	After enzyme treatment
Linen	0.81	0.82	6.4	6.2
CV%	1.0	1.1	3.3	4.6
100% Tension mercerized	0.79	0.80	7.6	7.3
CV%	0.5	0.6	3.2	3.4
95% Tension mercerized	0.78	0.78	7.9	7.8
CV%	0.8	2.2	4.2	5.1
Slack mercerized	0.77	0.78	7.8	7.9
CV%	0.2	1.8	3.6	3.1

A significant reduction in the x-ray crystallinity was found for the slack mercerized sample when compared with the untreated sample. However, the magnitude of change was less prominent in the tension mercerized samples since the lateral movement of the polymer chains was restricted by the applied tension during the caustic swelling. There was no additional change in x-ray crystallinity and moisture regain brought about by the enzymatic treatments, indicating that there were no changes in either the accessible surface area or crystallinity. This phenomenon [79, 82, 258, 263, 266-267] might be attributed to the mechanism such that the large

enzyme molecules could not penetrate the structure but only attack the ends of accessible chains present on the crystallite surface.

The increased accessibility is probably due to the action of sodium hydroxide solution which swells and breaks the hydrogen and van der Waals bonds, thus allowing the polymers to rearrange and move further apart for reorientation leading to an expanded fiber structure. By evaluating the changes in absorption moisture regain, the accessibility of fibers can be determined since the quantity of moisture held by fibers is proportional to the non-crystalline, less ordered regions within the fiber.

Moisture regains of both the control and mercerized sample are shown in Table 7.2. A significant increase of the moisture regain value was obtained after the mercerization treatment especially for the slack mercerized sample. This observation was consistent with the previous report which showed that the fiber accessibility was increased to a greater extent under the slack condition in flax yarn mercerization [43].

7.3.1.2 Fabric weight loss and thickness

As the enzymatic hydrolysis can remove the surface fibrils from the fiber surface, the fabric weight loss is thus considered as the primary index for the degree of reaction. The results of fabric weight loss measurement are shown in Table 7.3. In most of the cases, the weight loss increased tremendously as the incubation time was prolonged particularly for those using 2% enzyme dosage. When doubling the enzyme dosage from 1% to 2%, approximately twice the weight loss was obtained.

Table 7.3: Fabric weight loss of untreated and mercerized linen after various periods using 1% or 2% enzyme

	Weight loss, %			
Fabric type	1 h	2 h	3 h	4 h
Linen, 1% enzyme	1.0	1.3	1.3	1.3
CV%	24.7	30.9	40.9	23.0
Linen, 2% enzyme	1.8	2.5	3.0	3.0
CV%	15.6	9.4	17.1	12.2
100% Tension mercerized, 1% enzyme	0.8	0.8	0.9	1.0
CV%	54.3	49.2	55.4	33.7
100% Tension mercerized, 2% enzyme	1.5	1.6	1.9	2.2
CV%	34.1	33.5	60.9	30.6
95% Tension mercerized, 1% enzyme	0.9	1.0	1.3	1.2
CV%	39.5	46.5	41.6	21.6
95% Tension mercerized, 2% enzyme	1.5	2.0	2.3	2.2
CV%	26.4	25.4	20.9	17.2
Slack mercerized, 1% enzyme	0.3	0.3	0.4	0.5
CV%	38.9	36.6	31.7	58.3
Slack mercerized, 2% enzyme	0.6	1.1	1.9	1.8
CV%	39.1	78.0	79.0	96.2

The highest weight loss occurred after enzyme treatment of the un-pretreated sample followed by the 95% and 100% tension mercerized samples. It seems that the weight retention ability of the enzyme treatment can be improved by mercerization as reflected by the increment in fabric thickness. The slack mercerized fabric was allowed to swell without any restriction, and had the highest fabric thickness followed by the 95% and 100% tension mercerized sample as shown in Table 7.4. Thicker fabrics appear to have lower weight loss in the enzymatic treatments. This may suggest that the macroscopic features such as fabric thickness and construction also can affect the rate of reaction especially at a short treatment time [29, 190].

Table 7.4: Fabric thickness of untreated and mercerized linen after various periods using 1% or 2% enzyme

	Fabric thickness, mm														
	Untreated			1 h			2 h			3 h			4 h		
Fabric type	T2[a]	T100[b]	ST[c]	T2	T100	ST	T2	T100	ST	T2	T100	ST	T2	T100	ST
Linen, 1% enzyme	0.57	0.27	0.30	0.46	0.29	0.17	0.45	0.29	0.16	0.46	0.29	0.17	0.46	0.30	0.16
Linen, 2% enzyme				0.46	0.29	0.17	0.45	0.29	0.16	0.43	0.29	0.14	0.45	0.29	0.16
100% Tension mercerized, 1% enzyme	0.61	0.32	0.29	0.58	0.31	0.27	0.46	0.30	0.16	0.47	0.30	0.17	0.47	0.30	0.17
100% Tension mercerized, 2% enzyme				0.54	0.31	0.23	0.46	0.30	0.16	0.48	0.31	0.17	0.47	0.30	0.17
95% Tension mercerized, 1% enzyme	0.60	0.36	0.24	0.50	0.33	0.17	0.52	0.35	0.17	0.53	0.35	0.18	0.50	0.34	0.16
95% Tension mercerized, 2% enzyme				0.47	0.33	0.14	0.49	0.35	0.14	0.50	0.34	0.16	0.49	0.34	0.15
Slack mercerized, 1% enzyme	0.66	0.38	0.28	0.60	0.37	0.23	0.62	0.38	0.24	0.61	0.38	0.23	0.61	0.38	0.23
Slack mercerized, 2% enzyme				0.61	0.38	0.23	0.59	0.37	0.22	0.61	0.38	0.23	0.61	0.38	0.23

[a] Fabric thickness at 2gf/cm^2 (196Pa), T2, in mm.

[b] Fabric thickness at 100gf/cm^2 (9.81kPa), T100, in mm.

[c] Surface thickness, ST, in mm, ST = T2 - T100.

There was no significant change in fabric thickness measured at 100gf/cm^2 before and after the enzyme treatment of all the samples. However, a significant difference in fabric surface thickness (T2-T100) was found. It was reduced very quickly after the first hour of the enzyme treatment and the changes then started to slow down and approach a maximum value. Even though the period of treatment was prolonged for four hours, there was no significant change in the maximum value. In the case of the reduction of surface thickness, the effect of concentration of enzyme was less significant than the fabric weight loss. However, the highest surface thickness loss could be found from the un-pretreated sample followed by the 95% and 100% tension mercerized samples. The observed variation of fabric surface thickness further supported the theory that the macroscopic features such as fabric thickness could affect the rate of reaction especially at a short treatment time, and the denser fabric structure could also retard the access of the enzyme.

7.3.1.3 Fabric strength

The data for breaking strength values of the untreated and enzyme treated linen are shown in Table 7.5. When comparing the initial fabric strength of the control with the mercerized samples, it was found that the mercerization apparently improved the fabric strength. The increase in fabric densities in the case of slack mercerized sample as well as the 95% tension mercerized sample confirmed that the strength loss actually occurred. According to the previous finding [43], the slack mercerized flax fibers exhibited a decrease in crystallinity as a result of the unrestrained lateral swelling of the fiber. Owing to the absence of primary wall to exert restraint on the lateral swelling and consequent disorientation of the swollen fibers, the strength of flax fiber would decrease after the slack mercerization. Nevertheless, the fiber

strength would increase after the tension mercerization because the lateral movement of the polymer chains in flax was restricted, so the strength loss did not occur.

Table 7.5: Fabric breaking strength of untreated and mercerized linen after various periods using 1% or 2% enzyme

	Breaking strength, N				
Fabric type	Untreated	1 h	2 h	3 h	4 h
Linen, 1% enzyme	709	673	651	652	593
CV%	1.8	3.3	4.1	4.9	6.2
Linen, 2% enzyme		627	564	504	441
CV%		4.0	6.2	6.4	5.9
100% Tension mercerized, 1% enzyme	748	702	694	687	650
CV%	2.3	6.3	4.2	3.0	5.5
100% Tension mercerized, 2% enzyme		636	638	540	450
CV%		6.8	3.9	6.3	6.0
95% Tension mercerized, 1% enzyme	761	696	692	672	659
CV%	6.1	3.6	2.7	4.8	4.3
95% Tension mercerized, 2% enzyme		661	655	628	616
CV%		5.5	4.7	3.7	5.0
Slack mercerized, 1% enzyme	803	758	757	749	733
CV%	5.4	4.2	3.2	5.4	6.9
Slack mercerized, 2% enzyme		708	665	612	537
CV%		4.6	4.3	4.0	3.5

The relative breaking loads of the un-pretreated and mercerized linen are shown in Figures 7.1 and 7.2. The breaking strengths of the enzyme treated fabrics reduced as the treatment time was increased and a significant reduction was found after one hour of incubation especially at 2% enzyme dosage. For 1% enzyme dosage, the strength of the mercerized samples after a prolonged incubation was higher than the un-pretreated sample. In the case of cotton, the reactivity would increase after mercerization making it more susceptible to chemical attack. However, mercerization may alter the molecular structure of cotton in such a way that it showed higher strength retention than the corresponding non-mercerized cotton when subjected to degradative treatment under the identical condition [186].

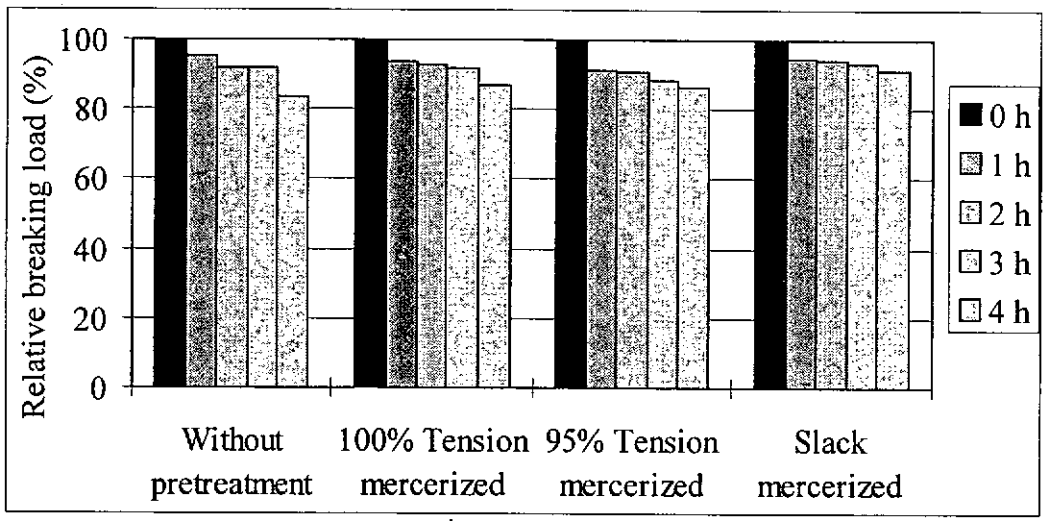

Figure 7.1: Relative breaking loads of untreated and mercerized linen after various periods using 1% enzyme

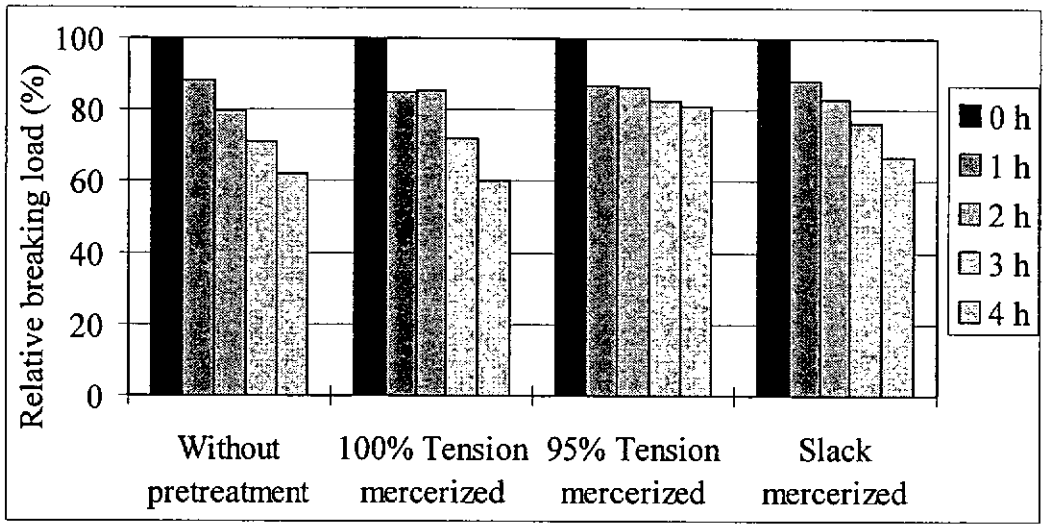

Figure 7.2: Relative breaking loads of untreated and mercerized linen after various periods using 2% enzyme

The higher retention of breaking strength of the mercerized samples is attributed to the removal of weak points present in the fiber structure so that the uniform structure was capable of distributing stress evenly along the fibers. However, the strength is reduced as the enzyme dosage is increased to 2%. A significant reduction of breaking strength was also found in the un-pretreated sample. For the slack mercerized sample, the strength reduction behavior was the least of all samples of 1% enzyme and less than all but the 95% tension mercerized samples of 2% suggesting that the reduction of fiber crystallinity could enhance the accessibility of

the substrate during the enzyme treatment at a higher enzyme dosage and prolonged treatment time.

7.3.1.4 Fabric bending properties

Of the most commonly used fibers in apparel textile, flax is one of the fibers having the highest stiffness and lowest resilience. The results of bending rigidity and hysteresis of the linen and mercerized linen after various periods of incubation time are shown in Table 7.6 and Table 7.7. The increase in bending rigidity of the mercerized sample was significantly under larger both 95% and 100% tension mercerization, and the fabric had a stiff and hard feel because of its compacted structure. For the slack mercerized sample, the increment of fabric stiffness was less predominant than the tension mercerized samples.

Table 7.6: Fabric bending rigidity of untreated and mercerized linen after various periods using 1% or 2% enzyme

	Bending rigidity, $gfcm^2/cm$				
Fabric type	Untreated	1 h	2 h	3 h	4 h
Linen, 1% enzyme	0.65	0.56	0.55	0.56	0.48
CV%	3.8	5.1	3.5	4.4	3.4
Linen, 2% enzyme		0.55	0.52	0.51	0.50
CV%		4.2	7.0	6.8	4.7
100% Tension mercerized, 1% enzyme	1.65	0.99	0.99	0.96	0.88
CV%	10.3	13.1	10.4	11.3	11.4
100% Tension mercerized, 2% enzyme		0.97	0.98	0.96	0.95
CV%		11.0	2.4	7.7	6.2
95% Tension mercerized, 1% enzyme	1.51	0.99	1.04	1.00	0.94
CV%	11.4	7.8	6.1	5.5	7.4
95% Tension mercerized, 2% enzyme		0.99	0.99	0.97	0.95
CV%		18.4	3.7	7.3	2.7
Slack mercerized, 1% enzyme	0.98	0.70	0.64	0.60	0.59
CV%	6.5	3.2	9.0	3.7	5.2
Slack mercerized, 2% enzyme		0.66	0.63	0.61	0.51
CV%		11.1	8.5	5.2	3.8

Table 7.7: Fabric bending hysteresis of untreated and mercerized linen after various periods using 1% or 2% enzyme

	Bending hysteresis, gfcm/cm				
Fabric type	Untreated	1 h	2 h	3 h	4 h
Linen, 1% enzyme	0.54	0.60	0.58	0.58	0.49
CV%	3.9	4.8	7.9	13.7	6.6
Linen, 2% enzyme		0.53	0.55	0.51	0.46
CV%		3.8	10.4	8.6	9.0
100% Tension mercerized, 1% enzyme	1.71	1.02	0.94	0.86	0.83
CV%	17.8	20.5	16.3	15.6	18.1
100% Tension mercerized, 2% enzyme		0.92	0.97	0.89	0.81
CV%		11.3	5.7	10.8	18.0
95% Tension mercerized, 1% enzyme	1.25	0.78	0.84	0.85	0.73
CV%	21.3	10.3	10.2	12.8	7.6
95% Tension mercerized, 2% enzyme		0.79	0.82	0.79	0.75
CV%		12.3	2.6	13.1	14.2
Slack mercerized, 1% enzyme	0.81	0.50	0.51	0.46	0.44
CV%	4.8	10.3	7.2	10.8	7.5
Slack mercerized, 2% enzyme		0.50	0.46	0.40	0.37
CV%		12.9	17.3	9.0	14.9

In general, the stiffness of a fiber depends partially on the degree of orientation and crystallinity of the polymers. As the proportion of amorphous area within a fiber becomes greater, the fiber tends to become less stiff. The more crystalline the fiber has, the stiffer it will tend to be. As a result, the slack mercerized sample was less stiff than the tension mercerized samples. On the other hand, the fiber diameter has greater influence on the bending properties than the flexural rigidity of fiber. Doubling a fiber diameter will produce a 16-fold increase in resistance to bending. Likewise, a 2-fold reduction in fiber diameter decreases the bending rigidity by 16-fold. Furthermore, the cross-sectional shape also influences the flexural rigidity of a fiber. Round fibers have high values of stiffness while flat fibers have relatively low values of stiffness [112]. Work has been reported that the major disadvantage of fabric mercerization was the large increment in fabric stiffness [179]. Moreover, fabric thickness and inter-fiber or inter-yarn friction also play an important role in bending rigidity.

For the un-pretreated sample, a slight reduction of bending rigidity was found. However, approximately 40% reduction of bending rigidity was found for the mercerized sample after the first hour of enzyme treatment. Even though the period of treatment was prolonged to four hours, there was still no significant change in the reduction of bending rigidity. A similar extent of reduction was found even with a higher enzyme dosage. The reduction of bending rigidity was probably due to the reduction of fiber diameter caused by the removal of surface fibrils. When the bending rigidity was reduced by the application of enzyme treatment, a similar reduction of bending hysteresis was found.

7.3.1.5 SEM observation

The appearance of fiber surface was investigated by means of scanning electron microscopy (SEM). When compared to the cotton fiber, the surface of the untreated flax fiber possessed a much larger amount of loose fibrils composed of debris and adhering fragmentary tissue components as shown in Figure 7.3 which exhibits the accumulation of surface fibrils on the yarn surface. Figures 7.4 and 7.5 show that after four hours of enzyme treatment, some of the surface fibrils still remain on the fiber surface implying that a longer incubation time might be required to remove all the surface fibrils completely.

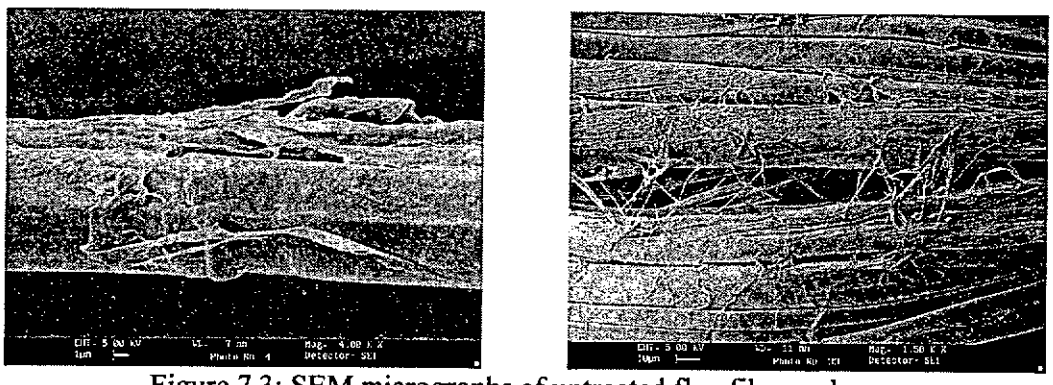

Figure 7.3: SEM micrographs of untreated flax fiber and yarn

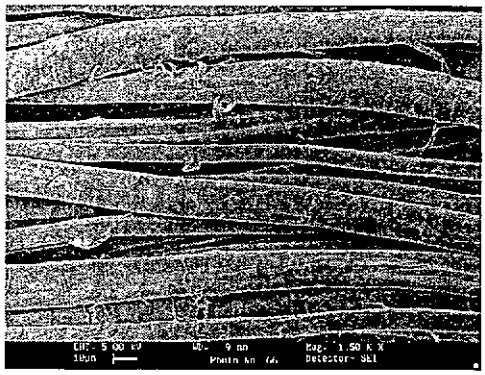

Figure 7.4: SEM micrograph of linen after 4 hours using 1% enzyme

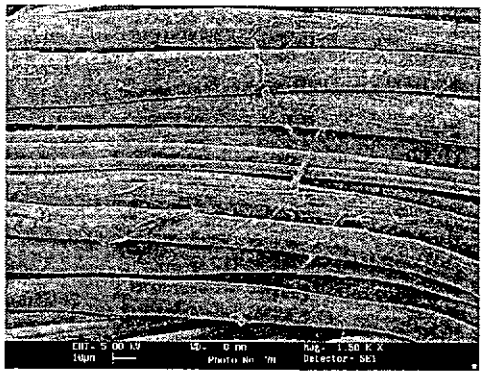

Figure 7.5: SEM micrograph of linen after 4 hours using 2% enzyme

SEM micrograph of the slack mercerized sample is shown in Figure 7.6. The shape of the slack mercerized fibers becomes rounder due to the unrestricted swelling, and a considerable amount of surface fibrils still remains on the fiber surface. After four hours of enzyme treatment, a comparatively smooth and clear surface was obtained and the effect was more predominant in the case of 2% enzyme dosage as shown in Figures 7.7 and 7.8.

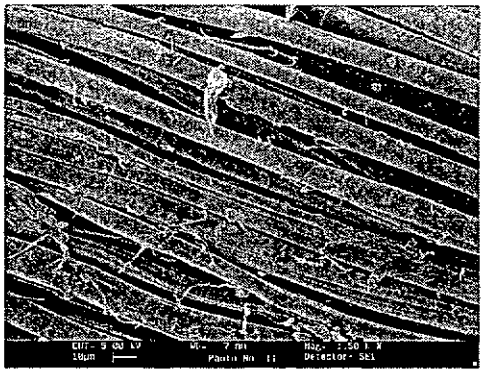

Figure 7.6: SEM micrograph of slack mercerized linen

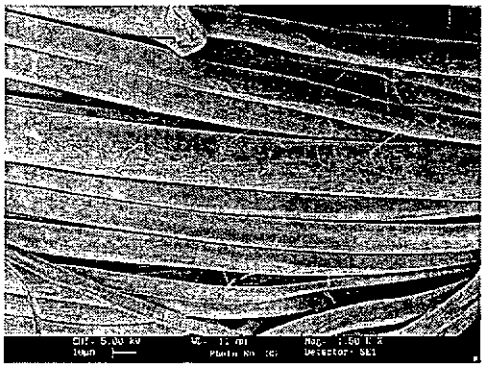

Figure 7.7: SEM micrograph of slack mercerized linen after 4 hours using 1% enzyme

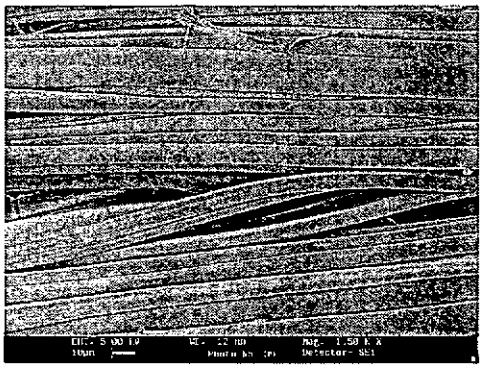

Figure 7.8: SEM micrograph of slack mercerized linen after 4 hours using 2% enzyme

As the mercerization tension was increased from slack to both 95% and 100% tension, the fiber cross-section would be progressively changed from round to relatively flat as shown in Figures 7.9 and 7.12. The SEM image shown in Figures 7.10-11 and 7.13-14 revealed that most of the surface fibrillar matter have been removed and the fiber surfaces have become smoother for both the tension mercerized and enzymatically treated samples.

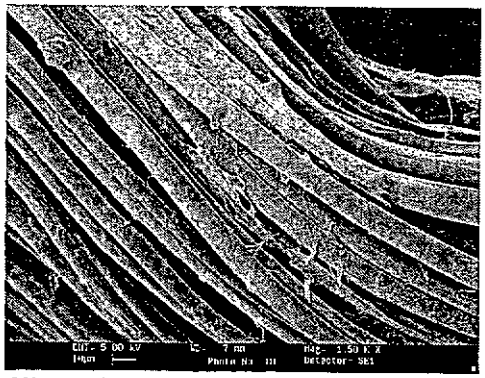

Figure 7.9: SEM micrograph of 95% tension mercerized linen

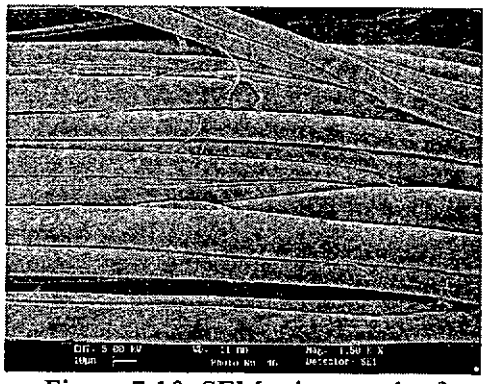

Figure 7.10: SEM micrograph of 95% tension mercerized linen after 4 hours using 1% enzyme

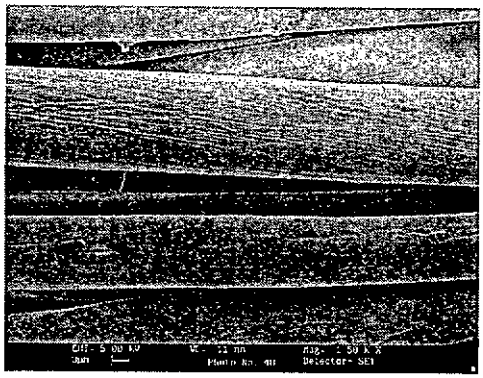

Figure 7.11: SEM micrograph of 95% tension mercerized linen after 4 hours using 2% enzyme

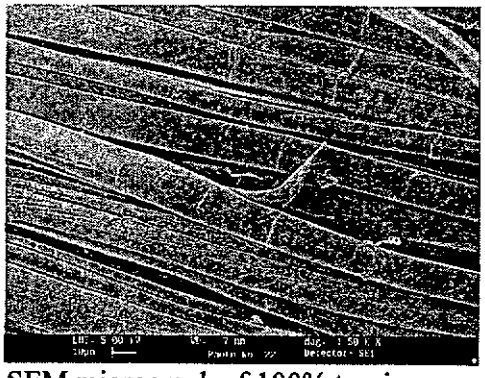

Figure 7.12: SEM micrograph of 100% tension mercerized linen

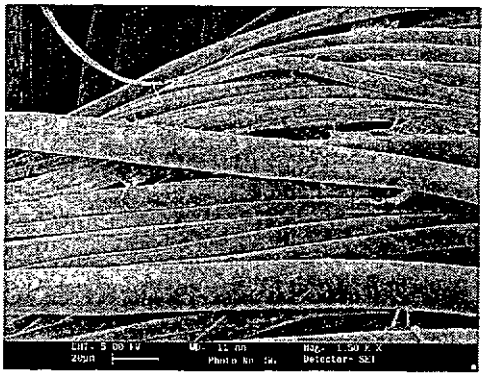

Figure 7.13: SEM micrograph of 100% tension mercerized linen after 4 hours using 1% enzyme

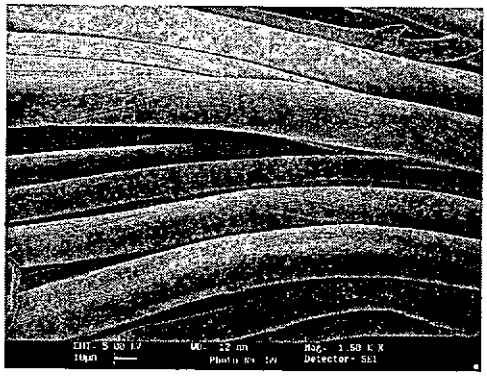

Figure 7.14: SEM micrograph of 100% tension mercerized linen after 4 hours using 2% enzyme

7.3.1.6 Dyeing properties

The dyeing properties of the slack, 95% and 100% tension mercerized are shown in Table 7.8. After the mercerization, the dyeing rate, final exhaustion and depth of shade are increased for all the mercerized samples. The slack mercerized sample exhibits higher increase in color yield than the tension mercerized sample.

With the direct dye of smaller molecular size (red dye), the mercerized samples show a faster dyeing rate especially for the slack mercerized sample. The dyeing rate is less influenced by the enzyme treatment. With regard to the final exhaustion, a significant improvement can be found for all the mercerized samples. The enzyme treatment does not affect the final exhaustion percentage. The K/S values of all the mercerized samples increase while the slack mercerized sample yields a higher increase. The increase of K/S value is significantly lowered by the enzyme treatment. On the whole, the mercerization process improves the dyeing performance including a faster dyeing rate, higher exhaustion of dye and higher depth of shade of the dyed material especially for the slack mercerized samples.

With the direct dye of a larger molecular size (green dye), the tension mercerized samples show a slower dyeing rate while the slack mercerized sample shows a faster dyeing rate. The faster dyeing rate of the slack mercerized sample may be simply due to the reduced crystallinity which become more susceptible to the larger dye molecule. The enzyme treatment reduces the dyeing rate of all the samples but does not change the final exhaustion percentage. However, the K/S values are improved significantly especially for the slack mercerized sample but the increase in K/S value is lowered by the enzyme treatment. Mercerization greatly improves the dyeing performance in terms of dyeing rate and depth of shade produced. The slack mercerized sample displays a higher increase of color yield than the tension mercerized samples because of the greater increase in accessibility. However, the enzyme treatment only slightly affects the increment of the final exhaustion of dye. Furthermore, the depth of shade increase is lowered by the enzyme treatment because of the removal of fiber surface amorphous region.

Mercerization improves the depth of shade of the dyed material significantly and especially for the slack mercerized sample. Although the slack mercerized sample has a similar exhaustion percentage when compared to the tension mercerized samples, the depth of shade produced is still higher. The changes of fiber internal scattering will greatly influence the depth of shade. Previous literature demonstrated that the mercerized flax fiber did not increase in size or shape as a result of the swelling treatment, but it did reduce the crystallinity of fiber [258, 267]. Therefore, the increase in apparent depth of shade found in the mercerized samples may be the reflection of increase in actual dye content and modification of internal scattering rather than the modification in fiber size or shape.

Increased fiber accessibility, as manifested by the increased dye adsorption, is the reflection of de-crystallization that occurs during the mercerization. The increase in dye adsorption obtained after the three mercerization treatments demonstrates that the slack treatment produces a greater increase in accessibility than the tension treatment. However, the magnitude of increase is also influenced by the size of entering dyestuff molecule [267]. This phenomenon is well illustrated by the mercerized samples dyed with the direct dye of a smaller molecular size. For the mercerized samples dyed with the direct dye of larger molecular size, the quantity of final dye exhaustion among the samples is similar but the apparent depths of shade obtained are different from each other. This demonstrates that the internal scattering of the dyed material on different structures of various crystallinity will greatly affect the resultant color depth of shade.

Table 7.8: Half time of dyeing, final exhaustion and K/S value of untreated, mercerized and enzyme treated sample dyeing with CI Direct Red 81 and Green 26

		CI Direct Red 81		CI Direct Green 26	
		Without enzyme treatment	Enzyme Treated	Without Enzyme treatment	Enzyme treated
Untreated	½ time of dyeing, min.	3.0	3.0	4.2	5.7
	Final exhaustion, %.	54.4	53.9	63.6	62.7
	K/S value	3.4	3.5	5.1	5.0
100% Tension mercerized	½ time of dyeing, min.	3.1	2.9	6.1	6.5
	Final exhaustion, %.	61.5	61.1	64.7	63.1
	K/S value	5.8	4.8	6.8	6.2
95% Tension mercerized	½ time of dyeing, min.	2.9	2.7	5.1	5.4
	Final exhaustion, %.	63.1	62.9	65.1	64.7
	K/S value	5.9	5.2	7.2	6.6
Slack mercerized	½ time of dyeing, min.	2.6	2.6	4.2	4.7
	Final exhaustion, %.	60.5	58.9	65.8	65.1
	K/S value	5.9	5.1	7.7	7.6

Apart from the improvement of dyeing performance after mercerization, Table 7.9 shows that the colorfastness properties of the mercerized linen are also improved particularly for those samples dyed with a smaller molecule dye. Again, the effect of enzyme treatment on the colorfastness properties of the dyed material is not significant.

Table 7.9: Colorfastness to washing of untreated, mercerized and enzyme treated sample dyeing with CI Direct Red 81 and Green 26

	CI Direct Red 81		CI Direct Green 26	
	Without enzyme treatment	Enzyme treated	Without enzyme treatment	Enzyme treated
Colour Change				
Untreated	3.7	3.5	4.5	4.7
100% Tension mercerized	4.7	4.3	4.5	4.5
95% Tension mercerized	4.2	4.5	4.3	4.5
Slack mercerized	4.5	4.2	4.5	4.5
Colour Staining on Cotton Fabric				
Untreated	2.2	2.0	4.5	4.8
100% Tension mercerized	2.3	2.5	4.7	4.7
95% Tension mercerized	2.3	2.3	4.8	4.5
Slack mercerized	2.5	2.2	4.8	4.8

7.3.2 Effect of Mechanical Agitation on Enzyme Treatment

7.3.2.1 X-ray crystallinity and moisture regain

Two levels of mechanical agitation with five stainless steel balls (medium agitation) and ten stainless steel balls (high agitation) were applied to the enzyme treatment respectively. It was used to study the effect of enzyme treatment with respect to the increased degree of mechanical agitation. As shown in Table 7.10, there was no significant change in x-ray crystallinity and moisture regain after the enzyme treatment because the large molecular size of enzyme could only attack the accessible fiber surface. Therefore, it did not lead to any significant change in the crystallinity. For the same reason, the moisture absorption properties of all the

enzyme treated samples were only slightly increased but not very significantly even when higher mechanical agitation was applied.

Table 7.10: X-ray crystallinity and moisture regain of linen at different levels of mechanical agitation after 4 hours using 2% enzyme

	X-ray crystallinity		Moisture regain, %	
Fabric type	Before enzyme treatment	After enzyme treatment	Before enzyme treatment	After enzyme treatment
Linen	0.81	0.82	6.4	6.2
CV%	1.0	1.1	3.3	4.6
Treated with 5 stainless steel balls		0.81		6.3
CV%		2.8		3.9
Treated with 10 stainless steel balls		0.81		6.5
CV%		1.1		3.5

7.3.2.2 Fabric weight loss and thickness

Table 7.11 shows the fabric weight loss of linen at different levels of mechanical agitation and various periods using 1% or 2% enzyme. Obviously, the fabric weight loss was significantly increased with the treatment time and enzyme dosage. However, there was no significant change in fabric weight loss between each level of mechanical agitation. Similar phenomena also appeared in the case of the reduction of fabric surface thickness as shown in Table 7.12.

Table 7.11: Fabric weight loss of linen at different levels of mechanical agitation after various periods using 1% or 2% enzyme

	Weight loss, %			
Fabric type	1 h	2 h	3 h	4 h
Linen, 1% enzyme	1.0	1.3	1.3	1.3
CV%	24.7	30.9	40.9	23.0
Linen, 2% enzyme	1.8	2.5	3.0	3.0
CV%	15.6	9.4	17.1	12.2
Treated with 5 stainless steel balls, 1% enzyme	1.0	1.1	1.2	1.3
CV%	34.0	15.2	32.2	49.6
Treated with 5 stainless steel balls, 2% enzyme	1.7	1.9	2.4	3.1
CV%	13.1	42.9	17.6	43.9
Treated with 10 stainless steel balls, 1% enzyme	1.0	1.3	1.3	1.4
CV%	36.0	49.3	41.5	19.4
Treated with 10 stainless steel balls, 2% enzyme	1.7	1.9	2.5	3.1
CV%	21.3	17.8	14.8	18.2

Table 7.12: Fabric thickness of linen at different levels of mechanical agitation after various periods using 1% or 2% enzyme

	Fabric thickness, mm														
	Untreated			1 h			2 h			3 h			4 h		
Fabric type	T2[a]	T100[b]	ST[c]	T2	T100	ST	T2	T100	ST	T2	T100	ST	T2	T100	ST
Linen, 1% enzyme	0.57	0.27	0.30	0.46	0.29	0.17	0.45	0.29	0.16	0.46	0.29	0.17	0.46	0.30	0.16
Linen, 2% enzyme				0.46	0.29	0.17	0.45	0.29	0.16	0.43	0.29	0.14	0.45	0.29	0.16
Treated with 5 stainless steel balls, 1% enzyme				0.46	0.28	0.18	0.47	0.29	0.18	0.47	0.29	0.18	0.45	0.29	0.16
Treated with 5 stainless steel balls, 2% enzyme				0.45	0.28	0.17	0.45	0.29	0.16	0.43	0.29	0.14	0.44	0.29	0.15
Treated with 10 stainless steel balls, 1% enzyme				0.46	0.29	0.17	0.46	0.29	0.17	0.45	0.29	0.16	0.45	0.29	0.16
Treated with 10 stainless steel balls, 2% enzyme				0.44	0.29	0.15	0.44	0.28	0.16	0.43	0.29	0.14	0.43	0.29	0.14

[a] Fabric thickness at 2gf/cm^2 (196Pa), T2, in mm.

[b] Fabric thickness at 100gf/cm^2 (9.81kPa), T100, in mm.

[c] Surface thickness, ST, in mm, ST = T2 - T100.

7.3.2.3 Fabric strength

Table 7.13 as well as Figures 7.15 and 7.16 show the reduction of breaking load of the linen at different levels of mechanical agitation and various periods using 1% and 2% enzyme.

Table 7.13: Fabric breaking strength of linen at different levels of mechanical agitation after various periods using 1% or 2% enzyme

	Breaking strength, N				
Fabric type	Untreated	1 h	2 h	3 h	4 h
Linen, 1% enzyme	709	673	651	652	593
CV%	1.8	3.3	4.1	4.9	6.2
Linen, 2% enzyme		627	564	504	441
CV%		4.0	6.2	6.4	5.9
Treated with 5 stainless steel balls, 1% enzyme		664	669	659	644
CV%		6.6	3.2	5.5	5.0
Treated with 5 stainless steel balls, 2% enzyme		634	622	554	552
CV%		5.6	6.2	5.1	7.7
Treated with 10 stainless steel balls, 1% enzyme		677	640	614	604
CV%		2.1	4.9	6.0	3.8
Treated with 10 stainless steel balls, 2% enzyme		594	575	562	560
CV%		5.7	5.3	4.1	7.8

The fabric strength of the enzyme treated fabrics was reduced as the treatment time was increased especially if 2% enzyme dosage was used. In the case of increasing the mechanical agitation with the aid of stainless steel balls, there was no significant difference in the fabric strength loss when 1% of enzyme dosage was used as shown in Figure 7.15.

Nevertheless, the difference among various levels of mechanical agitation could be found when 2% enzyme dosage was used as illustrated in Figure 7.16. The sample treated with higher agitation (10 stainless steel balls) showed a slightly higher reduction of breaking load after one hour of enzyme treatment. This could be explained by the higher reduction of inter-fiber friction as the damaged material was

removed from the fiber surface. However, an adverse effect was obtained when comparing the 4 hours enzyme treated sample under low agitation (no stainless steel ball) with the sample treated under high agitation (10 stainless steel balls). The fabric treated under higher mechanical agitation had higher resultant fabric strength than the sample treated under lower agitation. This was mainly due to the increased inter-fiber friction caused by the high levels of mechanical agitation which raised the fibrillar material from the fiber surface. As referred to previously, the results obtained from the fabric weight loss, most of the samples had a similar reduction when using the same amount of enzyme dosage and treatment time. This implies that the increased mechanical agitation applied to the enzyme treatment does not increase the weight loss but changes the fabric mechanical properties.

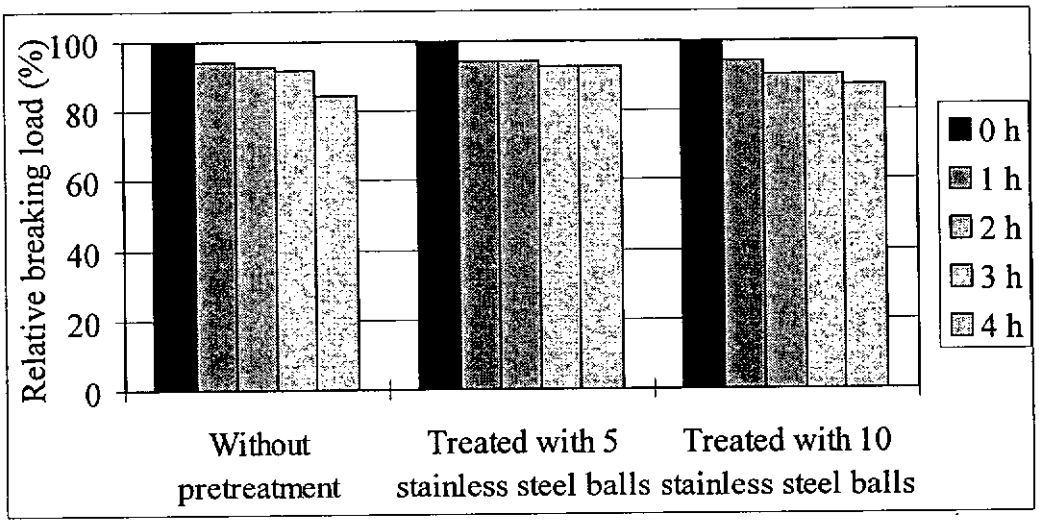

Figure 7.15: Relative breaking loads of linen at different levels of mechanical agitation after various periods using 1% enzyme

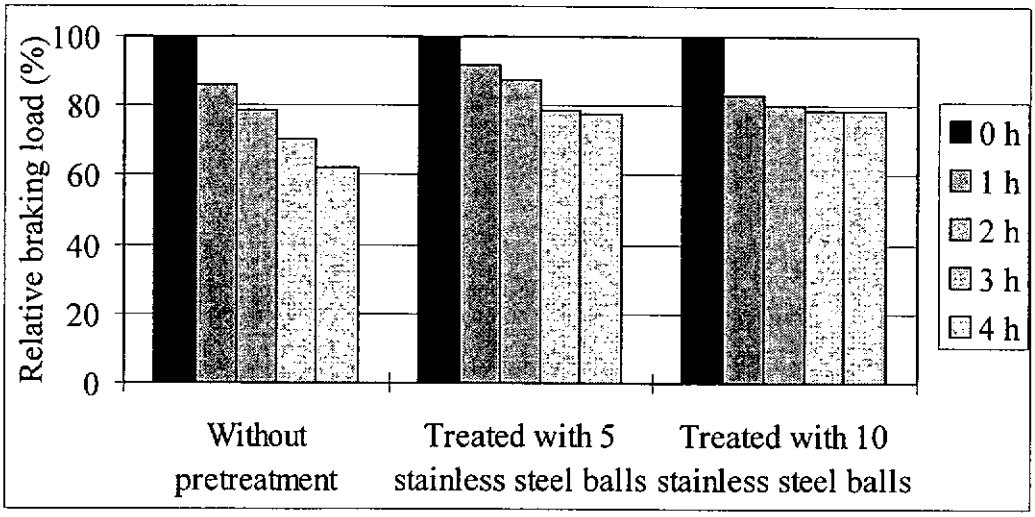

Figure 7.16: Relative breaking loads of linen at different levels of mechanical agitation after various periods using 2% enzyme

7.3.2.4 Fabric bending properties

Table 7.14 and Table 7.15 show the results of fabric bending rigidity and hysteresis of linen at different levels of mechanical agitation after various periods using 1% or 2% enzyme. The effect of mechanical agitation on the fabric bending rigidity and hysteresis was not obvious for most of the samples. However, a significant reduction in fabric bending rigidity and hysteresis was found for the sample treated for 1 hour with 2% enzyme dosage and high agitation. The reduction is attributed mainly to the reduced inter-fiber friction caused by the enzymatic removal of damaged material from the fiber surface. It has been confirmed that the removal of a small amount of cellulosic material from fibers could significantly reduce the fiber bending stiffness, particularly if cracks were formed [36].

Table 7.14: Fabric bending rigidity of linen at different levels of mechanical agitation after various periods using 1% or 2% enzyme

	Bending rigidity, gfcm^2/cm				
Fabric type	Untreated	1 h	2 h	3 h	4 h
Linen, 1% enzyme	0.65	0.56	0.55	0.56	0.48
CV%	3.8	5.1	3.5	4.4	3.4
Linen, 2% enzyme		0.55	0.52	0.51	0.50
CV%		4.2	7.0	6.8	4.7
Treated with 5 stainless steel balls, 1% enzyme		0.52	0.56	0.54	0.54
CV%		7.2	6.0	6.2	4.1
Treated with 5 stainless steel balls, 2% enzyme		0.52	0.57	0.58	0.57
CV%		4.1	4.4	6.0	5.9
Treated with 10 stainless steel balls, 1% enzyme		0.45	0.52	0.51	0.54
CV%		5.3	11.0	6.1	9.0
Treated with 10 stainless steel balls, 2% enzyme		0.46	0.53	0.54	0.53
CV%		7.0	6.4	6.4	9.4

Table 7.15: Fabric bending hysteresis of linen at different levels of mechanical agitation after various periods using 1% or 2% enzyme

	Bending hysteresis, gfcm/cm				
Fabric type	Untreated	1 h	2 h	3 h	4 h
Linen, 1% enzyme	0.54	0.60	0.58	0.58	0.49
CV%	3.9	4.8	7.9	13.7	6.6
Linen, 2% enzyme		0.53	0.55	0.51	0.46
CV%		3.8	10.4	8.6	9.0
Treated with 5 stainless steel balls, 1% enzyme		0.51	0.56	0.52	0.48
CV%		12.1	10.4	8.3	6.8
Treated with 5 stainless steel balls, 2% enzyme		0.47	0.58	0.58	0.56
CV%		9.6	10.0	13.9	6.6
Treated with 10 stainless steel balls, 1% enzyme		0.39	0.47	0.49	0.49
CV%		8.6	16.8	12.0	12.0
Treated with 10 stainless steel balls, 2% enzyme		0.36	0.45	0.47	0.48
CV%		6.2	6.4	7.3	15.3

The increases in fabric bending rigidity and hysteresis were found as the enzyme treatment time was prolonged from one hour to four hours with high agitation and 2% enzyme dosage. This supported the explanation mentioned in Section 7.3.2.3 that the fabric mechanical properties would be changed if high levels of mechanical agitation during the enzyme treatment could raise the fibrillar material from fiber surface.

7.3.2.5 SEM observation

Figures 7.17 - 7.20 show the SEM micrographs of linen after 4 hours using 1% or 2% enzyme with medium and high agitation. A comparatively smooth and clear surface was obtained in the case of 2% enzyme dosage.

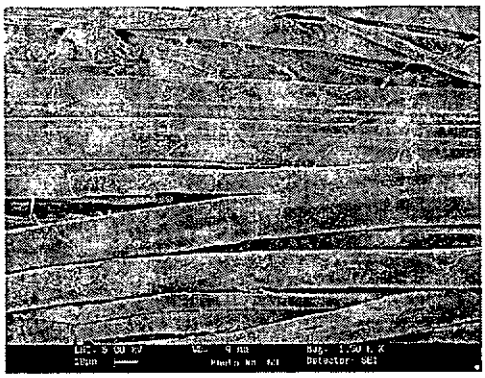

Figure 7.17: SEM micrograph of linen after 4 hours using 1% enzyme and 5 stainless steel balls

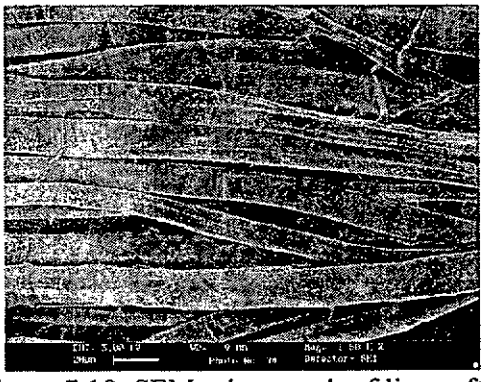

Figure 7.18: SEM micrograph of linen after 4 hours using 2% enzyme and 5 stainless steel balls

Figure 7.19: SEM micrograph of linen after 4 hours using 1% enzyme and 10 stainless steel balls

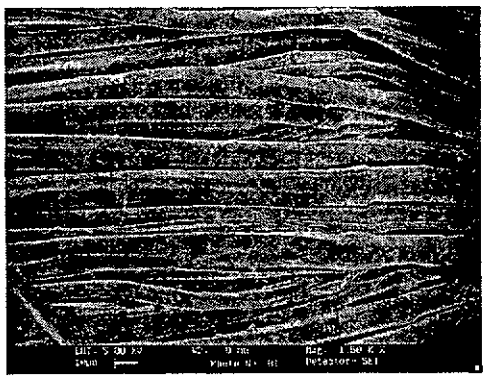

Figure 7.20: SEM micrograph of linen after 4 hours using 2% enzyme and 10 stainless steel balls

7.4 CONCLUSION

Mercerization has been employed as a pretreatment of linen material prior to enzymatic hydrolysis in order to attain a reduction of crystallinity and improvement of fiber accessibility. Mercerization pretreatments under different tensions also altered the fabric sett, tensile strength and bending properties of linen. Tensile strength was increased under the tension mercerization but reduced under the slack

condition. In addition, large increase in bending rigidity were found especially when tension was applied during the pretreatment. Significant changes were obtained for the moisture regain and x-ray crystallinity ratio under different tensions of mercerization.

Owing to the fact that the accessible regions of the cellulosic material are often too narrow for the large enzyme molecules to penetrate effectively, then both the moisture absorption and the crystallinity ratio can not be further changed after the enzyme treatment. Macroscopic features such as fabric thickness and packing density have also influenced the rate of enzymatic reaction as reflected by the reductions in both fabric weight loss and fabric surface thickness while the enzyme treatment was applied to the slack mercerized sample. Furthermore, the strength retention ability during the enzymatic hydrolysis was enhanced by the mercerization pretreatment. Enzyme treatments effectively reduced the fabric stiffness of the mercerized material implying that the crystallinity of the material was important for the reduction of bending rigidity caused by the enzyme treatment. The fiber surface appearance was revealed by SEM micrographs which showed that the fiber surface smoothness was improved by the pretreatment.

With regard to the time effect of enzyme treatment, significant reductions of fabric surface thickness, strength and bending rigidity were obtained after the first hour of incubation. The effect of increasing the concentration from 1% to 2% results in higher fabric weight and strength losses but with smoother fiber surfaces. However, the effect was less predominant in the reduction of fabric surface thickness and bending rigidity.

Mercerization greatly improved the dyeing performance in terms of dyeing rate and depth of shade produced. Enzyme treatment did slightly affect the increment of final exhaustion of dye and the depth of shade produced. Dye fastness was improved by mercerization pretreatment, whereas enzyme treatment did not affect the dye fastness.

On the other hand, a significant reduction in fabric bending rigidity and hysteresis could be achieved by applying higher mechanical agitation for one hour treatment with 2% enzyme dosage. It had been shown that a certain level of mechanical agitation applied during treatment affected the mechanism of enzyme finishing and also the resultant fabric mechanical properties. These findings suggest that the choice of processing method should be varied in order to attain the desired enzyme finishing effects.

CHAPTER 8

CONCLUSIONS

This thesis attempts to provide a comprehensive and systematic investigation on modification of linen by plasma and enzyme treatments. A range of advanced analytical instruments and characterization techniques was used to describe the variations in structure and properties brought about by the treatments. This chapter will provide a brief summary of the research results and conclusions. Remaining problems and possible further research work will also be discussed.

8.1 SUMMARY

This thesis covers a literature review, characterizations of the structure and properties modification of linen by low temperature plasma, mercerization, enzyme treatments as well as their synergetic effects.

8.1.1 Literature Review

A literature survey was reported in Chapter 2 on the chemical composition, morphological structure, properties and modification technology of flax fibers. It revealed the importance of using environmentally friendly textile finish and surface modifications to replace the harsh and energy-demanding chemical processes. Background knowledge and recent development of the modification technology as well as the characterization techniques were outlined. Further investigations of plasma and enzyme treatments were especially useful for flax fiber modification.

8.1.2 Characterizations of Plasma Treated Linen

In order to examine the effects of plasma treatment on the flax fiber, an experiment was conducted by using plasma treatments with oxygen and argon gases, two levels of discharge power (100W and 200W) and various exposure times (2.5, 5, 10, 20, 40, 60 minutes) to modify linen as described in Chapter 3. A range of analytical methods was used to determine the effects of plasma treatments on the fiber bulk structure and properties, surface morphology and properties, and fabric mechanical properties.

Oxygen or argon plasma treatments resulted in changes in the surface morphology and chemical properties of flax fibers. It was found that plasma treatment on linen with a short exposure time results in a substantial increment of surface polar groups and water uptake. Furthermore, a slight improvement of fabric strength, bending rigidity, hysteresis and wrinkle recovery was achieved without interfering with the bulk fiber structure, with minimal loss of fabric weight and whiteness.

Under the experimental conditions, all plasma treated linen showed no significant changes in the degree of polymerization and crystallinity but slight reductions of moisture regains were observed. The fabric weight loss was increased with the exposure time. The appearance of cracks and voids was less noticeable when using the argon plasma, while considerable voids and cracks appeared on the oxygen plasma (200W) treated linen. The oxygen content (O_{1s}/C_{1s} ratio) of the plasma treated linen was dramatically increased especially when using a higher discharge power (200W) of both gases and for 60 minutes of exposure. The fabric whiteness was reduced greatly after being exposure to the argon plasma with a higher discharge

power. Substantial improvement of fabric water uptake was achieved by exposing linen to oxygen plasma for 10 minutes or to argon plasma for 5 minutes with a discharge power of 100W. The effect remained after a storage time up to 1000 hours. The fabric water uptake and strength were increased initially and then decreased with the prolonged exposure whereas the fabric bending rigidity, hysteresis and wrinkle recovery were slightly improved. A significant reduction in both fabric bending rigidity and hysteresis was achieved after 2.5 minutes of oxygen plasma exposure or 10 minutes of argon plasma exposure.

During the treatment, the fabric samples treated with the oxygen plasma generated higher heat as well as suffered higher weight and strength loss than those treated with the argon plasma. However, a higher level of yellowing was found in the argon plasma treated linen. It was observed that the prolonged exposure time, regardless of type of gas and power, did not result in better fabric water uptake and even caused adverse effects on linen such as excessive reduction of fabric strength, increased bending stiffness and reduction in fabric water uptake.

Chapter 4 presented a comprehensive study on the morphological and topographical change in plasma treated flax fibers by using the Environmental Scanning Electron Microscopy (ESEM) and Atomic Force Microscopy (AFM) for the first time. Time-series images of fiber surface appearance were studied by the ESEM. Suitable operational parameters were selected to examine the fiber surface without the degradation caused by electron beam. As the exposure time was accumulated, the depth of the micro-pores etched by the plasma would increase with increasing width of the pores. The surface fibrils remained on the surface for up to 40 minutes of

oxygen plasma exposure or 60 minutes of argon plasma exposure. The dominant fabric weight loss of the linen during plasma treatment was mainly attributed to the fiber surface etching. Fiber contraction was also observed during the plasma treatment. The ESEM micrographs showed a good correlation with the SEM micrographs without obscuring the surface details of the fibers.

Furthermore, AFM was used to measure the depth of etching pits induced by the argon and oxygen plasma. From a relatively smoother surface of an untreated flax fiber, the argon plasma created pits with the sizes (both depth and diameter) in mainly sub-micrometer while the oxygen plasma created pits with the sizes in a few micrometers. A quantitative description of the surface topography of plasma treated flax fibers was obtained by the use of a few image processing techniques. The FFT power spectra were used to describe the periodic surface features of plasma treated fibers. The changes in surface roughness of the plasma etched flax fiber were quantified by the RMS values. The RMS value was increased from 40.9 of the untreated sample to 98.0 of the argon and 308.4 of the oxygen plasma treated fiber.

The wetting behavior of plasma treated linen was presented in Chapter 5. The measurements of surface contact angles as well as the determination of critical surface tension by the Zisman's plots were first considered. It was found that these methods alone were not adequate to quantify the wetting properties of plasma treated linen. Further investigation on the wicking abilities of plasma treated linen was conducted using both upward and downward water wicking methods. The respective experimental set-up and testing procedures were developed. It was found that the

downward wicking method was more suitable to distinguish the effects of plasma treatment under various conditions.

8.1.3 Plasma and Mercerization Pretreatments and their Synergy with the Enzymatic Reaction

In order to improve the reaction rates and minimize the reduction in fabric strength, the possibilities of using plasma or mercerization as pretreatments have been explored for the enzymatic hydrolysis. On one hand, the accessibility of crystallinity region could be increased by the introduction of cracks on the fiber surface after the plasma treatment. On the other hand, mercerization could reduce the fiber crystallinity and increase the fiber accessibility. Therefore, the effects of the pretreatments and their synergy with enzyme treatments were assessed in terms of the changes in fiber bulk structure and properties, mechanical properties, surface morphology and properties, and dyeing properties with direct dyes.

8.1.3.1 Plasma pretreatments

Chapter 6 reported the application of enzyme treatment to the plasma pretreated linen. Plasma treatments with oxygen and argon gases (200W) for various periods of exposure time (2.5, 5, 10, 20, 40, 60 minutes) were applied to linen prior to the cellulase treatment. The results showed that the plasma pretreatment did enhance the effectiveness of enzymatic hydrolysis. With regard to the oxygen plasma with an exposure time of 2.5 minutes, a faster reaction rate and acceptable strength loss percentage were achieved. Increase of fabric water uptake was further enhanced by the enzyme treatment. Fabric bending rigidity, hysteresis and wrinkle recovery were

slightly improved by both treatments. Plasma pretreatment could improve dyeing performance when dealing with a direct dye of small molecular size.

No significant change in the degree of polymerization and crystallinity was found after both enzyme and plasma treatments. However, a slight reduction of moisture regain was observed from all the plasma pretreated linen and a similar phenomenon was also found after the enzyme treatment. The fabric weight loss increased with the plasma exposure time and a distinct reduction was found after the subsequent enzyme treatment. Both the depth and width of the voids created by the plasma treatment were further deepened and smoothed by the enzyme treatment. Fabric yellowing occurred after plasma exposure and the whiteness was almost recovered after the enzyme treatment. Increase of fabric water uptake was further enhanced by the enzyme treatment. The plasma pretreatment could enhance the effectiveness of enzyme treatment, and a severe strength reduction would occur inevitably. Fabric bending rigidity, hysteresis and wrinkle recovery were slightly improved by both treatments. With the aid of plasma pretreatment, the dyeing rate of the smaller dye molecule (red dye) was slightly increased with a shorter exposure time for all cases, but the dyeing rate of the larger dye molecule (green dye) was reduced. Final exhaustion increased for both types of dyes. The K/S value of the linen dyed with smaller dye molecule was moderately improved, but it is slightly reduced when dyeing with larger dye molecule. Prolonged plasma exposure alone apparently reduced the dyeing rate slightly, while the cellulase treatment further reduced the dyeing performance especially with the direct dye of larger molecular size. When considering the washing fastness properties, improvement could be achieved by the plasma pretreatment whereas the enzyme treatment did not affect the dye fastness.

8.1.3.2 Mercerization pretreatments

Chapter 7 presented the application of the enzyme treatment on mercerized linen. The factors concerned were the mercerization tension (slack, 95% tension, 100% tension), concentration of cellulase (1%, 2%), incubation time (1h, 2h, 3h, 4h) and levels of mechanical agitation (medium, high). The mercerization pretreatment can be applied to reduce crystallinity and improve fiber accessibility. The effectiveness of mercerization pretreatments was assessed.

Mercerization significantly reduced the crystallinity of flax fiber and increased the moisture regain. It was confirmed by the experiments that the fiber structure, accessibility and physical properties of mercerized linen were enhanced by exhibiting a high reduction of fabric stiffness, minimizing the loss of tensile strength, shortening the original treatment time and better removal of fiber surface fibrils.

With regard to the enzyme incubation time effect, significant reductions of fabric surface thickness, strength and bending rigidity were obtained after the first hour of incubation. The effect of increasing the concentration from 1% to 2% would result in higher fabric weight and strength loss but with a smoother fiber surface. On the other hand, a significant reduction of bending rigidity and hysteresis was achieved by applying a higher mechanical agitation with 2% enzyme for 1 hour.

Mercerization greatly improved the dyeing performance in terms of dyeing rate and depth of shade produced. Enzyme treatment slightly affected the final exhaustion of dye and the depth of shade produced. When considering the washing fastness

properties, great improvement was achieved by the mercerization pretreatment. The enzyme treatment did not affect the fastness property apparently.

8.2 CONCLUSIONS

The present thesis illustrated a comprehensive and systematic investigation on the variations of the structure and properties of the modified linen with the major conclusions being summarized as follows.

Substantial increase surface polar groups and water uptake, a slight improved fabric strength, bending stiffness, wrinkle recovery and dyeing performance were achieved after a short exposure of linen to oxygen or argon plasma. Increasing the exposure time of plasma treatment, the depth of the micro-pores etched on the fiber surface increased with enlarged width of the pores. From a relatively smoother surface of an untreated flax fiber, pits with the sizes (both depth and diameter) in sub-micrometer were etched by the argon plasma while pits with sizes of a few micrometers were created by the oxygen plasma.

Fabric softness and fiber smoothness were improved by the application of enzyme treatment. Significant reduction of the bending rigidity could be achieved by applying higher mechanical agitation during the enzyme treatment. Plasma or mercerization pretreatments were used to enhance the effectiveness of enzyme treatment. It was found that the pretreated linen with plasma could provide a faster enzymatic reaction rate with acceptable strength loss.

Mercerizations increased the accessibility and improved the dyeing performance of linen. The fabric sett, tensile strength and bending properties were also altered under different mercerization tensions. It was found that enzyme treatment effectively reduced the fabric stiffness and fiber surface smoothness of the mercerized linen. Considering the improvement in the enzymatic reaction rate, plasma pretreatment seems to offer a better enhancement. These findings suggested that the choice of processing method should be varied in order to attain the desired enzyme finishing effects as well as the desired end product properties.

A characterization system covering fiber bulk structure and properties, surface morphology and properties, fabric properties and dyeing properties was used to investigate the variations of the modified linen. The advanced analytical instruments and techniques employed included ESEM, AFM, image processing techniques and downward wicking measurement. On the whole, a comprehensive surface evaluation was achieved.

8.3 RECOMMENDATION FOR FUTURE WORK

The major objectives of the research project have been achieved. However, further work is necessary in order to improve and further develop effective techniques for industrial applications.

In the present work, the effectiveness of enzyme treatment was determined based on the fabric weight loss and the variations of the fabric properties before and after the treatment. Since reduced glucose will be liberated during the enzymatic hydrolysis of cellulose, it is possible to evaluate the extent of such hydrolysis by determining

the amount of the liberated glucose. The degree of glucose liberated can be used to determine the effectiveness of cellulase treatment and establish the correlation between the variation of fiber and fabric properties. The established relationship will be useful in the control of the enzyme treatment for industrial application and is highly recommended for further investigation.

The developed downward wicking technique can be used to investigate the wicking properties of a wider range of fabrics in terms of fabric structure, fiber contents as well as the effects of textile finishing. Therefore, an advanced study of this technique is highly recommended in the future.

The zeta potential measurement is important to quantify the average charge density at the surface. Besides, the FTIR-ATR characterization technique offers the determination of chemical functional groups on the fiber surface. These two techniques may be used in conjunction with the techniques employed in the present work to monitor the changes occurring on the fiber surfaces at various stages of textile processing particularly where surface modifications are used.

ESEM has been shown to be a very useful tool for observing the surface morphology of textile fiber. Similarly, AFM is also a powerful tool to study the fiber surface topographically in nano-meters scale. Both characterization techniques make it possible to carry out the on-going observation of the fiber surface affected by the surface treatment or modification. Further study is highly recommended to improve these two characterization techniques and their application to other areas of textile research.

REFERENCES

1. AATCC 153-1985, Color Measurement of Textiles: Instrumental, *AATCC Technical Manual* (1992).

2. AATCC 61-1994, Colorfastness to Laundering, Home and Commercial: Accelerated, *AATCC Technical Manual* (1994).

3. AATCC 66-1990, Wrinkle Recovery of Fabrics: Recovery Angle Methods, *AATCC Technical Manual* (1992).

4. AATCC 79-1986, Absorbency of Bleached Textiles, *AATCC Technical Manual*, 106 (1991).

5. AATCC Evaluation Procedures 1, Grey Scale for Color Change, *AATCC Technical Manual* (1992).

6. AATCC Evaluation Procedures 2, Grey Scale for Color Staining, *AATCC Technical Manual* (1992).

7. Achari, A. E., Ghenaim, A., Wolff, V., and Caze, C., Topographic Study of Glass Fibers by Atomic Force Microscopy, *Textile Research Journal*, **66**, (8), 483-490 (1996).

8. Adamson, A. W., *Physical Chemistry of Surfaces*, John Wiely, NY, 784pp (1997).

9. Akin, D. E., Henriksson, G., Morrison III, W. H., and Eriksson, K. E. L., Enzymatic Retting of Flax, *Enzyme Applications in Fiber Processing, ACS Symposium Series 687*, American Chemical Society, 269-278 (1998).

10. Akin, D. E., Morrison, W. H., Gamble, G. R., Rigsby, L. L., Henriksson, G., and Eriksson, K. E. L., Effect of Retting Enzymes on the Structure and Composition of Flax Cell Walls, *Textile Research Journal*, **67**, (4), 279-287 (1997).

11. Asferg, L. O., and Videbaek, T., Softening and Polishing of Cotton Fabrics by Cellulase Treatment, *International Textile Bulletin Dyeing/Printing/Finishing*, (2), 5-8 (1990).

12. ASTM D2654-89a, Moisture Content and Moisture Regain of Textiles, Annual Handbook of American Society of Testing and Material Standard (1995).

13. ASTM D5035-95, Breaking Force and Elongation of Textile Fabrics (Strip Test), Annual Handbook of American Society of Testing and Material Standard (1995).

14. Bahners, T., and Schollmeyer, E., Application of Low Temperature Plasma Technology for Textile Pretreatments – Part 1: Procedures of Low Temperature Plasma Technology, *Textile-Parxis-International*, (7/8), XV-XVI (1994).

15. Batra, S. K., *Handbook of Fiber Science and Technology: Fiber Chemistry*, Dekker, NY, 727-807 (1983).

16. Bayard, J., Desizing with Enzymes, *Canadian Textile Journal*, (6), 168-169 (1983).

17. Benerito, R.R., Ward, T. L., Soignet, M., and Hinojosa, O., Modifications of Cotton Cellulose Surfaces by Use of Radiofrequency Cold Plasmas and Characterization of Surface Changes by ESCA, *Textile Research Journal*, **51**, (4), 224-232 (1981).

18. Bertoniere, N. R., and Rowland, S. P., Spreading and Imbibition of Durable Press Reagent Solutions in Cotton-Containing Fabrics, *Textile Research Journal*, **55**, (1), 57-64 (1985).

19. Betrabet, S. M., Prospects and Problems in Application of Enzymes in Wet Processing, *Colourage,* **41**, (5), 21-25 (1994).

20. Bhattacharyya, S. K., Enzymes and Textiles, *The Textile Industry and Trade Journal,* **2**, (1/2), 11-13 (1983).

21. Boenig, H. V., Principle Parameters in Plasma Adhesion, *Fourth Annual International Conference of Plasma Chemistry and Technology*, 63-85 (1989).

22. Bozzola, J. J., and Russell, L. D., *Electron Microscopy, Principles and Techniques for Biologists*, Jones and Bartlett Publishers, Boston, 184-213 (1992).

23. Bracewell, R. N., *The Fourier Transform and Its Applications*, McGraw-Hill, NY, 241-274 (1986).

24. Brown, P. W., Hellmann, J. R., and Klimkiewicz, M., Examples of Evolution of Microstructure in Ceramics and Composites, *Microscopy Research and Techniques*, **25**, (5/6), 474-486 (1993).

25. BS 3090:1978, The Determination of the Cuprammonium Fluidity of Linen Materials, British Standard Institutes (1978).

26. BS 4554:1970, Wettability of Textile Fabrics, *British Standard Handbook 11*, British Standard Institution, 4/204-4/212 (1974).

27. Buchle-Diller, G., and Zeronian, S. H., Enhancing the Reactivity and Strength of Cotton Fibers, *Journal of Applied Polymer Science*, **45**, 967-979 (1992).

28. Buchle-Diller, G., Zeronian, S. H., Enzymatic and Acid Hydrolysis of Cotton Cellulose After Slack and Tension Mercerization, *Textile Chemist and Colorist*, **26**, (4), 17-24 (1994).

29. Buchle-Diller, G., Zeronian, S. H., Pan, N., and Yoon, M. Y., Enzymatic Hydrolysis of Cotton, Linen, Ramie and Viscose Rayon Fabrics, *Textile Research Journal*, **64**, (5), 270-279 (1994).

30. Buschle-Diller, G., and Traore, M. K., Influence of Direct and Reactive Dyes on the Enzymatic Hydrolysis of Cotton, *Textile Research Journal*, **68**, (3), 185-192 (1998).

31. Buschle-Diller, G., El Mogahzy, Y., Inglesby, M. K., and Zeronian, S. H., Effects of Scouring with Enzymes, Organic Solvents, and Caustic Soda on the Properties of Hydrogen Peroxide Bleached Cotton Yarn, *Textile Research Journal*, **68**, (12), 920-929 (1998).

32. Byrne, G. A., and Brown, K. C., Modifications of Textiles by Glow-discharge Reactions, *Journal of the Society of Dyers and Colorist*, **88**, (3), 113-117 (1972).

33. Cameron, R. E., Environmental SEM: Principles and Applications, *Microscopy and Analysis*, **6**, (17), 11-13 (1994).

34. Carroll, B. J., The Accurate Measurement of Contact Angle, Phase Contact Areas, Drop Volume, and Laplace Excess Pressure in Drop-on-Fibre Systems, *Journal of Colloid and Interface Science*, **57**, (3), 488-495 (1976).

35. Carroll, B. J., The Determination of the Contact Angle of a Liquid Droplet on a Thin Fiber, *Textile Research Journal*, **47**, (8), 561-562 (1977).

36. Cavaco-Paulo, A., Almeida, L., and Bishop, D., Effects of Agitation and Endoglucanase Pretreatment on the Hydrolysis of Cotton Fabrics by a Total Cellulase, *Textile Research Journal*, **66**, (5), 287-294 (1996).

37. Cavaco-Paulo, A., Almeida, L., and Bishop, D., Hydrolysis of Cotton Cellulose by Engineered Cellulases for *Trichoderma reesei*, *Textile Research Journal*, **68**, (4), 273-280 (1998).

38. Cavaco-Paulo, A., Processing Textile Fibers with Enzymes: An Overview, *Enzyme Applications in Fiber Processing, ACS Symposium Series 687*, American Chemical Society, 180-189 (1998).

39. Chan, C. M., Ko, T. M., and Hiraoka, H., Polymer Surface Modification by Plasmas and Photons, *Surface Science Reports*, **24**, 1-54 (1996).

40. Chan, C. M., *Polymer Surface Modification and Characterization*, Hanser Publishers, NY, 35-76 (1993).

41. Chatterjee, P. K., Capillarity and Surface Phenomena, *Nonwovens-Theory,*

Process, Performance & Testing, 39-55 (1993).

42. Chatterjee, P. K., Mechanism of Liquid Flow and Structure Property Relationships, *Absorbency*, Chatterjee, P. K., Elsevier science Publishing Company Inc., NY, 29-84 (1985).

43. Cheek, L., and Roussel, L., Mercerization of Ramie: Comparisons with Flax and Cotton, Part I: Effects on Physical, Mechanical, and Accessibility Characteristics, *Textile Research Journal*, **59**, (8), 478-483 (1989).

44. Cheek, L., and Roussel, L., Mercerization of Ramie: Comparisons with Flax and Cotton, Part II: Effects on Dyeing and Behavior, *Textile Research Journal*, **59**, (9), 541-546 (1989).

45. Chikkodi, S. V., Determining Fiber Loss in Biofinishing of Cotton and Cotton/Wool Blended Fabrics, *Textile Chemist and Colorist*, **28**, (3), 28-31 (1996).

46. Chikkodi, S. V., Khan, S., and Mehta, R. D., Effects of Biofinishing on Cotton/Wool Blended Fabrics, *Textile Research Journal,* **65**, (10), 564-569 (1995).

47. Choe, E. K., Park, S. Y., Cha, H. C., and Jeon, B. D., Effect of Pre-existing Dyes and Fabric Type on Cellulase Treatment of Cotton Fabrics, *Textile Research Journal*, **67**, (3), 155-162 (1997).

48. Clark, D. T., Dilks, A., and Shuttleworth, D., The Application of Plasmas to the Synthesis and Surface Modification of Polymers, *Polymer Surface*, Clark, D. T., and Feast, W. J., John Wiley & Sons, NY, 185-211 (1978).

49. Clarkson, K., Collier, K., Larenas, E., and Wesis, G., Opportunities for Use of Biochemicals in Textile Finishing, *AATCC Book of Papers,* 319-323 (1994).

50. Collins, S. P., Pope, R. K., Scheetz, R. W., Ray, R. I., Wagner, P. A., and Little, B. J., Advantages of Environmental Scanning Electron Microscopy in Studies of Microorganisms, *Microscopy Research and Technique*, **25**, (5/6), 398-405 (1993).

51. Cook, J. G., *Handbook of Textile Fibres, 1. Natural Fibres*, Fifth Edition, Shildon, Merrow, 4-12 (1984).

52. Cowling E. B., Physical and Chemical Constraints in the Hydrolysis of Cellulose and Lignocellulosic Materials, *Cellulose as a Chemical and Energy Resource, Biotechnology & Bioengineering Symposium*, Wilke, C. R., Eds., John Wily & Sons, NY, 163-181 (1975).

53. Csiszar, E., Szakacs, G., and Rusznak, I., Bioscouring of Cotton Fabrics with Cellulase Enzyme, *Enzyme Applications in Fiber Processing, ACS Symposium Series 687*, American Chemical Society, 204-211 (1998).

54. Csiszar, E., Szakacs, G., and Rusznak, I., Combining Traditional Cotton Scouring with Cellulase Enzymatic Treatment, *Textile Research Journal*, **68**, (3), 163-167 (1998).

55. Dai, J., Application of Plasma Technology in Textile Processing, *Journal of Textile Research* (in Chinese), No. 17, (6), 384-390 (1996).

56. Danilatos, G. D., An Atmospheric Scanning Electron Microscope (ASEM), *Scanning*, **3**, 215-217 (1980).

57. Danilatos, G. D., and Brooks, J. H., Environmental SEM in Wool Research – Present State of the Art, *Proceedings of The 7th International Wool Textile Research Conference, Tokyo*, Vol. I, 263-272 (1985).

58. Danilatos, G. D., and Postal, R., Design and Construction of an Atmospheric or Environmental SEM-2, *Micron*, **14**, (1), 41-52 (1983).

59. Danilatos, G. D., and Postle, R., The Environmental Scanning Electron Microscope and its Applications, *Scanning Electron Microscopy*, (I), 1-16 (1982).

60. Danilatos, G. D., Beam-radiation Effects on Wool in the ESEM, *Proceedings of the 44th Annual Meeting of the Electron Microscopy Society of America*, 674-675 (1996).

61. Danilatos, G. D., Design and Construction of an Atmospheric or Environmental SEM (Part 3), *Scanning*, 7, 26-42 (1985).

62. Danilatos, G. D., Design and Construction of an Atmospheric or Environmental SEM (Part 1), *Scanning*, **4**, 9-20 (1981).

63. Danilatos, G. D., Design and Construction of an Environmental SEM (Part 4), *Scanning*, **12**, 23-27 (1990).

64. Danilatos, G. D., Introduction to the ESEM Instrument, *Microscopy Research and Technique*, **25**, 354-361 (1993).

65. Danilatos, G. D., Mechanisms of Detection and Imaging in the ESEM, *Journal of Microscopy*, **160**, (1), 9-19 (1990).

66. Danilatos, G. D., Review and Outline of Environmental SEM at Present, *Journal of Microscopy*, **162**, (3), 391-402 (1991).

67. Danilatos, G. D., The Examination of Fresh or Living Plant Material in an Environmental Scanning Electron Microscope, *Journal of Microscopy*, **121**, (2), 235-238 (1980).

68. David, R. L., *CRC Handbook of Chemistry and Physics*, 73th edition, Clefeland, CRC Press, Ohio, 6-127 (1992/93).

69. DeBoer, J. J., The Wettability of Scoured and Dried Cotton Fabrics, *Textile Research Journal*, **50**, (10), 624-631 (1980).

70. Denes, F., Hua, Z. Q., Barrios, E., and Young, R. A., Influence of RF-Cold Plasma Treatment on the Surface Properties of Paper, *Pure Appl. Chem.*, A32 (8&9), 1405-1443 (1995).

71. Dezert, M. H., Viallier, P., and Wattiez, D., Continuous Control of an Enzymatic Pretreatment on Linen Fabric Before Dyeing, *Journal of the Society of Dyer and Colorist*, **114**, (10), 283-286 (1998).

72. Digital Instruments Internet Web Site, http://www.di.com. (January 1999)

73. DIN 53924-1978, Determination of the Rate of Absorption of Water by Textile Materials (Height of Rise Method), DIN Deutsches Institut Fur Norming E V. (1978).

74. Egitto, F. D., and Matienzo, L. J., Plasma Modification of Polymer Surfaces for Adhesion Improvement, *IBM Journal Research Development*, **38**, (4) 423-439 (1994).

75. El-Rafie, M. H., Higazy, A., and Hebeish, A., Bleaching of Linen Fabrics Using A Hydrogen Peroxide/Urea System, *American Dyestuff Reporter*, **81**, (3), 48, 50, 53-55, 67 (1992).

76. Enari, T., and Niku-Paavola, M, Enzymatic Hydrolysis of Cellulose: Is the Current Theory of the Mechanism of Hydrolysis Valid?, *CRC Critical Review in Biotechnology*, **5**, (1), 67-87 (1987).

77. Engel, A., Biological Applications of Scanning Probe Microscopes, *Ann. Rev. Biophys. Biophys. Chem.*, **20**, 79-108 (1991).

78. Felix, J. M., and Gatenholm, P., The Nature of Adhesion in Composites of Modified Cellulose Fibres and Polypropylene, *Journal of Applied Polymer Science*, **42**, 609-620 (1991).

79. Finch, P., and Roberts, J. C., Enzymatic Degradation of Cellulose, *Cellulose Chemistry and its Applications*, Nevell, T. P., and Zeronian, S. H., John Wily & Sons, NY, 312-343 (1985).

80. Flamm, D. L., and Herb, G. K., Plasma Etching Technology – An Overview, *Plasma Etching – An Introduction*, Manos, D. M., and Flamm, D. L., Academic Press Inc, NY, 1-89 (1988).

81. Focher, B., Marzetti, A., and Sharma, H. S. S., Changes in the Structure and Properties of Flax Fiber During Processing, *The Biology and Processing of Flax*, Sharma, H. S. S., and Van Sumere, C. F., Eds., M Publications, Belfast, Northern Ireland, 329-342 (1995).

82. Focher, B., Marzetti, A., Beltrame, P. L., and Carniti P., Structural Features of

Cellulose and Cellulose Derivatives, and their Effects on Enzymatic Hydrolysis, *Biosynthesis and Biodegradation of Cellulose*, Haigler C. H., and Weimer, P. J., Marcel Dekker, NY, 293-310 (1991).

83. Focher, B., Physical Characteristics of Flax Fiber, *The Biology and Processing of Flax*, Sharma, H. S. S., and Van Sumere, C. F., Eds., M Publications, Belfast, Northern Ireland, 11-32 (1995).

84. Forsberg, P., and Lepoutre, P., Environmental Scanning Electron Microscope Examination of Paper in High Moisture Environment: Surface Structural Changes and Electron Beam Damage, *Scanning Microscopy*, **8**, (1), 31-34 (1994).

85. Gerristead, W. R., Link, Jr., L. F., Paciej, R. C., Damiani, P., and Li, H., Environmental Scanning Electron Microscopy for Dynamic Corrosion Studies of Stainless Steel Piping Used in UHP Gas Distribution Systems, *Microscopy Research and Technique*, **25**, 523-528 (1993).

86. Ghali, K., Jones, B., and Tracy, J., Experimental Techniques for Measuring Parameters Describing Wetting and Wicking in Fabrics, *Textile Research Journal*, **64**, (2), 106-111 (1994).

87. Ghali, K., Jones, B., and Tracy, J., Modeling Moisture Transfer in Fabric, *Experimental Thermal and Fluid Science*, **9**, 330-336 (1994).

88. Godau, D. E., Using Plasma Technology, *Textile Technology International*, 109-110 (1996).

89. Good, R. J., Contact Angle, Wetting, and Adhesion: A Critical Review, *Journal of Adhesion Science and Technology*, **6**, (12), 1269-1302 (1992).

90. Good, R. J., Contact Angles and the Surface Free Energy of Solids, *Surface and Colloid Science, Volume 11 Experimental Methods*, Plenum Press, NY, 1-29 (1979).

91. Goswami, K. K., and Mukherjee, A. K., Bleaching of Linen (*Linum usitatissimum*), *Indian Journal of Fibre and Textile Research*, **18**, (6), 82-86 (1992).

92. Goswami, K. K., and Mukherjee, A. K., Effects of Alkali on Linen (*Linum usitatissimum*), *Indian Journal of Fibre and Textile Research*, **17**, (9), 136-143 (1992).

93. Goto, T., Wakida, T., Nakanishi, T., and Ohta, Y., Application of Low Temperature Plasma Treatment to the Scouring of Gray Cotton Fabric, *Sen-i Gakkaishi*, **48**, (3), 133-137 (1992).

94. Goynes, W. R., Surface Characterization of Textiles Using SEM, *Modern Textile Characterization Method*, Raheel, M., Marcel Dekker, NY, 145-174 (1996).

95. Greaves, P. H., Microscopy, Imaging and Analysis, *Advance in Fibre Science*, Kumar, M. S., Textile Institute, Manchester, 48-66 (1992).

96. Gregorski, K. S., and Pavlath, A. E., Fabric Modification Using the Plasmod: The Effect of Extensive Treatment in Nitrogen and Oxygen Plasma in Low Pressure, *Textile Research Journal*, **50**, (1), 42-46 (1980).

97. Grill, A., *Cold Plasma in Materials Fabrication, From Fundamentals to Applications*, Piscataway, N. J., IEEE Press, NY, 258pp (1994).

98. Grindstaff, T. H., Patterson, H. T., A Common Error in Contact-Angle Measurments on Fibers Using the Level-Surface Method, *Textile Research Journal*, **45**, (10), 760-761 (1975).

99. Hamilton, I. T., Great Scope for Flax!, *Textile Horizon*, **4**, (5), 22-23 (1984).

100. Hamilton, I. T., Linen, *Textiles*, **15**, (2), 30-34 (1986).

101. Hamlyn, P., The Impact of Biotechnology on the Textile Industry, *Textile Magazine*, (3), 6-10 (1995).

102. Hansma, P. K., Elings, V. B., Marti, O., and Bracker, C. E., Scanning Tunneling Microscopy and Atomic Force Microscopy: Application to Biology and Technology, *Science*, **242**, 209-216 (1988).

103. Hardin, I. R., Li. Y., and Akin, D., Cotton Wall Structure and Enzymatic Treatments, *Enzyme Applications in Fiber Processing, ACS Symposium Series 687*, American Chemical Society, 190-203 (1998).

104. Harnett, P. R., and Mehta, P. N., A Survey and Comparison of Laboratory Test Methods for Measuring Wicking, *Textile Research Journal*, **54**, (7), 471-178 (1984).

105. Harper Jr., R. J., and Lambert, A. H., Stone Finishing and Dyeing of Cotton Garments, *AATCC Book of Papers*, 278-286 (1991).

106. Harrision, G., Silva, A. P., Horrocks, A. R., Rhodes, D., Improving the Performance of Bleached Cotton Fibre in Terms of Increased Absorbency, *Proceedings of the Textile Institute Yarn and Fiber Science Joint Conference*, Manchester, UK, 1-6 (1996).

107. Harrison, P. W., Absorbent Incontinence Products, *Textile Progress*, **20**, (3), 1-35 (1990).

108. Harry, P. R., *Textile Chemistry*, Amsterdam Elsevier, 88-95 (1963).

109. Hartzell, M. M., and Hsieh, Y. L., Enzymatic Scouring to Improve Cotton Fabric Wettability, *Textile Research Journal*, **68**, (4), 233-241 (1998).

110. Hartzell, M. M., and Hsieh, Y. L., Pectin-Degrading Enzymes for Scouring Cotton, *Enzyme Applications in Fiber Processing, ACS Symposium Series 687*, American Chemical Society, 212-227 (1998).

111. Hatch, K. L., *Textile Science*, West Publishing Company, St. Paul, 119-121 (1993).

112. Hatch, K. L., *Textile Science*, West Publishing Company: St. Paul, 113-114 (1993).

113. Heikinheimo, L., C., Cavaco-Paulo, A., Nousianen, P., Siika-aho, M., and Buchet, J., Treatment of Cotton Fabrics with Purified *Trichodermna reesei* Cellulases, *Journal of the Society of Dyer and Colorist*, **114**, (7/8), 216-220 (1998).

114. Hemmpel, W. H., The Surface Modification of Woven and Knitted Cellulose Fibre Fabrics by Enzymatic Degradation, *International Textile Bulletin. Dyeing/Printing/Finishing*, **37**, (3), 5-6, 8, 10, 12-14 (1991).

115. Henriksson, G., Akin, D. E., Rigsby, L. L., Patel, N., and Eriksson, K. E. L., Influence of Chelating Agents and Mechanical Pretreatment on Enzymatic Retting of Flax, *Textile Research Journal*, **67**, (11), 829-836 (1997).

116. Henriksson, G., Eriksson, K. L., Kimmel, L., and Akin, D. E., Chemical / Physical Retting of Flax Using Detergent and Oxalic Acid at High pH, *Textile Research Journal*, **68**, (12), 942-947 (1998).

117. Herlinger, H., Kuster, B., and Volz, W., Methods for Characterizing the Wetting Behavior of Textile Fabrics, *Melliand English*, (11), E330-E332 (1986).

118. Hersh, S. P., Resistively and Static Behavior of Textile Surfaces, *Surface Characteristics of Fibers and Textiles*, Rebenfeld, L., Marcel Dekker, NY and Basel, 225-293 (1975).

119. Hoke. L., Segars, R. A., and McDermott, R. B., Methods to Evaluate Solid Surface Tension for Military Fabrics, U. S. Army Matick RD&E Center, 1-50 (1990).

120. Hollander, A., and Behnisch, J., Semicontinuous Plasma Treatment of Textiles, *Asian Textile Journal*, (8), 49-51 (1997).

121. Hsieh, Y. L., and Yu, B., and Hartzell, M. M., Liquid Wetting, Transport, and Retention Properties of Fibrous Assemblies, Part II: Water Wetting Properties and Retention of 100% and Blended Woven Fabrics, *Textile Research Journal*, **62**, (12), 697-704 (1992).

122. Hsieh, Y. L., and Yu, B., Liquid Wetting, Transport, and Retention Properties of Fibrous Assemblies, Part I: Water Wetting Properties of Woven Fabrics and Their Constituent Single Fibres, *Textile Research Journal*, **62**, (11), 677-

685 (1992).

123. Hsieh, Y. L., Liquid Transport in Fabric Structures, *Textile Research Journal*, **65**, (5), 299-307 (1995).

124. Hsieh, Y. L., Miller, A., and Thompson, J., Wetting, Pore Structure, and Liquid Retention of Hydrolysed Polyester Fabrics, *Textile Research Journal*, **66**, (1), 1-10 (1996).

125. Hsieh, Y. L., Thompson, J., and Miller, A., Water Wetting and Retention of Cotton Assemblies as Affected by Alkaline and Bleaching Treatments, *Textile Research Journal*, **66**, (7), 456-464 (1996).

126. Hua, Z. Q., Sitaru, R., Denes, F., and Young R. A., Mechanisms of Oxygen- and Argon-RF-Plasma-Induced Surface Chemistry of Cellulose, *Plasma and Polymers*, **2**, (3), 199-224 (1997).

127. Inagaki, N., and Yasukawa, Y., Improvement of Wicking Property of PET Fabrics by Plasma Polymerization of Nitro Compounds, *Sen-i Gakkaishi*, **44**, (7), 333-338 (1988).

128. Inagaki, N., Plasma Interactions Between Plasma and Polymeric Materials, *Plasma Surface Modification and Plasma Polymerization*, Technomic Publishing Company, Pennsylvania, 21-42 (1996).

129. Inagaki, N., Tasaka, S., and Kawai, H., Improved Adhesion of Ploy (tetrafluoroethylene) by NH_3-plasma Treatment, *Journal of Adhesion Science and Technology*, **3**, (8), 637-649 (1989).

130. INDA Standard Test: IST 10.1 (95), Standard Test Method for Absorbency Time, Absorbency Capacity and Wicking Rate, INDA, Association of the Nonwoven Fabrics Industry (1995).

131. Instruction Manual for Contact Angle Meter Model CAM-MICRO, Tantec Inc., (1996).

132. Instruction Manual for Model S-2380N Scanning Electron Microscope, Hitachi Ltd., (1995).

133. Janca, J., and Czernichowski, A., Wool Treatment in the Gas Flow from Gliding Discharge Plasma at Atmospheric Pressure, *Surface and Coatings Technology*, **98**, 1112-1115 (1998).

134. Jenkins, L. M., and Donald, A. M., Use of the Environmental Scanning Electron Microscope for the Observation of the Swelling Behavior of Cellulosic Fibers, *Scanning*, **19**, 92-97 (1997).

135. Jerde, J., *Encyclopedia of Textiles*, Facts On File, Inc., NY, 119-127 (1992).

136. Jung, H. Z., and Ward, T. L., Water Absorption of Toweling as Affected by

Argon Cold Plasma, *Textile Research Journal*, **47**, (8), 563-564 (1977).

137. Jung, H. Z., Ward, T. L., and Benerito, R. R., The Effect of Argon Plasma on Water Absorption of Cotton, *Textile Research Journal*, **47**, (3), 217-223 (1977).

138. Kaczynski, S., Linen Asserts Itself in Knit Fabrics, *Filiere Maille,* (33), 27-28 (1995).

139. Kawase, T., Fujii, T., Minagawa, M., Sawada, H., and Nakayama, M., Novel Fluoroalkylation of Polyester Surfaces: Grafting with Perfluoroalkanoyl Peroxides, *Textile Research Journal*, **64**, (7), 375-380 (1994).

140. Kawase, T., Uchita, M., Fujii, T., and Minagawa, M., Acrylic Acid Grafted Polyester Surface: Surface Free Energies, FT-IR(ATR), and ESCA Characterization, *Textile Research Journal*, **61**, (3), 146-152 (1991).

141. Kernaghan, K., and Kiekens, P., Bleaching and Dyeing of Linen, *The Biology and Processing of Flax*, Sharma, H. S. S., and Van Sumere, C. F., Eds., M Publications, Belfast, Northern Ireland, 343-445 (1995).

142. Kernaghan, K., Physical Properties of Linen and Their Influence on Finishing, *The Biology and Processing of Flax*, Sharma, H. S. S., and Van Sumere, C. F., Eds., M Publications, Belfast, Northern Ireland, 475-500 (1995).

143. Kidd, B., Carr, C. M., Dodd, K. J., Vickerman, J., and Byrne, K., X-Ray Photoelectron Spectroscopic Study of Wool Modified by Gaseous Fluorine, *Textile Research Journal,* **65**, (9), 504-506 (1995).

144. Kirk, T. K., Ligin-Degrading Enzyme System, *Cellulose as a Chemical and Energy Resource, Biotechnology & Bioengineering Symposium,* Wilke, C. R., John Wily & Sons, NY, 139-150 (1975).

145. Kissa, E., Wetting and Wicking, *Textile Research Journal*, **66**, (10), 660-668 (1996).

146. Klahorst, S., Kumar, A., and Mullins, M. M., Optimizing the Use of Cellulases for Denim Finishing, *AATCC Book of Papers*, 243-249 (1991).

147. Kochavi, D., Videbaek, T., Cedroni, D., Optimizing Processing Conditions in Enzymatic Stonewashing, *American Dyestuff Reporter,* **79**, (9), 24, 26, 28 (1990).

148. Koo, H., Ueda, M., Wakida, T., Yoshimura, Y., and Igarashi, T., Cellulase Treatment of Cotton Fabrics, *Textile Research Journal*, **64**, (2), 70-74 (1994).

149. Koztowski, R., and Manys, S., Flax: The Oldest Fibre in Civilisation?, *Textiles,* **22**, (4), 8-9 (1993).

150. Koztowski, R., and Manys, S., Old Fibre, New Uses, *Textile Asia*, **27**, (1), 66-

70 (1996).

151. Kramar, L., Plasma Techniques Versus Wet Pretreatment, *Textile Month*, (3), 24-25 (1994).

152. Kramar, L., Plasma Techniques Vs Wet Pretreatment, *International Dyer*, (4), 30-31 (1991).

153. Kratz, G., and Funder, A., Finishing of Woven Linen and Ramie Fabrics with Liquid Ammonia, *Melliand Textilberichte*, **68**, (10), E341-E345 (1987).

154. Kubota, S., and Emori, K., Abrasive Finishing of Cotton Fiber by Low Temperature Plasma, *Sen-i Gakkaishi*, **50**, (8), 343-348 (1994).

155. Ladchumanandasivam, R., Miles, L. W. C., and Hawkyard, C. J., The Accessibility of Cotton to Anionic Dyes, *Journal of the Society of Dyer and Colorist*, **110**, (10), 300-301 (1994).

156. Lambrinou, I., Outerwear of Linen (Part 1), *Melliand Textilberichte [Eng. Ed.]*, **11**, (7), 528-530 (1982).

157. Le, C. V., Ly, N. G., and Stevens, M. G., Measuring the Contact Angles of Liquid Droplets on Wool Fibres and Determining Surface Energy Components, *Textile Research Journal*, **66**, (6), 389-397 (1996).

158. Leijala, A., and Hautojarvi, J., Characterizing Spin Finish Layers on Polypropylene Fiber Surfaces by Means of Scanning Force Microscopy Techniques, *Textile Research Journal*, **68**, (3), 193-202 (1998).

159. Li, Y., and Hardin, I. R., Treating Cotton with Cellulases and Pectinases: Effects on Cuticle and Fiber Properties, *Textile Research Journal*, **68**, (9), 671-679 (1998).

160. Magonov, S. N., and Whangbo, M. H., *Surface Analysis with STM and AFM: Experimental and Theoretical Aspects of Image Analysis*, Weinheim, NY, 323pp (1996).

161. Magonov, S. N., Goreberg, A. Y., and Cantow, H. J., Atomic Force Microscopy on Polymers and Polymer Related Compounds, *Polymer Bulletin*, **28**, 577-584 (1992).

162. McEvoy, G., Linen: One of the World's Oldest Fibres is Ideal for the '90s, *Canadian Textile Journal*, **111**, (8), 20-21, 25 (1994/1995)

163. Merkel, R. S., *Absorbency and Repellency, Textile Product Serviceability*, Maxwell Macmillan International, NY, 307-234 (1991).

164. Meyer, E., Atomic Force Microscopy, *Prog. Surf. Sci.*, **41**, 3-49 (1992).

165. Miller B., Friedman, H. L., Johnson, R. A., and Holmes, C. E., Pro and Anti-

gravity Wicking Compared, *INDA-TEC 96 Book of Papers*, 13.1-13.15 (1996).

166. Miller, B., and Tyomkin, I., An Extended Range Liquid Extrusion Method for Determining Pore Size Distributions, *Textile Research Journal*, **56**, (1), 35-40 (1986).

167. Miller, B., and Tyomkin, I., Liquid Porosimetry: New Methodology and Applications, *Journal of Colloid and Interface Science*, **162**, 163-170 (1994).

168. Miller, B., and Tyomkin, I., Spontaneous Uptake by Heterogeneous Fabric Structures, *Nonwovens Industry*, **19**, (10), 58-62 (1988).

169. Miller, B., and Young, R. A., Methodology for Studying the Wettability of Filaments, *Textile Research Journal*, **45**, (5), 359-365 (1975).

170. Miller, B., Experimental Aspects of Fiber Wetting and Liquid Movement Between Fibers, *Absorbency*, Elsevier Science, NY, 121-147 (1985).

171. Miller, B., The Wetting of Fibres, *Surface Characteristics of Fibres and Textiles, Part II*, Schick, M. J., Marcel Dekker, NY and Basel, 417-446 (1975).

172. Millett, M. A., Baker, A. J. and Satter, L. D., Pretreatments to Enhance Chemical, Enzymatic and Microbiological Attack of Cellulosic Materials, *Cellulose as a Chemical and Energy Resource, Biotechnology & Bioengineering Symposium,* Wilke, C. R., Eds., John Wily & Sons, NY, 193-219 (1975).

173. Mitchenko, Y. I., Genis, A. V., Fenin, V. A., Kadontseva, T. I., and Chegolya, A. S., Properties of Fibrous Materials Which Have Been Treated in a Gas Discharge, *Fibre Chemistry*, **19**, (2), 152-154 (1987).

174. Montgomery, S. M., Miller, B., and Rebenfeld, L., Spatial Distribution of Local Permeabilities in Fibrous Networks, *Textile Research Journal*, **62**, (3), 151-161 (1992).

175. Mori, R., Haga, T., and Takagishi, T., Relationship Between Cellulase Treatment and the Dyeability with a Direct Dye for Various Kinds of Cellulosic Fibers, *Journal of Applied Polymer Science,* **48**, 1223-1227 (1993).

176. Mori, R., Haga, T., and Takagishi, T., Relationship Between Cellulase Treatment and Direct Dye Dyeing for Cotton, *Journal of Applied Polymer Science,* **45**, 1869-1872 (1992).

177. Morton, W. E., and Hearle, J. W. S., *Physical Properties of Textile Fibres*, The Textile Institute, Manchester, 159-177 (1993).

178. Morton, W. E., and Hearle, J. W. S., *Physical Properties of Textile Fibres*, The Textile Institute, Manchester, 502-563 (1993).

179. Murphy, A. L., Margavio, M. F., Cooper, Jr., A. S., and Welch, C. M., Yarn Mercerization Techniques in Preparing High-Strength Wash-Wear Cottons, *Textile Research Journal*, **38**, (5), 544-553 (1968).

180. Myers. D., *Surfaces, Interfaces and Colloids: Principles and Applications*, VCH Publishers, 87-109 (1991).

181. Neumann, A. W., and Good, R. J., *Techniques of Measuring Contact Angles, Surface and Colloid Science, Volume 11 Experimental Methods*, Plenum Press, NY, 31-91 (1979).

182. Olson, L., A New Technology for Stoneless Stone-Washing Applications, *American Dyestuff Reporter*, **77**, (5), 19-22 (1988).

183. Olson, L., Stone Washing, *Textile Rental*, (9), 26-31 (1987).

184. Orlepp, G., Weiss-Quasdorf, M., Mieck, K. P., Cellulases Open up New Possibilities for Textile Recycling, *Melliand English*, **78**, (11-12), E199-E200 (1997).

185. Pailthorpe, M. T., and Curiskis, J. I., Sun Protection and Apparel Textiles, *Proceedings of International Textile Conference*, Coimbatore, India, (11), 19-21 (1995).

186. Pandey, S. N., and Nair, P., Mercerized and Crosslinked Cotton Yarns Part II: Effect of Stretching During Mercerization on Physical Properties and Degradation of Crosslinked Yarns, *Textile Research Journal*, **57**, (9), 532-538 (1987).

187. Park Scientific Instruments Internet Web Site, http://www.park.com. (January 1999)

188. Pavlath, A. E., *Techniques and Applications of Plasma Chemistry*, Hollahan. T. R., and Bell, A. T., Wiley, NY, 149-175 (1974).

189. Pedersen, G. L., Screws, Jr. G. A., and Cedroni, D. M., Bio-Polishing of Cellulosic Fabrics, *Textile Industries Dyegest Southern Africa*, **13**, (6), 4-10 (1994).

190. Pedersen, G. L., Screws, Jr., G. A., and Cedroni, D. M., Bio-Polishing of Cellulosic Fabrics, *Canadian Textile Journal*, **109**, (12), 31-35 (1992)

191. Peeling, J., Courval, G., and Jazzar, M. S., ESCA and Contact-Angle Studies of the Surface Modification of Poly (ethylene Terephthalate) Film: Photooxidation and Aging, *Journal of Applied Polymer Science: Polymer Chemistry Edition*, **22**, 419-428 (1984).

192. Phillips, T. L., Horr, T. J., Huson, M. G., Turner, P. S. and Shanks, R. A., Imaging Wool Fibre Surfaces with a Scanning Force Microscope, *Textile*

Research Journal, 65 (8), 445-453 (1995).

193. Radmacher, M., Tillmann, R. W., Fritz, M., and Gaub, H. E., From Molecules to Cells: Imaging Soft Samples with the Atomic Force Microscope, Science, 257, 1900-1905 (1992).

194. Rahman, M. M. M., and Sayed-Esfahani, M. H., Scanning Electron Microscopy Study of Flax Fibres, *Indian Journal of Textile Research*, **4**, (12), 149-152 (1979).

195. Rakowki, W., Plasma Modification of Wool Under Industrial Conditions, *Melliand English*, (10), E334-337 (1989).

196. Rakowki, W., Plasma Treatment of Wool – From Lab Curiosity to Industrial Reality, *Fibres & Textiles in Eastern Europe*, (9/10), 45-49 (1995).

197. Rakowki, W., Plasma Treatment of Wool Today. Part 1 – Fibre Properties, Spinning and Shrinkproofing, *Journal of Society of Dyers and Colorist*, **113**, (9), 250-255 (1997).

198. Rakowski, W., Okoniewski, M., Bartos, K., and Zawadzki, J., Plasma Treatment of Textiles - Potential Applications and Future Prospects, *Melliand Texilberichte (Eng. Ed.)*, E301-E308 (1982).

199. Rebenfeld, L., and Miller, B., Using Liquid Flow to Quantity the Pore Structure of Fibrous Materials, *Journal of Textile Institute*, **86**, (2), 241-251 (1995).

200. Rebenfeld, L., Fibrous Materials, *Absorbency*, Chatterjee, P. K., Elsevier Science Publishing Company Inc., NY, 1-27 (1985).

201. Rebenfield, L., Miller, B., and Tyomkin, I., Pore Structure in Fibrous Networks as Related to Absorption, *Modern Textile Characterization Methods*, Marcel Dekker, NY, 291-309 (1996).

202. Rhee, H., Young, R. A., and Sarmadi, A. M., The Effect of Functional Finishes and Laundering on Textile Materials, Part I: Surface Characteristics, *Journal of Textile Institute*, **84**, (3), 394-405 (1993).

203. Rhee, H., Young, R. A., and Sarmadi, A. M., The Effect of Functional Finishes and Laundering on Textile Materials, Part II: Characterization of Liquid Flow, *Journal of Textile Institute*, **84**, (3), 406-418 (1993).

204. Rochow, T. G., and Tucker, P. A., *Introduction to Microscopy by Means of Light, Electrons, X- rays, or Acoustics*, 2nd ed., Plenum Press, NY, 297-327 (1994).

205. Rolf, S., and Petry, G., Enzymes- Biocatalysts in Textile Finishing, *Melliand English*, **76**, E253-256 (1995).

206. Rudolf, W. K., Blum, A., and Werner G., Development of Objective Quality Criteria for Fiber Flax/Flax Part I: Chemical and Morphological Investigations, *Melliand English*, **69**, (12), E428-E429 (1988).

207. Rybkin, V. V., Maximov, A. L., Gorberg, B. L., and Titov, V. A., Plasma Technology and Equipment for the Modification of Textiles and Polymer Films, *Asian Textile Journal*, (10), 30-34 (1997).

208. Ryu, J., Dai, J., Koo, K., and Wakida, T., The Effect of Sputtering Etching on the Surface Characteristics of Black-dyed Polyamide Fabrics, *Journal of the Society of Dyer and Colorist*, **108**, (5/6), 278-281 (1992).

209. Ryu, J., Wakida, T., and Takagishi, T., Effect of Corona Discharge on the Surface of Wool and Its Application to Printing, *Textile Research Journal*, **61**, (10), 595-601 (1991).

210. Saito, M., and Yabe, A., Dispersion and Polar Force Components of Surface Tension of Some Polymer Films, *Textile Research Journal*, **53**, (1), 54-59 (1983).

211. Sarmadi, A. M., Young, A. K., and Young, R. A., Wettability of Nonwoven Fabrics. 1. Effect of Fluorochemical Finishes on Water Repellency, *Industrial Engineering Chemical Research*, **32**, 279-287 (1993).

212. Sarmadi, A. M., Young, A. K., and Young, R. A., Wettability of Nonwoven Fabrics. 2. Effect of Cationic Surfactant Treatment, *Industrial Engineering Chemical Research*, **32**, 287-293 (1993).

213. Sarmadi, M., Denes, A. R., and Denes, F., Improved Dyeing Properties of $SiCi_4$ (ST)-Plasma Treated Polyester Fabrics, *Textile Chemist and Colorist*, **28**, (6), 17-22 (1996).

214. Sato, Y., Tokino, S., Iino, H., Shim, Y., Ryu, J., and Wakida, T., Regression of Surface Characteristics of Oxygen Low Temperature Plasma-Treated Films by Heat Treatment, *Sen-i Gakkaishi*, **51**, (12), 580-585 (1995).

215. Sato, Y., Wakida, T., Tokino, S., Niu, S., Ueda, M., Mizushima, H., and Takekoshi, S., Effect of Crosslinking Agents on Water Repellency of Cotton Fabrics Treated with Fluorocarbon Resin, *Textile Research Journal*, **64**, (6), 316-320 (1994).

216. Sawada, K., Tokino, S., and Ueda, M., Bioscouring of Cotton with Pectinase Enzyme in a Non-aqueous System, *Journal of the Society of Dyer and Colorist*, **114**, (12), 355-359 (1998).

217. Sawada, K., Tokino, S., Ueda, M., and Wang, X. Y., Bioscouring of Cotton with Pectinase Enzyme, *Journal of the Society of Dyer and Colorist*, **114**, (11), 333-336 (1998).

218. Sawbridge, M., and Ford, J. E., *Textile Fibres Under the Microscope*, Shirley

Institute, Manchester, 17pp (1987).

219. Schaefer, D. M., Carpenter, M., Gady, B., Reifenberger, R., Demejo, L. P., and Rimai, D. S., Surface Roughness and its Influence on Particle Adhesion Using Atomic Force Techniques, *Fundamentals of Adhesion and Interface*, Rimai, D. S., DeMejo, L. P., and Mittal, K. L., Utrecht, Netherlands, 35-48, (1995).

220. Schunke, H., Sanio, C., Pape, H., Schunke, U., and Matz, C., Reduction of Time Required for Dew Retting of Flax, Influence of Agricultural, Mechanical and Microbiological Techniques on Fiber Processing, *Melliand English*, **76**, (6), E101-E104 (1995).

221. Segal, L., Creely, J. J., Martin, Jr., A. E., and Conrad, C. M., An Empirical Methods for Estimating the Degree of Crystallinity of Native Cellulose Using the X-Ray Diffractometer, *Textile Research Journal*, **29**, (10), 786-794 (1959).

222. Sharma, H. S. S., An Alternative Method of Flax Retting During Dry Weather, *Ann. Appl. Biol.*, 109, 605-611 (1986).

223. Sharma, H. S. S., and Van Sumere, C. F., Enzyme Treatment of Flax, *The Genetic Engineer and Biotechnologist*, **12**, (3/4), 19-13 (1992).

224. Sharma, H. S. S., Studies on Chemical and Enzyme Retting of Flax on a Semi-industrial Scale and Analysis of the Effluents for their Physico-chemical Components, *International Biodeterioration,* **23**, 329-342 (1987).

225. Sheehan, J. G., and Scriven, L. E., Assessment of Environmental Scanning Electron Microscopy for Coating Research, *1991 Tappi Coating Conference*, 337-383 (1991).

226. Sheth, G. N., Mayboo. C., Musale, A. A., Betrabet, A. M., Application of Enzyme Treatment to Cellulosic Fabrics for Imparting Specific Functional Properties, *Technological Conference, Resume of Papers, BTRA, SITRA, NTRA, ATIRA*, 99-111 (1995).

227. Shroff, J. J., Enzymes and Enzyme-Desizing, *Textile Industry & Trade Journal*, **23**, (5/6), 5-7 (1985).

228. Smiley, R. J., and Delgass, W. N., AFM, SEM and XPS Characterization of PAN-based Carbon Fibers Etched in Oxygen Plasmas, *Journal of Materials Science*, **28**, 3601-3611 (1993).

229. Sotton, M., Improvements and Innovations in Processing Techniques New Approaches in the Finishing of Linen, *European Textile Research – Competitiveness Through Innovation,* 266-277 (1985).

230. Sparrow, J. T., Applications to Fibers and Polymers, *The Use of the Scanning Electron Microscope*, Hearle, J. W. S., Sparrow, J. T., and Cross, P. M., 1st

ed., Pergamon Press, Oxford, NY, 139-163 (1972).

231. Stone, R. B., and Barrett, J. R., U.S.D.A. Study Reveals Interesting Effects of Gas Plasma Radiations on Cotton Yarn, *Textile Bulletin*, **88**, (1), 65-69 (1962).

232. Tao, Weiying and Collier, B. J., The Environmental Scanning Electron Microscope: A New Tool for Textile Studies, *Textile Chemist and Colourist*, **26**, (2), 29-31 (1994).

233. Thompson, C. M., and Shure, L., *Imaging Processing Toolbox*, The Math Works Inc., Mass, 187pp (1993).

234. Thorsen, W. J., Modification of the Cuticle and Primary Wall of Cotton by Corona Treatment, *Textile Research Journal*, **44**, (6), 422-428 (1974).

235. Tissington, B., Pollard, G., and Ward, I. M., A Study of the Effects of Oxygen Plasma Treatment on the Adhesion Behavior of Polyethylene Fibres, *Composites Science and Technology*, **44**, 185-195 (1992).

236. Tonks, L., and Langmuir, I., A General Theory of Plasma of Arc, *Physics Review*, **33**, 876-922 (1929).

237. Tonks, L., and Langmuir, I., Oscillations in Ionised Gases, *Physics Review*, **33**, 195-210 (1929).

238. Tonks, L., and Langmuir, I., The Interaction of Electron and Positive Ion Space Charges in Cathodes Sheaths, *Physics Review*, **33**, 954-989 (1929).

239. TopoMetrix Internet Web Site, http://www.topometrix.com. (January 1999)

240. Tsai, P. P., Wadsworth, L. C., and Roth, J. R., Surface Modifications of Fabrics Using a One-Atmosphere Glow Discharge Plasma to Improve Fabric Wettability, *Textile Research Journal*, **67**, (5), 359-369 (1997).

241. Tyndall, R. M., Application of Cellullase Enzyme to Cotton Fabric and Garments, *AATCC Book of Papers*, 269-273 (1991).

242. Tyndall, R. M., Improving the Softness and Surface Appearance of Cotton Fabrics and Garments by Treatment with Cellulase Enzymes, *Textile Chemist and Colorist*, **24**, (6), 23-26 (1992).

243. Tyndall, R. M., Upgrading Garment Washing Techniques, *American Dyestuff Reporter*, **79**, (5), 22, 24, 26, 28, 29-30 (1990).

244. Ueda, M., and Tokino, S., Physico-chemical Modifications of Fibers and theirs Effect on Coloration and Finishing, *Review Progress of Coloration*, **26**, 9-19 (1996).

245. Ueda, M., Koo, H., Wakida, T., and Yoshimura, Y., Cellulase Treatment of

Cotton Fabrics, Part II: Inhibitory Effect of Surfactants on Cellulase Catalytic Reaction, *Textile Research Journal*, **64**, (10), 615-618 (1994).

246. Uyama, Y., Inoue, H., Ito, K., Kizshida, A., and Ikada, Y., Comparison of Different Methods for Contact Angle Measurement, *Journal of Colloid and Interface Science*, **141**, (1), 275-279 (1991).

247. Van Langenhove, L., and Bruggeman, J. P., Method of Fiber Analysis, *The Biology and Processing of Flax*, Sharma, H. S. S., and Van Sumere, C. F., Eds., M Publications, Belfast, Northern Ireland, 311-327 (1995).

248. Van Sumere, C. F., Retting of Flax with Special Reference to Enzyme-retting, *The Biology and Processing of Flax*, Sharma, H. S. S., and Van Sumere, C. F., Eds., M Publications, Belfast, Northern Ireland, 157-198 (1995).

249. Varghness, J., Bhattacharyya, N., and Sahasrabudhe, A. S., Aftertreatments on Cellulosic Textiles Dyed with Direct Dyes – A Review, *Colourage*, **36**, (6), 15-31 (1989).

250. Vladimirtseva, E. L., Sharnina, L. V., and Blinicheva, I. B., Application of the Low-Temperature Plasma in Preparation Processes of Linens, *Fiber and Textiles in Eastern Europe*, **3**, (2), 30-31 (1995).

251. Vohrer. U., Muller, M. and Oehr, C., Glow-discharge Treatment for the Modification of Textiles, *Surface and Coatings Technology*, **98**, 1128-1131 (1998).

252. Wakida, T., and Tokino, S., Surface Modification of Fibre and Polymeric Materials by Discharge Treatment and Its Application to Textile Processing, *Indian Journal of Fibre & Textile Research*, **21**, (3), 69-78 (1996),

253. Wakida, T., Cho, S., Choi, S., Tokino, S., and Lee, M., Effect of Low Temperature Plasma Treatment on Color of Wool and Nylon Fabrics Dyed with Natural Dyes, *Textile Research Journal*, **68**, (11), 848-853 (1998).

254. Wakida, T., Kawamura, H., Song, J. C., Goto, T., and Takagishi, T., Surface Free Energy of Poly (ethylene Terephthalate) and Nylon 6 Films Treated with Low Temperature Plasma, *Sen-i Gakkaishi*, **43**, (7), 384-389 (1987).

255. Wakida, T., Takeda, K., Tanaka, I., and Takagishi, T., Free Radicals in Cellulose Fibers Treated with Low Temperature Plasma, *Textile Research Journal*, **59**, (1), 49-53 (1989).

256. Wakida, T., Tokino, S., Niu, S., Kawamura, H., Sato, Y., Lee, M., Uchiyama, H., and Ingaki, H., Surface Characteristics of Wool and Poly (ethylene Terephthalate) Fabrics and Film Treated with Low-Temperature Plasma Under Atmospheric Pressure, *Textile Research Journal*, **63**, (8), 433-438 (1993).

257. Wakida. T., and Tokino, S., Surface Modification of Fibre and Polymeric

Materials by Discharge Treatment and Its Application to Textile Processing, *Indian Journal of Fibre and Textile Research*, **21**, (3), 69-78 (1996).

258. Walker, L. P. and Wilson, D. B., Enzymatic Hydrolysis of Cellulose: An Overview, *Bioresource Technology*, **36**, 3-14 (1991).

259. Ward, T. L., and Benerito, R. R., Testing Based on Wettability to Differentiate Washed and Unwashed Cotton Fibers, *Textile Research Journal*, **55**, (1), 40-45 (1985).

260. Ward, T. L., and Benerito, R.R., Modification of Cotton by Radiofrequency Plasma of Ammonia, *Textile Research Journal*, **52**, (4), 256-263 (1982).

261. Ward, T. L., Benerito, R. R., Hilda, Z., and Use of Cold Plasma in the modification of Cotton, *16th Textile Chemistry and Processing Conference*, 8-11 (1976).

262. Watt, I. M., *The Principles and Practices of Electron Microscopy*, Cambridge University Press, NY, 30-262 (1997).

263. Weimer, P. J., Quantitative and Semiquantitative Measurements of Cellulose Biodegradation, *Biosynthesis and Biodegradation of Cellulose*, Haigler C. H., and Weimer, P. J., Marcel Dekker, NY, 263-291 (1991).

264. Wood, E. J., and Hodgson, R. M., Carpet Texture Measurement Using Image Analysis, *Textile Research Journal*, **59**, (1), 1-12 (1989).

265. Wood, E. J., Applying Fourier and Associated Transforms to Pattern Characterization in Textiles, *Textile Research Journal*, **60**, (4), 4212-220 (1990).

266. Wood, T. M., Fungal Cellulases, *Biosynthesis and Biodegradation of Cellulose*, Haigler C. H., and Weimer, P. J., Marcel Dekker, NY, 491-525 (1991).

267. Woodward, J., Synergism in Cellulase Systems, *Bioresource Technology*, **36**, 67-75 (1991).

268. Worbel, A. M., Kryszewski, M., Rakowski, W., Okoniewski, M., and Kubacki, Z., Effect of Plasma Treatment on Surface Structure and Properties of Polyester Fabrics, *Polymer*, **19**, (8), 908-912 (1978).

269. Xu, B., Identifying Fabric Structures with Fast Fourier Transform Techniques, *Textile Research Journal*, **66**, (8), 496-506 (1996).

270. Yamagishi, M., and Kako, G., Weight Loss Treatment to Soften the Touch of Cotton Fabric, *JTN*, **23**, (46), 64 (1988).

271. Yamagishi, M., Weight Loss Treatment to Soften the Touch of Cotton Fabric, *Kako Gijutsu*, **23**, 46 (1988).

272. Yan, H., and Guo, W., A Study on Change of Fiber Structures Caused by Plasma Action, *Journal of China Textile University*, (2), 1-9 (1987).

273. Yan, H., and Guo, W., A Study on Change of Fiber Structures Caused by Plasma Action, *Fourth Annual International Conference of Plasma Chemistry and Technology*, 181-188 (1989).

274. Yan, H., and Yu, W., Application of Plasma Etching Techniques to the Investigation of Fibre Structures, *Journal of East China Institute of Textile Science and Technology*, (2), 10-21 (1985).

275. Yasuda, H., Glow Discharge Polymerization, *Macromolecular Review*, **16**, 199-293 (1981).

276. Yasuda, H., *Plasma Polymerization*, Academic Press Inc., 178-195 (1985).

277. Yasuda, T., Gazicki, M., and Yasuda, H., Effects of Glow Discharges on Fibers and Fabrics, *Journal of Applied Polymer Science: Applied Polymer Symposium 38*, 201-214 (1984).

278. Yatagai, M., Correlation Between Wettability and Water Absorbency of Soiled Fabrics, *Textile Research Journal*, **64**, (8), 461-465 (1994).

279. Yoon, N. S., and Lim, Y. J., Tahara, M. and Takagishi, T., Mechanical and Dyeing Properties of Wool and Cotton Fabrics Treated with Low Temperature Plasma and Enzymes, *Textile Research Journal*, **66**, (5), 329-336 (1996).

280. Youan, M., Surface Acid-Base Characteristics of Fibre Materials by Contact Angle Measurements, *Journal of Applied Polymer Science*, **50**, 851-853 (1993).

281. Young, R. A., Denes, F., Hua, Z. Q., and Sitaru, R., ESCA Analysis of Plasma Modified Cellulose, *Proceedings of the 1997 9th International Symposium on Wood and Pulping Chemistry*, 129-1 – 129-4 (1997).

282. Zisman, W. A., Influence of Couritution and Adhesion, *Industrial and Engineering Chemistry*, **55**, 18-38 (1963).

APPENDIX 4-I

FeSEM Micrographs of Untreated Flax Fiber

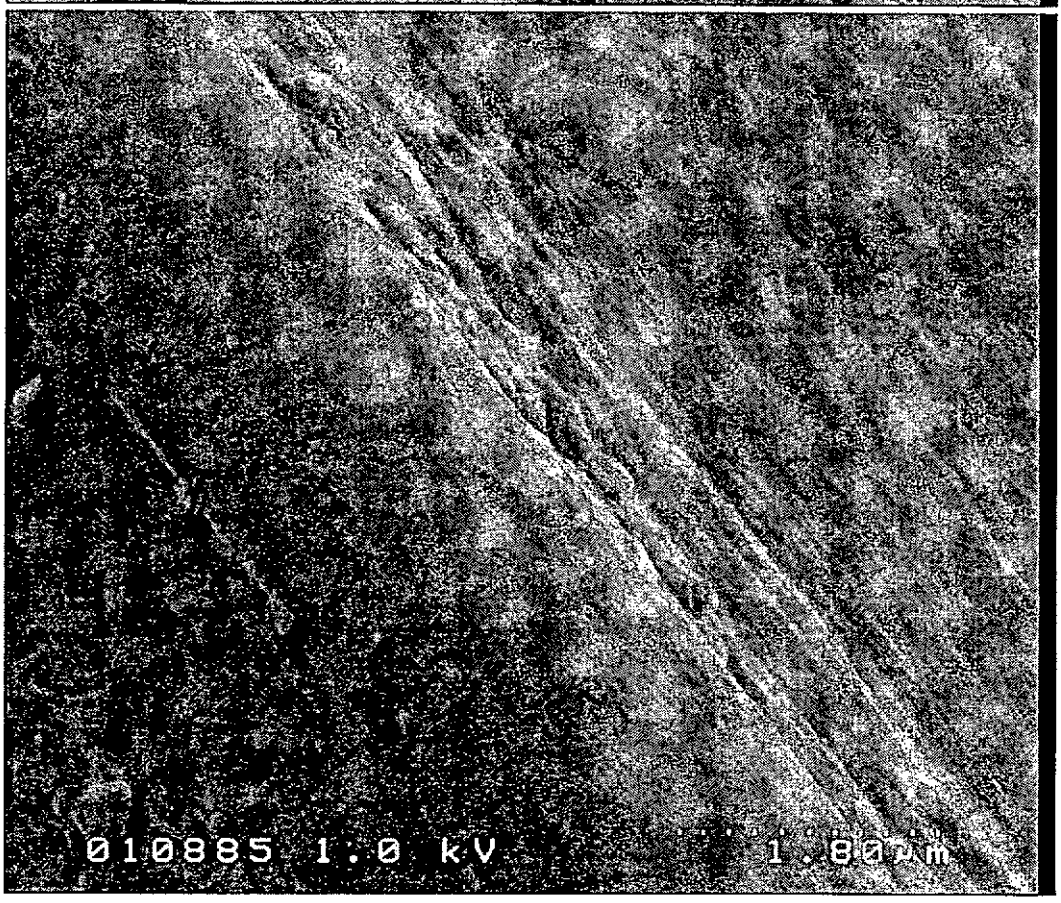

FeSEM Micrographs of Argon Plasma Treated Flax Fiber

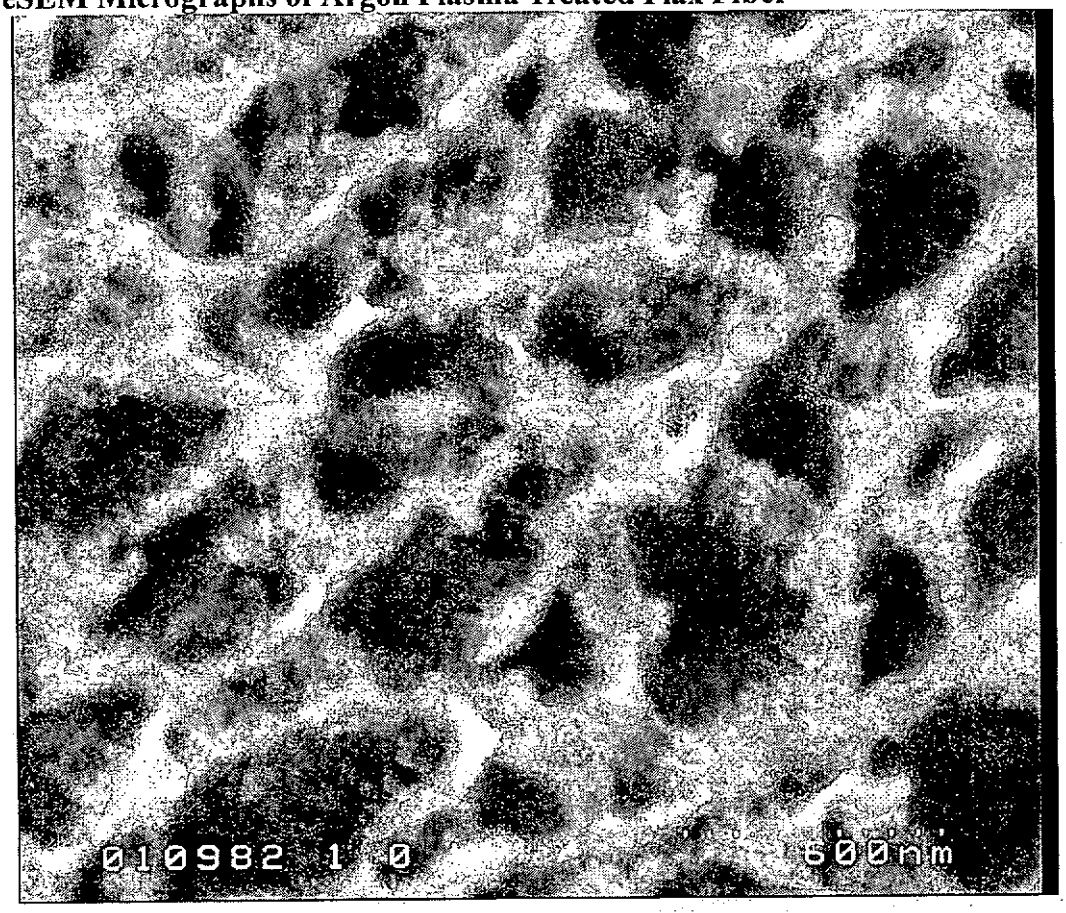

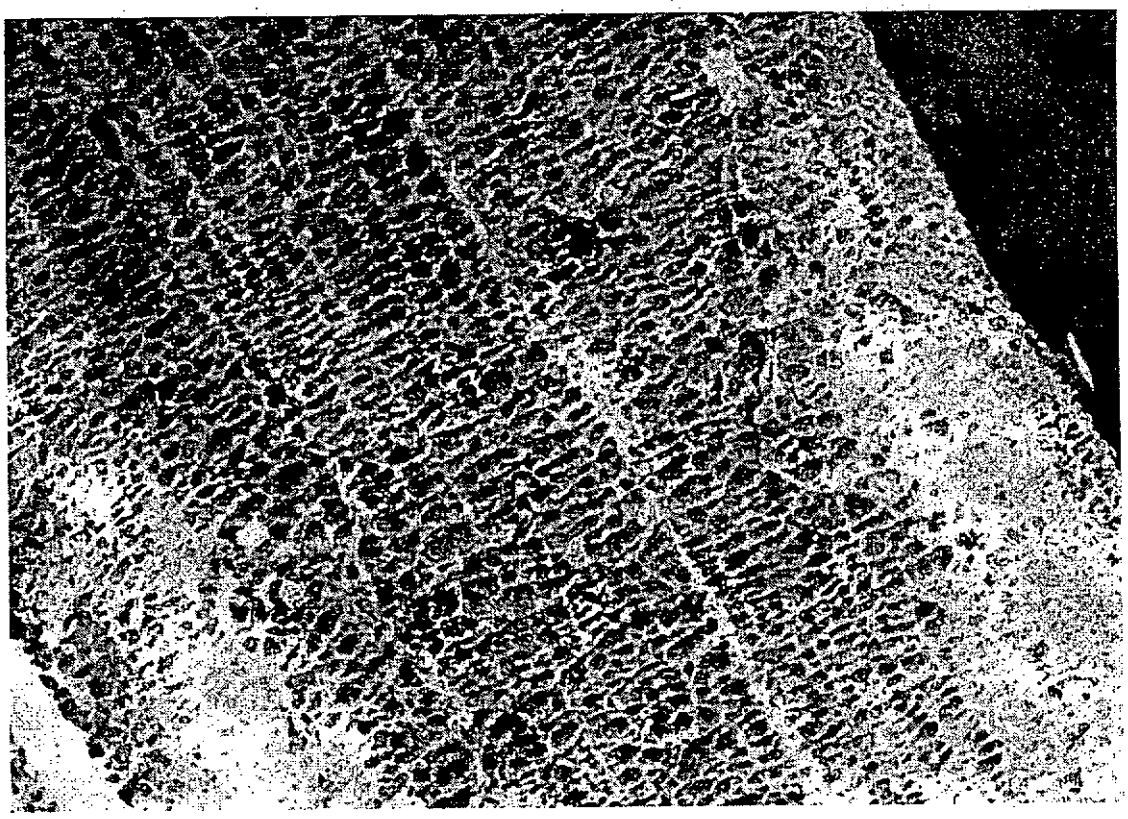

FeSEM Micrographs of Oxygen Plasma Treated Flax Fiber